Skeletal changes after post-mortem exposure to fire as an indicator of decomposition stage

Submitted by:

Natalie Keough

A thesis submitted to the Department of Anatomy, School of Medicine, Faculty of Health Sciences, University of Pretoria, in fulfilment of the requirements for the degree

Of

PhD in Anatomy

Pretoria, 2013

Supervisor: Prof EN L'Abbé

Co-supervisor: Prof M Steyn

DECLARATION

I, Natalie Keough, declare that this dissertation is my own work. It is being submitted for the degree of PhD in Anatomy at the University of Pretoria. It has not been submitted before for any other degree or examination at this or any other Institution.

Sign: _____

This _____ Day of _____, 2013

TABLE OF CONTENTS

LIST OF FIGURES

LIST OF TABLES

ABSTRACT

Forensic anthropologists and taphonomists are often tasked with interpreting the sequence of events from death through decomposition to skeletonisation. Discovery of burnt bone often evokes questions as to the condition of the body prior to the burn event. The purpose of this study was to evaluate features of thermal damage on bones in relationship to the condition of the bone (dry/wet) and progression of decomposition. Twenty-five pigs in various stages of decomposition (fresh, early, advanced, early & late skeletonisation) were exposed to fire for 30 minutes. The skeletal elements were scored and features included: colour change (unaltered, charred, calcined), brown and heat borders, heat lines, delineation, greasy bone, joint shielding, predictable and minimal cracking, delamination and heat-induced fractures. Colour changes were scored according to a ranked percentage scale (0 – 3) and the remaining traits as absent or present (0/1). Cohen's Kappa statistics evaluated intra- and interobserver error. Density plots and frequency distributions were constructed and multiple regression (categorical variables) and transition analysis were employed. The majority (8) of the 13 traits displayed potential to predict decomposition stage from burned remains. An increase in calcined and charred bone occurred synchronously with an advancement in decomposition. The organic composition of bone and presence of flesh affect the characteristics features of burned bone. Greasy bone occurred most often in the early/fresh stages (fleshed bone). Heat borders, heat lines, delineation, joint shielding, predictable and minimal cracking were associated with wet tissue/bone; whereas brown burn/borders, delamination and other heat-induced fractures were associated with early and late skeletonisation. No statistically significant differences were noted among observers for the majority of the traits except for predictable and minimal cracking and heat-induced fractures in the cranium. Heat-induced changes may assist in estimating decomposition stage from unknown, burnt remains and thereby aid in a providing an indication as to the condition of the bone prior to the burn event.

Keywords: Taphonomy, Burned bone, Patterned thermal destruction, Transition analysis, Heat-induced changes

ACKNOWLEDGEMENTS

Taphonomic studies, especially those that involve fire, are not for the feint hearted. If it were not for the myriad of strong supporters in my life, this project would have been more challenging. I would like to thank my two-person supervisory team, Prof Maryna Steyn and Prof Ericka L'Abbé for their unquestionable assistance in this project. Thank-you for providing countless amounts of freedom, patience and, encouragement in order to tackle the field of taphonomic observation, interpretation and quantification. Throughout this project, through many, many obstacles, Prof Steyn and Prof L'Abbe always believed in this project to produce results in the end.

I am forever in debt to my colleagues at the Department of Anatomy (UP); Professor Marius Bosman, Gert Lewis, Liefie Du Plessis, Prof JH Meiring, Claire Venter and Albert van Schoor for helping in hours of need, whether it was collecting rotten carcasses or providing a supportive word; you all made this task bearable. Jolandie Myburgh, partner in crime, thank-you for all the man hours spent establishing the body farm, procuring pigs, recording decomposition, chasing cows, burning decomposed pig carcasses and collecting burn fragmented remains. You provided the much needed support and motivation to this project and as we say; there was never a dull moment on the body farm. Thank-you, sincerely, for travelling along down this research path.

I would like to extend my thanks to Roelf Coertze, without whom there would be no pig body farm nor pigs to place there. Thanks for understanding and accepting the strange requests made to initiate this project and for providing the space, man-power and facilities to conduct this research. A special thanks to Melvin Trollope and Tommy van Deventer for

supplying the pig carcasses for this study. Their help and continual support proved to be invaluable and without it this project would have had no sample.

I would like to thank the following individuals for their invaluable contributions to this project:

- NRF and Navkom: for supplying the research funding for this project.
- Eric Marakalla: for all the assistance in the maceration of the pig carcasses.
- Steve Symes and Steve Ousley: for all the supportive words of encouragement and the excited trips to the FABF – cameras ready.
- Prof Piet Becker and Samantha Pretorius: thank-you both for your enthusiastic input into the statistical part of this study. Prof Becker thanks for the patience and the utter interest you showed in this work when we were punching in numbers during the late afternoon hours. Samantha, thank-you for showing interest in this new field and going to the effort to learn how to use a new program just so you could help me soup up my statistics and make for a more impressive outcome. A word of thanks also to Kyra Stull for her help with the statistics program R.
- Students at the Department of Anatomy: thanks for voluntarily going out to the pig farm in the middle of summer in the heat and helping with collection and recording data. Your help was greatly appreciated and I hope it served as a learning platform as well.
- Marinda Pretorius for help with the illustrations for this project.

Lastly, I would just like to express my heartfelt gratitude and love towards my family members. To Jean, the love of my life, who in his own way pushed, supported and believed in me through this long journey. To my Dad, for always believing in me even when I thought that this would never end. To my Mom (who unfortunately could not see me graduate) – who so believed in my abilities that to her I already had already finished my degree. She never missed an opportunity to brag about my achievements and for that I am eternally grateful. I know she will be sitting in on my graduation to share this amazing feat – she is missed. To my Sister who also never stopped believing and really supporting me through this project. Her constant and enthusiastic interest in my progress always kept me on edge and made me make sure that I had new news to give her every time we met for an update.

- Thank-you

Chapter 1: Introduction

In South Africa, fire had often been used either to execute a person or destroy evidence on a body. Under the previous South African government, informal death squads, associated with the South African Police Service (SAPS), used fire, and in later years explosives, to dispose of the remains of anti-government activists (Pauw 1991, 1996). Former death squad commander Dirk Coetzee recalled that "the bodies were placed on a pyre constructed from wood, bushveldt grasses and tyres. In order to reduce the remains to ashes, the fire was tended for 7 to 9 hours after which the ashes were deposited in the river" (Pauw, 1991, 1996). Similarly, in various experimental studies, DeHaan (2012) noted a period of 7 to 9 hours to destroy completely a fully fleshed body, which corroborates with the findings of Bohnert *et al*. (1998).

In response to police brutality and lawlessness in the rural communities, "necklacing" originated in the South African townships in the 1980's as a form of mob execution for suspected traitors to the apartheid struggle (SAPA, 1997; Bornman *et al*., 1998; Frater, 2007). The procedure involved placing tyres around the intended victim's arms and chest, dousing them with petrol and setting the entire construction alight. With the recent immigration of foreigners into South Africa, continual dissatisfaction with service delivery (water supply, sanitation), unemployment and rising crime rates, the practice of necklacing has reappeared in the townships and rural communities (Fihlani, 2011).

According to the 2011 National Injury Mortality Surveillance System (NIMSS) annual report for the Gauteng province, the leading cause of unintentional, non-transport related deaths in individuals between 15 and 64 years of age is fire-related (NIMSS, 2012). In 2009, an estimated 200 million people died globally as a result of shack fires with one third being in sub-Saharan countries (UN Reports, 2009). Historically, South Africa, South America and other regions of South Asia present with the highest prevalence of shack related fire deaths (Raphela, 2011). Approximately 9% of fatal deaths in South Africa are from fire-related injuries (NIMSS, 1999). Burned or charred remains make up approximately 5% (22/424) of all forensic cases received in the Forensic Anthropology Research Center (FARC) analysed for the SAPS between 2005 and 2011. Burned skeletal remains represent a challenge in terms of identification and reconstruction of possible peri-mortem events, particularly with regard to cases of necklacing and bodies recovered from the veldt. The

analysis of burned human remains fulfils an important area of research in modern taphonomic studies. Skeletal remains that require anthropological analysis vary from the freshly dead, to early stages of decomposition (fleshy or desiccated tissue) to the final stages of skeletonisation. Forensic anthropologists provide presumptive identifications (or biological profiles) of unidentified human skeletal remains and interpret skeletal injuries within context and known taphonomic circumstances.

Taphonomy can be described as the scientific reconstruction of all postmortem events influencing the preservation, observation and recovery of remains (Haglund & Sorg, 1997; Denys, 2002). Reconstructing the events in a forensic context leading to and following death involves the analysis of depositional context and peri- and postmortem injuries on bone (Haglund & Sorg, 1997). The research outcomes of taphonomic studies provide valuable data that can be applied to forensic casework (Pope, 2007). Forensic taphonomy is thus specifically concerned with the various processes that occurred directly to or for a period after death (postmortem interval) as well as decomposition and all influencing factors involved in these processes (Mann *et al*., 1990; Denys, 2002; Sorg & Haglund, 2002; Adlam & Simmons, 2007). In recent years, an area of taphonomic research associated with the impact of modifying agents such as temperature, insect and scavenger access, burial depth, and of relevance to this study, fire exposure, on the process and sequence of decomposition has evolved (Sorg & Haglund, 2002). Fire influences the standard models used for the estimation of the rate and sequence of decomposition (Mayne Correia, 1997; Kolver & Van der Linde, 2005; Symes *et al.,* 2008).

A body may be intentionally set on fire in an attempt to destroy both identity and evidence of a crime (Fanton, 2006), but the burn event may only occur days or weeks after death. During this period, decomposition progresses from autolysis through putrefaction with biomass reduction from arthropod, carnivore or rodent activity. Decomposition takes place at varying rates and systematically degrades soft and hard tissues with numerous variables contributing to the final condition of the remains. Decomposition reduces soft tissue and results, eventually, in a dry skeleton, which is structurally different from fresh/fleshed remains. Burning of remains during any one of the decomposition stages will create discernable differences that are linked to the presence of the tissue, fat/grease and organic materials in bone.

The South African veldt is the perfect location for the disposal of a human body as it comprises a large part of the country, the grass is long, and few individuals venture into the

remote areas. Data obtained from the Advanced Fire Information System (AFIS) show that on average 30 000 veldt fires occur each year in South Africa, affecting 3 million hectares of land. Every year, fields are burnt either as a means to prepare the grass for land clearing, hunting, pasture management or crop production or by accident (Nkomo & Sassi, 2009). During the time that the land is being processed, numerous burnt, decomposed or decomposed and burnt bodies are discovered and subsequently require skeletal analysis.

Fire is a destructive force that often thwarts forensic anthropologists' ability to identify and analyse human remains (Mayne Correia, 1997). For decades, researchers have been interested in the condition of a body (fleshed, wet or dry) prior to the burn event, time since death and bone trauma (Krogman, 1939; Webb & Snow, 1945; Baby, 1954; Binford, 1963; Thurman & Wilmore, 1981; Grevin *et al.,* 1998; Pope, 2007; Symes *et al.,* 2008). Studies focused on burned remains evolved from simple fragment quantification of early cremation sites to a more descriptive and systematic macroscopic approach of skeletal material (Scott *et al.,* 2010).

One question that arises when examining burnt remains is whether investigators can identify evidence of traumatic injury or criminal activity from the skeleton. Another question is whether the body burnt at the time of death or some time afterwards decomposition had progressed (Pope, 2007). Remains recovered from burn events can be in various states of destruction ranging from charred with soft tissue to completely incinerated, with minimal to no soft tissue. Victims exposed to fire for a short duration usually display superficial damage or charring of the skin and are often visually recognised. However, in cases of prolonged exposure to fire and other taphonomic elements, recognisable features are often destroyed and alternative methods for identification are required (Pope, 2007). The ability to interpret thermal damage with regard to colour changes, structural changes (shrinkage, warping) and bones burnt in flesh from those burnt dry, are some of the requirements of practicing forensic anthropologists. Knowledge of how and why a body is affected by heat is critical for fire investigation studies. Current research provides little direction in distinguishing between accidental trauma and criminal activity (i.e., differentiating between a normal burn pattern and an abnormal burn pattern), especially when only skeletal remains are recovered. Even less information is available with regard to whether the body was burned fresh or in a specific stage of decomposition (Pope, 2007).

Due to heat-related fragmentation and deformation, burnt bone is often unrecognizable as bone. More experimentation relating to scene recovery, reconstruction,

trauma interpretation, thermal correlations with colouration, morphological and microscopic changes, distinguishing between bones burned with flesh and those burned without flesh, and chemical extraction techniques, are required (Arora *et al.*, 2010). When a fleshed body burns, a predictable sequence of tissue distortion and body repositioning occurs and is known as the pugilistic posture. This pose may appear within 10 minutes of exposure to a fire (Bohnert *et al.,* 1998; Pope, 2007). The pugilistic posture is the systemic reaction of the body to fire, and results in contraction of the muscles from the neck and upper and lower limbs. With continual exposure to fire, the pugilistic posture allows for differential tissue shielding of exposed areas (Symes *et al.,* 2008). Areas protected with large amounts of skin, fat and muscle burn last and areas with minimal layers of protection burn first. The ability to identify, reconstruct and understand a normal pattern of thermal destruction in human remains is important so that deviations in this pattern due to natural (decomposition), accidental or criminal (accelerants, restraints) intentions can possibly be identified.

Patterned thermal destruction of human remains is well-described, but various influencing factors on this pattern are not yet fully understood. One factor influencing a normal burn pattern is the level of decomposition of the body. If a body was in a more advanced state of decomposition, the normal pattern of thermal destruction for fleshed remains does not apply, as the body cannot strongly flex, or not flex at all, into a pugilistic posture. It is important to note that an abnormal burn pattern can only be seen as possible evidence of criminal intent if the condition of the body prior to burning is already known, as once the body can no longer enter a pugilistic posture (i.e., no normal pattern), all evidence of burning is abnormal. Most researchers agree that burned fleshed bone displays different characteristics regarding colour, texture and fractures when compared to dry burned bone (Binford, 1963; Thurman & Wilmore, 1981; Pope, 2007; Symes *et al.,* 2008). However, burn patterns between fleshed and dry bone are not well described in the literature.

To date, no studies have been performed involving the exposure of several bodies that are in various stages of decomposition to a fire and then observing the characteristics of the burn patterns. The purpose of this study is to describe and quantify macroscopic changes associated with fire in skeletal material exposed to fire in five stages of decomposition, namely, fresh, early, advanced and early and late skeletonisation. To accomplish the aims this study has to establish whether a relationship between the levels of decomposition (fresh, early, advanced, early skeletonisation, late skeletonisation) and burn damage exist and to statistically quantify these concomitant changes. Frequency distributions with density plots,

multiple regression analysis (categorical variables) and transition analysis provide both descriptive and predictive insights into the relationship between heat-related alterations to the skeleton and the stages of decomposition.

The primary objective of this study is to assess whether a trend exists (with various levels of decomposition) in the proportion and degree of burn-related changes on bone. To achieve this, three levels of procedural analyses are employed. First, the burn-related characteristics are tested for statistical significance with advancement of decomposition; this would also determine if various components of burn-related damage (heat borders, heat lines, joint shielding) accurately depict the stage of decomposition when using multi-variable data analysis. Second, the burn-related characteristics are tested using two prediction models (multiple regression and transition analysis) to determine whether scoring a suit of traits can be used to estimate decomposition stage and thirdly, repeatability is tested to determine the accuracy and reliability of scoring burn-related traits on skeletal material.

Chapter 2: Literature Review

The aim of the present study is to evaluate the significance of 13 burn-related traits to establish whether there is marked relationship between these traits and the stages of decomposition and the condtion of bone. This literature review outlines the fundamentals of the process of decomposition and the morphological changes that take place during those stages. This review will also provide a detailed description of the study and interpretation of burnt human remains.

2.1. Decomposition

Decomposition is a sequential process that involves a variety of complex mechanisms such as autolysis, putrefaction and decay. The result thereof is the reduction of a fleshed body to a skeleton (DiMaio & DiMaio, 1989; Clark *et al.*, 1997; Fiedler & Graw, 2003; Powers, 2007). Although the sequence of decomposition is relatively consistent, no two individuals decompose in the same way or at the same time. Variation in decomposition creates difficulty in estimating the exact postmortem interval (PMI) and, the longer the PMI the more uncertain the estimation (Pinheiro, 2007). Postmortem changes are observed within 4 minutes to 2 hours after death (Clark *et al.*, 1997; Vass, 2001). These changes result from a lack of cardiac activity, which previously supplied oxygenated blood to the tissues and skin. Initial changes include the loss of the normal skin and mucous membrane colour (Clark *et al.*, 1997; Gunn, 2009) and an increase in enzymatic and bacterial activity, which initiates the process of degradation (Fiedler & Graw, 2003).

2.1.1. Autolysis

Autolysis is an aseptic process where intracellular hydrolytic enzymes, which are present in the cytoplasmic granules of all cells, are released into the cytoplasm and result in a breakdown of both cells and organs (DiMaio & DiMaio, 1989; Clark *et al.,* 1997; Powers, 2007). All cellular components have the potential to undergo autolytic and enzymatic breakdown due to the presence of innate, biochemical mechanisms for nutrient processing, degradation of toxic substances and recycling of both structural and functional molecules

(Powers, 2007). Various sections of the body contain different quantities of enzymatic complements per functional requirement, which renders variable rates of autolysis for each distinct cell, tissue and organ (Powers, 2007). For example, the liver contains a broad spectrum of catabolic enzymes that allow for a more rapid onset of autolysis when compared to that of muscle tissue, which has limited biochemical activity and a delay in the onset of autolytic processes (Powers, 2007).

The trigger mechanism for autolysis is also influenced by a decrease in intracellular pH that results from the absence of oxygen intake (Cormack, 1987; Clark *et al.,* 1997; Vass, 2001). Since cellular membranes are disrupted, the by-products of protein and carbohydrate (via hydrolytic enzymes) digestion are released into surrounding tissue and are subsequently utilised by other micro-organisms (Clark *et al.,* 1997). Following death, carbon dioxide accumulates in the blood as well as chemicals from the degradation of tissue. This causes the blood to become acidic, i.e. decreased pH (Cotran *et al.*, 1994). In addition to this, cell integrity is compromised by various cellular enzymes such as lipases, proteases and amylases, which dissolve the cells from the inside-out and cause a release of nutrient-rich fluids into the surrounding tissues (Vass, 2001). Changes which occur as a by-product of autolysis are initially only observable microscopically. Approximately 48 hrs after death, these changes are apparent to the naked eye (Clark *et al.*, 1997). External phenomena such as skin slippage or fluid-filled blisters (bullae) are macroscopic occurrences which are due to a release of hydrolytic enzymes that cause an accumulation of fluid under the dermis and a loosening of the epidermis from the dermis (Clark *et al.,* 1997; Vass, 2001). The chemical changes that take place do not occur in a uniform fashion throughout the body. Some areas present with a faster conclusion of energy metabolism (e.g., blood) when compared to other areas (e.g., vitreous humor of eye) (Gunn, 2009).

Autolysis is a chemical process and is dependent on the surrounding temperature. Heat accelerates the process where cooler temperatures slow it down. If temperatures become extreme (hot or cold), then the process of autolysis ceases completely (DiMaio & DiMaio, 1989; Clark *et al.,* 1997). During the process of autolysis, the body eventually adjusts to the surrounding environmental temperature (algor mortis); the blood settles in the capillaries resulting in external skin colour changes (livor mortis); and the muscles stiffen on the account molecular alteration to the cellular cytoplasm (rigor mortis).

2.1.1.1. Algor mortis

The PMI is estimated within the first 24 hours after death with the use of body core temperature, otherwise known as algor mortis or the coldness of death (Pounder, 2000; Tracqui, 2000; Gunn, 2009). Algor mortis results from an absence of internal core temperature regulation. The use of a decrease in core body temperature to estimate PMI is classified as a rate method. This implies that the event was either initiated or ceased at time of death. Therefore, the measured change in rate (increase or decrease) is used to provide an estimated PMI (Gunn, 2009). The core body temperature, however, may not always be the most reliable method to measure PMI, as with all rate methods, the longer the elapsed time the more inaccurate the method (Gunn, 2009). Various extraneous factors (e.g, environment, activity prior to death, location) are highly influential on core body temperature. Furthermore, the application of methods used to calculate body temperature need to two assume two facts that one may not always know. The first assumption is that the body temperature, at time of death, was normal (average = 37°C). The second assumption implies that the process of body cooling follows a uniform and consistent pattern. If these constraints are not known, estimation of PMI may be inaccurate (DiMaio & DiMaio, 1989; Gunn, 2009).

An individual's core body temperature at death should not be estimated, because normal body temperature varies between individuals, and depends on various external and internal factors surrounding the cause and manner of death (DiMaio & DiMaio, 1989; Gunn, 2009). Furthermore, death may not have occurred immediately after an attack or incident. If a victim had been assaulted but death only occurred after a prolonged period of time, the core body temperature may be influenced if the victim was in an extremely hot or cold environment (higher or lower) prior to death. Body temperature varies depending on time of day, physical activity (running, sleeping, and swimming), weather (snow, desert) and disease/infection (viral/bacterial infection) (DiMaio & DiMaio, 1989).

In a corpse, internal body heat is lost in a variety of ways which influence the rate at which body temperature cools (Table 2.1). The manner in which a body cools is best represented by a sigmoid curve in which internal temperature is plotted against time (Figure 2.1). In the beginning there is maintenance of body temperature that can last for several hours - the temperature plateau. This phase is followed by a linear rate of temperature cooling and slows rapidly as the body approaches environmental temperature. This phase (temperature plateau) can last from 30 minutes to 5 hours (Clark *et al.,* 1997). Under normal

circumstances, core body temperature decreases at an average of 16.94°C per hour after death (Clark *et al.,* 1997). The temperature of the body reaches equilibrium with the surrounding environmental temperature within 18 – 20 hours (Fisher, 2007; Goff, 2009). Variability is often observed in the temperature plateau and is attributed to factors such as the body temperature (at time of death); body mass, clothing, movement of air, humidity, and location (Pounder, 2000; Tracqui, 2000).

The intermediate phase results in a rapid linear decline in core body temperature that slows down when equilibrium with the surrounding environmental temperature is achieved. The optimal time to measure the core body temperature is during the intermediate phase. However, the rate of postmortem cooling, as previously mentioned, is affected by various environmental factors and cadaveric factors other than the environmental temperature and the body temperature at the time of death. These are summarised in Table 2.1.

2.1.1.2. Livor mortis

Livor mortis (i.e., hypostasis/lividity) is an early postmortem change that results from the gravitational accumulation of blood in veins and capillaries due to cessation of blood flow, the result is a dark reddish-purple to purple discolouration/staining of the skin that is easily observed and is often referred to as the colour of death (DiMaio & DiMaio, 1989; Clark *et al.,* 1997; Henssge *et al.*, 2002; Powers, 2007; Gunn, 2009) (Figure 2.2). The red patches/blotches gradually darken to a purplish hue owing to the dissociation of oxygen molecules from red blood cell haemoglobin (Clark *et al.,* 1997). Due to the release of a fibrinolytic enzyme (plasmin) which forces red blood cells and plasma to remain in liquid form throughout the vascular system, blood is rendered incoagulable within 30 – 60 min postmortem. Due to gravity, blood sinks into the dependent parts of the body and fills the inert veins and capillaries (Henssge *et al.,* 2002; Powers, 2007; Gunn, 2009). To the inexperienced eye, livor mortis could be mistaken for bruising, which could cause problems when interpreting peri-mortem traumatic injuries (DiMaio & DiMaio, 1989).

Due to the compression of capillaries, lividity does not occur on areas of the body that are resting against a firm surface or are in direct contact with another object (DiMaio & DiMaio, 1989; Henssge *et al.*, 2002). For example, under normal conditions, a body that is lying in anatomical position (supine/on back), does not form lividity on the shoulder blades, elbows, buttocks, thighs or calves as these areas are in direct contact with the ground

(DiMaio & DiMaio, 1989; Green, 2000, Henssge *et al.*, 2002; Gunn, 2009). In addition to the absence of lividity formation on contact surfaces, pressure lividity (pressure pallor) (Figure 2.3) is observed in circumstances where ligatures (rope around neck, tied hands) or tight clothing (belts, bra straps) prevented blood accumulation in associated blood vessels. This results in distinct colour differences between pressure areas and non-contact areas (Gunn, 2009).

Livor mortis presents within 15 minutes postmortem (Clark *et al.,* 1997) but becomes visually evident within 20 to 120 minutes and reaches maximum colouration at approximately 8 to 12 hours after death. At this time, lividity becomes and remains visible until putrefaction (DiMaio & DiMaio, 1989, Pounder, 2000; Tracqui, 2000; Green, 2000). If the body is moved from its original position prior to fixation (< 8 hours after death), the blood, due to gravitational changes, relocates and accumulates in another position (DiMaio & DiMaio, 1989). To determine whether lividity is fixed or not, the researcher needs to gently press a finger against a patch of livor mortis on the skin. If lividity disappears when the finger is removed, then it is not fixed. If the lividity does not disappear, it is considered fixed (Pounder, 2000; Tracqui, 2000; Green, 2000).

When lividity is fixed and the body is relocated, secondary lividity takes place. This phenomenon occurs faster when the body is moved within the first few hours after death (Camps *et al.*, 1976). Secondary lividity patterns are observed at least 24 hours after death and are associated with the repositioning of the body. Since the coagulation of blood and fibrinolyis occur in a variable timeframe, the use of secondary lividity to estimate PMI is of no value (Henssge *et al.*, 2002). However, secondary lividity is useful to determine relocation of the body within the first 24 hours after death.

The appearance of lividity varies among individuals and its rate of development can be influenced by certain medical conditions and disease (Gunn, 2009). Therefore, this method is not a highly useful indicator of PMI.

2.1.1.3. Rigor mortis

Rigor mortis is the generalised stiffness of the voluntary and involuntary muscles of the body after death. Ordinarily, death is immediately followed by muscular and joint relaxation which is known as primary muscular flaccidity (Gunn, 2009). Generalised muscular stiffening succeeds this relaxation. During the initial flaccid stage, urine and faeces

are released and gastric contents regurgitated owing to relaxation of the muscle sphincters (Clark *et al.*, 1997; Gunn, 2009).

The process that leads to rigor mortis is considered to be a reversible chemical change that takes place during the denaturation and complete depletion of adenosine triphosphate (ATP) (DiMaio & DiMaio, 1989; Gill-King, 1997; Clark *et al.,* 1997; Powers, 2007). The integrity of the sarcoplasmic reticulum of muscle cells is lost after death and results in an influx of calcium ions into the sarcomere, which elevates the intracellular calcium concentration (Marieb, 1992; Gunn, 2009). The sarcomere is a contractile unit that is comprised of alternating parallel protein filaments of actin and myosin. During the release of calcium ions, binding sites present on actin filaments normally occupied by regulatory proteins (troponin and tropomysoin) are unblocked. This allows the myosin filament to bond via a cross-arm to the actin filament (Gunn, 2009). When the cross-arm retracts, the actin is pulled along the thick myosin fibre. As a consequence the sarcomeres join together (end-to-end) and shorten the muscle fibres (Marieb, 1992).

In a living individual, ATP-driven transport pumps shift calcium back into the sarcoplasmic reticulum, which detaches the actin-myosin bond and brings about muscle relaxation. After death ATP production ceases and its availability diminishes; this causes calcium ions to accumulate in the sarcomeres and to produce a state of contraction/rigidity (Marieb, 1992; Gunn, 2009). Therefore, actin and myosin filaments become permanently contracted in the absence of ATP (DiMaio & DiMaio, 1989). However, muscle contraction is not permanent. As a result of protein denaturation, actin filaments from the ends of the sarcomeres detach, and rigor dissapates (Marieb, 1992; Gunn, 2009).

The sequence in which rigor mortis arises is fairly predictable and is referred to as Nysten's Law (Tracqui, 2000). Nysten, in 1811, was first to publish a reference for rigor mortis. He stated that rigor mortis is a successive manifestation of muscle rigidity with certain muscles showing signs of rigor before others. Rigor mortis initially appears in the masticatory muscles, the muscles of the eyelids, the lower jaw, the neck, the trunk and upper extremities and then finally the lower extremities (DiMaio & DiMaio, 1989; Clark *et al.,* 1997; Gill-King, 1997; Henssge *et al.*, 2002) and usually also develops faster in the muscles that were most active prior to death (Gunn 2009). The distal joints of the hands and feet are affected before the larger proximal joints of the elbows, knees, shoulders and hips (Pounder, 2000).

The manifestation of rigor mortis for isolated muscle fibres is divided into four distinct phases (Henssge *et al.*, 2002). Phase I (delay period) occurs directly after death. The muscle maintains a normal state due the presence of ATP, which allows the splitting of the actin-myosin cross-bridges. Phase II (onset period – reversible) occurs when ATP concentration falls to a critical level and causes the cross-bridges to remain intact. This phase is reversible, because the muscle activity relaxes when it receives either external sources of ATP or oxygen. In phase III (rigor – irreversible) rigor is fully developed and irreversible on account of postmortem modifications to the muscle fibres which inhibit them to relax. Phase IV (resolution) is the cessation of rigor. The muscle fibre returns to a limp/flaccid state, which is possibly related to protein denaturation. In Table 2.2, variability regarding onset, duration and cessation of rigor is shown. As can be seen, rigor mortis starts within the first 7 hours after death, is generally complete after 2 days and disappears within a week after death.

The onset and duration of rigor mortis is affected by surrounding temperature (ambient), the degree of muscular activity and muscular development, and the metabolic state of an individual prior to death (Gill-King, 1997; Clark *et al.,* 1997; Pounder, 2000; Tracqui, 2000; Gunn, 2009). Rigor mortis is a chemical process that is often accelerated with heat (Clark *et al.,* 1997). High environmental temperatures increase the onset of rigor mortis but delay its duration. In cold temperatures (below 10 °C), the onset of rigor mortis is delayed but its duration is increased (Gordon *et al.,* 1988; DiMaio & DiMaio, 1989). Likewise, excessive muscular activity, such as heavy exercise, severe convulsions, or fever prior to death, results in a decrease in ATP production which hastens the onset of rigor mortis and decreases its duration (DiMaio & DiMaio, 1989; Clark *et al.,* 1997). In the absence of strenuous muscular activity, the onset of rigor mortis is delayed, but its duration is increased. In individuals with well-developed muscles, rigor mortis is more intense than those with poor muscular development.

When examining a body, the degrees (complete, partial, or absent) and distribution of rigor are assessed. A forced flexion of the different joints indicates the amount and location of rigor mortis in the body. The general rule applies that the faster the onset of rigor mortis, the shorter its duration. Although rigor may not be highly reliable owing to the fact that it is a progressive event, its manifestation has been used as an estimator of the PMI (Pounder, 2000; Tracqui, 2000; Henssge *et al.,* 2002).

2.1.2. Putrefaction

In contrast to autolysis, putrefaction is a septic process. It begins with the proliferation of bacteria and endogenous enzymes within the anaerobic environment of the intestines and is a consequence of the cessation of homeostatic mechanisms that prevent bacterial overgrowth in a living individual (Gill-King, 1997; Clark *et al.,* 1997; Pounder, 2000; Tracqui, 2000; Green, 2000; Powers, 2007).

Throughout putrefaction, soft tissues are destroyed via micro-organisms like bacteria and fungi that are found in the gastrointestinal tract (DiMaio & DiMaio, 1989; Pounder, 2000; Tracqui, 2000; Vass, 2001; Powers, 2007). In living organisms the gastrointestinal tract contains roughly 96 to 99% anaerobic and 1 to 4% aerobic bacteria, both of which act quickly upon host cells in their immediate environment after death (Jawetz *et al.,* 1982). Micro-organisms, owing to the process of autolysis, penetrate cellular membranes and disseminate through the body (Powers, 2007). The actions of these micro-organisms are enhanced from the catabolism of soft tissues (carbohydrates, proteins and fat) into gases, liquids and simple molecules (Clark *et al.,* 1997; Vass, 2001). Putrefaction begins inevitably in the stomach and intestines. Due to the release of heme by-products, both organs will attain a dark purple-brownish colour (Powers, 2007). Destructive changes in organ macro-structure are observed with thinning of the myocardium, honeycombing of the liver (gas formation), disintegrating brain structures, softening of the spleen and spreading oedema of the lungs and surrounding spaces (Powers, 2007). In addition to these changes, accumulated gaseous and metabolic products generate physical and chemical alterations that are observed on a decomposing body (Clark *et al.,* 1997; Powers, 2007). These changes are often observed in areas of prominent lividity, because red blood cells are a food source for multiplying bacteria.

The most noticeable sign of putrefaction is an external greenish discolouration on the skin that covers the abdominal area (DiMaio & DiMaio, 1989; Gill-King, 1997; Vass, 2001; Pinheiro, 2007; Powers, 2007) (Figure 2.4). A main component of these gaseous by-products is hydrogen sulphide (H_2S). This chemical reacts with the haemoglobin in red blood cells and produces the compound sulfhemoglobin (green pigment) (Clark *et al.,* 1997). This by-product of initial decay lines the superficial blood vessels and, as putrefaction continues, it causes a distinct greenish hue to appear on the skin (Clark *et al.,* 1997). With the accumulation of H_2S in the tissues and the continuing oxidation of bile pigments, a change in colour from green to purple to black is observed (Gill-King, 1997).

During life the outer layer of skin is being constantly shed and replaced from cells in the underlying epidermis. Following death, this dermal layer becomes separated from the underlying epidermis. Due to hydrolytic enzyme production at junction points between these two layers, the result is the easy removal of the epidermal layer (Goff, 2009). With continuing colour changes, the structural integrity of the tissue is compromised and results in characteristic skin slippage observed in the phases of decomposition (Powers, 2007). Thin, opaque sheets of epidermis are sloughed off by the slightest touch (Figure 2.5). An interesting phenomenon often observed in this stage of decomposition is the presence of marbling or suggillation. Marbling results from intravascular haemolysis of the intestinal bacteria which colonise the venous system and produce deoxyhaemoglobin, which is bluish in colour (DiMaio & DiMaio, 1989, Clark *et al.,* 1997, Pinheiro, 2007). Marbling appears as darkened streaks beneath the skin and along some of the superficial vessels (Figure 2.6). It is often seen over the chest, shoulders and abdomen.

Skin blisters or postmortem bullae are present at this stage of decomposition. These blisters are most often filled with a red-purple, serous fluid (Clark *et al.,* 1997; Pinheiro, 2007). On occasion, maggots colonise the fragile blisters that easily rupture (Figure 2.7). In addition to these fluid-filled blisters, the lining of the gastrointestinal tract decomposes and produces a dark, coagulated fluid, commonly referred to as purging fluid (Clark *et al.,* 1997).

Gaseous accumulation (hydrogen sulphide, carbon dioxide and methane) causes distension of most tissues, especially those of the intestines (Vass, 2001; Powers, 2007) (Figure 2.8). The abdominal gases provoke oedema which appears in the head, neck and on occasion, the limbs (DiMaio & DiMaio, 1989; Pinheiro, 2007). Distention and bloating are associated with anaerobic fermentation by the release of rich, volatile fatty acid by-products (butyric and propionic acids). Muscle tissue yields to the formation of additional volatile fatty acids via bacterial action and further protein and fat decomposition creates phenolic compounds and glycerols (Vass, 2001).

With continuous gas and fluid build-up, pressure in the abdomen, scrotum and penis increases. This results in a separation of necrotic tissue layers and a purging of malodorous fluids (Figure 2.9) from any open orifice (Clark *et al.,* 1997; Vass, 2001; Pinheiro, 2007; Powers, 2007). The face and neck may also increase in size from a build-up of gas. This results in protrusion of the eyes and tongue, which can project through everted lips (Clark *et al.,* 1997; DiMaio & DiMaio, 1989; Pinheiro, 2007; Gunn, 2009). In some cases, natural orifices are insufficient in the release of large amounts of gas and fluid, and the distension in

the abdominal region reaches a point where the skin of the abdomen may rupture which results in additional postmortem injuries (Vass, 2001). Active decay commences once purging of gases and accumulated fluids has terminated. At this stage of putrefaction various factors such as seeping electrolytes, large numbers of anaerobic and aerobic bacteria, insect activity and carnivores contribute extensively to the decline of the body. Another change observed at this stage of decomposition is the gradual darkening of the abdomen from green to purple-brown to black.

Skeletonisation is the final stage of decomposition and involves the removal of all soft tissue from the bones (Figure 2.10). The time necessary for a body to skeletonise is variable (DiMaio & DiMaio, 1989). Once a body is skeletonised, decomposition does not cease, but a process known as diagenesis (degradation or decomposition of bone) continues to take place (Vass, 2001). During diagenesis the organic (collagen) and inorganic (calcium, hydroxyapatite) components of bone exposed to environmental influences undergo chemical alterations in their constituent proportions.

Three mechanisms exist that contribute to the degradation of bone. The first mechanism involves chemical degradation of the organic fraction of bone, namely collagen (Collins *et al.*, 2002). The destruction of collagen leads to structural disorganisation, which results in gelatinisation, rendering the bone into a mineral shell that is filled with small interconnecting pores (Collins *et al.,* 1995; Nielson-Marsh & Hedges, 1999; Miles *et al.,* 2000). On occasion, these pores may be filled with secondary minerals from the surrounding environment and represent one of the key mechanisms in the formation of fossils (Collins *et al.*, 2002). The rate at which collagen is lost is dependent on external factors such as environmental temperature, pH and time (Collins *et al.*, 2002).

The second mechanism involves chemical degradation of bone minerals, which have an unbalanced, thermodynamic equilibrium with rain water (White & Hannus, 1983). Therefore, the burial location of bone with regard to the underground water table (either above or around) has an ultimate effect on its survival (Hedges & Millard, 1995; Pike *et al.,* 2001; Hedges, 2002). The mineral transformation of bone because of rain water results in accelerated chemical and biological degradation of collagen (Collins *et al.*, 2002). The third mechanism is the most common form of diagenesis and occurs soon after death. It involves degradation of bone via microbial interference (Yoshino *et al.,* 1991; Bell *et al.,* 1996). The rate of chemical degradation is dependent on environmental temperature, pH and time,

whereas microbial activity performs at optimal capacity when the pH is close to neutral (Collins *et al.,* 2002).

Although the stages of decomposition progress in a predictable sequence, the time of onset and the rate of decomposition are considerably variable due to numerous internal and external influencing factors.

2.1.3. Variations observed in decomposition

2.1.3.1. Saponification

Saponification or adipocere formation occurs after the onset of putrefaction in warm, moist, environments and is seen as yellowish-white, greasy, wax-like deposits composed of oleic, palmitic and stearic acids (DiMaio & DiMaio, 1989; Gill-King, 1997; Vass, 2001; Fielder & Graw, 2003; Fründ & Schoenen, 2009; Schoenen & Schoenen, 2013). Adipocere develops via neutral fat hydrolysis and hydrogenation with the release of saturated fatty acids (Forbes *et al.,* 2005). This conversion allows the pH of the surrounding tissue to decrease, inhibiting bacterial growth, which results in soft tissue preservation. Ideal conditions for the development of adipocere include heat and water (exogenous or from the body itself) for development of the required microbes and the hydrolysis and hydrogenation of the fatty tissues respectively (Clark *et al.,* 1997; Fielder & Graw, 2003; Pinheiro, 2007; Fründ & Schoenen, 2009; Schoenen & Schoenen, 2013). For these reasons, adipocere is most commonly found on bodies that have been exposed to warm, damp environments or submerged in cold water with low percentage of oxygen (anaerobic bacteria) (Clark *et al.,* 1997; Fielder & Graw, 2003; Pinheiro, 2007; Fründ & Schoenen, 2009; Schoenen & Schoenen, 2013). Adipocere may take several weeks or months to form (Fielder & Graw, 2003; Fründ & Schoenen, 2009; Schoenen & Schoenen, 2013).

The consistency of adipocere varies with the type of material to which it is bound and gives some indication as to the rate of decomposition. Rapid decomposition is indicated by a hard and crumbly composition of bound with sodium (intestinal fluids), but a soft, paste-like consistency when it is bound with potassium (breakdown of cell membranes). The postmortem invasion of tissues by bacteria accelerates the formation of adipocere, especially putrefactive species such as *Clostridium.*

Although some points are debatable, the formation of adipocere and the sequence of biochemical processes involved are well-established (Fielder & Graw, 2003; Pinheiro, 2007;

Fründ & Schoenen, 2009; Schoenen & Schoenen, 2013). The process of adipocere formation begins immediately after death and usually first develops within the subcutaneous tissues such as the cheeks, breasts and buttocks (Camps *et al.,* 1976; Pinheiro, 2007). Since adipocere formation requires reservoirs of fat, this process is more commonly observed in female and infant than male corpses (Gill-King, 1997). In individuals with low body fat (emaciated), adipocere formation is fairly limited (Clark *et al.,* 1997). Internal structures which contain adipose tissue such as the mesentery, omentum or perirenal fat and organs may be influenced by lipidic metabolizing pathological conditions and may also undergo the process of saponification (Pinheiro, 2007).

Adipocere may become evident 3 – 12 months after death. The first signs of adipocere may appear as early as 3 weeks postmortem. If the conditions are ideal, adipocere may last for decades, sometimes even centuries (Pinheiro, 2007). This preservation is always of interest to forensic investigators, as evidence relating to a crime may be preserved (Clark *et al.,* 1997; Fielder & Graw, 2003; Fründ & Schoenen, 2009; Schoenen & Schoenen, 2013).

2.1.3.2. Mummification

Dehydration and desiccation of the tissue arrests active decay and facilitates mummification (Vass, 2001). The skin is converted into a leathery or parchment-like sheet (dry and brittle) that clings to the bones, particularly the cheeks, forehead, and sides of the back and hips. Mummification can occur either partially or in conjunction with other forms of putrefaction (Pinheiro, 2007; Parks, 2011; Marella *et al*., 2013). The process of mummification is often found with adipocere formation. These two processes are dependent on each other. The hydrolysis of fatty tissue requires the use of water, which contributes to the desiccation of body tissues (Pinheiro, 2007).

Mummification often develops in dry, ventilated areas. These areas may be icy, have very low humidity and low bacterial growth, such as arctic regions or deserts (Pinheiro, 2007; Parks, 2011; Marella *et al*., 2013). The mummification of bodies in temperate climates is unusual, unless the body was placed in a favourable environment such as air-conditioned buildings. Although the required environmental conditions for mummification to occur are well known, the exact time it takes for a body to mummify is not (Pinheiro, 2007; Parks, 2011; Marella *et al*., 2013). The problem with establishing a suitable timeline for mummification is that a long period can pass before the body is discovered (Pinheiro, 2007).

2.1.4. Factors that influence the rate of decomposition

Forensic scientists need to estimate accurately the PMI of a corpse and need adequate and accurate techniques to back-up their conclusions. PMI estimation is a popular topic of research and one of the main concerns involves factors that influence the rate of decomposition and what effect they would have on estimating PMI. Table 2.4 provides a summary as to which factors increase and decrease the rate of decomposition.

A body progresses through the stages of decomposition in a relatively sequential order but at different rates. According to most authors (Mann *et al.,* 1990; Gill-King, 1997; Campobasso *et al*., 2001; Adlam & Simmons, 2007; Kelly *et al*., 2009; Simmons *et al*., 2010; Zhou & Byard, 2011) ambient, environmental temperature has the greatest influence on the rate of decomposition. In temperate climates (ideal conditions) the degree of putrefaction after 24 hours during warm to hot weather may require approximately 10 times the amount of days in winter (cold, snow) to reach the same stage (Polson *et al.,* 1985; Mann *et al.,* 1990).

Rapid cooling of a body after sudden death (exposure to cold or freezing temperatures) will delay the onset of decay and in extreme cases cease it completely because of the reduced access by insects. Although flies and other insects infest a carcass in cold temperatures (5 – 13°C), fly eggs will die at temperatures below zero degrees Celsius. Should eggs manage to hatch and the maggots leave the carcass to become exposed to extreme cold temperatures, they will die (Mann *et al.,* 1990). As is most often the case in colder climates, maggots tend to conceal themselves within the carcass (organs, head, and chest), feed, develop and survive as they colonise in large masses and produce their own heat which in turn ensures their survival (Mann *et al.,* 1990). One of the stages in the metamorphosis of the fly is "maggot migration" during which maggots relocate themselves some distance from the carcass to burrow a few centimetres in the ground for pupation. If the cold environmental temperature continues, they remain in the ground until the warm weather returns (Mann *et al.,* 1990).

The ideal/optimal temperature for putrefaction ranges between 21 and 38°C. Temperatures below 10°C or exceeding 38°C will delay the progression of putrefaction (Polson *et al.*, 1985). The presence or absence of flies in the initial stages of decomposition, regardless of the temperature, has a large influence on the decomposition rate. Studies have revealed that when a body with an external wound is laid down to decompose, it will decay at a much faster rate than a body that has no trauma (Galloway *et al*., 1989; Mann *et al.,* 1990;

Rodriguez, 1997; Campobasso *et al*., 2001) although a recent study has found no difference in the rate of decomposition because Diptera prefer natural orifices to trauma sites (Cross & Simmons, 2010). However, flies are attracted to the scent of blood and therefore should an external wound with be present, fly activity will commence sooner and, therefore, so will the destructive activity of maggots.

Although temperature has a significant role in the rate of decomposition because it influences the rapid or delayed exposure of insects, the ambient temperature at which a body decomposes may not relate to the outside, environmental temperature but also various other external or internal factors such as movement of air, clothing, water involvement or depth of burial (Gill-King, 1997). Burial depth has a significant influence on the rate of decomposition. A buried body can decompose up to four times slower than a body that either decomposes under normal circumstance above the ground or even submerged in water (Mann *et al.,* 1990; Rodriguez, 1997; Dent *et al.,* 2004; Pinheiro, 2007). Bodies buried between 0.3 and 0.6 m below the ground decay at a faster rate than bodies buried at depths between 0.9 and 1.2 m (Mann *et al.,* 1990). This decrease in decomposition rate when a body is buried deeper results from the restricted access of carrion insects such as blowflies and beetles as well as oxygen and carnivores to the cadaver (Rodriguez & Bass, 1985). Bodies buried at depths of about 0.3 m provide albeit limited access to carrion insects (particularly blow flies), because they lay eggs in the soil directly above the carcass and migration of the larvae developing from these eggs to the corpse takes place (Rodriguez & Bass, 1985). Some flies known as coffin flies can locate buried bodies as far down as a meter or more (Gunn, 2009). Overall, the buried environment provides an insulation barrier against solar radiation, insect access and carnivore activity as well as the absence of air, and lower temperatures that all result in a delayed onset of decomposition (Rodriguez & Bass, 1985; Mann *et al.,* 1990; Rodriguez, 1997; Pinheiro, 2007).

Carnivores and scavengers tend to have a considerable impact on the rate of decomposition since carnivores eat soft tissues, especially those of the face and hands and play a huge role in body disarticulation (Haglund *et al*., 1988; Galloway *et al*., 1989; Mann *et al*., 1990; Galloway, 1997; Rodriguez, 1997; O'Brien *et al*., 2007; Steadman & Worne, 2007; Moraitis & Spiliopoulou, 2010). Carnivores, especially Canis families, are notorious for disarticulating skeletons and scattering the elements around the corpse. The majority of the carnivore activity takes place after the early stages of decomposition (Galloway, 1997). Rodents tend to cause extensive damage to the soft tissues of the face, hands, feet and

abdomen (Mann *et al.,* 1990; Rossi *et al*., 1994) during the early stages of decomposition as well as damage to mummified and skeletonised remains (Haglund & Sorg, 1997).

Decomposition studies related to aridity and humidity are limited (Galloway *et al.,* 1989; Mann *et al.,* 1990; Galloway, 1997; Rhine & Dawson, 1997; Aturaliya & Lukasewycz, 1999). Humidity and aridity affect the amount of water loss and water retention of a body (Mann *et al.,* 1990, Aturaliya & Lukasewycz, 1999). This results in either an increase or decrease in the rate of decomposition. Early studies (Galloway *et al.,* 1989, Mann *et al.,* 1990) established that insect activity increases in high humidity environments due to moisture retention in the soft tissues maintaining their accessibility to fauna. Research in dry environments has revealed that rainfall has no effect on the activity of maggots while they are on/in the carcass as they seek refuge within the body cavities where they continue to feed and develop (Reed, 1958; Mann *et al*., 1990). However, rainfall has a direct influence on the activity of flies around the carcass that results in the reduction of eggs being laid or even the complete cessation thereof, which in turn influences the number of maggots present (Lopes De Carvalho & Linhares, 2001). Arid environments (extreme dry cold and extreme dry heat) demonstrate rapid increase in decomposition rates in the early stages followed by desiccation and mummification due to extreme moisture loss with little signs of insect activity, resulting in the preservation of the carcass and prolonging of the decay and dry stages of decomposition (Galloway, 1997). Mummification in arid regions usually results in hardened, leathery skin encasing softer underlying tissues which may still exude a foul odour (Galloway, 1997).

A study conducted by Mann *et al.* (1990) revealed that large/obese individuals do not decompose at a different rate to that of an average sized individual. It was noted that obese individuals lost their excess fat quite rapidly after death via liquidation (melting away). A similar study by Hewadikaram and Goff (1991), however, established that although there may not be a difference in the sequence/pattern of decomposition, there is a distinct difference in the rate of decomposition between bodies of varying size. This difference in rate was observed most significantly between 5 to 16 days of decomposition. Their study found that the insects responsible for the greatest reduction of a corpse's biomass (Diptera larvae) were more attracted to the larger of the two carcasses, with a resultant increase in maggot activity.

Water has both physical and chemical effects on the process of decomposition (Gill-King, 1997). The high specific heat of water acts as a temperature stabiliser and a buffer

which regulates the effects of tissue and environmental pH (Gill-King, 1997). Water is a source of hydrogen, which is essential for the biochemical reactions within cells (Gill-King, 1997). Decomposition may be either accelerated or decelerated in a body that has been partially/completely submerged in water, although most believe that a body submerged in water will decompose at a slower rate than a body exposed to air due to the protection offered against land insects and predators (Pinheiro, 2007). However, decomposition rate in water is dependent on the composition of the water (fresh or salty), the pH and movability (Gill-King, 1997). Salt acts as a preservative and therefore could delay the process of decomposition (Micozzi, 1991).

2.2. Thermal destruction of human remains

2.2.1. Early cremation studies

Cremation is the process of exposing fleshed or defleshed remains to a controlled fire until soft tissue and skeletal components are reduced to small fragments and ash (Shipman *et al.,* 1984). Cremated bone (cremains) usually has been heated to temperatures over 600°C, and the resultant effect is recrystallization of the mineral content producing larger and better-structured crystals (Lanting *et al.,* 2001). Many cultures utilise cremation as a primary means to dispose of their dead. In some countries, cremation has become popular due to land restrictions and to the high cost of burial (de Gruchy & Rogers, 2002).

Research into cremains (archaeological or modern) has intrigued archaeologists and anthropologists for decades (Krogman, 1939; Haury, 1945; Baby, 1954; Wells, 1960; Binford, 1963). Although many studies on cremains originate from archaeological sources, the study and interpretation of modern cremains in a forensic context has recently increased. With increased popularity of modern crematory practices, forensic anthropologists are exposed to cremains at some point in their careers (Murad, 1998). Criminal investigators of commercial cremation practices also implore the help of forensic anthropologists in cases of disputed identity, commingling of remains and negligent cremation practices (Schultz *et al.,* 2008).

Numerous observational and experimental studies aimed to define unique features of bone that was burnt while dry, fleshed and wet/green were conducted throughout the 20th century and 21st century (Krogman, 1943; Webb and Snow, 1945; Baby, 1954; Trotter &

Peterson, 1955; Wells, 1960; Stewart, 1979; Binford, 1963, 1972; Thurman & Willmore, 1980; Bradtmiller & Buikstra, 1984; Shipman *et al*., 1984; Gilchrist & Mytum, 1986; Buikstra & Swegle, 1989; Mayne, 1990; Grupe & Hummel, 1991; Nelson, 1992; Stiner *et al*., 1995; Symes *et al*., 2001; Whyte, 2001; de Gruchy & Rogers, 2002; Dunlop, 2004; Bontrager & Nawrocki, 2008; Symes *et al*., 2008; Gonçalves *et al*., 2011; Keough *et al*., 2012).

In the early forties, Webb and Snow (1945) sought the opinion of Wilton M. Krogman on the burial and crematory practices of two prehistoric Native American groups, the Hopewell and Adena people. Due to the different burn patterns observed on the skeletal remains, Krogman reasoned that these two groups of people had practiced different cremation methods. According to Krogman (1943), the Adena people had cremated fleshed remains, whereas the Hopewell people had cremated defleshed remains, or dry bones (Webb & Snow, 1945; Stewart, 1979). Unlike dry bone, burnt wet/green bone or bone with a thin tissue layer demonstrates clear-cut, patina-like heat-induced fractures along with charring, calcination and splintering (Fairgrieve, 2008). Krogman (1943) used these characteristics to distinguish whether the bones of the Hopewell and Adena societies had been wet or dry prior to the burn event.

In 1954, Baby re-evaluated not only the Adena and Hopewell cremains but also performed burn experiments using whole, unembalmed, fleshed bodies, dissected cadavers (embalmed) and dry bone. Baby (1954), in contrast to Krogman (1943), suggested that checking or cracking on the surface of burnt bone may not be related to the nature of the bone prior to exposure but was more so a trait that is dependent on the duration of exposure. When exposing bones to a crematory fire, Baby (1954) found that dry bones remained intact with superficial checking, splintering and fine, deep longitudinal striae, whereas fleshed and green bones presented with deep cracks, warping and both transverse and diagonal fractures. Both Baby (1954) and Krogman (1943) concluded that burnt fleshed bone and green/wet bone were difficult to distinguish.

Following the disparate results of Krogman (1943) and Baby (1954), Binford (1972 [1963]) repeated Baby's (1954) experiments in order to confirm or refute them and to establish a controlled comparative sample to conduct his own experiments on post-burn cooling methods and bone calcination. Binford's sample included dry bone (archaeological), recently macerated bone (Anatomy department; University of Michigan) and green and partially fleshed bones (head, arm, and feet) from a partially dissected monkey.

The dry and recently macerated bone presented with the same thermal alternations. Long bones exhibited superficial cracking, fine longitudinal striae, deep longitudinal fracturing or splintering, but no signs of warping. Spongy bone had modest checking (patina fractures) with small fractures along the longitudinal axis of the bone. The observations were in agreement with those obtained from Baby (1954). Changes to the cooling off period of hot or recently heat-exposed bone did affect the morphology of thermal alteration. Cooling heated bone with water caused fragmentation with splitting along the heat-induced fractures and longitudinal striae, but no increase in the amount of superficial checking was noted. With natural cooling, the bone remained intact and no warping was observed.

Binford (1972 [1963]) found the experiments with fleshed and green bone (partially dissected monkey) more difficult to replicate than with dry and recently macerated bone. The skull of the monkey showed differential calcination patterns. Areas that displayed complete calcination included the fronto-orbital, maxillary and masto-parietal regions. Incomplete calcination was observed on the basilar and nuchal regions of the skull and on the mandible at the attachment sites for the internal pterygoid muscles, which were charred and still adhered to the bone. Warping was noted in all burn-affected areas, especially along the cracks that had developed during burning. Long bones had a similar morphology with deep longitudinal and transverse fractures and warping. Transverse fractures were curved and serrated as opposed to the straight cracking seen on the dry and recently macerated bone. Angular and curved checking was found on the green and fleshed bone that opposed the observations on the dry bone. Unlike the superficial checking on dry bone, the checking on green bone extended completely through the bone. Rapid cooling broke bone along the heat-induced fracture lines in all cases.

Based on the above literature, Krogman (1939), Baby (1954) and Binford (1972 [1963]) agreed that dry bone could be distinguished from fleshed or green/wet bone after burning. Baby (1954) and Binford (1972 [1963]) agreed that dry bone displayed longitudinal fractures, no warping and superficial, angular cracking while green/wet or fleshed bone displayed deep transverse fractures (may be curved) and warping. From Binford's (1972 [1963]) study it was also concluded that the degree of calcination observed on bones is directly proportional to the exposure time, heat intensity, protective muscle thickness and position of bone in relation to fire.

Based on the early cremation studies of Krogman (1939, 1943), Webb and Snow (1945), Baby (1954) and Binford (1972 [1963]), Thurman and Willmore (1980-81) devised

an experiment to analyse differences between fleshed and defleshed (green) remains after exposure to fire. While large areas of agreement among these studies were found, several disparities in results and terminology were noted. Binford (1972 [1963]) used words like "fleshed" and "fresh" bone, but it is unclear whether the terms relate to the same bone condition. The same can be said for the use of the term, "green" bone. There is confusion as to whether the green bone analysed by Baby (1954) and Krogman (1943) is the same green bone used by Binford (1972 [1963]) in his replicative study (Thurman & Willmore, 1980-81). Unlike previous studies, Thurman and Willmore (1980-81) did not find extensive warping in green bone, but they did observe surface checking. Wet/green bone was more likely to have serrated fractures near epiphyseal ends, parallel-sided fractures along checking lines and reduced warping than fleshed bone. Fleshed bone displayed signs of serrated, deep transverse fractures and diagonal cracking accompanied by warping.

Following Thurman & Willmore's (1980-81) replicative study, Shipman *et al.* (1984) and Buikstra & Swegle (1989) conducted experiments to evaluate differences in fleshed and dry burnt bone. Buikstra and Swegle (1989) did not agree with Baby (1943) or Binford (1972 [1963]) with regard to the sole presence of warping and deep transverse fractures on fleshed bone. Buikstra & Swegle (1989) experimented with bovine, canine and human bone. The authors reported that warping occurred in bone that was burnt wet/green and dry. Deep transverse fractures, previously associated with fleshed bone, were also observed on wet and dry bone.

In summary, dry bone (no flesh, no grease) predominantly displays longitudinal fractures, absence of warping and superficial angular cracking. Green/wet (recently defleshed, greasy) bone has deep, and frequently curved, transverse fractures, warping and occasional endosteum and longitudinal splitting. Bones burned while fleshed (adhering flesh/soft tissue) display serrated, transverse fractures that transect the bone completely together with diagonal cracking and warping. The extent of thermal destruction to bone is related to the duration of exposure; the intensity of the heat; the thickness of the overlying muscle tissue; and the position of the bone in relation to the point of oxidation of fire. Unless these factors are controlled, the replication of burn characteristics on fleshed, wet and dry bone is difficult.

2.2.2. Trauma interpretation

The accurate interpretation of perimortem, postmortem and antemortem trauma is difficult in thermally altered remains as evidence of injuries (gunshot, blunt force and sharp force) are often concealed or obscured from the heat and fire (Herrmann & Bennett, 1999; Bohnert *et al.,* 2002; de Gruchy & Rogers, 2002; Pope & Smith, 2004; Arora *et al.*, 2010). In addition to concealing perimortem trauma, burned bones often present with extensive fracturing. Differentiating between heat-induced fractures and those of forensic significance requires an understanding of fracture biomechanics. Previous studies (Herrmann & Bennett, 1999; de Gruchy & Rogers, 2002; Pope & Smith, 2004; Arora *et al.,* 2010) have analysed gunshot, blunt and sharp force traumas to determine whether the classic characteristics of each could be identified after burning.

2.2.2.1. Sharp force trauma

Defects associated with sharp force trauma can remain recognisable after exposure to fire. Based on the comprehensive reconstruction of the remains, incisions from sharp objects can be identified (Symes *et al.,* 1999). Stryker and rip saws display clear, identifiable kerf walls as do cut and chop marks from knives and cleavers (Rockhold, 1996; Herrmann & Bennett, 1999; de Gruchy & Rogers, 2002). However, chop marks from cleavers are difficult to distinguish from straight, transverse heat-induced fractures (de Gruchy & Rogers, 2002).

Preservation of incised features is dependent on factors such as saw type, position of bone in fire, duration of fire, presence of accelerants, atmospheric conditions and fluctuating temperatures (de Grunchy & Rogers, 2002; Marciniak, 2009). Although most incisions remain distinguishable after burning, interpretation of these fractures should be performed with caution. Shrinkage and warping of burnt bone may obscure cut mark morphology as well as distort the impact site and fracture patterns (Herrmann & Bennett, 1999; Marciniak, 2009).

2.2.2.2. Ballistic trauma

Ballistic trauma may produce extensive fragmentation of bone prior to burning. Post-burning of these fragments makes it more difficult to reconstruct than sharp or blunt force

traumas, since often the fragments are lost or not retrieved, making reconstruction difficult. Therefore, depending on the degree of fragmentation, minimal interpretation of fracture morphology can be performed (Herrmann & Bennett, 1999). Heat-induced fractures on the skull often resemble the classic spider-web pattern (elliptic & circular) observed in gunshot wounds. However, the typical radiating fractures associated with gunshot wounds are absent (Herrmann, 1976). Radiating fractures advance from the impact site in both gunshot and blunt force trauma. Bohnert *et al.* (2002) reported on a case regarding a captive bolt injury to a burnt skull that was identified because of the associated radiating fractures emanating from the impact site. A captive bolt pistol is used on animals prior to the slaughtering process in order diminish pain and suffering during exsanguination. The report corresponded with original observations made by Herrmann (1976). The presence of these radial fractures is what sets this type of injury aside from heat-induced fractures.

Most ballistic trauma is recognisable and interpretable in burned bone (Pope & Smith, 2004). Entrance defects retain a distinctive circular shape and internal bevelling, even in calcined remains. Large linear fractures related to both trauma and heat-induced changes are observed (Pope & Smith, 2004). Difficulties in interpreting burnt ballistic trauma include misinterpretation of thermal delamination of the outer table as the characteristic bevelling at entrance and exit wounds. Fracture margins of gunshot defects are distorted and may change in shape, size and orientation (Pope & Smith, 2004).

2.2.2.3. Blunt force trauma

The recognition and interpretation of blunt force trauma is possible, provided an accurate reconstruction of the remains is performed (Herrmann & Bennett, 1999; Pope & Smith, 2004). Characteristic features of blunt force trauma such as radiating fractures and plastic deformation may be obscured and confused with heat-induced fractures. Although these features can become obscured and mingled, Pope and Smith (2004) noted that careful and precise examination of the surfaces related to the impact site may reveal subtle markings of blunt force trauma (depressions, inward crushing and margins) that are distinct from heat-induced trauma. Fractures due to thermal alteration will not display tension and compression responses associated with blunt force trauma.

During reconstruction of fragmented remains, Herrmann and Bennett (1999) noted that large fragments are associated with the blunt force trauma, whereas small fragments are

associated with the heat-induced fractures. The authors made an interesting assessment of the relationship between heat-induced fractures and trauma; transverse fractures (or perpendicular) were often associated with the heat-induced alterations. Alternatively, longitudinal fractures were associated with both traumatic and heat-induced fractures. In order to separate fracture types, surface morphology of the fracture lines was analysed. Trauma induced longitudinal fractures display a smooth, sparsely contaminated surface when compared to the more sharpened, clean and richly coloured margins of heat-induced fractures (Herrmann & Bennett, 1999; Pope & Smith, 2004).

In many cases, skeletal remains are too incomplete for reconstruction and/or identification of peri-mortem or postmortem trauma. Characteristics from previously mentioned studies are only applied when all cremated or thermally altered elements are recovered. With prolonged exposure to heat or fire, features of ballistic, blunt and sharp force trauma deform and cannot be recognised.

2.2.3. Thermal destruction of human remains

Fire is an exothermic oxidative reaction between a fuel (in this case, a body and skeletal elements) and an oxidizer (oxygen). Any combustible material may comprise the fuel source, and air provides the oxidizing agent. Oxygen must be present in order to sustain the combustion process (Fairgrieve, 2008). Fire can manifest as either a smouldering (solid-gas reaction) fire or a flame (gas-gas reaction) fed with adjacent chemicals or flammable materials (Eckert, 1981; DeHaan, 2008). The reaction becomes a self-sufficient entity that emits both heat and light (Icove & DeHaan, 2003; DeHaan, 2008). Sustenance of a fire requires four elements, namely fuel, oxygen, heat and the uninhibited exothermic chemical oxidation (Holck, 2005; DeHaan, 2008; Fairgrieve, 2008). Heat is an important and obvious factor in the burning process (DeHaan, 2008; Fairgrieve, 2008). If the heat source is not sufficient to ignite the fuel, combustion cannot occur (Fairgrieve, 2008). Lastly, chemical oxidation is necessary to sustain combustion (Icove & DeHaan, 2003; Fairgrieve, 2008).

The quantity of all four elements determines the degree of destruction and thermal alteration to a body. Fuel sources can range from a solid to a liquid or a gas and can also change from one biochemical component to another (Pope, 2007). A well-fuelled and ventilated fire can reduce a fleshed body to calcined ash within hours. In the case of a uncontrolled fire (e.g., veldt fire), limited fuelling agents and drafty conditions can

differentially burn a body, with heavy alterations to some areas and no alternations to other areas (Walker *et al.*, 2005).

2.2.3.1. The body's response to fire

Body tissues exposed to fire often display blistering/scalding, scorching and charring (DeHaan *et al.,* 1999). The resultant surface alterations are either from direct or indirect thermal exposure such as electrocution, friction or chemical exposure (Cooper, 2006). In order to understand thermal destruction of a human body, the properties of fire and the insulative properties of skin, muscle and fat need to be examined.

Skin, fat and muscle

In a fire, a body's skin, muscle and fat comprises fuel for combustion. With limited thermal involvement, body tissues exhibit minimal charring and scorching. When a body represents a large percentage of the fuel in a fire, significant tissue destruction occurs (DeHaan *et al.*, 1999).

While the following terminology is more applicable to the recognition and treatment of burn injuries in living individuals, it does provide a means to describe soft tissue damage on the deceased (Pope, 2007). Skin is the first area susceptible to thermal alteration and may change colour, shrink, blister, split and rupture. Severity of damage is dependent on differential anatomical distributions of soft tissue structures (Cooper, 2006). For example, thick skin on the palmar surface of the hand and the plantar surface of the feet is more resistant to heat than the thin skin on the flexor and extensor surfaces of the arms and forearms (Cooper, 2006). Initial macroscopic alterations include slight skin blistering (pseudo-blisters) and singeing of head and facial hair (Glassman & Crow, 1996). Pseudo-blisters form when steam fills the space between the epidermis and dermis. They differ from antemortem blisters in that they do not have circumferential reddening or underlying redness (Adelson, 1954). Heat blisters are weakened areas in the skin that eventually result in the skin splitting or rupturing (Pope, 2007). Heat ruptures occur when the skin undergoes dehydration and heat-induced contraction (Cooper, 2006; Pope, 2007; Fairgrieve, 2008). Skin rupturing is most common in the extensor region of muscles and areas of the head (Cooper, 2006).

First and second-degree burns are identified during initial exposure and involve only partial thickness burning (epidermal penetration) (Cooper, 2006). Fluid-filled blisters

associated with second-degree burns occur, and partial detachment of the epidermis may be observed (Whyte, 2001). The hands and feet of second-degree burn victims may present with a whitish discolouration and a swollen epidermis which resembles a "washerwoman's skin" (Whyte, 2001; Bohnert & Pollack, 2003).

Total destruction of a body via fire requires a pronounced external ignition to start it and a rigid, porous wick to sustain it (Cook & Ide, 1985; DeHaan, 1997; DeHaan *et al.*, 1999; DeHaan & Nurbakhsh, 2001; Bohnert *et al.*, 2002; Christensen, 2002; Dehaan, 2008). With fire, fat is liquefied and is rendered combustible. While fat may serve as a fire's wick, its sustainability is dependent on preheating from an external source (DeHaan *et al.*, 1999). Fat alone may be able to sustain a fire, particularly in fat rich areas such as the torso, abdomen and thighs.

After the fat has burned the muscle tissue is exposed. Muscle tissue is denser than skin and because of its moisture content and thickness serves as a great insulator to underlying bone. Muscle tissues are a layered material that progressively burns along the shafts of long bones and in the opposite direction to the origin of the heat. Thin and thick muscle groups react differently to heat and fire and allow differential thermal injury to bone. Flat muscles, abdominal muscles and muscles covering the skull burn from externally to internally and gradually expose the bone. Thicker muscles groups, limbs and neck, burn through several layers of tissue, and as these layers slowly shrink, they recede along the bone's shaft (Pope, 2007).

Skin, fat and muscle insulate the skeleton. Soft tissue is unevenly distributed throughout the body with some areas presenting with thicker muscle mass than other areas. As expected, bones covered with dense, thicker muscle fibres, such as the thigh, are more protected than thin tendons and ligaments covering joints, hands and feet. Areas with little skin and muscle are quickly destroyed, and the underlying bone is exposed and altered. Differential tissue thickness refers to the predictable arrangement of soft and hard tissue in the body. The principle of differential tissue thickness is used to determine the sequence of skeletal element exposed under thermal conditions and to predict burn patterns (Symes *et al.,* 1999).

Four variables associated with fire exposure are summarised in Table 2.5. While the source of fire exposure varies, some characteristics, such basic human anatomy, physiology and bone composition, remain constant and are due to both the protective nature of the soft tissue surrounding bone and to the properties of a fire which can produce predictable burn

patterns (Symes *et al*., 1999, 2008). Burnt bone is often analysed without considering these predictable patterns or the protective insulation of muscle and fat (Smith *et al*., 2001).

2.2.3.2. Thermal destruction of a body under controlled conditions and the manifestation of a skeletal burn pattern

The reaction and process of thermal destruction to a body, under controlled conditions, has been studied and documented in detail (Bohnert *et al.*, 1998; Pope, 2007; Symes *et al.,* 2008). Destruction of soft tissues is progressive and starts at the skin, advances through fat and muscle, and eventually bone. The rate of destruction depends on the construction of the body part and its position in the fire. The course of thermal destruction to a human body follows a set pattern; the following paragraphs provide a detailed description of this pattern and how a human body undergoes thermal alteration with approximately one hour of fire exposure:

0 – 10 minutes

Gross morphological identification of a body is possible and injuries are often associated with smoke inhalation (Glassman & Crow, 1996). At this level, thermal injury involves little soft tissue loss, exhibits varying degrees of charring to the hands, feet, genitalia, and ears and minimal rupturing of the abdominal wall (Glassman & Crow, 1996; Gerling *et al.,* 2000).

Initial heating of the cranium immediately distorts facial identification, as it causes facial bloating, retraction of the lips, protrusion of the tongue and a distinct shortening of the nose (Bohnert *et al*., 1998; DiMaio & DiMaio, 2001; Pope & Smith, 2004; Pope, 2007) (Figure 2.13). The skin and supporting tissues of the head and neck then shrink and undergo distortion with effects such as skin splitting, elastic retraction and blistering. Heat may also cause shrinkage of the eyelids with exposure of the eyeballs (Pope, 2007).

10 – 20 minutes

After ten minutes of exposure, a body assumes the pugilistic posture or pugilistic attitude (Adelson, 1955; Bass, 1984; Spitz, 1993; Bohnert *et al*., 1998; DiMaio & DiMaio, 2001; Icove & DeHaan, 2003). Originally, this position of the upper limbs was considered a

defensive pose from the victim before being burned. However, this position is purely attributed to the effect of heat on the tissue of the human body.

The pugilistic pose is an alteration of three factors, namely the anatomical position of the body, the arrangement of the muscles and the increasing strain on the muscle and bone. Knowledge as to the body's change in position contributes to understanding the patterns of thermal destruction (Smith *et al.,* 2001). With an increase in duration of heat exposure, the body experiences intense muscular contraction of the stronger, bulky flexor muscles which, in turn, forces the body into a pugilistic pose (Adelson, 1955; Cooper, 2006). The contraction is quite strong such that the muscles may tear when the limbs are forcibly extended (Adelson, 1955). With continual exposure to fire, the pugilistic position allows for differential tissue shielding of exposed areas (Symes *et al.,* 2008). Areas protected with large amounts of skin, fat and muscle burn last and areas with minimal layers of protection burn first. Since the pugilistic pose is the body's natural reaction to heat, an unconfined body's original position prior to exposure does not influence the pose (Smith *et al.,* 2001).

Bodies recovered from intense fires often present with extreme flexion of the arms, wrists, ankles and legs (Adelson, 1955; Arora *et al*., 2010) (Figure 2.11). The wrists undergo pronation, the elbows hyperflex, the humerus medially rotates, the shoulder adducts and the phalanges flex (Smith *et al.,* 2001). This movement exposes the dorsal surface of the hand, wrist and elbow to heat and fire, such that these areas on the upper limb are the first to experience thermal alteration (Symes *et al.,* 1999). Likewise, the lower limbs flex with inversion of the feet and plantar-flexion at the ankle (Symes *et al.,* 2008) (Figure 2.12). Areas on the anterior surfaces of both the femur and tibia are exposed first with the posterior surfaces protected due to flexion and subsequent accumulation of tissue over the joint surfaces.

With protracted exposure, the posterior neck muscles contract and the head is forced backwards. The occipital area is protected from the fire but the face is directly exposed to the flames. Burn variability of this region is attributed to the flexible position of the head as well as its unique anatomy and distribution of soft tissues (Symes *et al.*, 1999; Pope, 2007). Due to the thin layer of muscles on the scalp and the thick nuchal muscles at the cranial base, thermal destruction first appears on the calvarium and advances to the cranial base (Symes *et al.,* 1999). The dynamic retraction of the scalp from skin splitting, elastic retraction and blistering subjects the forehead and vertex to rapid destruction, such that broad areas of the cranial bone are exposed to fire (Bohnert *et al.,* 1998).

Prominent facial bones are exposed after 10 minutes (Bohnert *et al*., 1998; Symes *et al.*, 1999). As mentioned above, the frontal bone burns first and is followed with the face, namely the anterior parietal bones, supra-orbital ridges, infraorbital margins, the zygomatic arches and the nasal and pre-canine maxilla (Figure 2.14). The inferior, lateral margin of mandibular body is also exposed. The mentalis muscle protects the mandible anteriorly, and the masseter and buccinator muscle protects it posteriorly. Between these two muscle attachments, burning travels posteriorly towards the gonial angle and up along the ascending ramus. The second exposed site is the lateral aspect of the mandibular condyle. The last areas to burn are the coronoid process and the mandibular notch (Symes *et al.,* 1999). Heat-induced mandibular fractures may occur, but these fractures follow the contours of the mandible and the associated receding muscles (Bohnert *et al*., 1998; Pope, 2007).

A skull does not explode when burned. Previous research implied that the brain boiled, released steam and with increased intracranial pressure exploded into various pieces (Bass, 1984; Rhine, 1998; Sachs, 2002; Bass & Jefferson, 2003; Spitz, 1993, 2006). However, this is not the case. Within twenty minutes, the calvarium is completely exposed. The coronal and sagittal sutures separate, and fissures are evident on the external table. Heat hematomas may form at this stage and present as dark, thickened and coagulated masses of blood between the dura mater and the skull. When heat is applied to the cranium the blood boils out from the venous sinuses and collects in the space between the dura mater and the cranium (Cooper, 2006). The blood formed in a heat hematoma is spongy, brown in colour and bilateral. In contrast, a true extra-dural hematoma is a localised, thick and unilateral pooling of dark blood and is not a result of heat exposure (Cooper, 2006).

Fracture lines, specifically on the frontal bone, manifest and evolve into wide gaps between 15 and 20/25 minutes of direct fire exposure (Bohnert *et al.,* 1998, Symes *et al.,* 1999). Protected areas include the occipital bone and cranial base; lower portion of the temporal bone; the sphenoid, nasal spine, post-canine maxilla and palate; and the posterior portion of the parietal bones (Symes *et al.*, 1999) (Table 2.6). Sparse tissue may remain on the cheeks and face throughout this stage (Bohnert *et al*., 1998). However, exposed areas on mandible become brittle, fragment or even delaminate. With delamination the alveolar dental sockets are exposed. The fact that the roots of the teeth lie deep within the sockets provides the internal portions with protection against the flames (Pope, 2007).

The torso is heavy and bulky and tends to avoid damage in the early stages of thermal exposure (Pope, 2007). When compared to skin, muscle and fat, moisture-rich organs take

longer to dehydrate and burn. By 20 minutes, the anterior thoracic wall is charred, associated muscles are shrunk and the anterior surfaces of the sternum, ribs, clavicle and scapula are exposed (Bohnert *et al*., 1998; Pope, 2007) (Figure 2.15).

Skin and superficial soft tissues of the upper and lower limbs are destroyed around 20 minutes. Heat damage to bones of the lower limbs is delayed due to the thicker, heavier tissue and muscle protection (Pope, 2007). The formation of the pugilistic posture in the upper limbs starts with flexion of the fingers and wrist and progresses up the arm to the shoulder joint (Pope, 2007). Initial heat quickly removes soft tissues covering the dorsal hand and wrists and exposes the underlying bone (Figure 2.16). Due to the flexed position of the hand, the posterior metacarpals are immediately burned, and a canoe-shaped pattern is formed on the metacarpals (Symes *et al.,* 1999) (Figure 2.17). With flexion of the wrist, the distal ulna and radius undergo thermal alteration within 20 minutes of exposure (Symes *et al.,* 2008). Within 20 minutes, skeletal elements of the hand are calcined and are connected to the wrist via charred soft tissue (Bohnert *et al*., 1998).

With continual heat exposure, deeper layers of soft tissue and muscle of the forearm and arm burn and contract, which causes flexion at the elbow (Pope, 2007). When the elbow flexes, the anterior humerus, ulna and radius are covered with more tissue and are spared destruction. This is referred to as cubital sparing. The olecranon fossa is somewhat protected by the presence of the olecranon process which delays thermal damage in this area. However, the medial and lateral epicondyles of the humerus, the posterior olecranon process, and the radial head are exposed to the flame and burn in conjunction with the wrist and hand (Bohnert *et al*., 1998; Symes *et al.,* 1999; Pope, 2007) (Figure 2.18). Charring and shrinkage of muscle is observed which leaves the distal aspects of the ulna and radius partially exposed (Bohnert *et al*., 1998). Heat-induced fractures dislocate the forearm (ulna and radius) from the wrist, after which the lateral and medial borders of the forearm bones begin to burn. Soft tissue protects the interosseous borders of the ulna and radius, the radial tuberosity, and the area below the coronoid process; these areas are the last to burn (Pope, 2007) (Figure 2.18).

On the arm, the fire progresses both proximal and distal towards the center of the shaft. In later stages of heat progression, the bulky muscles of the brachium and shoulder are exposed and result in flexion of the shoulder joint. With flexion, the anterior humeral head is protected while the posterior humeral head is exposed and burns first (Symes *et al.,* 1999). The deltoid tuberosity is the first area to be burned on the humeral shaft (Figure 2.18).

20 – 30 minutes

By thirty minutes, gaps in the calvarium widen, and the outer table disintegrates (Bohnert *et al*., 1998). With this continued exposure the facial bones become calcined, and only small amounts of burnt tissue remain.

Destruction of the upper limbs progress with continuing shrinkage and charring of the muscle tissue that is adhered to underlying bones. The distal radius and ulna are completely destroyed, and only the proximal ends of both bones are articulated at the elbow joint (Bohnert *et al.,* 1998).

Early signs of heat-related change to the lower limbs occur over areas with sparse tissue protection (Pope, 2007). Thermal damage of the lower limbs progresses from the dorsal foot and ankle to the shin and knee and eventually to the thigh and hip (Figures 2.16 & 2.19). Similarly with the fingers, the toes curl into the ball of the foot, and the sparsely covered tarsals, metatarsals and phalanges are then destroyed (Pope, 2007). In contrast, accumulation of soft tissue on the plantar side of the foot spares this region from the flames. The proximal tibia first exhibits thermal alteration on the tibial tuberosity and the medial and lateral condyles (Figure 2.19). The distal tibia starts to burn on the medial malleolus and travels upwards along the medial and anterior borders of the shaft (Figure 2.19). The broad, unprotected, medial border is quickly exposed and damaged, whereas the lateral and posterior borders have more muscular protection and burn last. The unique flattened shape of both medial and anterior borders of the tibia causes a canoe-like pattern to emerge. Because of the canoe pattern the posterior tibia experiences minimal burning on the medial surface (Symes *et al.,* 1999).

By 30 minutes most of the tibial surface and the distal thigh are free from tissue and are calcined (Bohnert *et al*., 1998). The fibula is less protected than the tibia. After the soft tissue has receded, the lateral malleolus and the lateral head of the fibula burn, respectively (Pope, 2007) (Figure 2.19). Fire eventually penetrates into the deep muscles of the upper leg. This results in flexion of the knee and is similar to the pattern observed in the elbow. The anterior medial and lateral condyles of the distal femur are exposed first. The knee joint, various muscle attachments, popliteal region and the intracapsular knee ligaments offer protection to the posterior condyles of the tibia and femur (Figure 2.19).

The shaft of the femur has a unique burn pattern which is attributed to both the muscle compartments of the thigh and their positioning in the pugilistic posture. Most burning occurs on the distal femur and progressively moves up the shaft. Initially, the anterior surface of the

shaft is more exposed than the posterior surface (Figure 2.19). Around the midshaft directionality changes, and the posterior surface is more exposed than the anterior surface. From this point, burning predominantly continues proximally along the linea apsera. This pattern is attributed to the morphology of *rectus femoris*, of which the distal portion is a thin ligament and proximal portion a fleshy, muscular belly, as well as the protective positioning of the lateral rotators of the hip and the anterior, posterior and medial muscles of the thigh in a pugilistic pose.

The thoracic and abdominal cavities are completely exposed by half an hour. The lateral surfaces of the ribs are visible, and the previously exposed anterior surfaces are calcined and warped (Bohnert *et al*., 1998; Pope, 2007). Due to the exposed thoracic and abdominal regions, the associated organs loose moisture, shrink and blacken.

30 – 40 minutes

By forty minutes under controlled conditions, the calvarium is gone and the brain is exposed. The facial bones are calcined. Any soft tissue present on the neck is charred and shrunken. Soft tissue of the anterolateral ribs is burned up to the posterior axillary line and the rib shafts are completely, calcined and warped. Organs associated with the both the thorax and abdomen are destroyed. The forearms are destroyed. The upper limbs are tissue free but the head of the humerus is intact. At this stage, heat-induced longitudinal fractures are commonly noted on the long bone shafts. Due to the thick musculature of the lower torso, the pelvis and lower spine are protected from thermal damage (Bohnert *et al*., 1998; Pope, 2007).

40 – 50 minutes

The entire upper limb is destroyed and with sections of calcined femora intact (Bohnert *et al*., 1998). The calcined facial bones disintegrate, and the base of the skull is exposed (Bohnert *et al*., 1998). Due to continuous shrinking of the nuchal muscles, the neck is further hyper-extended, the soft tissues are destroyed and the anterior vertebral bodies are calcined. Most of the internal organs associated with the thorax and abdomen are unrecognizable. The ilium is slightly charred with some adhering tissue. Early thermal damage to the pelvis is noted on the iliac crests and is due to their superficial position when compared to the deeper, more protected regions of the pubis and ischium (Figure 2.20). The muscles covering the broad iliac surface retract and expose the ilium from a posterior to an anterior direction (Pope, 2007). As the soft tissues further recede, surfaces of the pubis and

ischium become visible. The pubis is first exposed along the superior border and progresses anteriorly between the legs (Figure 2.20). Pelvic organs are destroyed (moisture loss and charring).

With extensive burning the anterior aspect of the greater trochanter is the first area exposed at the proximal femur (Symes *et al.* 1999) (Figure 2.19).

50 – 60 minutes

Complete destruction of the skull, with only small parts of mid-face and cranial base remain intact at this stage of exposure. At this stage it is most likely that the brain will have shrunk into a small charred mass positioned at the cranial base (Pope, 2007). With increasing dorsal flexion of the vertebral column, intervertebral disks are destroyed. Organs are mostly ash, and the tissues of the pelvis are entirely consumed. The ischium and sacrum are exposed.

To summarise; the complete destruction of a body in a fire is not an easy task. Uniform burning, as described above, is the exception and not the rule. A general rule is that areas with the highest concentration of soft tissue (thorax, pelvis and abdomen) are last to burn, whereas areas with little tissue concentration are the first to burn. While the subcutaneous fat ignites the fire, the produced heat cooks the internal organs from the outside to the inside. More often than not, soft tissue remains and may be useful for toxicological and even histological analysis. However, many forensic cases are received with complete destruction of soft tissue, post-burn decomposition and thermal damage to the hard tissue (bone) (Fairgrieve, 2008).

2.2.3.3. Bone response to thermal alteration

Thermal alteration of bone is dependent on temperature, stage of tissue reduction, pyrolysis of organic content, oxygen availability, and duration of exposure (Karmani, 2006; Pope, 2007). In order to understand the alteration that heat and fire has on the composition of bone, the basic structure and function of bone is described (Symes *et al.*, 2008).

Bone structure

Bone is a specialised form of connective tissue that serves to support, protect and move the body. Bone is highly vascularised and is constantly remodelling. As a tissue, bone comprises of a cortex in which long collagen chains are embedded within crystallised

inorganic particles to form a bony matrix (Freemont, 1998; Lanting *et al.,* 2001). Bone is a visco-elastic structure that is a weight-bearing support system, a powerful anchor for muscular forces (contraction) and is light in weight to compensate for swift movement (Freemont, 1998).

"Visco" refers to the rigid, unyielding and brittle hydroxyapatite crystal and calcium salts component (mineral component) of the bone matrix. Hydroxyapatite also provides compressive strength when bone is exposed to an external force (Herrmann & Bennett, 1999). The elastic component responsible for the tensile strength, yielding and ductile nature of bone is made up of collagen (Herrmann & Bennett, 1999; Zioupos *et al.,* 1999; Viguet-Carrin *et al.,* 2006).

When bone is exposed to fire, the inorganic and organic components undergo a series of biochemical changes (Schurr *et al.,* 2008). The crystalline collagen triple helical structure is transformed into a random amorphous coil, and the collagen content of bone is reduced (Gonçalves *et al*., 2011). Further evaporation, organic degradation and transformation of the inorganic matrix alter the chemical nature of bone which produces microscopic changes, colour changes, shrinkage, distortion, deformation and fracturing (Herrmann & Bennett, 1999; Cooper, 2006; Brickley, 2007; Symes *et al*., 2008).

Because of these extreme morphological alterations, standard anthropological methods often fail to aid in the identification of cremains (Devlin & Herrmann, 2008). While the precise mechanisms involved in chemical and structural thermal alteration of bone are not fully understood, heat alterations are shown to result in dehydration, shrinkage, warping, delamination, fracturing, fragmentation and discolouration of bone (Mayne Correia, 1997; Thompson, 2005, 2009; Karmani, 2006; Symes *et al.*, 2008; Dehaan, 2008; Marciniak, 2009).

Microscopic changes

Changes in gross morphology and histology of bone after exposure to various temperatures of heat and fire has been investigated (Table 2.12). Thompson (2005, 2009) reported on the macroscopic, dimensional changes in bone and the subsequent influence of these changes on histological age estimation techniques, while authors such as Forbes (1941), Herrmann (1976), Bradtmiller and Buikstra (1984), Shipman *et al.* (1984), Holden *et al.* (1995), Hanson and Cain (2007), and Nelson (1992), focused on describing the histology of burnt bone.

Hydroxyapatite comprises the inorganic (calcium phosphate) and organic (collagen) composition of bone and diretctly dictates it histology (Fairgrieve, 2008). Initial thermal alteration occurs to the lamellae with an increase in the prominence of the canaliculi. This is followed with changes in the lamellae from a smooth, normal structure to a coarser, more granular formation (Forbes, 1941). As the granularity of the lamellae increases with heat exposure, the canaliculi and lacunae disappear. The lamellar structure of the Haversian systems begins to degrade, and the periphery of the Haversian canals becomes ragged and ill-defined (Forbes, 1941). Complete lamellar structure is lost at temperatures around 800°C and is attributed to rapid crystal growth (Table 2.12)

When exposed to heat, the organic constituents of bone are lost, and a porous structure is created. With continued exposure, this porous network condenses and becomes a closed, interlocking structure (Figueiredo *et al.,* 2010). Using X-ray diffraction patterns, Shipman *et al.* (1984) demonstrated that hydroxyapatite crystals remain regardless of the temperature of the fire. However, the mineralogy of the bone is altered when exposed to heat and promotes an increase in crystal size and crystallinity of bone derived from hydroxyapatite (Shipman *et al.,* 1984; Figueiredo *et al.,* 2010). In contrast, at low temperatures changes to the structure of collagen fibrils can be observed in bone tissue (Arora *et al.,* 2010). Holden *et al.* (1995) observed variations in the orientation of structural collagen fibres between areas of the medullary, mid-cortex and outer cortex at various stages of burning (charred – calcined). The collagen fibres in the blackened (charred) medullary cortex had little fraying and a structured orientation. The collagen fibres in the mid-cortex (grey area) had fraying of individual mineralised collagen fibrils as well as the association of small spherical-type crystals within the mineralised residue of the fibres. The calcined, outer cortex had no mineralised collagen fibres, but it was replaced with hexagonal-type crystal growth. The relative sizes of the crystals formed are temperature dependant: the higher the temperature, the larger the crystal size (Shipman *et al.,* 1984).

Collagen is removed from bone at temperatures over 600°C and causes the formation of carbonite apatite which is later removed at calcination (900 to 1200°C) (Figueiredo *et al.,* 2010). During calcination, Haversian systems lose concentric lamellar bone. Heat does not affect the number of osteons in bone, but diameters of both Haversian systems and Haversian canals are altered. Bradtmiller and Buikstra (1984) and Nelson (1992) produced conflicting results on this subject. Bradtmiller and Buikstra (1984) observed an overall increase in the size of the Haversian systems when exposed to heat. This implies that heat does not affect the

concentric lamellae of the Haversian systems as much as it affects the interstitial lamellae (Fairgrieve, 2008). Nelson (1992) concluded opposite results and stated that the diameter of the Haversian systems decreased by almost 17%, while the Haversian canals increased by 10% (Nelson, 1992).

Cancellous bone becomes unidentifiable much faster than compact bone (Forbes, 1941). Similar to compact bone, microscopic changes first relate to the increasing prominence of the canaliculi of the lamellar bone. In cancellous bone, the lamellar structure disintegrates, and the lacunae appear hazy and ill-formed. The end-product is an unidentifiable, uniform granular matrix (Forbes, 1941).

Morphological/Macroscopic changes

Bone experiences definite structural alterations such as warping, deformation, shrinkage, and fragmentation when exposed to heat. The distortion, warping and shrinkage of bone are not uniform but rather dependent on cortical thickness, shape, size and distribution of trabecular bone (Pope, 2007). Poor reconstruction of burned remains that have been fragmented and warped can negatively influence the accuracy of standard anthropological methods (Eckert *et al.,* 1988; Whyte, 2001; Marciniak, 2009; Arora *et al.,* 2010). Well-reconstructed remains can be used to make accurate morphological interpretations, form distinctions between nonhuman and human bone, and identify specific skeletal elements (Owsley *et al.,* 1995; Arora *et al.,* 2010). The anthropological investigation of human remains (burned or unburned) involves observation of gross morphological traits and osteometrics (Fairgrieve, 2008).

Heat-induced dimensional changes to bone limit the osteometric and morphological assessment of sex and age. The heat physically alters the shape and size of the bones, and often only small fragments are recovered from the scene (Fairgrieve, 2008). For example, the pubic symphysis and auricular surface of the ilium are often used to estimate age (Todd, 1920; McKern & Stewart, 1957; Lovejoy *et al.,* 1985; Brooks & Suchey, 1990). While these two surfaces retain their structure when exposed to heat, they lose their organic components and become drier and more porous. This porosity makes the structure appear older than it is (Pope, 2007). The skull, being a common element used to estimate sex, often fragments when exposed to thermal conditions (Grèvin *et al.,* 1998; Thompson, 2002, 2009). Few discriminate features such as muscle insertion points, skull relief and prominent or less

marked crests may be identifiable when splintered and fractured burnt bones are reconstructed (Grèvin *et al.,* 1998).

Due to shrinkage and warping of burnt bone, osteometry and the use of long bones to estimate sex becomes less accurate, if not near impossible. When bone is exposed to low temperatures for a short duration of time, minimal shrinkage occurs (Murray & Rose, 1993; Arora *et al.*, 2010). However, both adult and juvenile remains have been shown to shrink between 5 and 10% when exposed to heat for an extended period of time. However, this depends on bone density, temperature, and duration of the fire (Van Vark, 1970; Krogman & İşcan, 1986; Warren & Maples, 1997; Thompson, 2005, 2009). Shipman *et al.* (1984) established a direct correlation between temperature of a fire and percentage of bone shrinkage. Shrinkage is recognised as the most influential factor to hinder the estimation of sex from burnt remains and is said to affect both length and width of bones (Fairgrieve, 2008).

The distortion of skeletal remains also affects the estimation of stature. Various methods based on the diameters of the humeral, femoral and radial heads as well as the length of the respective shafts have been adapted to estimate stature from burnt skeletal remains. These methods take into account the retraction (shrinkage or contraction) that occurs during the burning process (Grévin *et al.,* 1998). The methods involve careful reconstruction of the remains such that proximal to distal measurements can be taken. These values are then integrated into various formulae that take into account the contraction correction factor (Grévin *et al.,* 1998). Contraction correction factors use colour differentiations observed on the burnt remains to calculate the degree of distortion and may vary between 8 – 14% (Grévin *et al.,* 1998).

Dimensional changes such as warping, shrinkage, and fragmentation influence the identification and visual classification of cremains. The study of bone warping in fleshed/wet or dry bone, as a consequence of the heating process, is limited, contradictory and uncertain (Baby, 1954; Binford, 1963; Buikstra & Swegle, 1989; Spenneman & Colley, 1989). Several authors have not observed warping on dry human or nonhuman bone (Baby, 1954; Binford, 1963). Yet, recently, this has been discredited, and warping has been noted on dried bone (archaeological or recent) exposed to heat (Whyte, 2001; Gonçalves *et al*., 2011). When collagen degrades, the elastic nature of bone is lost, and the bone is unable to bend or warp prior to fracture. However, the time it takes for collagen to degrade varies, and therefore the possibility of collagen being present in apparently dry bone exists. While bone contains

collagen as a component, warping and distortion is a possibility. Heat-induced fractures are often associated with bone that was fleshed/wet/green prior to exposure (Gonçalves *et al*., 2011). If dry bone displays warping when exposed to thermal conditions, the collagen component was large enough to initiate warping (Gonçalves *et al*., 2011). Studies have suggested that bone warping could indicate the condition of the bone prior to burning, i.e. cremation immediately after death versus cremation as a secondary process (Gonçalves *et al*., 2011).

Colour changes in burnt bone

The colour changes observed in thermally altered bone signify the various stages of pyrolysis, tissue reduction, the direction of the fire, duration of exposure and the organic composition of bone. Temperature was previously thought to be the major colour influence, but due to more research it has been shown that temperature does not result in a specific colour change; instead, it is the duration of exposure that influences the colour manifestations on bone (Mays, 1998). These changes have been utilised in prior studies to analyse thermal alteration of archaeological collections (Connelly *et al.,* 2010). Colour change involves the gradual decomposition of organic components that form the bony matrix such as water, lipids, collagen and protein (Shipman *et al.,* 1984; Buikstra & Swegle, 1989; David, 1990; Mayne Correia, 1997; Bennet, 1999; Pope & Smith, 2004; Thompson, 2004). Oxygen availability, duration of exposure and tissue shielding all influence colour change and collagen content of bone (Shipman *et al.,* 1984; Mayne Correia & Beatie, 2002; Walker *et al.,* 2005; Symes *et al.,* 2008; Arora *et al*., 2010).

When exposed to fire/heat, bone progresses through four stages of cremation: dehydration, decomposition, inversion and fusion. Each stage displays unique colour changes and includes unburnt beige, to yellow, to dark brown and black, to blue-grey and ends in white (Schwark *et al.,* 2010). These observed colour changes can provide information as to the chemical process that took place in the bone, to the condition of remains prior to exposure, and to the environment in which the exposure took place (Walker *et al.,* 2005; Symes *et al.*, 2008). Insulative layers of soft tissue provide protection to the skeleton but are eventually lost during burning and bone experiences a sequential change in colour (Pope, 2007).

Areas between exposed soft tissues covering bone undergo heat-induced alteration. Even when protected within tissue, bone can experience dehydration from the radiating heat.

Majority of organic components are present in early-exposed bone and the periosteum often remains intact over these areas (Fairgrieve, 2008). When subjected to temperatures less than 200°C, the moisture content is lost in the bone matrix when the hydroxyl-bonds, that maintain the integrity of loosely-bound water and bonded water, are broken (Thompson, 2005; Pijoan *et al.,* 2007).

The above-mentioned tissue protected area is referred to as a heat border and is often ignored as thermal alteration even though it represents the initial stage of organic coagulation (Symes *et al.,* 2008). The border presents as an off-whitish, yellow or brown area located adjacent to the charred area (blacked, carbonised material). The heat border follows the contours of the soft tissue, and the overlying, receding tissues protect it from direct contact with the fire. Small, superficial, heat-related fractures, which are associated with continued shrinkage and moisture loss experienced within the protected bone area, are often observed within the heat border.

The heat border is an important element of fire destruction as it is more durable than either charred or calcined areas and may be the only indicator of a fire when the other areas are destroyed (Pope, 2007). In the case of fleshed remains, a heat line (white line/translucent bone) which represents the initial line of contact between unaltered and heat-altered bone is usually found adjacent to the heat border (Symes *et al.,* 1999). With more direct heat exposure, bone experiences organic pyrolysis and carbonisation and turns black (charred). This phase encompasses the decomposition of the organic and inorganic constituents and inversion, which is the loss of carbonates and the associated conversion of the hydroxyapatite to β-tricalcium phosphate (Thompson, 2005). At this stage, the periosteum is destroyed (Fairgrieve, 2008).

Charring is initiated on the external surface and gradually penetrates into the deeper cortical layers (Pope, 2007). Charred bone outlines the soft tissue contours that continue to expose more bone during retraction (Pope, 2007). Despite severe moisture loss, charred bone is semi-durable and often displays tensile shrinkage fractures which run parallel to the heat border and is known as predictable cracking (Symes *et al.,* 1999). Thick cortical bone (e.g., femur shaft) is more durable than the thin cortical bone (e.g., skull) to heat exposure. Thin cortical layers may be completely destroyed prior to discovery, and only partially charred trabecular bone is noted (Pope, 2007). In some cases, sufficient organic material is present in the bone, and the charred area appears greasy due to the release of marrow from the inner

cavity. This feature is important, as it will aid in determining the condition of the remains prior to the burn event (Pope, 2007).

Calcination is the final stage of heat-induced bone degradation and is a consequence of fusion (melting & coalescence) of the bony crystal matrix. Due to the post-organic destruction and modification of bone mineral content, bone transforms into a grey-white-blue colour (Symes *et al.,* 1999). For this degree of alteration, temperatures need to range over 800°C for a short period or at lower temperatures for an extended period (Buikstra & Swegle, 1989; Shipman *et al*., 1984; Van Vark, 1970; Pope, 2007). During this stage, bone experiences severe dehydration, and any remaining moisture is lost. Carbon released from the degradation of organic material bonds with oxygen to form carbon dioxide and carbon monoxide, and the calcined bone becomes an ashen framework of fused bone salts (Mayne Correia, 1997). The main composition of calcined bone is inorganic hydroxyapatite crystals and basis mineral components (Pope, 2007). This is the most damaging stage in thermal alteration, and often produces numerous heat-related fractures. The longer calcined bone is exposed to heat and fire, the greater the degree of fragmentation and deformation. Often only small brittle pieces of unidentifiable bone survive the process (Symes *et al*., 2008).

On occasion when heat-related fractures occur, the organic material present in the bone vents through the fractures lines and offers protection to the underlying structures. In calcined bone, the margins of the fracture lines are black (charred) and the external cortical colour is grey/white (Figure 2.21). Both cranial and postcranial demonstrate these changes and indicates that organic material in the bone has not yet undergone pyrolysis (Pope, 2007).

Heat-induced fractures

Heat stress as well as a traumatic injury can cause a bone to fracture. Evaluation of heat-induced fractures and fracture patterns originated with studies that focused on the crematory practices of archaeological groups (Krogman, 1939; Baby, 1954; Binford, 1963). Early studies focused on fracture patterns associated with the condition of the remains before exposure to fire in order to determine whether previous civilizations cremated fully fleshed or defleshed bodies. The more recent studies have focused on burn and fractures patterns and their application in the modern forensic field; are bodies of forensic significance burnt while fleshed or defleshed.

In extreme cases of cremation often only the bones remain for analysis and in the absence of significant colour changes and soft tissue, heat-induced fracture patterns may

provide information as to the condition of the remains prior to burning. Dry bone burns as a homogenous structure, because it lacks organic saturation and soft tissue protection. In contrast, fleshed remains have copious organic material and overlying tissue protection. When fleshed remains burn, destruction ranging from unburned bone to charred and calcined bones is present. Heat-induced fractures occur on the cortical surface of bone where the most heat is applied and tend not to travel through the entire bone except in cases of extreme cremation (Pope, 2007).

Bone fractures in heat due to the shrinking and loss of organic components. The most common heat-induced fractures are longitudinal and transverse and are found along the shafts of burnt fleshed, semi-fleshed and green/wet bone. While most commonly found on long bones, they can also form on flat and irregular bones. During the early stages of burning, longitudinal fractures form and result from a loss of structural integrity of the bone, protein denaturalization and dehydration (Pope & Smith, 2004). Longitudinal fractures may follow the lengthwise orientation of collagen fibres along the cylindrical Haversian systems or, when a broad area of bone is exposed to heat, radiate from the charred areas into the heat border (Binford, 1963; Stewart, 1979; Herrmann & Bennett, 1999; Symes *et al.,* 2001; Pope & Smith, 2004). Fractures that follow the line between burned and unburned bone are classified as burn line fractures and should not be confused with longitudinal fractures.

Step fractures are associated with longitudinal fractures and occur between the transverse margins of longitudinal fractures and across the entire shaft of the bone (Symes *et al.,* 2001). Similarly, transverse fractures also transect Haversian systems, but they do not break the entire bone shaft as seen with step fractures (Symes *et al.,* 2001). Both longitudinal and transverse fractures are classified as deep fractures, as they penetrate into the marrow cavity of the bone (Fairgrieve, 2008; Connelly *et al.,* 2010).

Curved transverse fractures, also known as soft tissue shrinkage lines, thumbnail lines or curved tissue regression heat fractures, are closely associated with the presence of flesh prior to burning (Thurman & Willmore, 1981; Eckert *et al*., 1988; Ubelaker, 1989; Binford, 1972[1963]; Herrmann & Bennett, 1999; Whyte, 2001; Symes *et al*., 2008). More recently, however, experiments by Gonçalves *et al*. (2011) suggested that curved transverse fractures are not exclusively linked to fleshed remains, but can been observed on burned dry remains. The presence of these fractures is considered a unique product of heat exposure as they bear no resemblance to defects attributed to trauma (Herrmann & Bennett, 1999). These fractures form a grouped arc running across the long axis of the bone shaft or in areas with dense,

accumulated tissue (cranial base, temporal region, nuchal region, frontal region and mandible) and indicate the direction of tissue regression (Herrmann & Bennett, 1999; Pope, 2007). When the body heats the protective soft tissue recedes, causing the periosteum to shrink and crack, forming fractures along these lines (Buikstra & Swegle, 1989) (Figure 2.22). A common effect of the curved transverse fracture is coning. This occurs when the fracture completely transects the shaft, leaving an arched fracture margin (Symes *et al*., 2008)

Curved transverse fractures also correlate with the colour changes discussed above. Aside from indicating the presence of flesh, curved transverse fractures also indicate the direction of fire. The apex of the highest arc points to the origin of the fire (Figure 2.23). Curved transverse fractures are also common on articular surfaces and surface near joints in which accumulating soft tissue, thickened connective tissue and cartilage protected the structure from encroaching heat (Pope, 2007). Concentric curvilinear fractures may also be observed on these surfaces and are due to the inward regression of soft tissue. These areas are also known as cold spots, and they are the last areas of a bone to burn (Symes *et al.,* 2008).

Delamination is a more destructive form of heat-induced fracture if compared to patina fracturing, longitudinal, step and curved transverse fractures. Delamination is often observed on the cranium (Pope & Smith, 2004). When the external table of the cranium is heated, small tensile cracks develop in the ever-shrinking outer table, which cause it to split/peel/flake away exposing the underlying diploë (Pope, 2007; Fairgrieve, 2008; Symes *et al.,* 2008) (Figure 2.24). In extreme cases, the external table of the cranium deforms, curls, and peels away from the underlying diploë (Pope, 2007). Postcranial remains display delamination most often at the epiphyseal ends where the cortical layer splits away from the underlying trabecular/spongy bone. Although delamination is a classic sign of heat damage it can also occur post-burning due to other taphonomic influences (Pope, 2007).

Burnt dry bone displays longitudinal splitting and sharp, clear-cut cracking/checking, or patina fractures, on the surface. Unlike longitudinal fractures, patina fractures are classified as superficial fractures that occur when a large surface of bone is exposed to a uniform amount of heat. These fractures do not penetrate the medullary cavity (Fairgrieve, 2008). They are mostly found in cortical bone overlying trabecular bone such as epiphyseal ends, vertebrae and cranial bones (flat bones). These fractures are less destructive and resemble a fine mesh of uniformly patterned cracks often seen in old paintings and old china. The patina-like surface can be destroyed with rough handling during the recovery and

transportation and results in delamination of the brittle surface. Dry bone exposed to fire is often calcined (white) with little charring and splintering (Symes *et al.,* 1999, 2001).

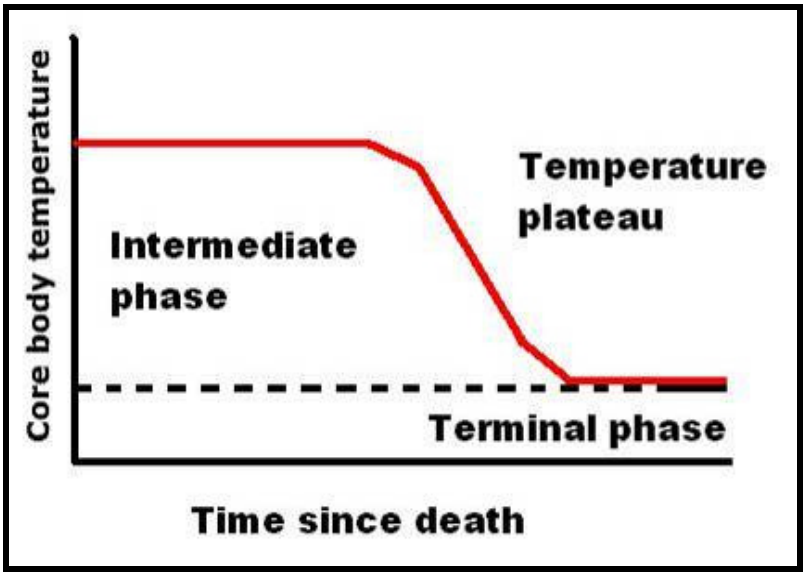

Figure 2.1 Body temperature after death

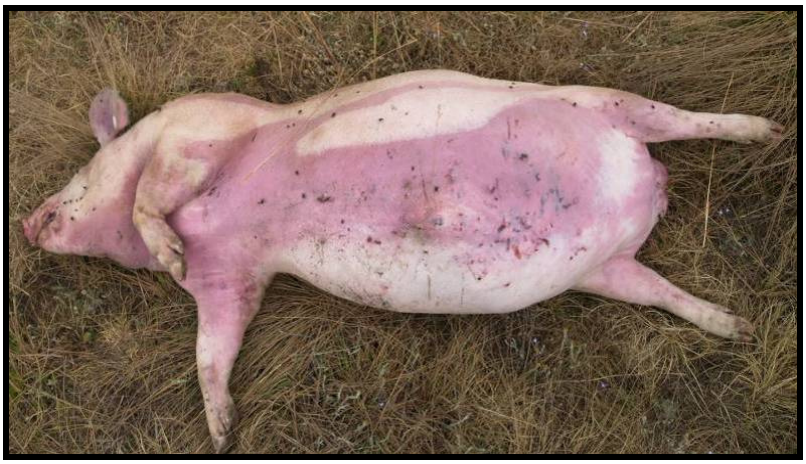

Figure 2.2 Livor mortis appearing as reddish-pink discolouration on a pig carcass

Figure 2.3 Pressure lividity on the back of a pig carcass

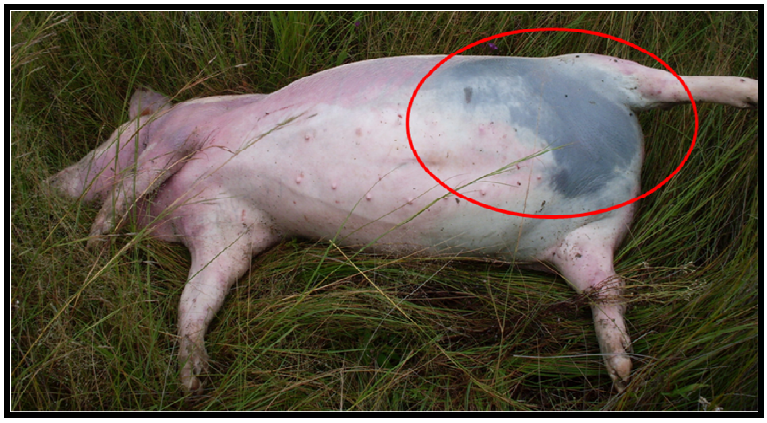

Figure 2.4 Greenish discolouration over the lower abdominal area

Figure 2.5 Skin slippage of head and neck region of a pig

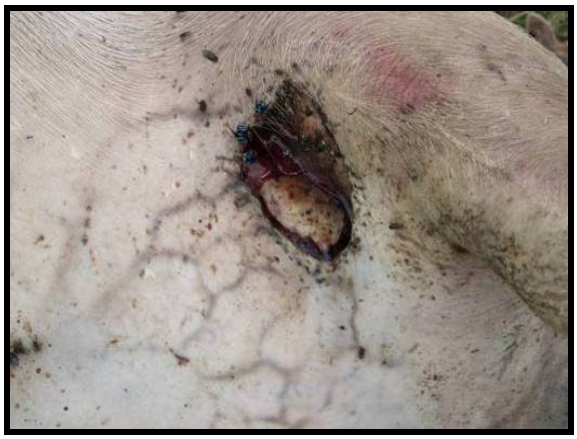

Figure 2.6 Marbling of the superficial blood vessels

Figure 2.7 Postmortem bullae present on the abdominal region

Figure 2.8 Progress in decomposition of a pig from PMI = 1 day to PMI = 3 days to PMI = 8 days showing the increase in abdominal volume due to gas build-up

Figure 2.9 Purging of fluids from the mouth and nostrils

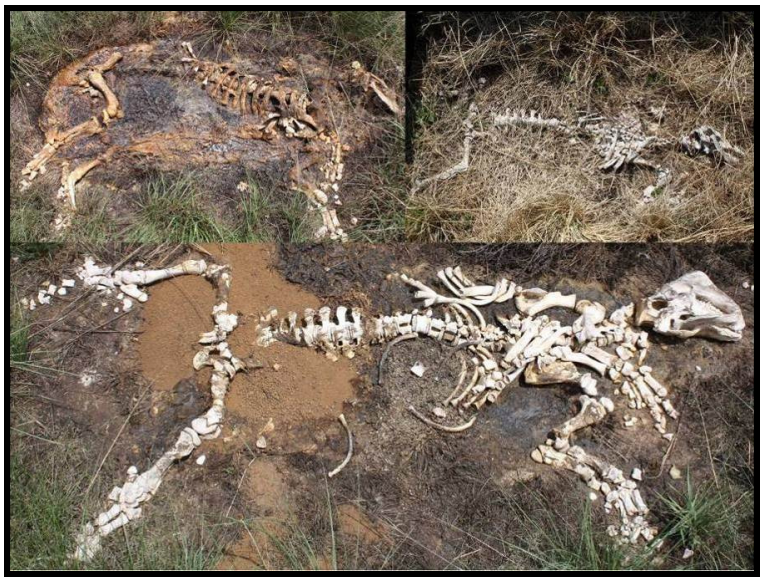

Figure 2.10 Skeletonisation: the final stage of decomposition

Figure 2.11 Pugilistic posture: extreme flexion of upper limb

Figure 2.12 Pugilistic posture: extreme plantarflexion of the foot

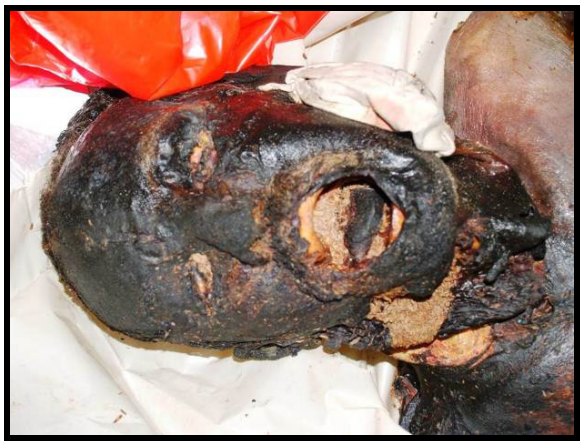

Figure 2.13 Distortion of facial features by fire: protrusion of tongue, bloated features

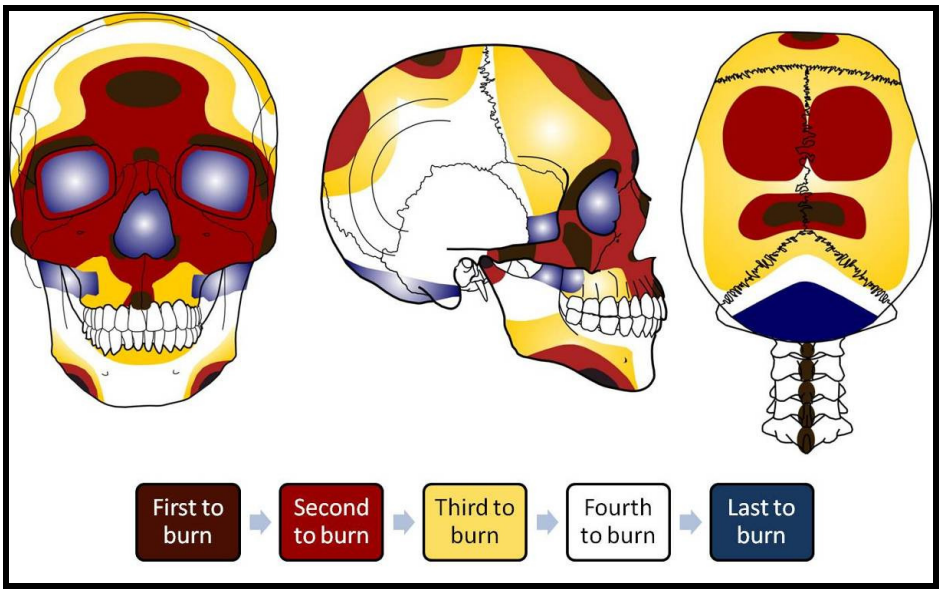

Figure 2.14 The manifestation of a burn pattern on the cranium (adapted from Symes *et al.*, 2008)

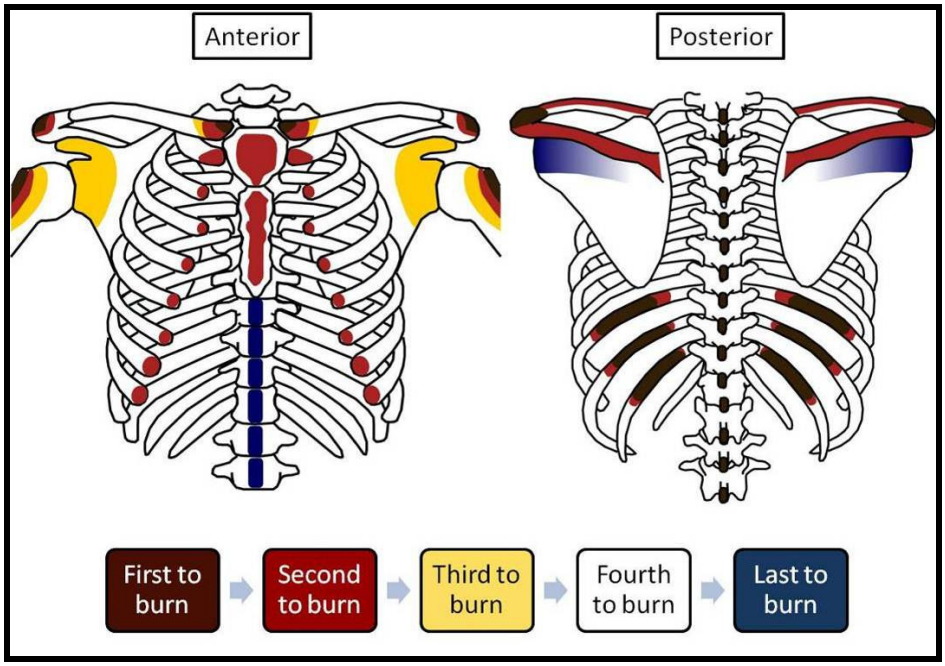

Figure 2.15 The manifestation of a burn pattern on the thorax (adapted from Symes *et al*., 2008)

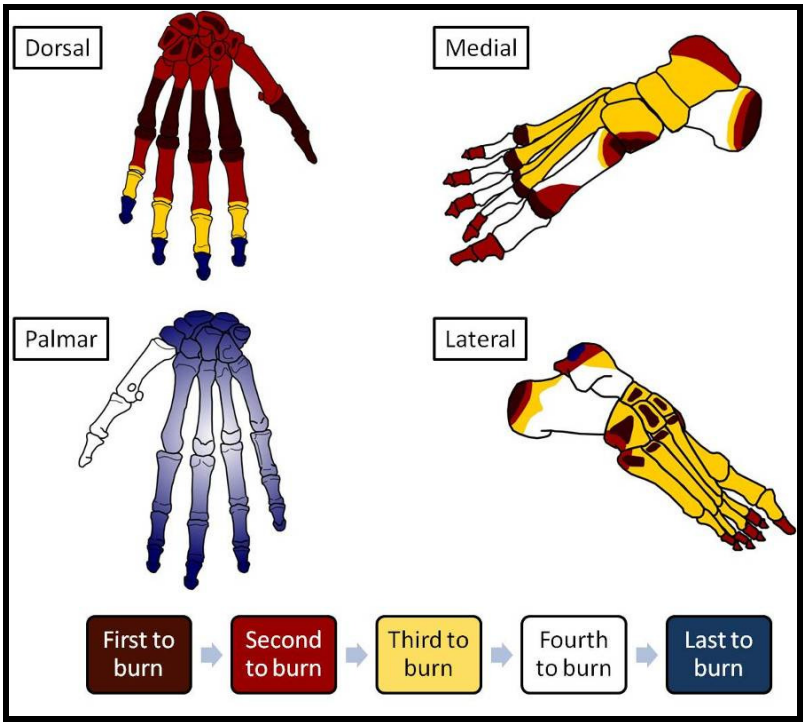

Figure 2.16 The manifestation of a burn pattern on the hands and feet (adapted from Symes *et al*., 2008)

Figure 2.17 Canoeing of the dorsal surface of the metacarpals

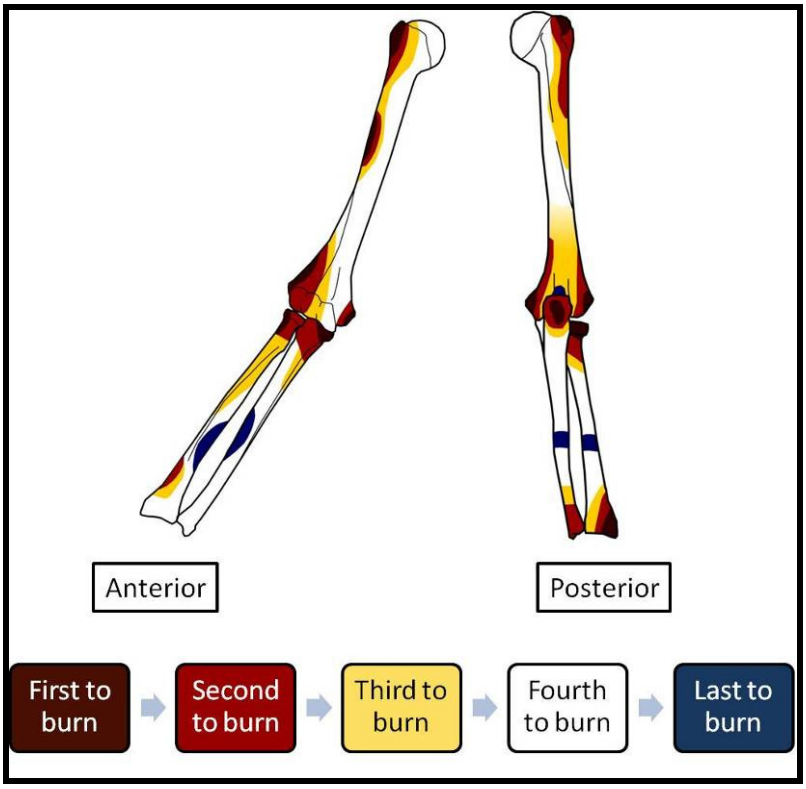

Figure 2.18 The manifestation of a burn pattern on the upper limb (adapted from Symes *et al*., 2008)

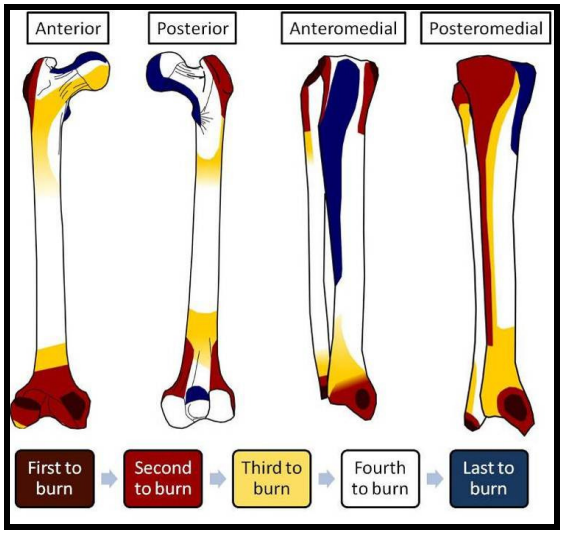

Figure 2.19 The manifestation of a burn pattern on the lower limb (adapted from Symes *et al*., 2008)

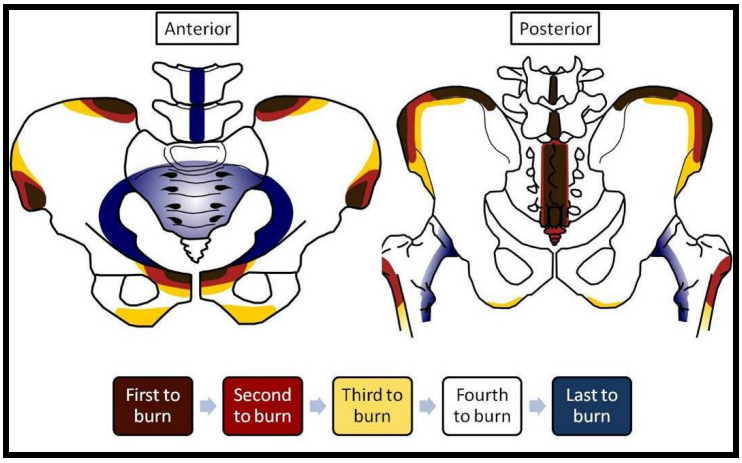

Figure 2.20 The manifestation of a burn pattern on the pelvis (adapted from Symes *et al*., 2008)

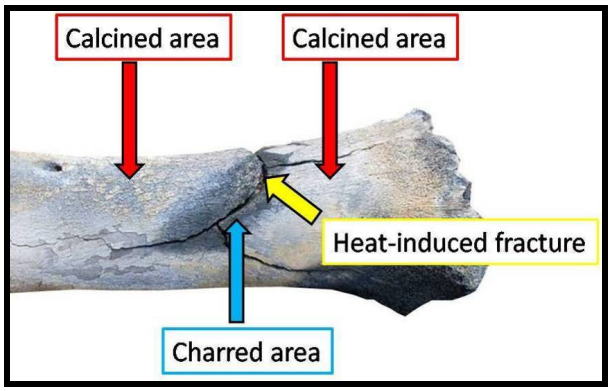

Figure 2.21 Charred organic material vented through a heat-induced fracture

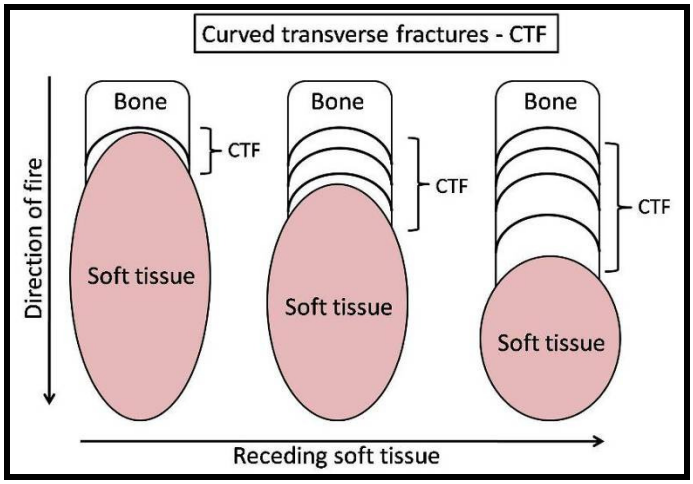

Figure 2.22 The formation of curved transverse fractures along the shaft of a long bone

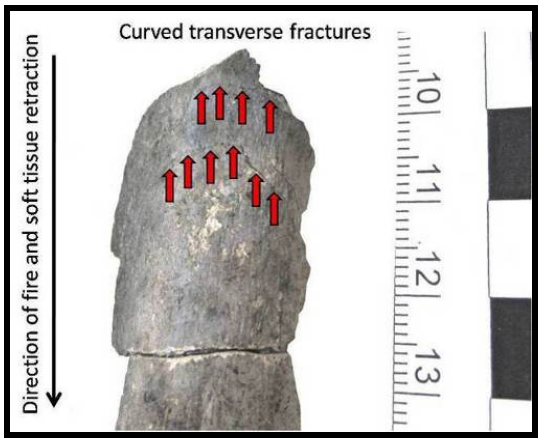

Figure 2.23 Curved transverse fractures on a femur shaft

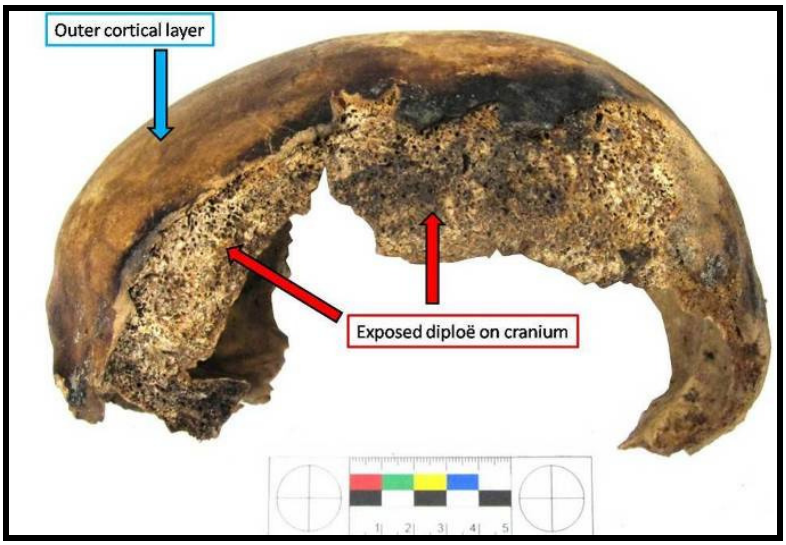

Figure 2.24 Delamination of the cranium

Table 2.1 Environmental and cadaveric factors affecting the rate of algor mortis (adapted from: Moritz & Henriques, 1947; Camps *et al.,* 1976; Polsen *et al.,* 1985; Simpson & Knight, 1985; Gordon *et al.,* 1988; DiMaio & DiMaio, 1989; Pounder, 2000; Tracqui, 2000; Fairgrieve, 2008)

Factors	Description	Example
Conduction	Heat, in the form of thermal energy, of an object is transmitted from a warmer area of a solid material to a cooler area, or when heat is absorbed by an object that is in contact with the body	Water is an excellent conductor. A body cools faster when submerged in water than when exposed to air
Convection	Movement of air around the body. Wind assists in carrying heat from the body	A body in a drafty room cools faster than a body in a room without air circulation
Radiation	Heat emitted from the body after death in the form of infrared heat rays	A body in a hot room will radiate more heat than if the room was temperate. The greater the temperature gradient between the body and the environment; the more heat loss via radiation
Evaporation	Conversion of body heat into water vapour	If water is present on the skin, heat loss via evaporation can occur
Surface area/mass ratio	Greater surface area of body relative to mass = more rapid cooling	Obesity slows cooling due to the added insulation
Clothing and coverings	Insulate the body from environment; thus cooling is slower	A clothed body is more insulated against the environment and will therefore cool at a slower rate

Table 2.2: General appearance of rigor mortis in the body after death

Rigor mortis stages	(Pounder, 2000; Tracqui, 2000)	(Gill-King, 1997)	(Gunn, 2009)
Onset of rigor mortis	0.5 – 7 hours (average 3 hours)	2 – 6 hours	3 – 4 hours
Completion of rigor mortis	2 – 20 hours (average 8 hours)	-	±12 hours
Retention of rigor mortis	Approximately 36 hours	24 – 84 hours	-
Disappearance of rigor mortis	2 – 3 days	>84 hours	>36 hours

Table 2.3 Summary of the stages of decomposition and their characteristics (adapted from: DiMaio & DiMaio, 1989; Clark *et al*., 1997; Galloway, 1997; Gill-King, 1997; Goff, 1997; Vass, 2001; Powers, 2007; Pinheiro, 2007; Gunn, 2009)

A: Fresh/Initial decay (0 – 7 days)
Begins at time of death – no discolouration. Autolysis takes place with few macroscopic changes observable on the remains. Slowly, signs of lividity become apparent. Insect activity is generally minimal with egg deposits in bodily orifices. Slight green discolouration over the anterior abdominal area, more specifically over the area of the caecum. No carnivore activity present at this stage
B: Early putrefaction/decomposition (1 – 8 days)
Pink-white appearance with skin slippage and some hair loss present with a deeper grey-green discolouration of abdominal area. Superficial veins of skin (purple-brown) – prominent around shoulders, upper chest, abdomen and groin (marbling/suggillation). Maggot colonisation becomes apparent during this stage (2nd day). Skin – glistening, dusky, reddish-green to purple-black appearance with some skin slippage present. Bloating of abdomen (as early as 2nd day) – formation of putrid gases in stomach and intestines. Purging of decomposition fluids from nose, mouth, vagina and rectum. Brown to black discolouration of skin especially around the fingers, nose and ears. Skin of arms and legs may discolour to brownish-black with a leathery appearance
C: Advanced/Black putrefaction/decomposition (4 days – 6-9 months)
Further darkening of the skin. Decomposition of tissues producing sagging of the flesh, caving in of the abdominal cavity due to the release of pent up gases. This is often accompanied by extensive maggot activity. Decomposition of internal organs resulting in organ shrinkage. Overall decomposition of the skin; head and face turn black, nails fall off and epidermal detachment is noted. The odour of decay is most prominent at this stage. Some bone exposure may be observed in the later phases of this stage. Butyric fermentation. Appearance of mould on the corpse, drying out of the remaining tissue (mummification)
D: Skeletonisation/Dry decay (2/9 months - years)
Bone exposure – greasy bone with some attached dried tissue may be present Total skeletonisation – dry bone with no tissue attached Extreme skeletonisation – skeletal elements are affected by environmental conditions resulting in weathering, cortical flaking and bleaching of bone. Skeletonisation with metaphyseal loss with long bones and cancellous exposure of the vertebrae

Table 2.4 Factors that influence the rate of decomposition (adapted from: Polsen *et al*., 1985; Rodriquez & Bass, 1985; Mann *et al*., 1989; Gill-King, 1997; Rodriguez, 1997; Dent *et al*., 2004; Pinheiro, 2007)

Variable	Increase rate	Decrease rate
Temperature - warm	X	X
Access by insects	X	
Burial and depth		X
Carnivores/Rodents	X	
Humidity/Aridity	X	X
Rainfall		X
Trauma to body	X	
Submerged: water	X	X

Table 2.5 Variables of fire exposure: (adapted from: DeHaan, 2008)

Variable	a	b	c	d	e
Size of fire	Single item burning	Multiple items burning	Full-room involvement (flashover)	Sustained post-flashover burning	
Exposure of body	On non-combustible floor for duration of fire	On top of burning items	On combustible floor that collapses during fire	In suspension on metal framework (eg; car seat)	Exposed to fire on all sides (commercia l cremation)
Duration of exposure	Antemortem	Postmortem			
Condition of bone	Fresh or Green	Dried			

Table 2.6 Areas of the cranium protected by differential tissue thickness

Area of the cranium	Muscle/s offering protection
Cranial base and occipital bone	Sternocleidomastoid, trapezius, occipitalis
Temporal region	Temporalis
Sphenoid bone	Temporalis
Post-canine maxilla	Buccinator
Palate	Tongue, teeth,lips
Posterior portion of parietal bones	Temporalis

Table 2.7 Summary of the first phase of skeletal elements to be exposed during the burning process (adapted from: Bohnert *et al*., 1998; Symes *et al*., 2008; Pope, 2007)

Stage	Skeletal element	Specific sites of sequential thermal destruction
First to burn	Cranium	Frontal bone (central forehead), glabella, supra-orbital ridges, lateral part: zygomatic process of temporal bone, orbital rims (superior & inferior), vertex, point superior to lambda, central part of alveolar process of maxilla, lateral to narale, inferior border of mandible, lateral surface of mandibular condyles
	Thorax	Clavicle: sternal end; Scapula: acromion process; Vertebrae: spinous processes; Ribs: posterior surfaces of lower ribs, anterior ends
	Upper limbs	Humerus: greater tubercle, deltoid tuberosity, medial & lateral epicondyles; Ulna: olecranon process, styloid process; Radius: styloid process, radial head, dorsal surface (distal): Hands: dorsal surface carpals (central), shaft and heads of metacarpals II – V, bases of proximal phalanges
	Pelvis	Os coxa: ASIS, posterior iliac crest, pubic tubercle; Sacrum: slight burn along median & medial sacral crests
	Lower limbs	Femur: lateral surface greater trochanter, medial condyle; Patella: base; Tibia: tibial tuberosity, medial malleolus, anterior border; Fibula: head, lateral malleolus; Feet: calcaneal tuberosity, lateral surface – base of first metatarsal, head of metatarsal V, bases of metatarsals

Table 2.8 Summary of the second phase of skeletal elements to be exposed during the burning process (adapted from: Bohnert *et al*., 1998; Symes *et al*., 2008; Pope, 2007)

Second in sequence to burn	Cranium	Frontal bone, supercilliary ridges, orbital rims (medial & lateral), zygomatic bones (arch), nasal bones, maxilla (frontal & zygomatic processes), maxilla (central part of alveolar part), parietal bones (central part), inferior border of mandible (extending anteriorly & posteriorly from first site), neck of mandibular condyle
	Thorax	Sternum: manubrium (anterior surface), sternal body (anterior surface); Clavicle: superior surface, sternal end; Ribs: anterior ends, posterior surface of lower ribs; Scapula: spine
	Upper limbs	Humerus: distal part of greater tubercle, deltoid tuberosity (periphery), medial & lateral supracondylar ridges; Ulna: olecranon process (periphery), anterior distal surface lateral to styloid process; Radius: neck, anterior distal surface medial to styloid process; Hands: dorsal surface of carpals (periphery to first burn site), metacarpal I, bases of metacarpals II – V, shafts of proximal phalanges
	Pelvis	Os coxa: posterior iliac crest (anterior to first burn site), posterior to ASIS, pubic crest; Sacrum: median & medial sacral crests, coccyx
	Lower limbs	Femur: peripheral to greater trochanter, medial & lateral condyles towards shaft, medial & lateral supracondylar lines; Patella: central part; Tibia: medial & lateral condyles (anterior parts), anterior border, medial malleolus (periphery to first burn site); Fibula: neck, lateral malleolus (periphery to first burn site); Feet: calcaneal tuberosity (periphery to first burn site), body of talus (trochlear surface), cuboid, heads of metatarsals I – IV, distal phalanges

Table 2.9 Summary of the third phase of skeletal elements to be exposed during the burning process (adapted from: Bohnert *et al*., 1998; Symes *et al*., 2008; Pope, 2007)

Third in sequence to burn	Cranium	Frontal bone, alveolar process of maxilla (lateral), coronal suture, parietal bones, lambdoid suture, alveolar process of mandible (central), angle of mandible
	Thorax	Clavicle: lateral to sternal end (first & second burn sites); Scapula: coracoid process, glenoid cavity(periphery on costal surface)
	Upper limbs	Humerus: intertubercular sulcus, shaft (lateral side), trochlear (posterior), posterior surface of distal end (excluding olecranon fossa); Ulna: distal shaft, olecranon process (distal); Radius: radial tuberosity, shaft (distal surface); Hands: dorsal surface of heads of proximal phalanges, dorsal surface of intermediate phalanges, bases of distal phalanges (dorsal)
	Pelvis	Os coxa: iliac crest (more central), ischial tuberosity, body of pubis & superior ramus, superior aspect of gluteal surface
	Lower limbs	Femur: head of femur (anteroinferior aspect), inferior aspect of neck towards lateral surface, superior to condyles, superior & inferior aspects of the linea aspera; Patella: apex; Tibia: medial surface, medial malleolus (superior aspect); Fibula: inferior to neck (superior shaft); Feet: talus (neck & head), navicular, 3 cunieforms, bases and shafts of metatarsals II – V, calcaneus (posterior), intermediate phalanges, cuboid

Table 2.10 Summary of the fourth phase of skeletal elements to be exposed during the burning process (adapted from: Bohnert *et al*., 1998; Symes *et al*., 2008; Pope, 2007)

Fourth in sequence to burn	Cranium	Frontal bone (directly anterior to coronal suture), inner orbital rims, inferior aspects of parietal bones, temporal bones, central section of occipital bone, styloid process, mastoid process, body of mandible, ramus of mandible, teeth
	Thorax	Sternum: manubrium & body (periphery), Clavicle: shaft & acromial end; Scapula: costal surface, infraspinous & supraspinous fossae; Vertebrae: all except for central portion of bodies (anterior); Ribs: all
	Upper limbs	Humerus: head, neck, medial surface of shaft; Ulna: central shaft (excluding center); Radius: central shaft (excluding direct center); Hands: palmar aspect of first metacarpal, proximal & distal phalanges (first digit)
	Pelvis	Os coxa: iliac fossa, superior & inferior ramus pubis, superior margin of acetabulum, gluteal surface, ischium, pubis; Sacrum: superior aspect of S1 & ala, dorsal surface (lateral aspects)
	Lower limbs	Femur: central aspect of head & neck, medial aspect of greater trochanter, central shaft, popliteal surface (excluding small spot in its center); Patella: posterior aspect; Tibia: medial border & surface; Fibula: shaft; Feet: body of calcaneus, head of talus, first metatarsal (shaft), proximal phalanges

Table 2.11 Summary of the last phase of skeletal elements to be exposed during the burning process (adapted from: Bohnert *et al*., 1998; Symes *et al*., 2008; Pope, 2007)

Last to burn	Cranium	Inner aspects of orbits, inner aspects of nasal cavity, lateral, most distal aspect of alveolar process of maxilla, temporal fossa, mastoid process, occipital bone, coronoid process of mandible
	Thorax	Scapula: small area inferior to spine in infraspinous fossa; Vertebrae: small section along central bodies (anterior)
	Upper limbs	Humerus: olecranon fossa; Ulna: small section on central shaft; Radius: small section on central shaft; Hands: remaining aspects of carpals, metacarpals and phalanges (palmar aspect)
	Pelvis	Os coxa: greater sciatic notch; Sacrum: ventral surface
	Lower limbs	Femur: superior aspect of head & neck (anterior), posterior head & neck, lesser trochanter, central part of popliteal fossa close to intercondylar fossa; Tibia: medial condyle (posterior); Fibula: medial aspect of shaft (central); Feet: joint surface (ankle)

Table 2.12 Compilation of histological changes observed in bone at varying temperatures (adapted from: Herrmann, 1976; Bradtmiller & Buikstra, 1984; Shipman *et al.,* 1984; Holden *et al.,* 1995; Figueiredo *et al.,* 2010)

Temperature (°C)	**Observed histological change**
< 185	Matrix unchanged in colour (tan/white), histological structures visible, no carbon deposition, no cracks through the matrix
200	Carbon accumulation in lacunae, general microscopic structure unchanged; Haversian systems, lamellae & osteocyte lacunae – intact; mineralised collagen fibres observed on Haversian system walls; endosteum start to disintegrate
300	Lamellar structure displays increased carbon and is tainted brown-black; cracks visible from Haversian systems radiating through bony matrix; H_2O removed from non-mineralised portion
400	Cracks radiate out further from Haversian systems through matrix; H_2O removed from non-mineralised portion
500	Majority of carbon is oxidized which renders the matrix a pale colour with many cracks; H_2O removed from non-mineralised portion
600	Cracks are numerous and abundant throughout the matrix; structure is visible; organic carbon burnt to CO_2 & eliminated; endosteum completely disintegrated; crystal formation occurs
700	Bony matrix shrinks, making the cracks wider; organic carbon burnt to CO_2 & eliminated
800	Microstructure largely disappeared due to fusion of apatite crystals; physiological hydroxyapatite changes to B-tricalcium phosphate; shrinkage due to recrystallization & crystal fusion
1400	Haversian canals and osteocyte lacunae still retain integrity
1600	All structural features of bone is lost; total melting & recrystallization of bone mineral (when cooled)

Chapter 3: Materials and Methods

An experimental, descriptive approach was used to investigate the relationship between thermal alteration of bone and five progressive stages of decomposition. This research attempts to quantify the varying suits of thermal alteration to the advancing process of decomposition.

3.1. Location of study

The study took place on the Forensic Anthropology Body Farm (FABF), which is located on the Miertjie Le Roux Experimental Farm and belongs to the Faculty of Natural and Agricultural Sciences of the University of Pretoria (Figure 3.1). The farm is 45 km outside of Pretoria along the N4 highway and is located at Kaalfontein 513 JR, District Cullinan in the Gauteng province. The farm icludes 570 hectares of dry land for maize production and pastures as well as a natural sour veldt for beef production. The map and satellite image show the terrain and provides an aerial view of the FABF enclosure and surrounding (Figures 3.2 & 3.3). The location of the FABF was selected in compliance with the regulations stipulated by the Department of Health (DoH). The enclosure needed to be 2 kms outside any urban housing or workplace and at least 200 m away from any natural water supply. Ethical clearance was obtained from the Environmental Biohazard Committee of the Faculty of Natural and Agricultural Sciences. Ethical approval was obtained from the Main Ethics Committee (134/2008). After the DoH received confirmation that the study adhered to all the above-mentioned criteria, the Faculty of Natural and Agricultural Sciences granted approval.

The enclosure was constructed in August of 2008. A 50 m x 50 m, 1.2 m high diamond-shaped wire fence was erected on a half hectare piece of land with an added gate to allow for entry and transport of the pig carcasses (Figures 3.2 and 3.3). The simple-style fence was chosen to reduce large, terrestrial carnivore activity, but scavenging from smaller mammals and birds was not prevented. Scavengers common to the area include jackals, muishonde and porcupines as well as crows and cattle egrets. All of these animals are capable of carrying off and therefore disturbing the original position of the carcass, especially in the later stages of decomposition when mostly skeletonised remains are left. On several

occasions (3 out of 25) larger scavenging animals such as jackals destroyed and relocated fresh pig carcasses. In these cases, the remains could not be utilised in the study, and new sample pigs were obtained. The 25 pigs that comprised the final sample did not have any damage from scavengers.

The South African climate is variable, ranging from sub-tropical (Eastern coastline) to desert and semi-desert regions (North Western parts), and is largely dependent on the altitude of the area and proximity to the ocean (Benhin, 2006). Climatic conditions are largely dependant on the altitude of the area and the proximity to oceans. Different altitudes and ocean proximity therefore allow climatic conditions of one region to vary considerably to the next (Benhin, 2006). The Miertjie Le Roux Experimental Farm is located inland on the central Highveld plateau. This area has warm, wind-free summers with an average temperature of 27.5^{o}C (January) and mild winters with temperatures averaging 18.3^{o}C (June); temperatures rarely drop below 0°C (http://www.saexplorer.co.za). Rainfall mainly occurs during the summer months. The humidity is low in most regions; however high humidity levels on the farm can be attributed to an underground river that runs through the region. South African vegetation can be defined as a homogeneous natural flora type comprised largely out of grassveld (Teie, 2005; Benhin, 2006). Five main vegetation types are predominant in South Africa and include; forestry plantations, savannah grasslands, fynbos, afromontane and lowland forest and Karoo (Teie, 2005). The study will only focus on climate and vegetation in one area of South Africa. Vegetation at the Miertjie Le Roux farm consists mostly of sour veldt grasslands. This collection of the data for this study took place between August 2008 to September 2011.

3.2. Materials

The sample was comprised of 25 adult, domesticated pigs (*Sus scrofa*) that were donated from two local pig farmers, Mr. T. van Deventer and Mr. M. Trollope, of Top Pig South Africa. Cause of death in all cases was attributed to common infections found in pigs living in large numbers and in close proximity to each other such as *Listeria monosytogenes*, *Escherichia coli* or *Clostridium perfringens*. Pigs with known dates of death and no signs of external trauma were used. Pigs ranged in mass from 50 to 100 kg. This range was used so as to reduce the effect of body size on the rate of decomposition and to ensure that a body size

similar to the range for adult humans was maintained. The pigs were classified as "Porkers" (60 to 70 kg) and "Baconers" (70 to 90 kg) (Agricultural Research Council, 1993).

Experimental research on decomposition and heat-induced changes has often made use of human and nonhuman models. The domesticated pig is the most common animal model used for taphonomic studies (DeHaan, 1997; DeHaan *et al.,* 1999; Herrmann & Bennett, 1999; de Gruchy & Rodgers, 2002; Adlam & Simmons, 2007; Megyesi *et al.,* 2005; Kolver *et al.,* 2001; van der Linde, 2003; Kolver *et al.,* 2003; Kolver & van der Linde, 2005). Animal models are primarily used due to the ethical issues involved in experimenting on cadavers and the restricted access to human remains for destructive research.

While animal models are not directly related to the human body, they do produce analogous results when the basic characteristics of heat-related changes such as colour change, burn pattern alteration (specific to pig anatomy) and limited fracture patterns to bone are examined. Nonhuman tissues (skin, fat, muscle, bone) serve as a good parallel model for experimenting with predictive modelling based on human remains, but limitations should be noted such as differential buttressing of the skeleton, differences in bone cortical thickness and tissue thickness comprising a portion quadrapedal anatomy (Pope, 2007).

3.3. Methods

3.3.1. Scoring the decomposition stage

The pigs were collected within 12 hours after death and placed, uncovered, on allocated spots on the FABF (Figure 3.4). The position of each pig was recorded on a grid (Figure 3.5), and a distance of at least 10 m separated all carcasses to ensure that insect colonisation from one pig did not cross-contaminate that of another. When placed on the ground, the pigs were randomly positioned on either their left or right sides.

From the sample of 25 pigs, five were exposed to fire in each of the four stages of decomposition; 5 for stage A (fresh), 5 for stage B (early decomposition), 5 for stage C (advanced decomposition) and 5 for stage D (skeletonisation). Since stage D (skeletonisation) is associated with adhering tissues and completely dry bone, the stage was subdivided into an early (D1) and late skeletonisation (D2) stage so that evaluations of burn pattern were performed on wet and completely dry bone.

The stage of decomposition (with TBS) was recorded for each pig prior to burning (Megyesi *et al.*, 2005). Total body scores (TBS) were calculated for each pig using the descriptions established by Megyesi *et al.* (2005) which are based on the original version of Galloway *et al*. (1989). An independent observer measured the decomposition stage for 10 randomly selected pigs as a means to test the reliability of scoring the stage of decomposition. As the manner and rate of decomposition differ between head and neck, thorax and limbs, scoring guidelines were separately applied to these three regions. Descriptions of the stages are shown in Tables 3.3., 3.4. and 3.5. (Megyesi *et al.*, 2005). The allotted point value was recorded from each region and added to reach the TBS, or the overall stage of decomposition for each pig. By taking the minimum and maximum scores possible for each stage, the following groups, pertaining to TBS, were established. A score equal to 3 places the pig in the fresh stage (A) of decomposition. TBS scores between and including 4 to 16 are assigned to the second stage of decomposition (stage B). TBS scores between, and including 17 to 24, fall within the third stage of decomposition (stage C). A TBS score that fell in the 25 to 32 range was considered to be in the early stage of skeletonisation (stage D1). Any TBS over 32 was considered to be in the late stage of skeletonisation (stage D2).

3.3.2. The burning process

For this project, an attempt was made to replicate a natural, outdoor veldt fire. Differential temperatures, ventilation, collapsing debris and reduction of the surrounding environment influence the complexity of natural fires. In order to start and maintain the fire, surrounding grass and bush was used in an open area. No accelerants (e.g., petrol or paraffin) were used.

According to the National Veldt and Forest Fires Act (No.101 of 1998) a veldt fire is defined as any fire that occurs outside the boundaries of an urban area and presents with the potential of getting out of control. Without preventative measures, veldt fires can continue to burn for as long as the weather is favourable and the vegetation remains a bountiful fuel source (Nkomo & Sassi, 2009; Siwele, 2011). To prevent the risk of creating an uncontrollable fire, a 1500 mm x 1200 mm perforated and mobile steel frame was constructed to surround the pig carcasses during the burning process (Figure 3.6). Each pig was exposed to fire for 30 minutes. The fire was intermittently (± every 5 mins) maintained with the addition grass and bush onto and around the carcass. Piling addional grass and flora

onto the carcass did not hinder the burning process. With this method, continuous exposure of the soft tissues to the flame was maintained. Sand was used to extinguish the fire after 30 minutes. The pigs were not disturbed or moved during the burning process.

The timeframe (30 min) of exposure was chosen not only to reduce the risk of losing control of the fire, but also because a body has been shown to display thermal alterations as soon as 10 minutes after exposure, and by 30 minutes the majority of bony elements are exposed enough to experience thermal damage (Bohnert *et al.*, 1998). A timeframe extending beyond 30 minutes was not considered, as many skeletal elements such as the cranium, small hand and foot bones and rib elements would have been destroyed. The aim was to expose the carcass to the fire for a period in which the majority of the skeletal elements could be recovered and therefore analysed for thermal alterations. The positions of the pigs were also noted prior to burning, because a carcass that is in direct contact with a hard surface may have protected areas that do not burn.

After the fire was extinguished, the steel frame was dismantled around the carcass. This cleared the immediate air of smoke. The direct areas surrounding the pigs were doused with water to prevent kindling a fire from the remnant ashes.

3.3.3. Recovery and processing

Approximately 10 minutes after burning, which was enough time for all the smoke to clear, photographs were taken of the pig carcass *in situ* (Figure 3.7). If large pieces of plant debris were obscuring the carcass, they were removed by hand without disturbing the under-lying remains. The pigs in the later stages of decomposition, which had little to no soft tissue present, were immediately collected. The remains were carefully packed into bags and transported to the Department of Anatomy, University of Pretoria, for further processing and analysis. Charred and calcined remains were packed in separate boxes so as to prevent postmortem damage during transport. Full and partially fleshed pigs were difficult to transport, so these pigs were left to decompose to a more advanced stage prior to removal.

If any of the pigs retained soft tissue, they were both processed and macerated. Pig elements were placed in linen bags and boiled in maceration pots at 100°C for approximately 6 to 12 hours (depending on amount of tissue present). Afterwards, bones were removed from the linen bags, and all adhering flesh was disposed of. Charred soft tissue that still adhered to

the bone was removed with gentle scrubbing under warm water; this did not damage the actual charred bone. The bones were left to dry for approximately 3 to 4 days. The pig elements were examined morphologically in a laboratory in the Department of Anatomy (Figure 3.8).

A scoring sheet with condensed definitions with associated ordinal values is provided in Appendix A. The state of decomposition of the pig was not known during analysis. One observer scored all 25 pigs. See Appendix A for the score sheet and Appendix B for the raw data collected.

3.3.4. Heat-related traits associated with burned bone

Thirteen heat-related traits were assessed and include a complete range of characteristics previously noted on burned remains (Mayne Correia, 1997; Thompson, 2005; Pope, 2007; Symes *et al*., 2008). Morphological features include 1) unaltered bone (Una), 2) charred bone (Cha), 3) calcined bone (Cal), 4) brown burn/border (BB), 5) heat border (HB), 6) heat line (HL), 7) delineation (D1), 8) greasy (Gr), 9) joint shielding (JS), 10) predictable cracking (PC), 11) minimal cracking (MC), 12) delamination (D2), and 13) heat-induced fractures (HIF). The scoring definitions, illustrations, scoring procedure and treatment of statistical analysis are described in the sections below.

Definitions for thermal alterations scored on the bones:

1) **Unaltered bone (Una):** displays no visual signs of thermal alteration (no colour change) (Figure 3.9). Tissue present at the time of exposure protected the bone from damage (Mayne Correia, 1997; Thompson, 2005; Pope, 2007; Symes *et al*., 2008).

2) **Charred bone (Ch):** represents carbonised skeletal material and is black in colour (Figure 3.9) (Mayne Correia, 1997; Thompson, 2005; Pope, 2007; Symes *et al*., 2008).

3) **Calcined bone (Ca):** is grey/white/blue/ash-brown coloured bone (Figure 3.10) (Mayne Correia, 1997; Thompson, 2005; Pope, 2007; Symes *et al*., 2008).

4) **Brown burn (BB)**: is brown discolouration due to heat exposure. Brown burn is located adjacent to a charred area and is not associated with a heat border (Figure 3.11) (Symes *et al*., 2008; Keough *et al*., 2012).

5) **Heat border (HB):** is an off-white/yellowish border located between charred and unaltered bone (Figure 3.12). The heat border has no direct contact with the fire and represents chemical alteration of the bone during heat exposure. Overlying albeit receding tissues protect the area during burning (Symes *et al*., 2008).

6) **Heat line (HL):** is a thin, whitish line directly adjacent to the heat border and represents the initial transition between unaltered and thermally altered bone (Figure 3.13) (Symes *et al*., 2008).

7) **Delineation (D1):** is present when a clear distinction is observed between unaltered bone, the heat line, heat border and charred area (Figure 3.12) (Symes *et al*., 2008; Keough *et al*., 2012).

8) **Greasy bone (Gr):** is a wet/oily surface and feel of the bone. All bones present with grease unless they are dry.

9) **Joint shielding (JS):** is when an area of joint articulation (e.g., mandibular fossa and mandibular condyle) is protected from thermal alteration often by surrounding ligaments (Symes *et al*., 2008; Keough *et al*., 2012). The area around the joint displays signs of thermal alteration, but the actual internal surfaces involved in the formation of the joint remain unaltered (Figure 3.14).

10) **Predictable cracking (PC):** is when small, clear heat fractures are observed parallel to the heat border (Figure 3.15). These fractures are present within the transition area between the heat border and the charred area (Pope, 2007; Symes *et al*., 2008; Keough *et al*., 2012).

11) **Minimal cracking (MC)**: is when a few random fracture lines are found within the heat-altered bone. These fractures are not associated with the mechanisms that create

predictable fractures, as described above, but result from direct exposure to heat/flame (Symes *et al*., 2008; Keough *et al*., 2012).

12) **Delamination (D2):** is the removal of the outer cortical layer of bone and subsequent exposure of the underlying spongy/cancellous bone (Figure 3.16) (Mayne Correia, 1997; Thompson, 2005; Pope, 2007; Symes *et al*., 2008).

13) **Heat-induced fractures (HIF):** are scored as present if one or more of the following are observed (Thompson, 2005; Pope, 2007; Symes *et al*., 2008):
    a) Longitudinal fractures: appear parallel to the long axis of the bone (Figure 3.17)
    b) Step fractures: occur in perpendicular lines on bone shafts and link two or more longitudinal fractures (Figure 3.17)
    c) Transverse fractures: occur perpendicular to the long axis of the bone but do not associate longitudinal fractures (Figure 3.18)
    d) Curved transverse fractures: also known as thumbnail or curvilinear fractures, form a group of curved arcs running along the long axis of the bone shaft (Figure 3.19)
    e) Patina fracturing: superficial checking on the bone that occur because of uniform heat exposure and resemble a fine mesh of uniformly patterned cracks to that which is in old paintings and china (Figure 3.20)

3.3.5. Scoring procedures for the colour changes associated with burned bone (features 1 – 3):

A ranking system was developed to score unaltered, charred and calcined bone. ***Each bone*** received a total of three scores; a score for the amount of unaltered bone, the amount of charred bone and the amount of calcined bone. These scores were dependant on the distribution of the colour changes observed on a single bone. The ranking system allows the quantification of the distribution of burn on a bone. The distribution of colour change on bone occurs in a uniform manner and is a cumulative process, i.e., one cannot have a score of 3 for all 3 categories. In order to use the ranking system, the following guidelines were developed:

- *Zero (0) score*: the surface presents with either no unaltered, no charred or no calcined areas. A zero is applied to either an unburned element or a uniformly burned element (Figure 3.21).

- *One (1) score*: if less than a quarter (<25%) of the bone surface remains thermally unaltered then a 1 is scored for unaltered bone; if less than a quarter (<25%) of the bone surface displays charred or calcined bone then the score of 1 is given and can be considered minimal thermal alteration (Figure 3.22).

- *Two (2) score*: if more than a quarter (>25%) but less than three quarters (<75%) of the bone surface remains unaltered a 2 is scored for unaltered bone; if charred or calcined bone is present on more than a quarter (>25%) but less than three quarters (<75%) of the bone surface then a 2 is scored for both charred and calcined and can be considered as moderate thermal alteration (Figure 3.23).

- *Three (3) score*: if more than three quarters (>75%) of the bone surface remains unaltered, then a 3 is assigned for unaltered bone; if more than three quarters (>75%) of the bone surface is charred or calcined then a 3 is scored for each and can be considered as extensive thermal alteration (Figure 3.24).

3.4. Inferential statistics: frequency distributions and density plots

3.4.1. Frequency distribution (Chi-squared statistics; Fisher's Exact Test)

Frequency distributions are the simplest method for analysing categorical (nominal) data and provide a display of the number of occurrences of a specific value in a data set (Samuels & Witmer, 2003). This form of analysis is often used to assess the distribution of categories (non-overlapping/mutually exclusive classes) in a sample. Chi-squared analysis is also a non-parametric test used to analyse data assumed not to reflect a normal distribution. This is calculated using the absolute frequencies of all the categories and utilising the observed frequency of a category as well as the expected frequency which would be expected according to the null hypothesis H_o (Samuels & Witmer, 2003). The chi-squared test is

commonly used to evaluate the significance of the observed relationship between categorical variables and whether the relationship can be used to make inferences about the sample and the larger population (Samuels & Witmer, 2003). Chi-squared analysis does not provide information about the strength of the relationship but only conveys the existence or nonexistence of the relationships between the variables investigated. The strength is determined with utilising the Fisher's Exact test.

Fisher's Exact test is used when two nominal variables as well as the expected vlaues are small. This test is more accurate than a chi-squared test when using a smaller sample size and is known as an "exact" test because it determines the p-value using exact calculations rather than a p-value based on asymptomatic approximation as with chi-squared statistics (Samuels & Witmer, 2003). When applying Fisher's Exact test of a null hypothesis against a directional alternative, the hypergeometric distribution is used to calculate the probability of getting the observed data. This provides evidence strongly against the null hypothesis, $H_{o.}$

3.4.2. Kernel density plots

A kernel density estimate is a non-parametric graph (no underlying probability density function) that is constructed based on the observations in the dataset (Crosbie & Corliss, 2012). The idea of a kernel estimate is to replace each datum point (x_i, $i = 1,..., n$) by a specified distribution which is centered on the point with a standard deviation designated by h (Thompson, 2006). The normal distributions are added together, resulting in smooth curves (kernel density estimate) that express the distribution having been scaled to a unit area; the kernel density estimate is given by:

$$\hat{f}(x,h) = \frac{1}{nh}\sum_{i=1}^{n} \emptyset\left(\frac{x - x_i}{h}\right)$$

where $\hat{f}(x,h)$ is the height of the curve at x, and $\emptyset$ is the standard normal density. The appearance of the kernel density is dependent on the value of the smoothing parameter h. When the kernel estimate is calculated with an appropriate value of h, a good estimate of the population density function is given but without making assumptions, i.e., it is a normal distribution.

3.5. Multi-variable regression analysis and transition analysis

3.5.1. Multi-variable regression analysis (categorical variables)

Regression analysis provides imformation as to the strength of a relationship between decomposition, represented as TBS, and one or more heat-related variables. The strength between variables is determined with correlation analysis and the mathematical equation used to predict one variable knowing the value of the other variable is determined with regression analysis (Greenfield *et al.*, 1998). By applying regression analysis, the relationship between the distribution of unaltered, charred and calcined bone and the progressive decomposition stages are more closely examined than with frequency distributions and density plots.

Multi-variable regression analysis for categorical variables is similar to directly standardised rates for regression but includes the possibility of adjusting for many variables at one time (Kahn, 1983). Once a relationship between variables is established, the strength and statistical significance of that relationship is determined (Greenfield et al., 1998). In order to accomplish this, the coefficient of determination (r2) is used and provides the percent of variance in the dependent variable that can be jointly explained by the variation in the independent variables (Greenfield *et al.*, 1998; Becker P, pers. comm.). In other words, r^2 provides the correlation between variables and the possible success of these variables in a predictive equation. However, the r^2 is not able to demostrate which of these variables are more important than the others.

Multi-variable regression analysis is a linear transformation of the X variables such that the sum of squared deviations of the observed and predicted Y is minimised. The prediction of Y is accomplished with the following equation:

$$Y_i = b_0 + b_1 X_{1i} + b_2 X_{2i} + \cdots + b_k X_{ki}$$

The "b" values are called regression weights and are computed in a way that minimises the sum of squared deviations. Normal multi-variable regression analysis can be extended to include categorical variables. In order to do this, dummy variables are created to add ordinal variables to the equation. The steps include recoding the categorical variables into a number of individual, dichotomous variables which in known as "dummy coding". Categorical variables with *k* levels are transformed in *k-1* variables each within two levels.

Two properties define a dummy variable which include the fact that they are categorical and non-ordinal. The number values associated with each category serve only to identify the various groups/categories it represents, but not to assign a value or order to any one category. The second (which makes a dummy variable a "dummy variable"), is that the variable binary as it has two values: 0 or 1. Technically, a variable like decomposition or distribution of calcined bone have more than 0 and 1 values, but when this type of dummy variable is used in a regression equation, coefficients are calculated for each category, while all other categories are equal to zero. Thus, if done correctly, even a multi-categorical variable can be used as a dummy variable, because ultimately, it is broken up into 0s and 1s (Institute for Digital Research and Education, 2013; Multiple Regression with Categorical Data, 2013; Stockburger, 2013).

Dummy variables are useful in that they control for membership within a particular category or group. If a categorical variable is not split into several dummy variables when using regression analysis, the results are invalid, because regression analysis assumes variables to be continuous unless told otherwise. Regression analysis revolves around the use of means and standard deviations, but with categorical variables, means and standard deviations do not have meaning (Institute for Digital Research and Education, 2013; Multiple Regression with Categorical Data, 2013; Stockburger, 2013).

The relationship between heat-induced colour changes and TBS was examined. The distribution of colour change on bone is measured in four categories (score = 0, 1, 2, 3). The **xi** command in STATA is used to create indicator variables (dummy variables) and then run the multi-variable regression, as shown in Table 3.7. The command **xi** includes the term i.cr_cal, i.cr_cha, i.cr_una in the model, with created dummy variables; Cr_Cal_1, Cr_Cal_2, Cr_Cal_3, Cr_Cha_1, Cr_Cha_2, Cr_Una_1, Cr_Una_2 and Cr_Una_3. Looking at calcined bone on the cranium the following dummy variables were developed: Cr_Cal_1, Cr_Cal_2 and Cr_Cal_3. Cr_Cal_1 is equal to 1 if Cr_Cal is scored as 1 and 0 otherwise. Likewise, Cr_Cal_2 is 1 if Cr_Cal is scored as 2, and 0 otherwise, and likewise with Cr_Cal_3 (Table 3.6).

When interpreting a multi-variable regression that uses dummy variables, if four dummy variables are present, only three are included in the equation. If all dummy variables are included the model would essentially become overspecified. Overspecification of a model arises when several correlated variables are related to a single response and if ignored can lead to unstable estimates of regression coefficients and large prediction errors (Elston &

Proe, 1995). Whenever a dummy variable is used, there should always be an default omitted category (reference category), in this study the omitted category is score =0. If a variable is omitted it does not mean that the equation is ignoring that group but rather specifying the coefficients for score =1, score = 2 and score = 3 are shown. However, the coefficient for the omitted category (score = 0) can be known from the results. In omitting score = 0 category, the cases were not dropped but rather shifted into the constant and used as a comparison group in that the constant equals the mean for the group where the score = 0. The interpretation of the coefficients is similar to binary variables. The coefficient for Cr_Cal_1 is the mean for the group scoring 1 minus the mean of the omitted group (score = 0) and the coefficient for Cr_Cal_2 is the mean of the group scoring 2 minus the mean of the group scoring 1.

The equations formulated when applying categorical variables is a basic extension of a general multi-variable regression equation. This equation, specifically for the cranium, shows the effect heat-induced colour changes with the increase in TBS (Table 3.7). The model explains almost 87% of the variation around our independent variable, or TBS (adj r-squared = 0.87). The equation from Table 3.7 looks as follows;

$$(TBS) = 6.4 + 8.3\ (cr\_cal\_1 = 1, else = 0) + 13.3\ (cr\_cal\_2 = 1, else = 0) + 16\ (cr\_cal\_3 = 1, else = 0) + 11.6\ (cr\_cha\_1 = 1, else = 0) + 7.77\ (cr\_cha\_2 = 1, else = 0) + 0.5\ (cr\_una\_1 = 1, else = 0) - 4.5\ (cr\_una\_2 = 1, else = 0)$$

The equation allows the calculation of the predicted TBS for a cranium that has 3 scores; calcined score, charred score and an unaltered score. For example; if a cranium is scored a 1 for calcined bone, a 2 for charred bone and a 2 for unaltered bone, a 0 or a 1 is used for whether the cranium falls within the particular category or not;

$$\begin{aligned}(TBS) &= 6.4 + 8.3(1) + 13.3(0) + 16(0) + 11.6(0) + 7.77(1) + 0.5(0) - 4.5(1)\\ &= 6.4 + 8.3 + 7.77 - 4.5\\ &= 17.97 \pm 4.2\ (MSE)\end{aligned}$$

Therefore, predicted TBS = 18 ± 4.2 for a cranium that was scored a 1 for calcined bone, a 2 for charred bone and a 2 for unaltered bone. Cr_Una_3 was omitted due to multi-

collinearity because of the dependency among the independent variables in the proposed model (Becker, pers. comm.).

Multi-collinearity is not considered a problem when the main outcome of the regression analysis is estimation/prediction (Becker, pers. comm.). If there is a near perfect relationship among predictors, the estimates for a regression model cannot be uniquely computed, and the variable is omitted. This correlation between independent variables is only seen as a hazard when interpretation of the variables themselves becomes the reason for the regression analysis. Table 3.7 shows the confidence intervals for each predictor value. The confidence interval provides the estimated range which is likely to include an unknown sample parameter, the estimated range being calculated from the given set of sample data. This interval is also ideal to quantify the degree of uncertainty around common parameters of interest, such as the sample mean, or its spread (Ramírez, 2009). In this study a 95% confidence interval was chosen which means that the probability of observing a value outside of the normal curve is less than 5%.

3.5.2. Transition analysis (Boldsen *et al*., 2002)

Transition analysis can be used with any trait/process that is arranged into an invariant series of senescent stages. While the precise timing of transition from one stage to the next presumably varies, the direction of the sequence is essentially fixed, for example, decomposition occurs in a unidirectional fashion. In order to determine the relationship between decomposition and the specific heat-related traits in the reference sample, some form of regression analysis is normally applied. The problem is deciding whether to regress c_j on a or a on c_j where c_j represents the set of heat-induced traits observed in the j-*th* skeleton in the sample and a represents the stage of decomposition. The two regression lines are often different. If a is regressed on c_j a value for a for each value of c_j, is estimated. In most cases this is the required outcome but modelled estimates are often sensitive to the specifics of the reference sample.

In many anthropological or taphonomy studies a point estimate of X (factor being estimated) or even a fixed interval is not necessarily needed, but rather the whole probability density function ($\Pr(a \backslash c_j)$) which is calculated separately for each skeleton and for every value of a. ($\Pr(a \backslash c_j)$) is the probability that the skeleton is in a specific stage of decomposition (a) given that it has characteristics c_j, where c_j is the set of skeletal traits (heat-related) observed

in the j-*th* skeleton in the sample. If the confidence interval should be estimated around the point estimate of stage for the *j-th* skeleton, it should be based directly on the density function ($\Pr(a \backslash c_j)$ or something closely related to it. This form of analysis eliminates the need for an arbitrary stage interval since some of the uncertainty with decomposition is statistically reconciled.

3.5.2.1. Transition analysis for heat-related traits and decomposition stage

The process followed in this study closely mimics that which is described Boldsen *et al*. (2002). However, the statistical process described in their study was for estimation of a continuous parameter (age), whereas in the present study the method was applied to a discrete classification system of the level of decomposition that exists in a bone element before thermal alteration. This is a novel approach to investigating the relationship between decomposition and burn-related characteristics on skeletal elements.

First, an exponential generalised linear model was fitted to the heat-related colour changes for each individual bone (McCullagh, 1980; McCullagh & Nelder, 1989). This was done using the program R, the code of which is provided in Appendix C. The assumption was made that the developmental trajectory for the skeletal element could be broken down into an invariant sequence of *s* distinct, non-overlapping stages, and that the heat-related changes are strictly unidirectional with respect to those stages. In other words all bones presumably start off in stage A (first stage of decomposition). This is a reasonable assumption, since all bone are considered fresh at death and subsequently progress through the other four stages of decomposition. This means that $P(y_i \geq 0 | j) = 1$, since one always starts by classifying in stage 0 and then bones can move from this stage as they continue to decompose. The continuation ratio model (Fienberg, 1977; Agresti, 1990; Lindsey, 1995a, 1995b; Long, 1997) was therefore used to fit a series of binary logistic models as:

$$P(y_i \geq i | j) = \prod_{k=1}^{i} \Lambda(\alpha_k + \beta_{k,j})$$

Where y_i is the category of classification that can be made for the level of heat-related indicators (0,1,2,3), *i* is the level 1, 2 or 3, *j* is the given level of decomposition (A, B, C, D,

E), $\Lambda\left(\alpha_i + \beta_k a_j\right)$ is the hazard function $\frac{\exp\left(\alpha_k + \beta_{k,j}\right)}{1+\exp\left(\alpha_k + \beta_{k,j}\right)}$ where α_k and $\beta_{k,j}$ are the parameter estimates. This is represented by P(Y>=*i*|*j*). The probability of a bone element being classified in exact indicator *i* given a specific stage of decomposition *j* is then:

$$P\left(y_i = i \middle| j\right) = P\left(y_i \geq i \middle| j\right) - P\left(y_i \geq i+1 \middle| j\right)$$

by Bayes's theorem which states that:

$$P\left[A \middle| B\right] = \frac{P\left[A\right] P\left[B \middle| A\right]}{P\left[B\right]}$$

If we assume a uniform prior distribution for the level of decomposition (i.e., any skeletal element found has an equal probability of being in any state of decomposition before classification), we can find the probability mass function for the level of decomposition conditional on the classification of specific heat-related alterations on individual bone elements:

$$P\left(j \middle| y_j = i\right) = \frac{P\left(y_j = i \middle| j\right)}{\sum_{k=0}^{3} P\left(y_j = k \middle| j\right)}$$

For the binary indicators a similar approach was used, except that a generalised linear model was fitted instead of the continuation ratio model, as only one binary logistic model had to be fitted and not a series. The additional step of finding $P\left(y_i \geq i \middle| j\right)$ is eliminated, since from the estimates of the parameters of the hazard function we can immediately deduce that:

$$P\left(y_j = 1 \middle| j\right) = \Lambda\left(\alpha_i + \beta_{i,j}\right).$$

3.6. Inter- and intraobserver statistics (Intraclass correlation determination & Kappa statistics)

Inter- and intraobserver errors were also determined using intraclass correlation and kappa statistics to establish the repeatability of scoring the decomposition stage as well as determining the repeatability of scoring the various burn characteristics. Ten randomly selected pigs were then re-scored by observer 1 (the author) as well as an independent observer 2 (the supervisor). While scoring, both observers were unaware of the actual PMI and stage of decomposition to prevent bias in scoring of the traits.

3.6.1. Interobserver analysis for scoring decomposition stage prior to burning

The aim of intraclass correlation (ICC) is to determine the reliability of the proposed method for scoring the stages of decomposition and estimating the TBS. An external observer scored decomposition for the head and neck, trunk, limbs and the resulting TBS for 10 randomly selected pigs in the sample on the same day as the primary observer. The two observers did not influence each other during scoring.

The procedure of ICC is based upon the analysis of variance and the estimation of variance components. The key difference between ICC and Pearson correlation is that the data are pooled to estimate mean and variance. Therefore, the advantage of determining ICC over Pearson correlation is that it adjusts for the effects of the scale of measurements and represents agreements among more than two raters or measuring methods (Shrout & Fleiss, 1979; McGraw & Wong, 1996).

A distinction is made among three study models: 1) each subject is rated by a different and random selection of a pool of raters, 2) each subject is rated by the same raters, and 3) the model makes no assumption regarding the subject or raters. In the first model, the ICC is always a measure for absolute agreement; in the second model a choice is made between two types: consistency when systematic differences between raters are irrelevant, and absolute agreement when systematic differences are relevant (Shrout & Fleiss, 1979; McGraw & Wong, 1996).

ICC can be interpreted as follows; 0 – 0.2 indicates poor agreement; 0.3 – 0.4 indicates fair agreement; 0.5 – 0.6 indicates moderate agreement; 0.7 – 0.8 indicates strong

agreement; and >0.8 indicates almost perfect agreement (Shrout & Fleiss, 1979; McGraw & Wong, 1996).

3.6.2 Inter- and intraobserver analysis for scoring the burn-related traits

Inter- and intraobserver error analysis was conducted to determine the level of repeatability of the scoring system. Kappa statistics were used to run inter- and intra-rater reliability in order to determine the consistency of scoring various burn-related traits among observers. The consensus for categorical data is measured by the number of agreements divided by the total number of observations. Two observers independently rated a set of ranked categorical variables. The first observer scored a set of 13 heat-related variables from a sample of 25 pig skeletons over a period of two years. For the purpose of intraobserver agreement, the scoring procedure was repeated on 10 pig skeletons 9 months after the original data collection. Similarly, a second observer scored the 13 heat-related traits on 10 pig skeletons.

The main focus of this classification procedure was to assess the precision with which the given material was classified by the two independent observers. If there were high measures of agreement, then consensus in the diagnosis and interchangeability of the observations is indicated. According to Banerjee *et al*. (1999), many statistical methods exist to measure agreement between observers. However, not all the methods incorporate the amount of agreement which can result from chance alone. Cohen's Kappa statistics (k) measures agreement between observers with a change-corrected factor incorporated in the equation. Cohen's Kappa reduces the observed proportion of agreement by the expected level of agreement, given the observed marginal distributions of the rater's responses and the assumption that the rater reports are statistically independent (Banerjee *et al.*, 1999).

If the raters are in complete agreement then $k = 1$. If there is no agreement among the raters, other than what would be expected by chance, then $k \leq 0$. Kappa can be interpreted as follows; 0 – 0.2 indicates poor agreement; 0.21 – 0.4 indicates fair agreement; 0.41 – 0.6 indicates moderate agreement; 0.61 – 0.8 indicates strong agreement; and 0.81 – 0.99 indicates almost perfect agreement. Table 3.6 presents an overall scale for interpretation of the kappa value.

Figure 3.1 Forensic Anthropology Body Farm (FABF): Location of study on the Miertjie Le Roux Experimental farm

Figure 3.2 A road map indicating the location of the FABF (black and red square) (Picture taken from Google maps, 2010).

Figure 3.3 The FABF enclosure indicated by red arrow (Picture taken from Google maps, 2010).

Figure 3.4 Pig carcass (fresh stage of decomposition, TBS = 3)

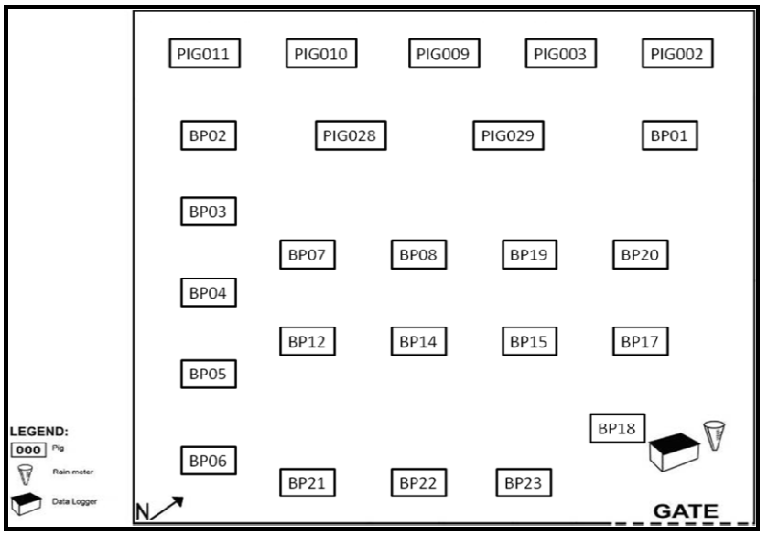

Figure 3.5 Grid layout of farm showing the positions of the 25 pigs

Figure 3.6 Steel framework for fire containment

Figure 3.7 Pig carcass: *in situ* before and after a burn event

Figure 3.8 Processed, post-burn pig elements

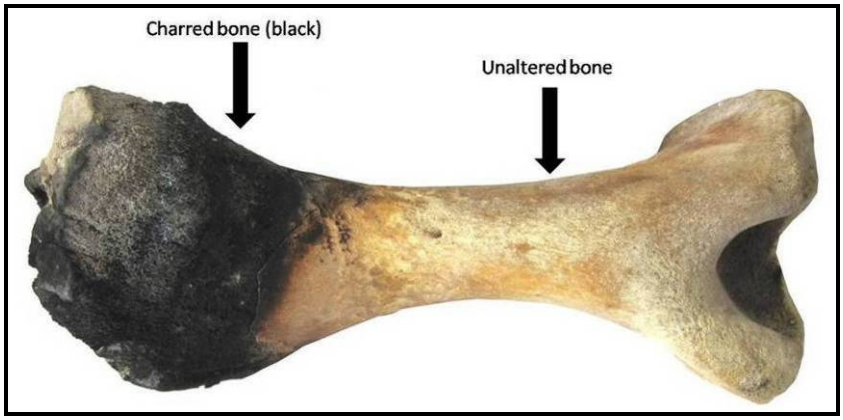

Figure 3.9 Charred proximal humerus of domesticated pig (blackened area)

Figure 3.10 Calcined tibia of domesticated pig (*Sus scrofa*)

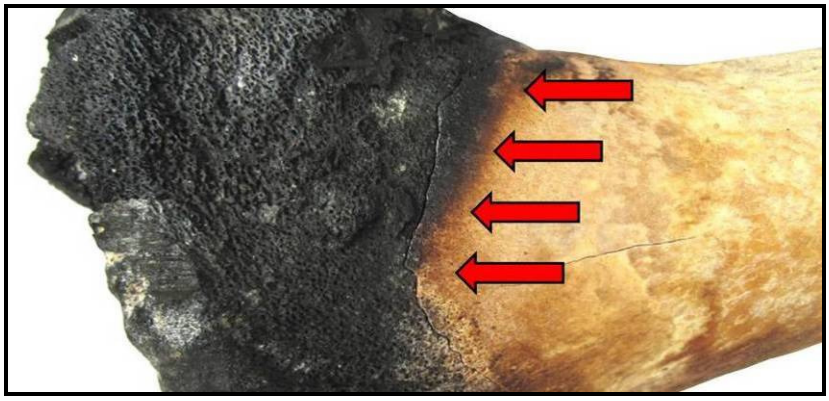

Figure 3.11 Brown burn adjacent to charred area

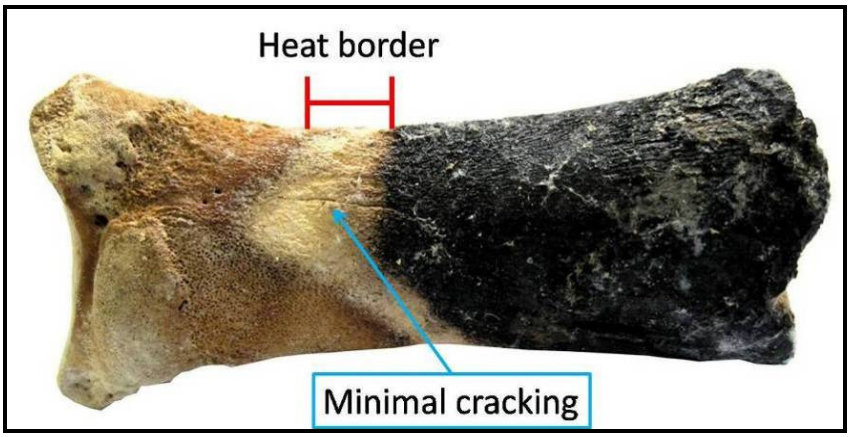

Figure 3.12 Heat border with clear distinction between charred bone, heat border and unaltered bone (delineation)

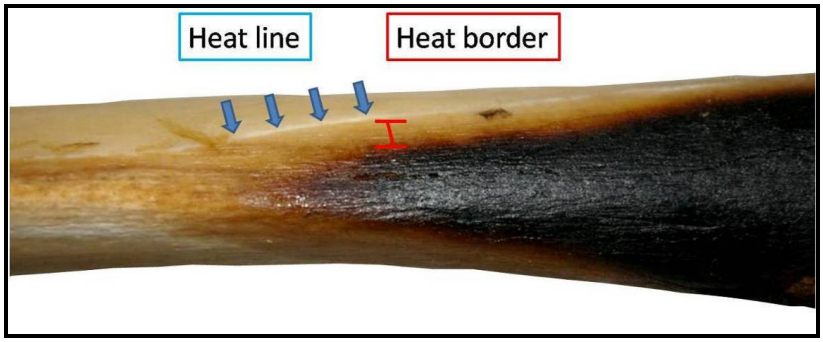

Figure 3.13 Heat line (blue arrows) adjacent to the heat border (red bracket)

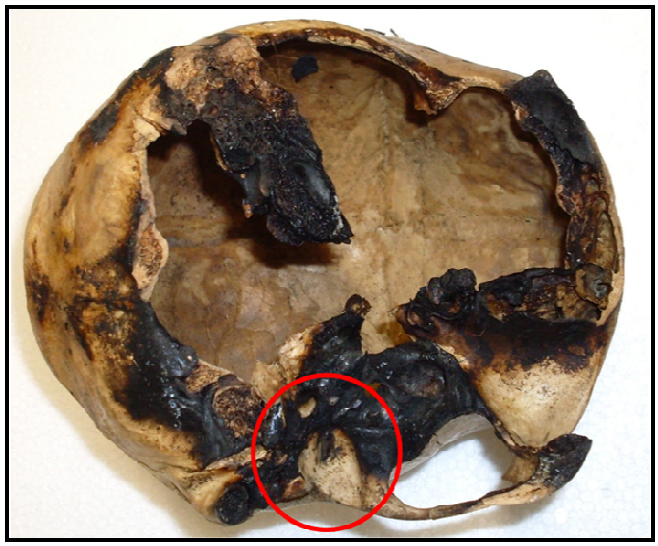

Figure 3.14 Basal view of human skull showing the unaltered mandibular fossa surrounded by charred bone (joint shielding)

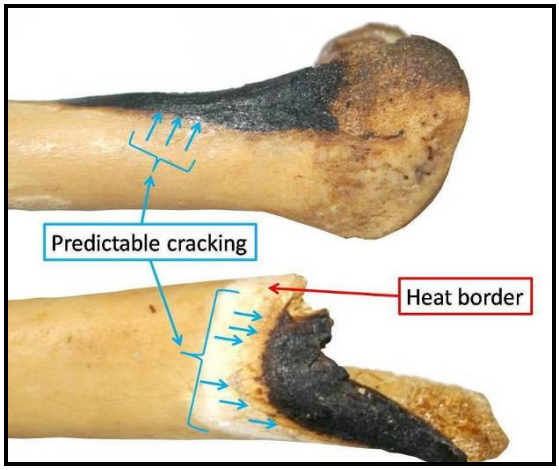

Figure 3.15 Predictable cracking along the transition area between charred bone and the heat border

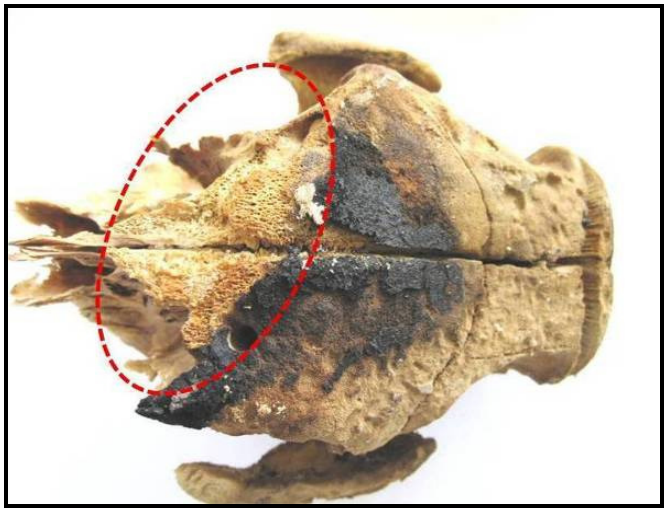

Figure 3.16 Delamination of the cranium with exposure of underlying cancellous bone

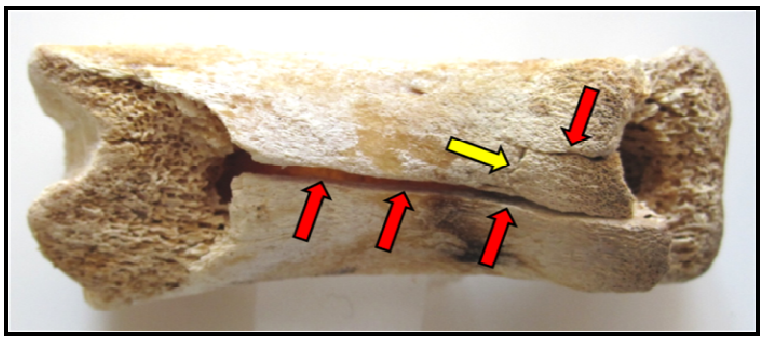

Figure 3.17 Longitudinal fractures (red arrows) and a step fracture (yellow arrow)

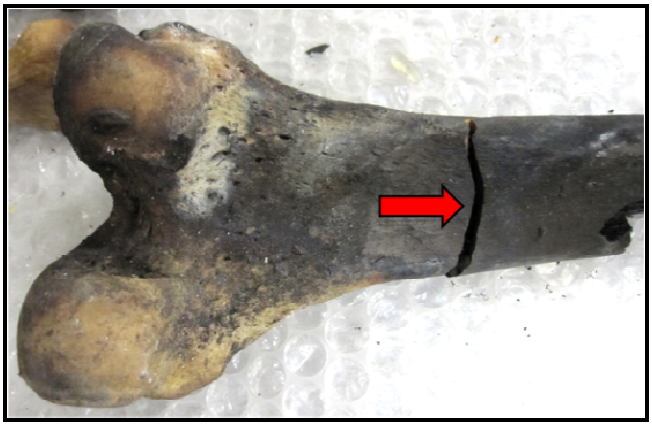

Figure 3.18 Transverse fracture of the distal femur shaft

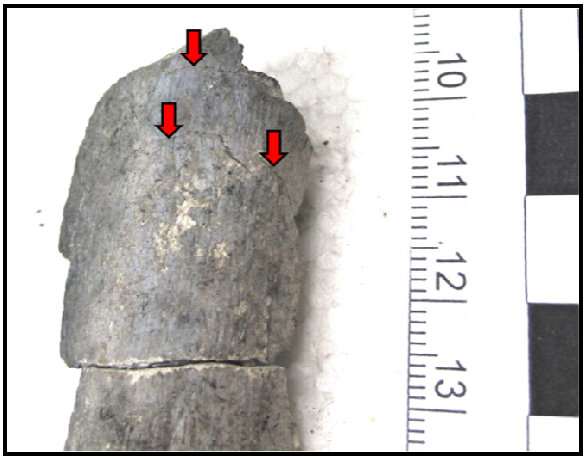

Figure 3.19 Curved transverse fractures along a femoral shaft

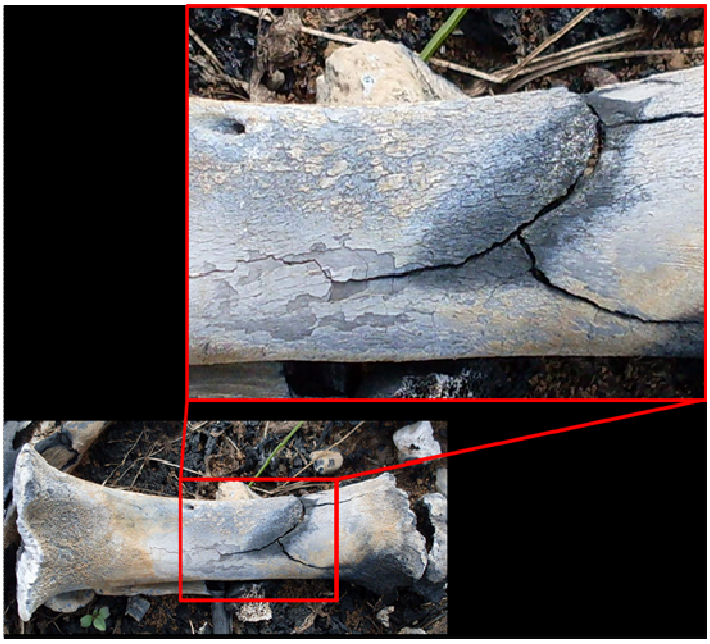

Figure 3.20 Patina fracturing on the shaft of a tibia

Figure 3.21 Completely unaltered bone (no thermal destruction). These bones would score a zero (0) for both calcined and charred and a three (3) for unaltered *[Score for bones above: Calcined = 0; Charred = 0; Unaltered = 3]*

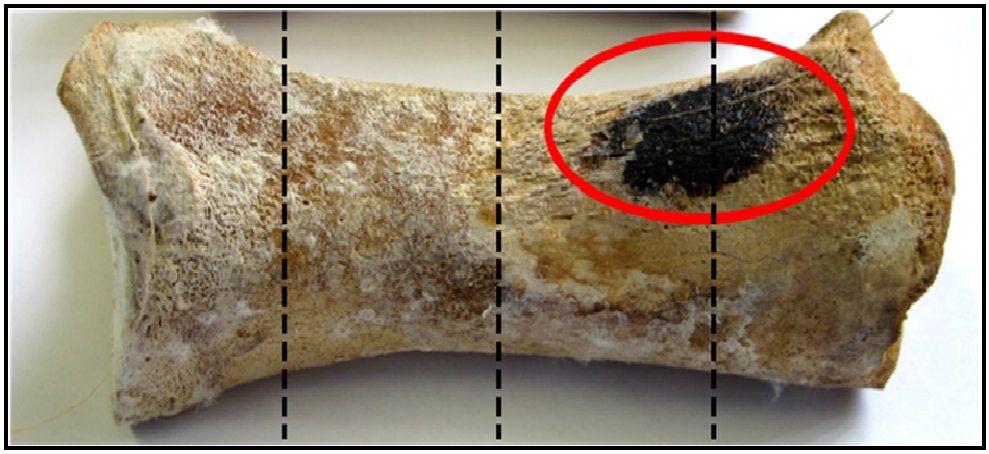

Figure 3.22 Score 1 for *charred bone* (red circle): thermal alteration in the form of charred bone is visible on less than a quarter (<25%) of the bone surface; the rest of bone remains thermally unaltered and would therefore score a 3 for unaltered bone. No calcined bone is present and would therefore score a 0 for calcined bone. *[Score for bone above: Calcined = 0; Charred = 1; Unaltered = 3]*

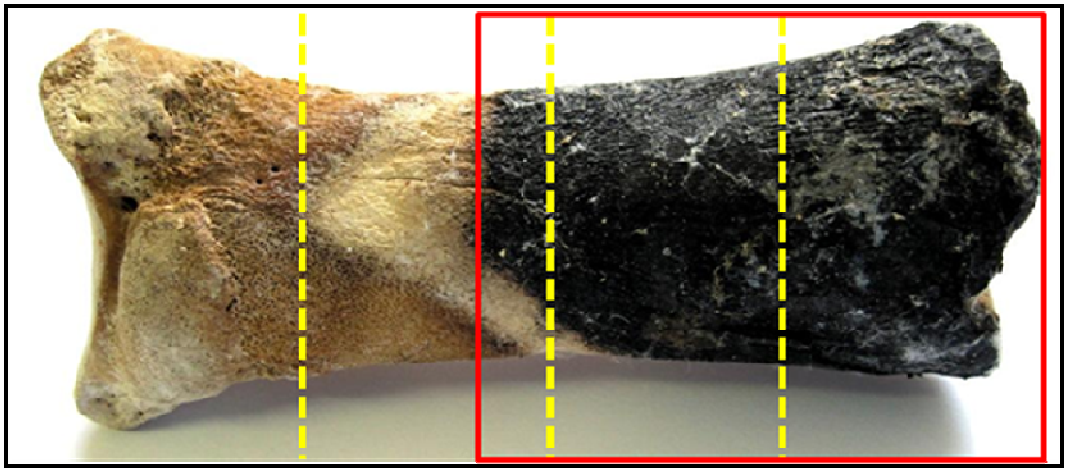

Figure 3.23 Score 2 for *charred bone* (red square): more than a quarter (>25%) but less than three quarters (<75%) of the bone displays charred thermal alteration. More than a quarter (>25%) but less than three quarters (<75%) of the remaining bone surface remains unaltered and would therefore score a 2 as well. No calcined bone is observed on the bone and therefore would score a 0 for calcined bone; *[Score for above bone: Calcined = 0; Charred = 2; Unaltered = 2]*

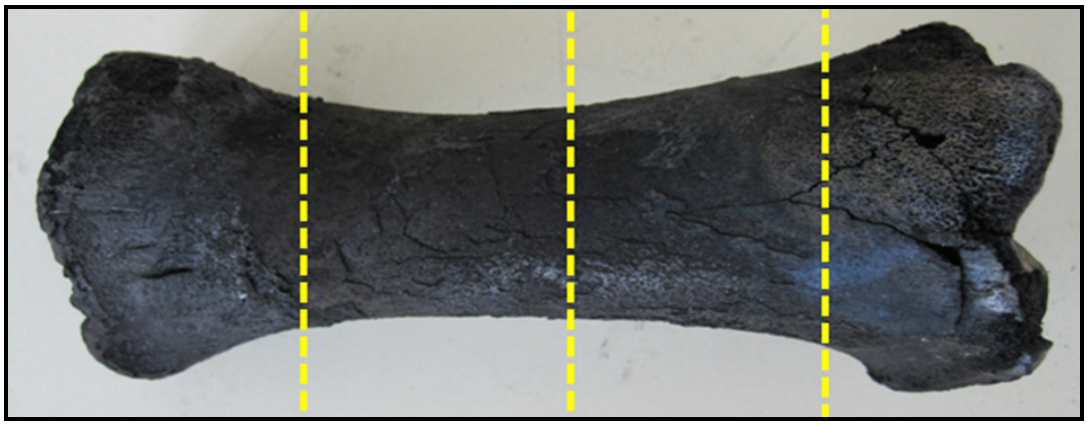

Figure 3.24 Score 3 for charred bone: thermal alteration covers more than three quarters (>75%) of the bone surface. No calcined or unaltered surfaces are present and would therefore score a 0 for both calcined and unaltered bone. *[Score for above bone: Calcined = 0; Charred = 3; Unaltered = 0]*

Table 3.1 Categories and stages of decomposition for the head and neck (Megyesi *et al.*, 2005)

Category	Points	Description
A: Fresh	1	Fresh, no discolouration
B: Early	2	Pink, white appearance with skin slippage & hair loss
	3	Grey to green discolouration: some flesh still relatively fresh
	4	Discolouration and/or brownish shades particularly at the edges, drying of nose, ears and lips
	5	Purging of decomposition fluids out of eyes, ears, nose and mouth, some bloating of neck and face may be present
	6	Brown to black discolouration of the flesh
C: Advanced	7	Caving in of flesh and tissues of eyes and throat
	8	Most decomposition with bone exposure of less than one half of the area being scored
	9	Mummification with bone exposure of less than one half of the area being scored
D: Skeletonisation	10	Bone exposure of more than one half of the area being scored with greasy substances and decomposed tissue
	11	Bone exposure of more than one half of the area being scored with desiccated or mummified tissues
	12	Bone largely dry, but retaining some grease
	13	Dry bone

Table 3.2 Categories and stages of decomposition for the trunk (Megyesi *et al*., 2005)

Category	Points	Description
A: Fresh	1	Fresh, no discolouration
B: Early	2	Pink, white appearance with skin slippage and marbling present
	3	Grey to green discolouration: some flesh still relatively fresh
	4	Bloating with green discolouration and purging of decompositional fluids
	5	Post-bloating following release of abdominal gases, with discolouration changing from green to black
C: Advanced	6	Decomposition of tissue producing sagging of flesh; caving in of the abdominal cavity
	7	Most decomposition with bone exposure of less than one half of the area being scored
	8	Mummification with bone exposure of less than one half of the area being scored
D: Skeletonisation	9	Bones with decomposed tissue, sometimes with body fluids and grease still present
	10	Bones with desiccated or mummified tissue covering less than one half of the area being scored
	11	Bone largely dry, but retaining some grease
	12	Dry bone

Table 3.3 Categories and stages of decomposition for the limbs (Megyesi *et al.*, 2005)

Category	Points	Description
A: Fresh	1	Fresh, no discolouration
B: Early	2	Pink, white appearance with skin slippage of hands and/or feet
	3	Grey to green discolouration, marbling, some flesh still relatively fresh
	4	Discolouration and/or brownish shades particularly at the edges, drying of fingers, toes, and other projecting extremities
	5	Brown to black discolouration, skin having a leathery appearance
C: Advanced	6	Most decomposition with bone exposure of less than one half of the area being scored
	7	Mummification with bone exposure of less than one half of the area being scored
D: Skeletonisation	8	Bone exposure of more than one half of the area being scored, some decomposed tissue and body fluids remaining
	9	Bone largely dry, but retaining some grease
	10	Dry bone

Table 3.4 Dummy variables for cranium calcined (Cr_Cal)

	Dummy variables			
Score	**Cr_Cal_0**	**Cr_Cal_1**	**Cr_Cal_2**	**Cr_Cal_3**
0	1	0	0	0
1	0	1	0	0
2	0	0	1	0
3	0	0	0	1

Table 3.5 Multiple regression for categorical variables example for the cranium (cr_cal = cranium calcined; cr_cha = cranium charred; cr_una = cranium unaltered)

```
xi: regress  tbs i.cr_cal i.cr_cha i.cr_una
note: 3.cr_una omitted because of collinearity

      Source |       SS       df       MS              Number of obs =      25
-------------+------------------------------           F(  7,    17) =   22.98
       Model |  2782.97333     7  397.567619           Prob > F      =  0.0000
    Residual |  294.066667    17  17.2980392           R-squared     =  0.9044
-------------+------------------------------           Adj R-squared =  0.8651
       Total |     3077.04    24      128.21           Root MSE      =  4.1591

------------------------------------------------------------------------------
         tbs |      Coef.   Std. Err.      t    P>|t|     [95% Conf. Interval]
-------------+----------------------------------------------------------------
      cr_cal |
          1  |   8.333333   3.796713     2.19   0.042     .3229682     16.3437
          2  |   13.33333   6.353117     2.10   0.051    -.0705712    26.73724
          3  |         16   4.362092     3.67   0.002     6.796791    25.20321
             |
      cr_cha |
          1  |       11.6   3.221618     3.60   0.002      4.80298    18.39702
          2  |   7.766667   7.000794     1.11   0.283    -7.003717    22.53705
             |
      cr_una |
          1  |         .5   3.221618     0.16   0.878     -6.29702     7.29702
          2  |       -4.5    3.94566    -1.14   0.270    -12.82462    3.824616
          3  |  (omitted)
             |
       _cons |        6.4    1.31522     4.87   0.000     3.625128    9.174872
------------------------------------------------------------------------------
```

Table 3.6 Interpretation of Kappa (Viera & Garrett, 2005)

Kappa	Agreement
< 0	Less than chance agreement
0.01 – 0.20	Slight agreement
0.21 – 0.40	Fair agreement
0.41 – 0.60	Moderate agreement
0.61 – 0.80	Substantial agreement
0.81 – 0.99	Almost perfect agreement

Chapter 4: Results

In order to associate heat-induced burn characteristics on bone with progressive stages of decomposition, **three** statistical procedures were used. The heat-related features include; heat-induced colour change (unaltered, charred, calcined), the presence/absence of brown burn/borders, heat borders, heat lines, delineation, greasy bone, joint shielding, predictable and minimal cracking, delamination and heat-induced fractures. This analysis was done in an attempt to associate the above-mentioned heat-related burn changes in bone with the various stages of decomposition in order to assist in the estimation of a PMI interval as well as to demonstrate differences between fleshed, wet and dry bone.

First, inferential statistics were established via the frequency distributions of the above-mentioned heat-related features within the five stages of decomposition (fresh, early, advanced, early skeletonisation, late skeletonisation); Chi-squared and Fisher's Exact tests are used to establish statistical significance and trends are graphically presented with density plots. Second, multiple regression analysis for categorical variables and transition analysis is used to assess whether heat-induced colour change can significantly estimate the stage of decomposition. Based on the nature of the sample as well as the variabilities in burned bone, these equations provide insight into the relationship of the variables with TBS and should not be used to predict TBS from an unknown case.

The repeatability and reproducibility of scoring the stage of decomposition and scoring heat-induced traits is evaluated with intraclass correlation (ICC) determination and Cohen's Kappa, respectively.

4.1. Inferential statistics

Frequency distributions and kernel density plots of the scores for the heat-induced colour changes, namely unaltered, charred and calcined bone are tabulated for all skeletal elements across the five stages of decomposition; A) fresh stage, B) early stage, C) advanced stage, D1) early skeletonisation and D2) late skeletonisation. Frequency distributions and kernel density plots for binominal traits, namely the presence or absence of a brown border, heat border, heat line, delineation, greasy, joint shielding, predictable cracking, minimal cracking, delamination and heat-induced fractures, are also constructed.

The usefulness of features related to heat exposure for evaluating decomposition is dependent on whether that change/alteration is useful in distinguishing fleshed, wet and dry bone from each other; basically one decomposition period from another. This point needs to be considered when these changes/alterations are used to estimate broad decomposition categories from remains that were burned for an unknown period of time. In Tables 4.1 to 4.19 and Figures 4.1 to 4.38, only the statistically significant ($p<0.05$) influences of heat-induced colour change and burn-related traits (brown burn/borders, greasy bone, delamination, heat-induced fractures) are presented; the full set of data is available in Appendix D and Appendix E.

4.1.1. Head and neck: Frequency distribution and kernel density plots

In Tables 4.1, 4.2 and 4.3, progressive colour changes in burned bone for the head and neck region are presented. With an advance in decomposition, calcined and charred bone gradually increase while unaltered bone decreases. Kernel densities for the scores (0, 1, 2 & 3) of heat-induced colour changes (calcined, charred and unaltered) on the cranium, mandible and cervical vertebrae for TBS are plotted (Figures 4.1, 4.2 & 4.3).

During fresh and early decomposition, no burn-related colour changes are observed (Tables 4.1 & 4.2). Figure 4.3 shows this distribution of unaltered bone, which decreases from scores of 2 and 3 in the early stages to scores of 0 and 1 in the advanced and final stages. In the advanced stage, changes in the distribution of unaltered, charred and calcined bone are noted. While the majority (80%) of the skeletal elements are unaltered (Table 4.3), minimal amounts (score = 1) of charred and calcined bone are noted on 60% and 27% of the remains, respectively (Tables 4.1 & 4.2). During early skeletonisation, moderate thermal changes (score = 2) are observed on the skeletal elements (charred = 73%; calcined = 60%) (Tables 4.1 & 4.2). In late skeletonisation, score 3 for calcined bone (33%) is more prevalent than charred bone across all bony surfaces (13%) (Tables 4.1 & 4.2). In Figure 4.1 calcined bone increases from minimal (score = 0 & 1) in the early stages to more substantial (scores = 2 & 3) in the final stages, and is also seen in Figure 4.2 which shows the distribution of charred bone increasing from zero in the early stages to varied amounts (score = 1 & 2) in the advanced and final stages.

For binary data, only the presence of greasy bone ($p = 0.0024$), delamination ($p = 0.0018$) and heat-induced fractures ($p = 0.0003$) display statistical significance with

decomposition (Tables 4.4, 4.5 & 4.6). Kernel densities for the absence (0) and presence (1) of greasy bone, delamination and other heat-induced fractures on the cranium, mandible and cervical vertebrae for TBS are plotted (Figures 4.4, 4.5 & 4.6).

During fresh and early decomposition, all skeletal elements are greasy with no delamination or other heat-induced fractures (Tables 4.4, 4.5 & 4.6). With advancing decomposition, the percentage of greasy bone declines from 100% (fresh and early) to 67% (advanced stage) and to 47% in early skeletonisation (Table 4.4). By late skeletonisation, none of the skeletal elements are greasy in either touch or appearance (Table 4.4). In Figure 4.4, this trend is evident, with greasy bone being grossly apparent in early decomposition (TBS < 20) and relatively absent in the later stages.

Delamination is observed on 67% of the skeletal elements from the advanced to late skeletonisation stage of decomposition (Table 4.5). Heat-induced fractures are present on 47% of the remains in the advanced stage and 100% of the remains in early and late skeletonisation (Table 4.6). This trend is noted in Figures 4.5 and 4.6, which show that delamination and heat-induced fractures are more prevalent in the advanced stages of decomposition than in the earlier stages (TBS>20/25).

4.1.2. Trunk: Frequency distribution and kernel density plots

As observed with the head and neck elements, calcined ($p = 0.0004$) and charred bone ($p = 0.0001$) significantly increases and unaltered bone significantly ($p = 0.0001$) decreases with a progression in decomposition (Tables 4.7, 4.8 & 4.9). Kernel densities for the scores (0, 1, 2 & 3) of heat-induced colour changes (calcined, charred and unaltered) on the ribs, scapulae, os coxae, thoracic and lumbar vertebrae for TBS are plotted in Figures 4.7 – 4.12.

In the fresh and early stages, no colour changes are observed (Tables 4.7 & 4.8). Figures 4.11 and 4.12 show that unaltered bone decreases from a score of 3 in early decomposition to scores of 1 or 2 in the advanced and final stages. The advanced stage shows only changes in the distribution of charred bone with minimal amounts (score = 1) observed on 16% of the remains (Table 4.8). In early skeletonisation, moderate changes (score = 2) are noted on 48% (charred) and 28% (calcined) of the skeletal elements (Tables 4.7 & 4.8). Late skeletonisation shows extensive charred bone (68%) (score = 3) in relation to calcined bone (8%) (Tables 4.7 & 4.8). Calcined bone increases from zero in the early stages of decomposition to scores of 1, 2 and 3 in the final stages. Figures 4.9 and 4.10 show that the

distribution of charred bone increases from zero in early decomposition to minimal amounts (score = 1) in the advanced stage and further increased amounts (score = 2 & 3) in the final stages.

For the binary data, the presence of greasy bone (p = 0.0036), delamination (p = 0.0001) and heat-induced fractures (p = 0.0001) displays statistical significance with decomposition. Kernel densities for the presence (1) or absence (0) of greasy bone, delamination and heat-induced fractures on the ribs, scapulae, os coxae, thoracic and lumbar vertebrae for total body score (TBS) are plotted (Figures 4.13 – 4.18).

All skeletal elements are greasy (Table 4.10) in the fresh and early stages with no delamination or other heat-induced fractures (Tables 4.11 & 4.12). With advancing decomposition, the percentage of greasy bone declines from 100% (fresh and early stages) to 80% (advanced stage) to 47% (early skeletonisation) and to 8% in late skeletonisation (Table 4.10). Figures 4.13 and 4.14 graphically represent this trend. Delamination is observed on 24% of the elements in the advanced stage and on 80% in early skeletonisation (Table 4.11). Heat-induced fractures are present on 12% of the elements in the advanced stages and on 76% in early skeletonisation (Table 4.12). By late skeletonisation, all recovered remains (100%) display both delamination and heat-induced fractures (Tables 4.11 & 4.12). Figures 4.15 – 4.18 illustrate this trend and show that delamination and heat-induced fractures are more prevalent in the advanced stages (TBS>20).

4.1.3. Limbs: Frequency distribution and kernel density plots

Calcined and charred bone observed on the limbs significantly increases (p = 0.0036; p = 0.0006), and unaltered bone significantly (p = 0.0063) decreases with advancing decomposition (Figures 4.13 – 4.15). Kernel density plots for the scores (0, 1, 2 & 3) of heat-induced colour changes (calcined, charred or unaltered) on the humerus, ulna, radius, metacarpals, femur, tibia, fibula and metatarsals are plotted against TBS (Figures 4.19 – 4.38).

In the fresh and early stages of decomposition, all elements display unaltered surfaces (score = 3), with 2.5% (radii & metacarpals) exhibiting minimal amounts of charred bone (score = 1) (Tables 4.15 & 4.14). In Figures 4.25 – 4.27, the distribution of unaltered bone decreases from a score of 3 in the early stages to scores of 0 or 1 in the advanced and final

stages. In the advanced stage, minimal charred and calcined bone (score = 1) are observed on 25% and 5% of the remains, respectively (Tables 4.13 & 4.14). In the early skeletonisation phase, moderate charred bone (score = 2) on 30%, and calcined bone on 17.5% of the elements (Tables 4.13 & 4.14) are noted; whereas extensive charred bone (score = 3) (60%) is more prevalent than calcined bone, which is observed on 2.5% of the remains in the final, late skeletonisation phase. In Figures 4.19 – 4.24 charred and calcined bone increases from zero in the early stages to scores of 1, 2 and 3 in the more advanced stages.

For binary data, brown burn/borders ($p = 0.0039$), greasy bone ($p = 0.0011$), delamination ($p = 0.0000$) and heat-induced fractures ($p = 0.0000$) display statistical significance with decomposition (Tables 4.16 – 4.19). Kernel density plots for the presence (1) or absence (0) of brown burn/borders on the radius, ulna, metacarpals and metatarsals (Figures 4.28 & 4.29) and the presence (1) or absence (0) of greasy bone, delamination and heat-induced fractures on the humerus, ulna, radius, metacarpals, femur, tibia, fibula and metatarsals are plotted against TBS (Figures 4.30 – 4.38).

Brown burn/borders are more common in the skeletonised stages (10% and 32.5%) (Table 4.16) and are absent in the earlier stages. This trend is observed in Figures 4.28 and 4.29. In early decomposition, all skeletal elements are greasy, and only 5% of all remains display both delamination and other heat-induced fractures (Tables 4.17 – 4.19). With the progression of decomposition, the percentage of greasy bone declines to 83% (advanced stage) to 58% (early skeletonisation) and to 2.5% in late skeletonisation (Table 4.17). Figures 4.30 – 4.32 are used to illustrate a decline in greasy bone from early to final stages. Delamination is observed on 20% of the elements in the advanced stage and on 67.5% in early and late skeletonisation (Table 4.18). Heat-induced fractures are present on 25% of the remains in the advanced stage, 80% in early skeletonisation and 98% in late skeletonisation (Table 4.19). Figures 4.33 – 4.38 are used to illustrate this trend and show that delamination and heat-induced fractures frequent in the advanced to the final decomposition stages.

4.2. Quantitative statistics

4.2.1. Multiple regression analysis with categorical predictors

Multiple regression analysis is used to predict the behaviour of independent variables (heat-related traits) with a dependent variable (TBS/decomposition) and provide information

as to the relationship of these traits to the dependent variable as well as the potential of these traits to supply an estimation of TBS. Multiple regression formulae for categorical data are presented in Tables 4.20 – 4.35 and contain the following information; the variable (heat-induced colour change on a specific skeletal element), the slope (Coef), the standard error (Std. Err.), the intercept (_cons), the mean standard error of estimate (MSE) and the r-squared (adjusted) value (coefficient of determination). Only the colour distribution on burned bone is regressed in this section, and only the most significant formulae are presented. The other formulae with lower r-squared values can be viewed in Appendix F. The binary variables are not represented well enough within the current sample to formulate statistically significant regression equations.

4.2.1.1. Head and neck

The multiple regression models for the cranium, mandible and cervical vertebrae with two predictors (charred & calcined) produced r-squared values of 0.87, 0.88, 0.77 respectively [F (5, 19) = 32.2; F (4, 20) = 44.5; F (4, 20) = 21.5)]. As can be seen in Tables 4.20 and 4.21, the distribution of charred and calcined bone is positively significant ($p<0.05$) with TBS. In Table 4.22, the distribution of calcined bone shows a significant positive relationship with TBS, while charred bone shows a significant inverse relationship for dummy variable 1 with TBS. When applying the formulae presented in Tables 4.20 – 4.22, the coefficient used is dependent on what the score for the variable (calcined, charred, unaltered).

For example (applicable to all equations in this chapter):

- Consider the equation for scoring heat-related colour change on the cranium (Table 4.20):
- X(TBS) = Constant (6.4) + 8.3(Cr_Cal_1 = 1, else = 0) + 16.5(Cr_Cal_2 = 1, else = 0) + 16.3(Cr_Cal_3 = 1, else = 0) + 11.6(Cr_Cha_1 = 1, else = 0) + 3.3(Cr_Cha_2 = 1, else = 0) ± MSE

- If the cranium scores as follows: Cal = 1, Cha = 2, the equation will be:

$$X\ (TBS) = 6.4 + 8.3(1) + 16.5(0) + 16.3(0) + 11.6(0) + 3.3(1) \pm MSE$$
$$= 6.4 + 8.3 + 3.3$$

$$= 18 \pm 4.1$$

$$TBS = 18 \pm 4.1 \text{ (range = 13.9 – 22.1)}$$

- Therefore the predicted TBS is 18 with a standard error of 4.1 (the Root MSE in Table 4.20). This score would place the cranium in an advanced or early skeletonisation stage.

4.2.1.2. Trunk

The multiple regression model for the ribs with two predictors (charred & calcined) produces an r-squared value = 0.80; F (5, 19) = 19.6. As can be seen in Table 4.23, the distribution of charred bone (dummy variables 1 and 3) has a significant positive relationship with TBS. The multiple regression model for the scapulae, os coxae, thoracic and lumbar vertebrae with two predictors (unaltered & charred) produces r-squared values = 0.68, 0.66, 0.69, 0.65 respectively [F (5, 19) = 11.24; F (4, 20) = 12.42; F (4, 20) = 14.53; F (5, 19) = 10.06]. As can be seen in Tables 4.24, 4.25 and 4.27, most of the distribution of charred and unaltered bone has a significant positive relationship with TBS. In Table 4.26, the distribution of charred bone is seen to have a significant ($p<0.05$) positive relationship with TBS and the distribution of unaltered bone a non-significant ($p>0.05$) negative relationship with TBS.

4.2.1.3. Limbs

The multiple regression model for the humerus with two predictors (unaltered & charred) produce an r-squared value = 0.67, F (4, 20) = 13.19. As can be seen in Table 4.28, the distribution of charred bone has a significant positive relationship with TBS.

The multiple regression model for the ulna, radius, femur, tibia, fibula and metatarsals with two predictors (charred & calcined) produced r-squared values of 0.62, 0.59, 0.63, 0.77, 0.62, 0.53 respectively [F (5, 19) = 8.97; F (4, 20) = 9.76; F (5, 19) = 9.2; F (6, 18) = 14.66; F (4, 20) = 10.88; F (4, 20) = 7.77]. As can be seen in Tables 4.29, 4.30, and 4.32 - 4.35, most of the distribution of charred and calcined bone has a significant positive relationship with TBS.

The multiple regression model for the metacarpals with three predictors (unaltered, charred & calcined) produced an r-squared value = 0.58, F (8, 16) = 5.11 (Table 4.31).

However, the relationship was not significant for any of the colour traits when the metacarpals were analysed.

In general, colour changes observed on the various skeletal elements display good potential to be predictors of decomposition stage.

4.2.2. Transition analysis

The distribution of colour change on skeletal elements of the head and neck (cranium, mandible and cervical vertebra) as a result of fire exposure across progressive decomposition is an example of single-trait analysis. These data are used to generate continuation ratio models which show the likelihood of a bone being in a specific stage of decomposition (A, B, C, D or E) if given a certain score for calcined, charred or unaltered bone (score = 0, 1,2 or 3) (Tables 4.36 to 4.38). Unlike regression analysis, which provides a description of the signifinace of heat-related variables to TBS, transition analysis provides the maximum likelihood (probability) that a certain skeletal element with a set of specific heat-related traits is in a particular stage of decomposition prior to a burn event.

The likelihood of a bone being in the early stages of decomposition declines as the percentage of thermal alteration increases to the point where the chances of a bone with extensive, uniform thermal alteration being in the early stages is almost zero.

4.2.2.1. Head and neck

Heat-induced colour change in the head and neck as an indicator of decomposition stage

With the absence of thermal alteration on the elements of the head and neck (cranium, mandible or cervical vertebrae), a 36 to 50% probability exists that the bones are in the first two stages, fresh and early. This is the collective probability if the skeletal elements presented in Tables 4.36 – 4.38 are combined. As the percentage of thermal alteration increases – more charred and calcined bone – the probability for being assigned to the later stages increases. As these likelihoods shift towards the later stages an increase in the probability is observed; i.e., the more decomposed and burned the remains, the higher the predicting factor for the decomposition stage.

If minimal amounts of calcination are observed on the head and neck, chances are that 50% of the remains had progressed into advanced decomposition and beyond. With moderate

amounts of calcined bone observed on the cranial surfaces, the chances that the remains are beyond the third stage of decomposition is highly probable (57% - 75%). If the elements of the head and neck display extensive calcination (score = 3) the remains were likely in the final stage of decomposition prior to burning (75% - 99%).

Minimal amounts (score = 1) of charred bone observed on the head and neck suggest that the remains were in an advanced stage of decomposition (50% - 99%). With minimal charred bone on just the cranium (i.e., no other bone recovered), the chances of the remains being in late skeletonisation is 50%. Increased amounts of charred bone (moderate (2) to extensive (3)) observed on the head and neck suggest a slightly higher probability (50% - 57%) that the remains are in a skeletonisation stage.

Binary indicators of decomposition stage for head and neck

In Tables 4.36 – 4.38, the presence of grease on the elements comprising the head and neck place remains in the fresh and early stages (28 – 33%). The presence of a heat border shows a 67% - 99% chance that the remains are in a state of advanced decomposition. A heat line, delineation, joint shielding and predictable cracking were only observed on the cranium and only in the advanced stage of decomposition (Table 4.36). Minimal cracking was only observed on the cranium and cervical vertebrae and allocates the remains to the advanced stage of decomposition (99%). Delamination or the presence of any other heat-induced fractures suggests that the cranial elements are in or have progressed beyond the advanced stage of decomposition (44% - 50%).

4.2.2.2. Trunk

Heat-induced colour change in the trunk as an indicator of decomposition stage

The absence of thermal alteration on the elements of the trunk suggests (28 to 39%) that the remains have not progressed beyond the advanced stage of decomposition (Tables 4.39 – 4.43). An investigation of the data reveals that no pig specimen scored a 0 for unaltered bone in the os coxae (Table 4.41); i.e., every pelvic element in the data set presented with some percentage of unaltered bone. Therefore, score 0 has a zero probability if being found in any unaltered pelvic remains.

If minimal amounts of calcined or charred bone are observed on the trunk, chances (50 - 99%) are the remains are in advanced or early skeletonisation. With increasing amounts

of calcined or charred bone (moderate – extensive) the remains were mostly beyond advanced decomposition (50% - 99%).

Binary indicators of decomposition stage

Tables 4.39 – 4.43 demonstrate that the presence of grease on the trunk elements places remains in fresh and early decomposition (27 – 39%). Predictable cracking is only noted on the ribs and scapulae and only in the advanced stage of decomposition (99%) (Tables 4.39 & 4.40). The presence of a heat border is only observed on the scapula and indicates a 50% chance that the remains are in the advanced stage or early skeletonisation (Table 4.40). Brown burn/border observed on the ribs, os coxae and lumbar vertebrae places the remains in early skeletonisation (99%). However if a brown burn/border is observed on the scapulae this suggests the remains are anywhere between advanced decomposition and late skeletonisation (33% probability each) (Tables 4.39 – 4.41, 4.43). Minimal cracking observed on the scapulae likely places the remains in early skeletonisation. Delamination or the presence of any other heat-induced fractures suggests the trunk elements are in or have progressed beyond early skeletonisation (39% - 63%).

4.2.2.3. Limbs

Heat-induced colour change in the extremities as an indicator of decomposition stage

With the absence of thermal alteration on the elements of the extremities, a 24 to 42% probability exists that the bones are in the fresh to advanced stages of decomposition (Tables 4.44 – 4.51). An investigation of the data reveals that no skeletal elements scored a 0 for unaltered bone in the femur and metatarsals (Tables 4.48 & 4.51); i.e., every femur and metatarsal in the data set presents with unaltered surfaces. Therefore, score 0 has a zero probability if being found in any unaltered femur or metatarsal remains.

Tables 4.44 – 4.51 show that if minimal or moderate calcined bone is observed on the extremities, chances are that the remains had progressed beyond advanced decomposition (50 - 75%). Extensive calcined bone (score = 3) likely places the remains in early or late skeletonisation (50 – 99%). Minimal or moderate amounts of charred bone observed on the extremities suggest that the remains are likely in or beyond advanced decomposition (33% - 99%). Increased amounts of charred bone (extensive) observed on the extremities suggest that the remains are in early or late skeletonisation prior to exposure (50 - 99%).

Binary indicators of decomposition stage

Tables 4.44 – 4.51 demonstrate that the presence of grease on the extremities would associate the remains with fresh, early or advanced decomposition (28 – 31%). The presence of a heat border observed on all the extremities, except the femur and fibula, shows a 50 – 99% chance that the remains are in advanced decomposition (Tables 4.41 – 4.47, 4.49 & 4.51). The presence of a heat line and delineation on the ulna, metacarpals, tibia and metatarsals suggest a 50 – 99% probability that the remains are in early or advanced decomposition (Tables 4.45, 4. 47, 4.49 & 4.51). Predictable cracking observed on the humerus, radius, metacarpals, tibia and metatarsals allocates the remains to the advanced stage of decomposition with a 50 – 99% probability (Tables 4.44, 4.46, 4.47, 4.49 & 4.51). Brown burn/border observed on all the elements, except the femur and fibula, associates the remains with late skeletonisation with probability of 60 – 99%. However, if observed on the ulna it places the remains in early or late skeletonisation (50% probability) (Tables 4.41 – 4.47, 4.49 & 4.51). Delamination or the presence of any other heat-induced fractures suggests the extremities are in or have progressed beyond the advanced stage of decomposition prior to burning (31% - 67%).

4.3. Inter- and Intraobserver error analysis

4.3.1. Intraclass correlation - ICC (scoring decomposition)

The ICC is a descriptive statistic that can be utilised to assess the consistency or reproducibility of a quantitative measure taken by different observers measuring the same features. These results are presented in Tables 4.52 – 4.54 (interobserver). The ideal result is to obtain a 1.00, which indicates a 100% agreement between two independent observers. An F-test was also conducted and a p-value obtained to assess significance between the two observers.

The interobserver results indicate that the highest agreement is found when scoring the trunk with an ICC of 0.997 and the lowest for scoring of the limbs (ICC = 0.923) (Tables 4.53 & 4.54). All the ICCs are well above 0.75 which indicates the method for scoring is repeatable. If the F-statistic and p-value are taken into account, no significant difference exists between the two independent observers.

4.3.2. Cohen's Kappa statistics

4.3.2.1 Head and neck

From Table 4.55, the intra- and inter-rater reliability for calcined bone is found to be almost perfect and substantial with agreements of 87.5% (k = 0.8159, p = 0.2231) and 79.2% (k = 0.7059, p = 0.2873), respectively. Intra- (k = 0.7538, p = 0.2615) and inter-rater (k = 0.7377, p = 0.1353) reliability for scoring charred bone on the head and neck is substantial with an agreement of 83%. Almost perfect levels of agreement are observed for unaltered bone (91.7%, k = 0.8737, p = 0.3679; 87.5%, k = 0.8204, p = 0.2231). These values indicate that calcined, charred and unaltered bone scored for the head and neck are all reliable burn-related traits and that the scores can be consistently recorded.

Intra-rater reliability for brown burn and heat border is substantial (agreement 91.7%, k = 0.7037, p = 0.1573; agreement 95.8%, k = 0.7778, p = 0.3173), while an almost perfect agreement of 95.8% (k = 0.8636, p = 0.3173) and a substantial agreement of 91.7% (k = 0.7037, p = 0.1573) is observed for the inter-rater error. Both these variables display considerable agreement between the two independent observers (Table 4.55).

Almost perfect agreements in both intra- and inter-rater reliability testing for greasy bone are observed (100%, k = 1.000, p = 1.000; 91.7%, k = 0.8125, p = 1.000). The p-values for both tests are non-significant and indicate that the scoring of this trait between observers is consistent. The inter-rater agreement for predictable cracking shows slight agreement (95.8%, k = 0.0000, p = 0.3173), whereas an almost perfect agreement for minimal cracking (95.8%, k = 0.8333, p = 0.3173) is observed. Both predictable and minimal cracking show non-significant p-values and indicate consistent scoring of these traits (Table 4.55).

Fair (66.7%, k = 0.2889, p = 1.000) and moderate (79.2%, k = 0.5455, p = 0.6547) agreements for delamination are observed. The non-significant p-values indicate that this trait is consistently scored. The reliability for heat-induced fractures (100%, k = 1.000, p = 1.000; 75%, k = 0.1910, p = 0.0143) is almost perfect for intra-rater but only slight for the inter-rater agreement. The first set of values indicates that one observer consistently scored the same trait in both rounds. The second set of values indicates that although the agreement percentage is high, a statistically significant p-value shows that the two independent observers could not consistently score the trait in the same manner.

In summary, calcined, charred and unaltered bone, brown and heat borders, greasy bone, delamination and heat-induced fractures can be consistently scored in elements of the

head and neck, while predictable and minimal cracking show some difficultly in scoring consistently between independent observers.

4.3.2.2 Trunk

From Table 4.56, the intra-rater reliability for calcined and charred bone is almost perfect and substantial with agreements of 90% (k = 0.8498, p = 0.5134) and 77.5% (k = 0.6552, p = 0.3796). The inter-rater reliability for calcined and charred bone is moderate for both traits with a shared agreement of 67.5% (k = 0.5307, p = 0.0074; k = 0.5586, p = 0.0117).

The reliability for unaltered bone (80%, k = 0.6998, p = 0.1490; 85%, k = 0.7521, p = 0.1116) is moderate for both intra- and inter-rater agreement, with non-significant p-values. Intra-rater reliability for brown burn is slight (agreement 82.5%, k = 0.1566 p = 0.0503). The p-value for this test was almost statistically significant, which implies that the observer selected the scores differently during the second round of analysis. However, inter-rater agreement for brown burn is substantial (97.5%, k = 0.7872, p = 0.3173). The reliability for the heat border (100%, k = 1.000, p = 1.000; 100%, k = 1.000, p = 1.000) is almost perfect for both the intra- and interobserver agreement. This trait shows a perfect score and the non-significant p-value indicates that the two independent observers scored consistently (Table 4.56). Almost perfect agreements in both intra- and inter-rater reliability tests for greasy bone are observed (100%, k = 1.000, p = 1.000; 100%, k = 1.000, p = 1.000) (Table 4.56).

The inter-rater agreement for predictable cracking shows substantial agreement (97.5%, k = 0.6552, p = 0.3173) with only slight agreement for minimal cracking (97.5%, k = 0.0000, p = 0.3173) is observed. Both predictable and minimal cracking show non-significant p-values. Moderate (87.5%, k = 0.6000, p = 0.02530) and substantial (85%, k = 0.6783, p = 0.0143) agreements for delamination are observed; this variable can be scored consistently among observers. However, the statistically significant p-value suggests that the observers failed to score the variable in the same manner. The reliability for heat-induced fractures (100%, k = 1.000, p = 1.000; 97.5%, k = 0.9390, p = 0.3173) is almost perfect for both intra- and inter-rater agreement; the p-value was not significant (Table 4.56).

In summary, calcined, charred and unaltered bone, brown and heat borders, greasy bone, predictable and minimal cracking, and heat-induced fractures can be consistently

scored in elements of the trunk, while delamination shows some difficultly in scoring consistently between independent observers.

4.3.2.3 Limbs

From Table 4.57 it can be seen that intra- and inter-rater reliability for calcined bone is substantial and almost perfect with agreements of 82.8% (k = 0.7433, p = 0.3208) and 89.1% (k = 0.8315, p = 0.0302) respectively. The statistically significant p-value demonstrates the inability of the observers to score consistently and suggests a chance agreement. Intra- (k = 0.6263, p = 0.2231) and inter-rater (k = 0.8544, p = 0.0719) reliability for charred bone scored on the extremities is substantial (75%) and almost perfect (89.1%) respectively. For unaltered bone, substantial and almost perfect levels of agreement are observed (82.8%, k = 0.7684, p = 0.0503; 87.5%, k = 0.8097, p = 0.5062). Calcined, charred and unaltered bone scored on the head and neck can be consistently recorded.

Intra-rater reliability for brown burn is substantial (agreement 87.5%, k = 0.6859, p = 0.0047), while an almost perfect agreement of 93.8% (k = 0.8072, p = 0.3173) is observed for the inter-rater. Although high agreements were found for scoring brown burn, the statistically significant p-value indicates that the observers failed to similarly score the trait. The reliability for the heat border (96.9%, k = 0.0000, p = 0.1573; 92.2%, k = 0.5722, p = 0.6547) shows slight and moderate agreements for the intra- and interobserver scores, respectively. Almost perfect agreements in both intra- and inter-rater reliability testing for greasy bone are observed (98.4%, k = 0.9592, p = 0.3173; 96.9%, k = 0.9376, p = 0.1573). The p-values are not significant (Table 4.57).

The inter-rater agreement for predictable cracking shows slight agreement (95.8%, k = 0.0000, p = 0.3173), whereas an almost perfect agreement for minimal cracking (95.8%, k = 0.8333, p = 0.3173) is observed; the p-values are not significant. Substantial (84.4%, k = 0.6541, p = 0.5271; 82.8%, k = 0.6563, p = 0.7630) agreements for delamination are observed. The reliability for heat-induced fractures (100%, k = 1.000, p = 1.000; 98.4%, k = 0.9631, p = 0.3173) is almost perfect for both intra- and inter-rater testing. The p-values are not significant (Table 4.57).

In summary, calcined, charred and unaltered bone, heat borders, greasy bone, predictable and minimal cracking, delamination and heat-induced fractures can be

consistently scored in elements of the limbs, while brown borders show some difficultly in scoring consistently between independent observers.

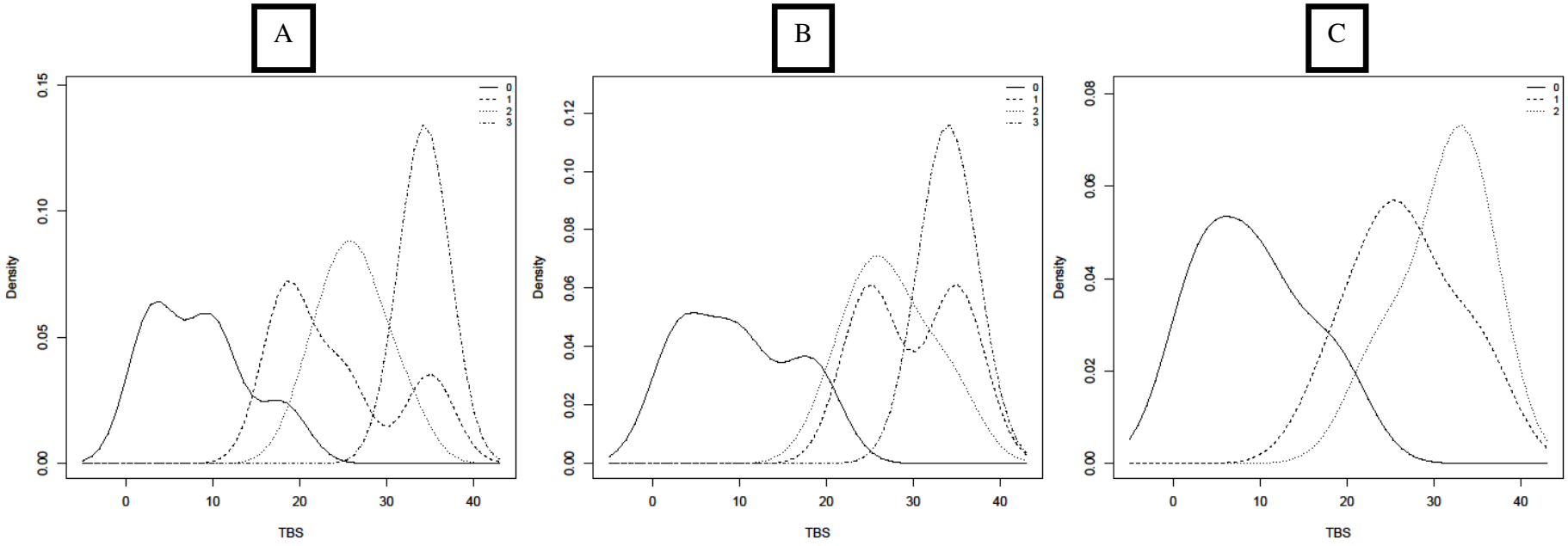

Figure 4.1 Kernel density estimates for the amount of calcined bone based on the ranked scores (0,1,2,3) in the cranium (A), mandible (B) and cervical vertebrae (C) [TBS = total body score]

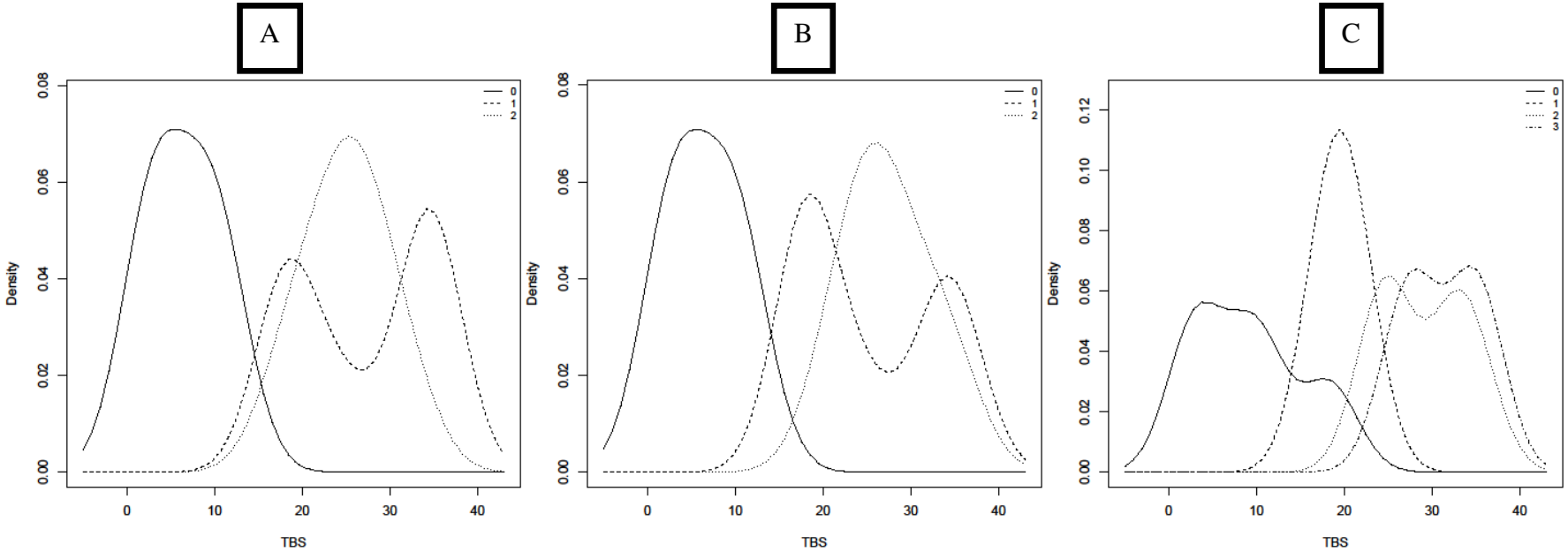

Figure 4.2 Kernel density estimates for the amount of charred bone based on the ranked scores (0,1,2,3) in the cranium (A), mandible (B) and cervical vertebrae (C) [TBS = total body score]

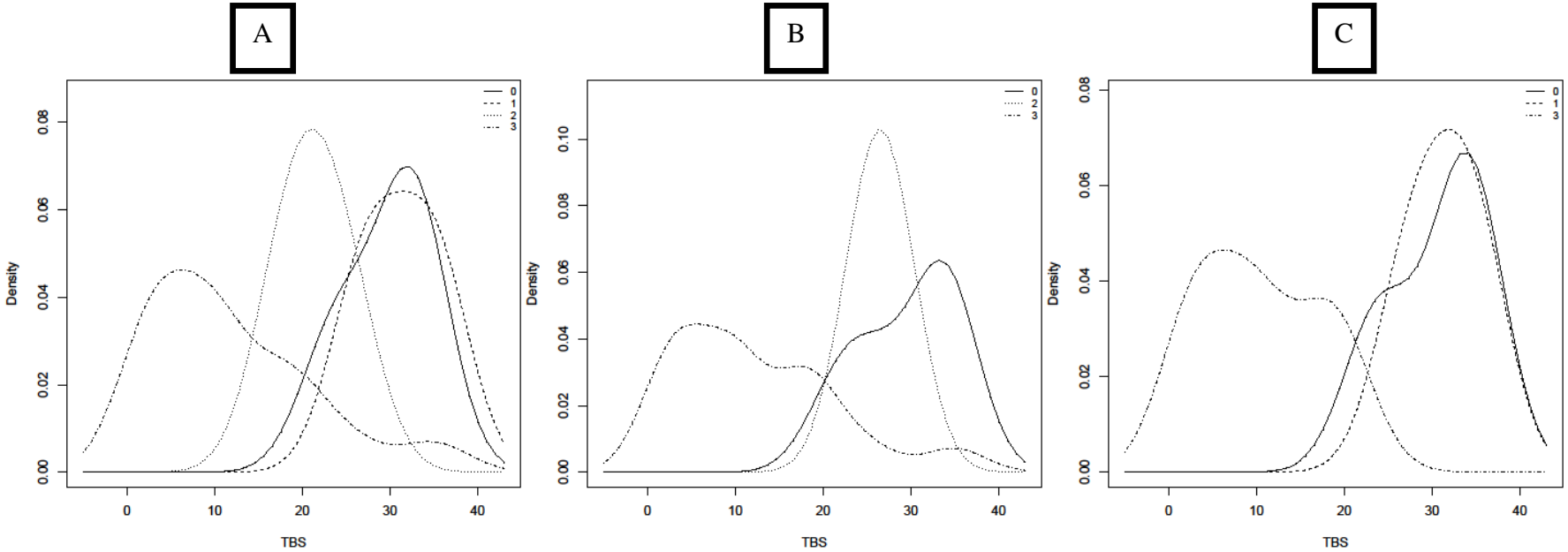

Figure 4.3 Kernel density estimates for the amount of unaltered bone based on the ranked scores (0,1,2,3) in the cranium (A), mandible (B) and cervical vertebrae (C) [TBS = total body score]

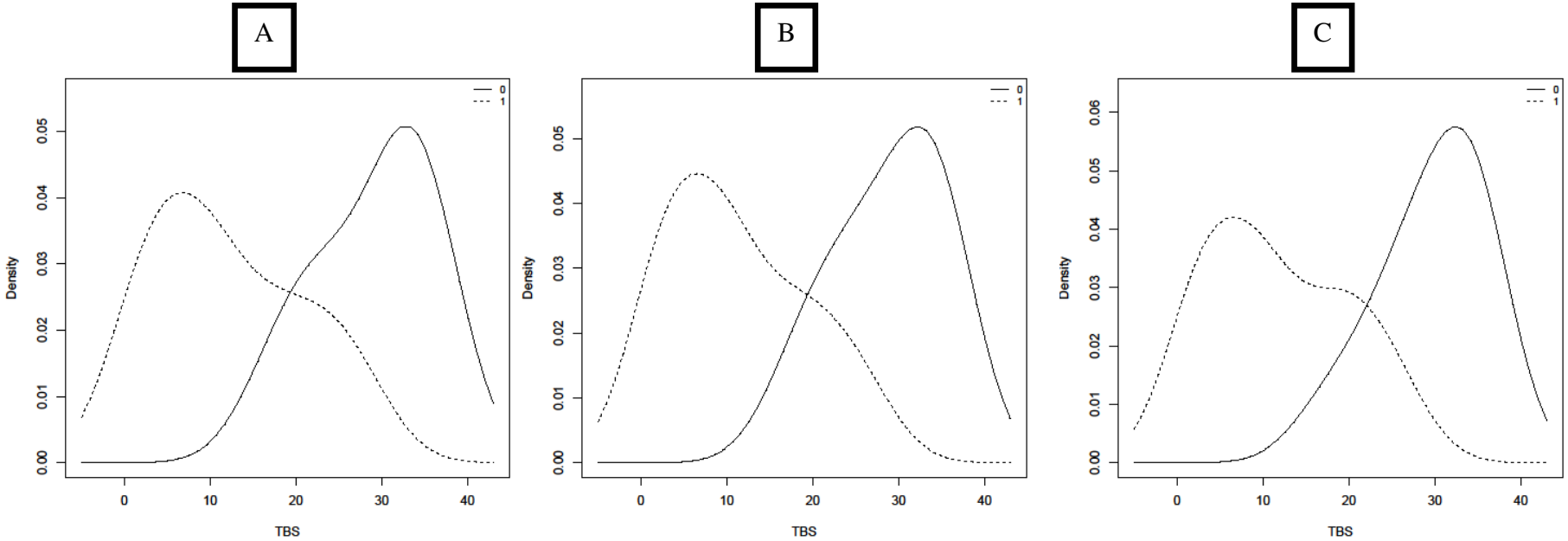

Figure 4.4 Kernel density estimates for greasy bone based on the binary scores (0,1) in the cranium (A), mandible (B) and cervical vertebrae (C) [TBS = total body score]

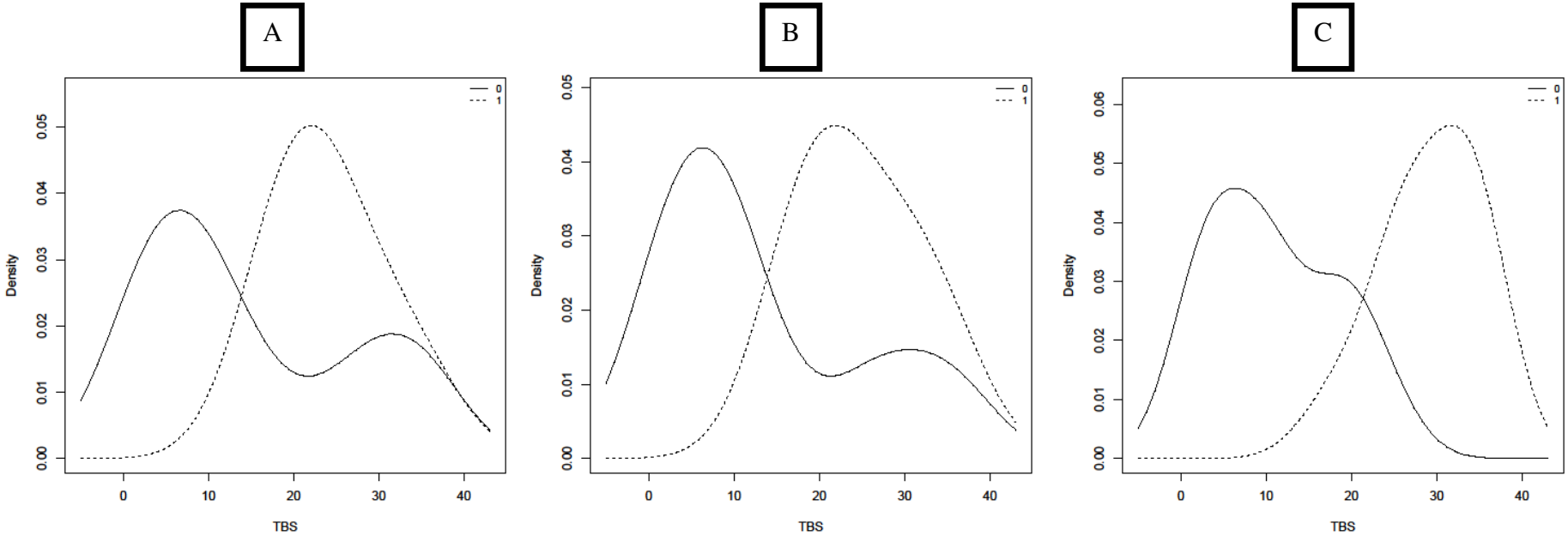

Figure 4.5 Kernel density estimates for delamination based on the binary scores (0,1) in the cranium (A), mandible (B) and cervical vertebrae (C) [TBS = total body score]

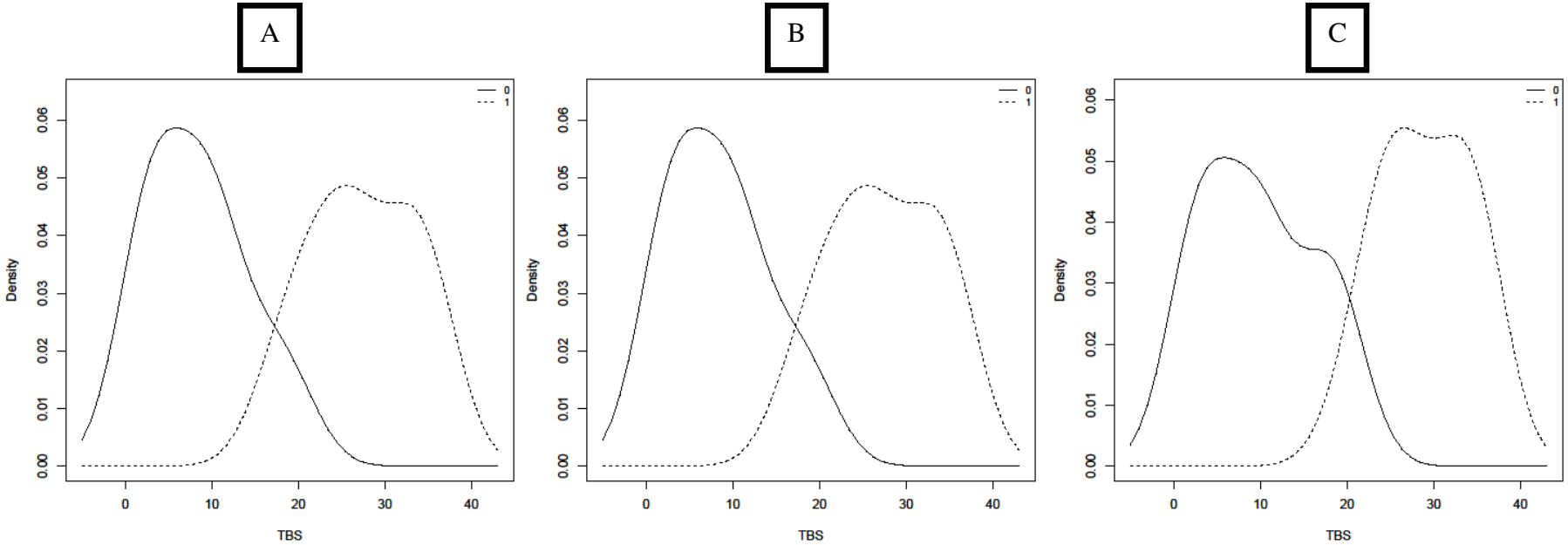

Figure 4.6 Kernel density estimates for heat-induced fractures based on the binary scores (0,1) in the cranium (A), mandible (B) and cervical vertebrae (C) [TBS = total body score]

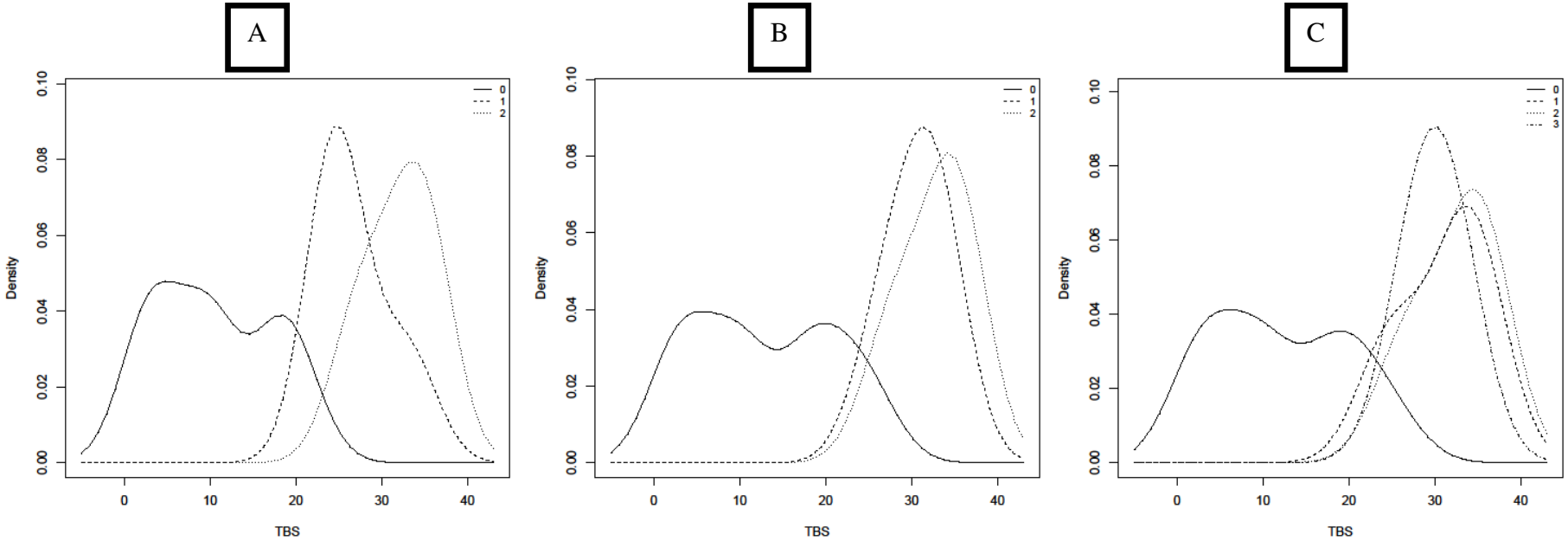

Figure 4.7 Kernel density estimates for the amount of calcined bone based on the ranked scores (0,1,2,3) in the ribs (A), scapula (B) and os coxa (C) [TBS = total body score]

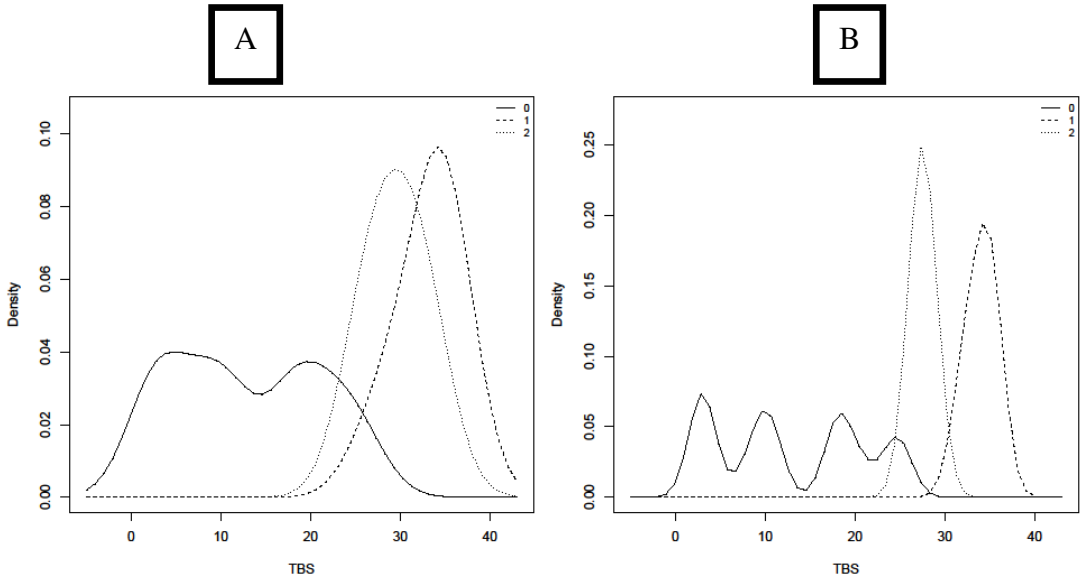

Figure 4.8 Kernel density estimates for the amount of calcined bone based on the ranked scores (0,1,2,3) in the thoracic vertebrae (A) and lumbar vertebrae (B) [TBS = total body score]

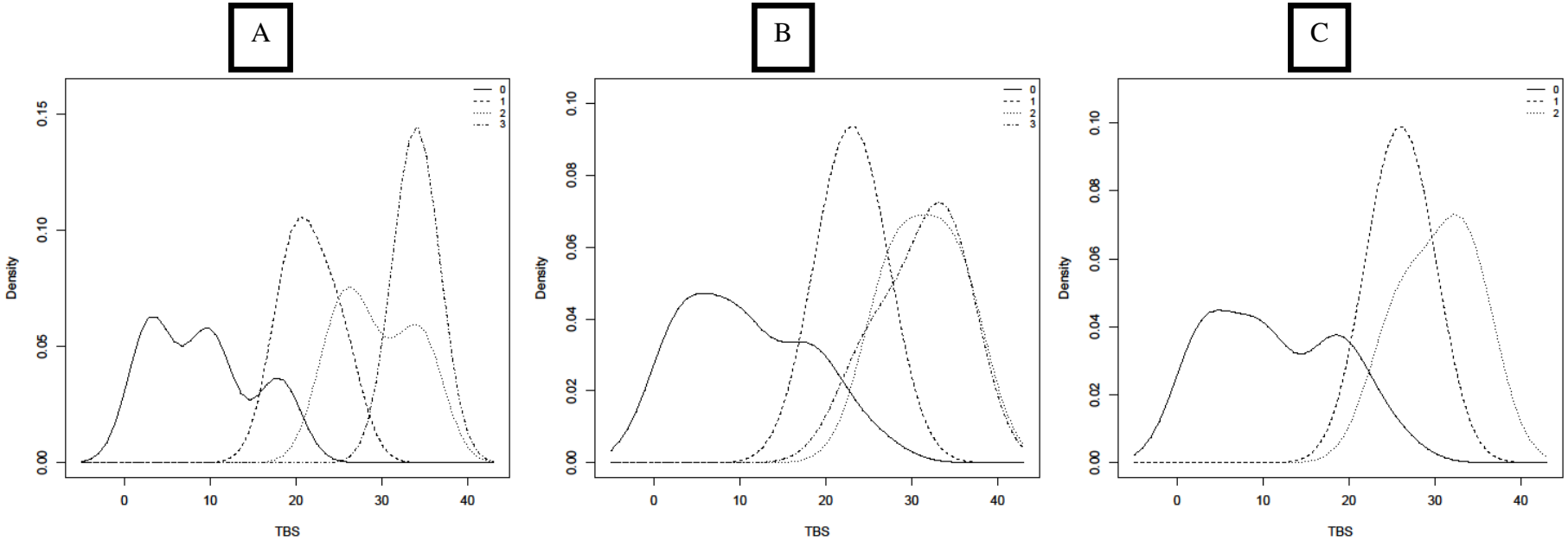

Figure 4.9 Kernel density estimates for the amount of charred bone based on the ranked scores (0,1,2,3) in the ribs (A), scapula (B) and os coxa (C) [TBS = total body score]

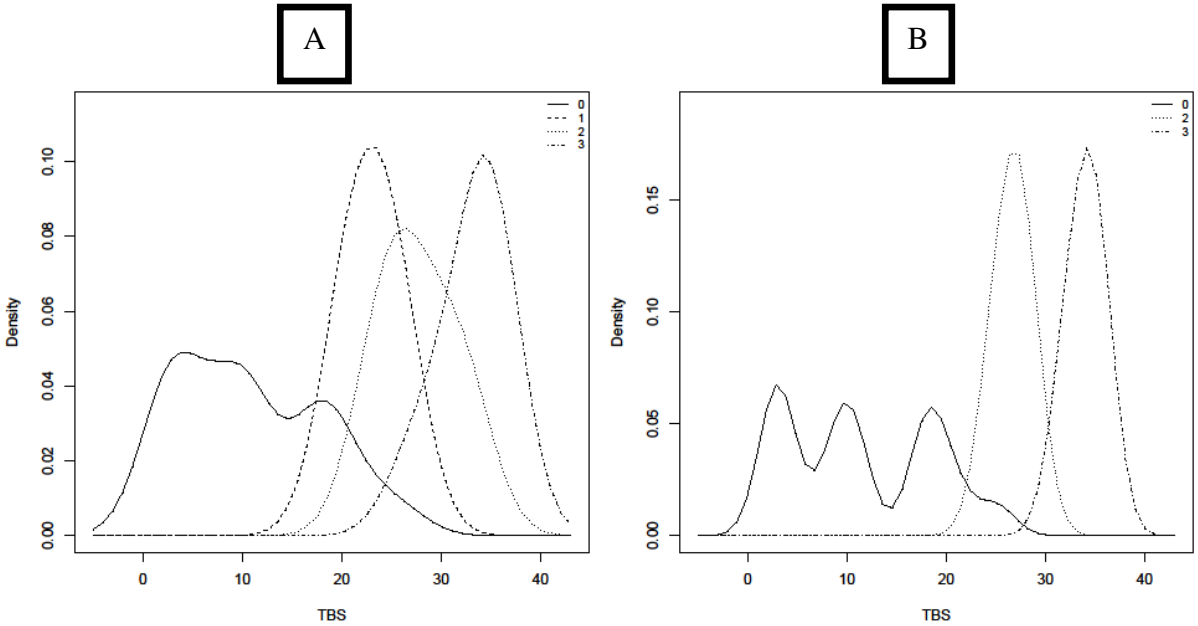

Figure 4.10 Kernel density estimates for the amount of charred bone based on the ranked scores (0,1,2,3) in the thoracic vertebrae (A) and lumbar vertebrae (B) [TBS = total body score]

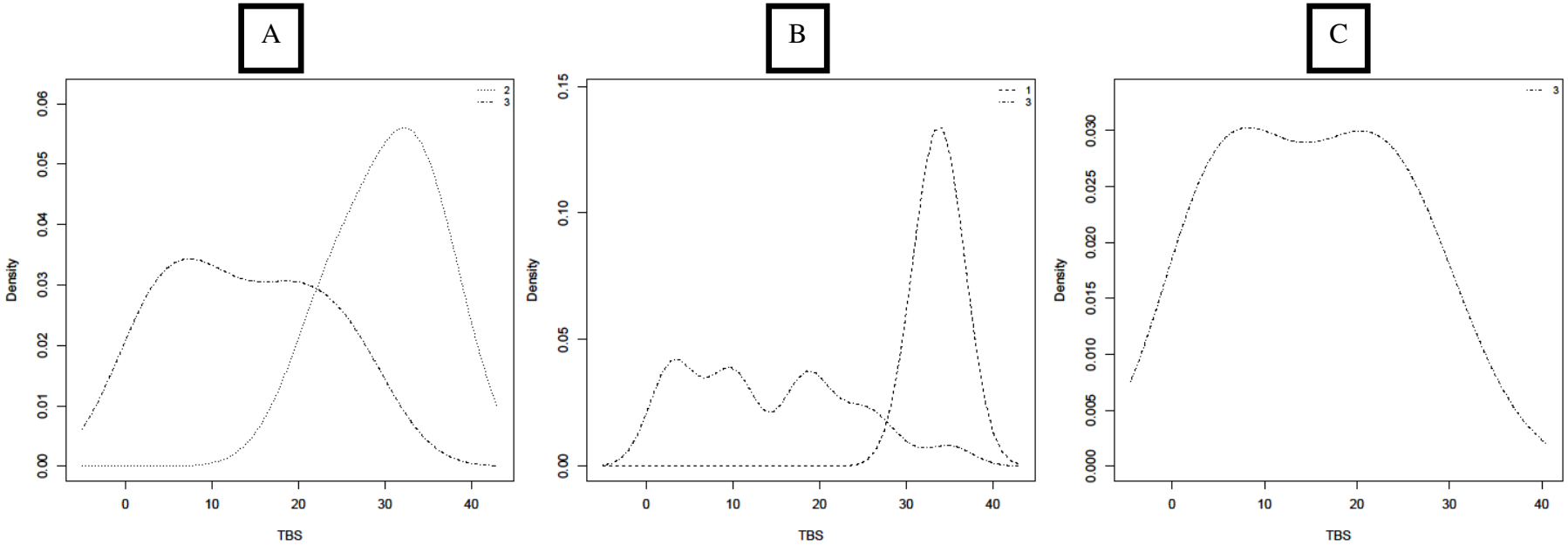

Figure 4.11 Kernel density estimates for the amount of unaltered bone based on the ranked scores (0,1,2,3) in the ribs (A), scapula (B) and os coxa (C) [TBS = total body score]

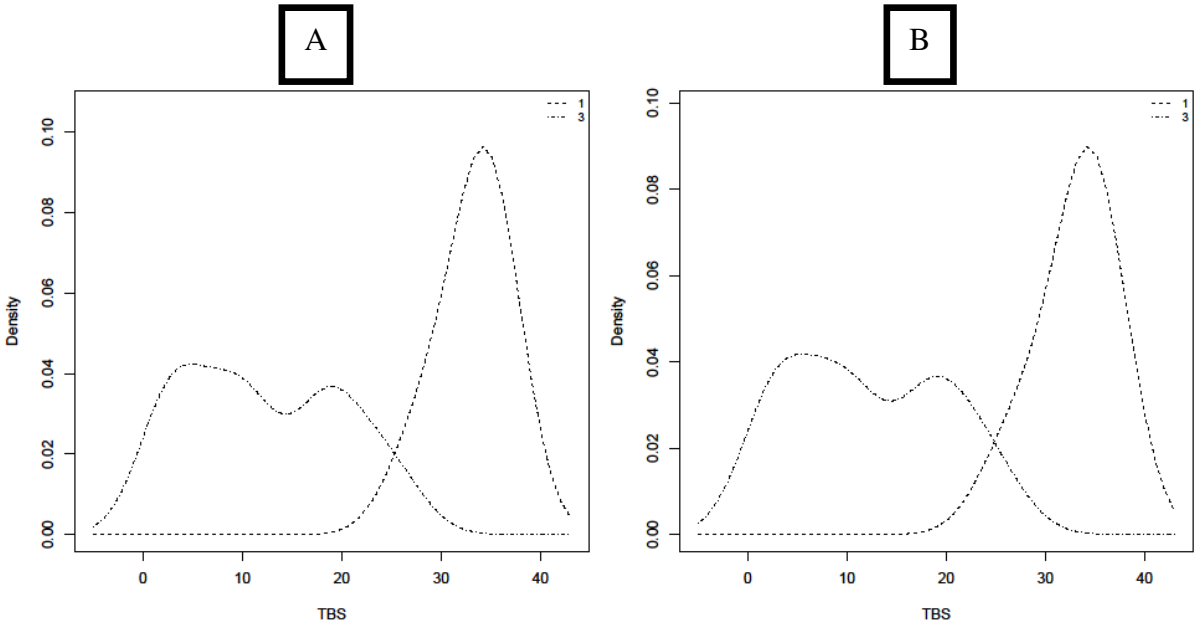

Figure 4.12 Kernel density estimates for the amount of unaltered bone based on the ranked scores (0,1,2,3) in the thoracic vertebrae (A) and lumbar vertebrae (B) [TBS = total body score]

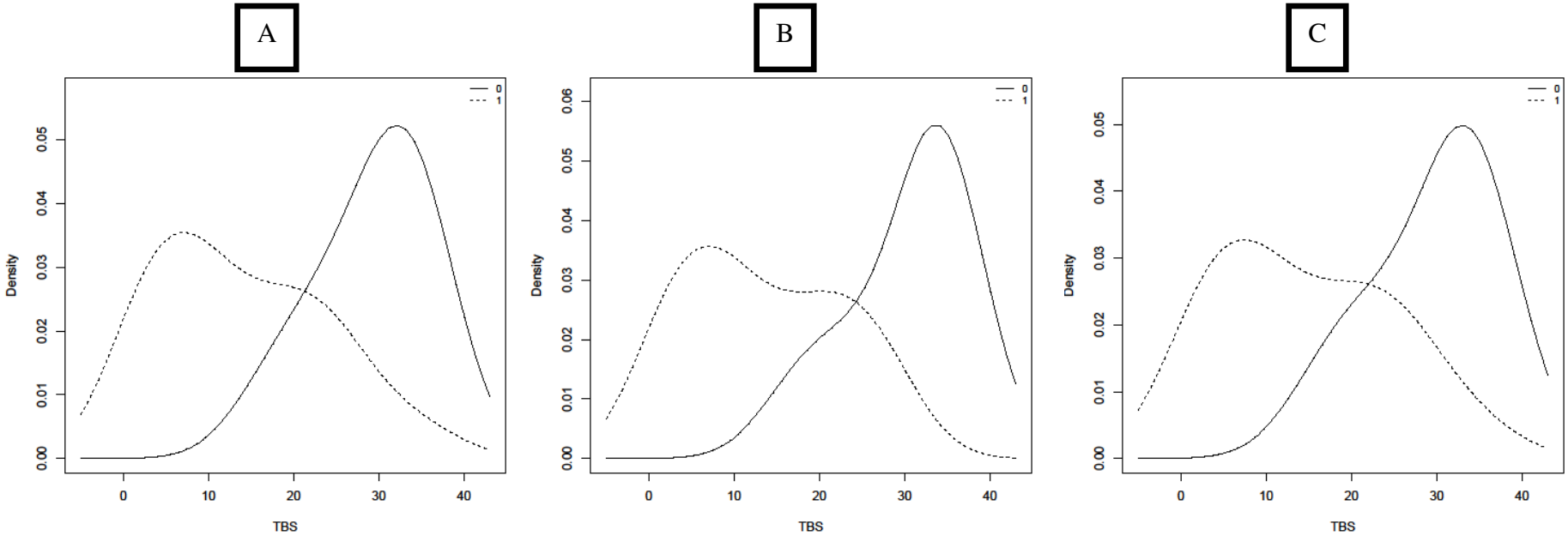

Figure 4.13 Kernel density estimates for the amount of greasy bone based on the binary scores (0,1) in the ribs (A), scapula (B) and os coxa (C) [TBS = total body score]

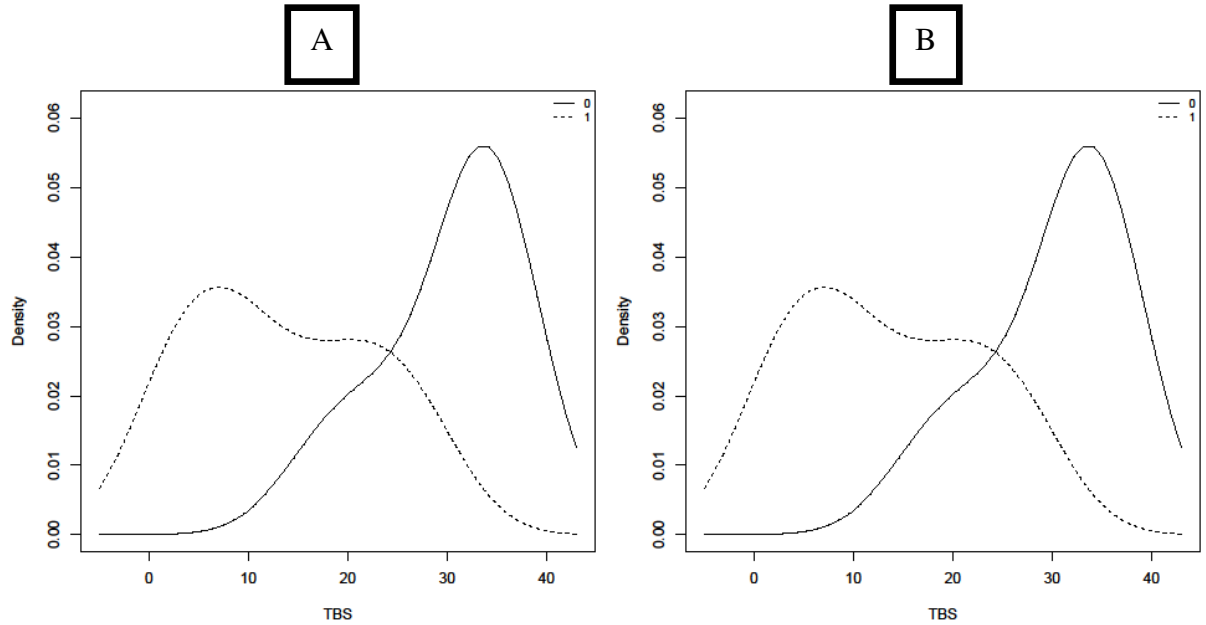

Figure 4.14 Kernel density estimates for the amount of greasy bone based on the binary scores (0,1) in the thoracic vertebrae (A) and lumbar vertebrae (B) [TBS = total body score]

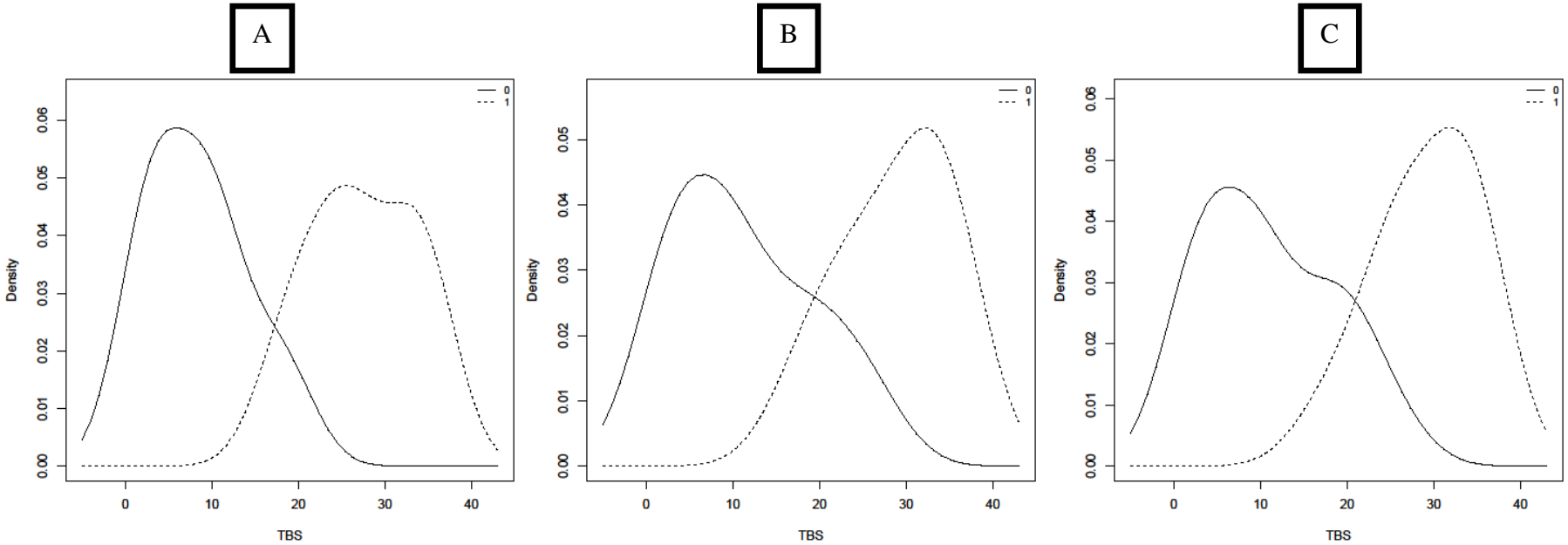

Figure 4.15 Kernel density estimates for the amount of delamination based on the binary scores (0,1) in the ribs (A), scapula (B) and os coxa (C) [TBS = total body score]

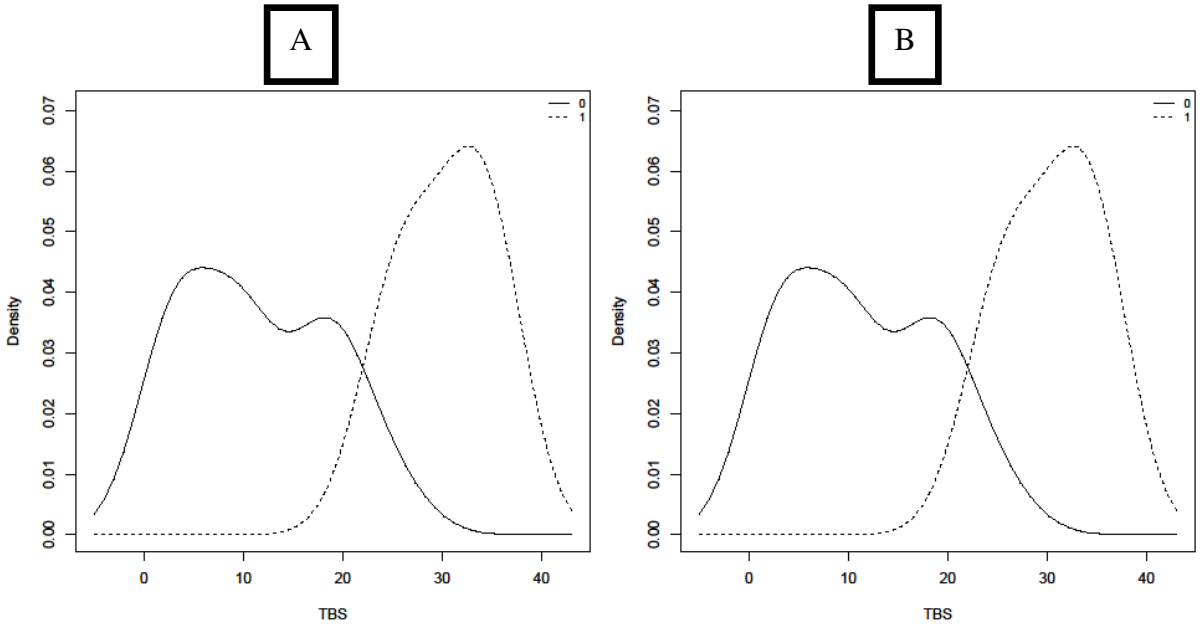

Figure 4.16 Kernel density estimates for the amount of delamination based on the binary scores (0,1) in the thoracic vertebrae (A) and lumbar vertebrae (B) [TBS = total body score]

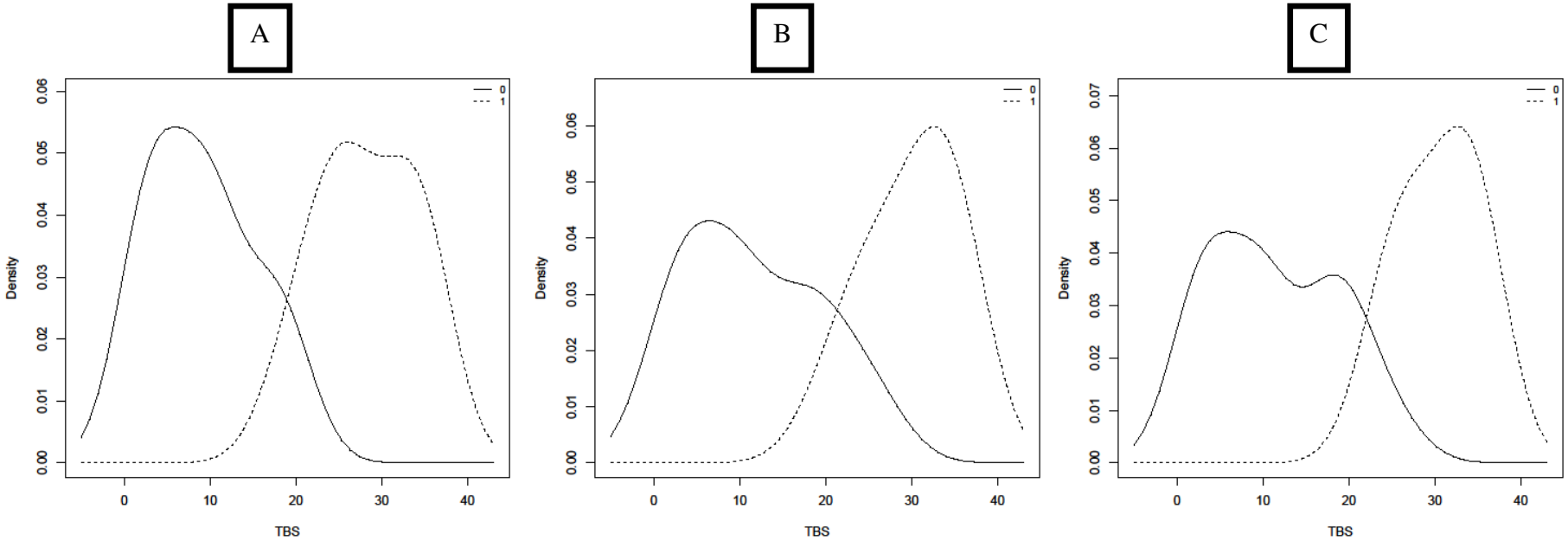

Figure 4.17 Kernel density estimates for the amount of heat-induced fractures based on the binary scores (0,1) in the ribs (A), scapula (B) and os coxa (C) [TBS = total body score]

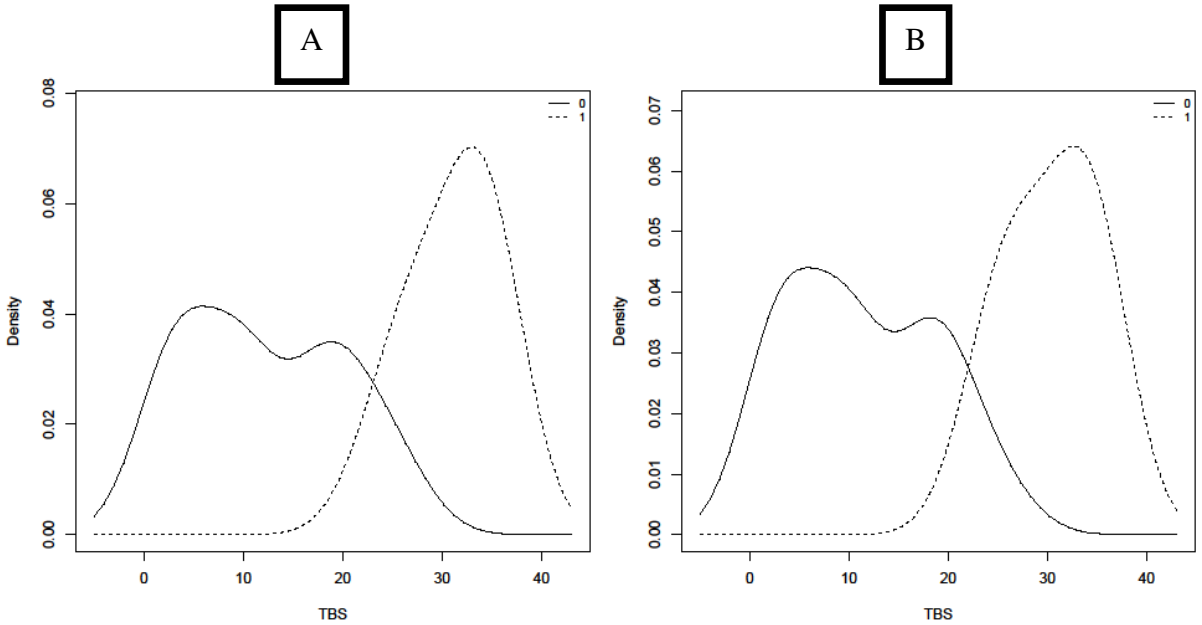

Figure 4.18 Kernel density estimates for the amount of heat-induced fractures based on the binary scores (0,1) in the thoracic vertebrae (A) and lumbar vertebrae (B) [TBS = total body score]

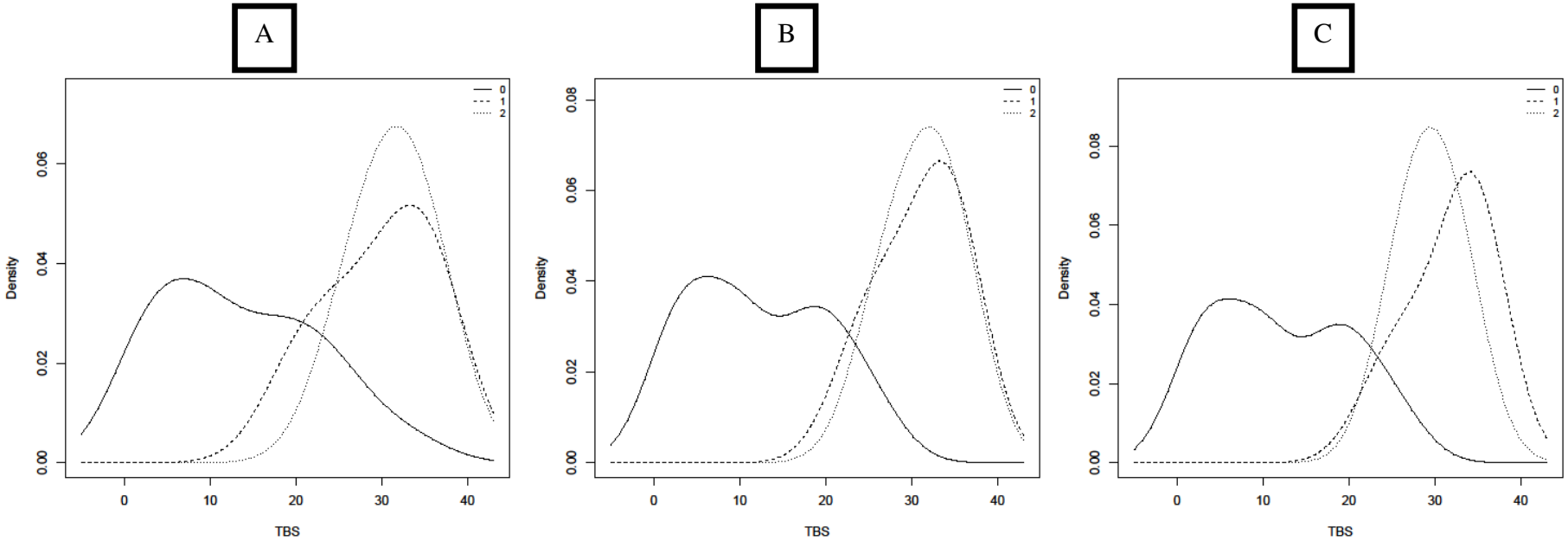

Figure 4.19 Kernel density estimates for the amount of calcined bone based on the ranked scores (0,1,2,3) in the humerus (A), ulna (B) and radius (C) [TBS = total body score]

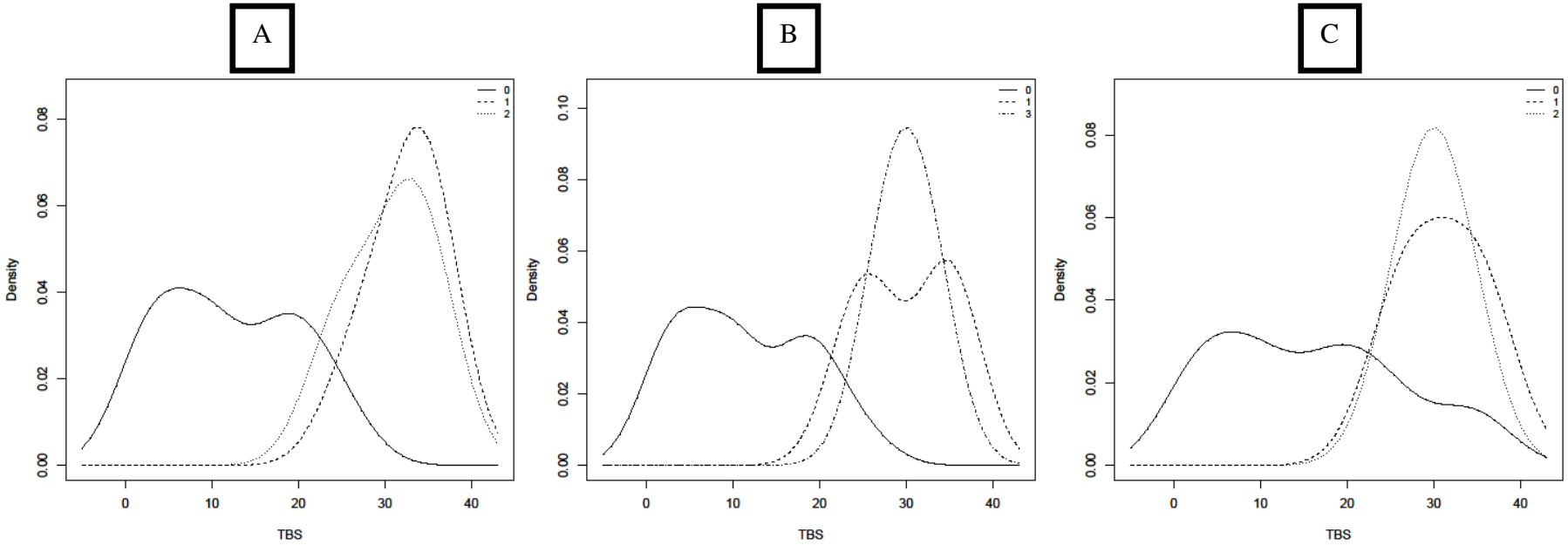

Figure 4.20 Kernel density estimates for the amount of calcined bone based on the ranked scores (0,1,2,3) in the femur (A), tibia (B) and fibula (C) [TBS = total body score]

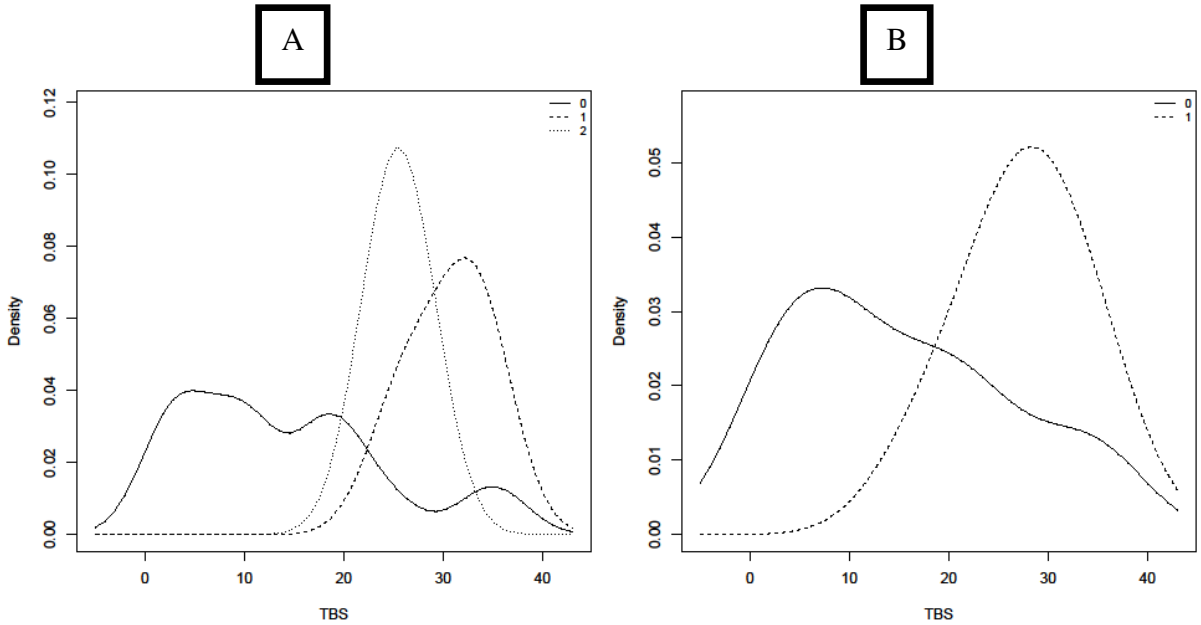

Figure 4.21 Kernel density estimates for the amount of calcined bone based on the ranked scores (0,1,2,3) in the metacarpals (A) and metatarsals (B) [TBS = total body score]

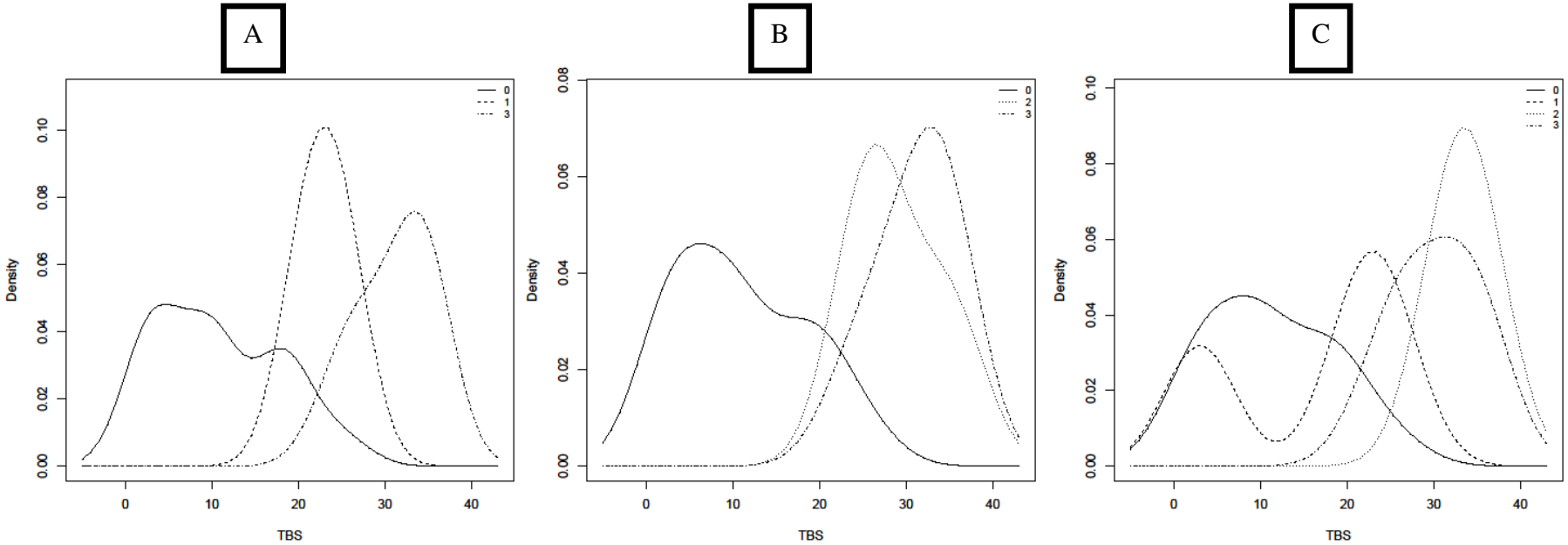

Figure 4.22 Kernel density estimates for the amount of charred bone based on the ranked scores (0,1,2,3) in the humerus (A), ulna (B) and radius (C) [TBS = total body score]

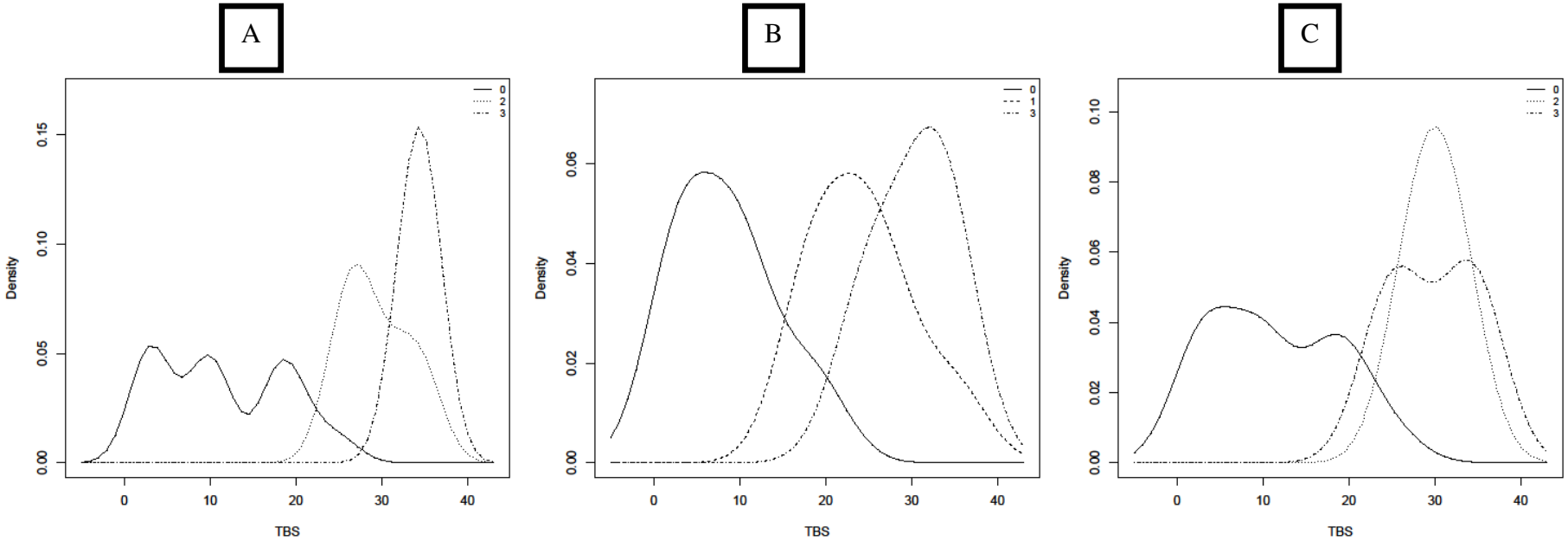

Figure 4.23 Kernel density estimates for the amount of charred bone based on the ranked scores (0,1,2,3) in the femur (A), tibia (B) and fibula (C) [TBS = total body score]

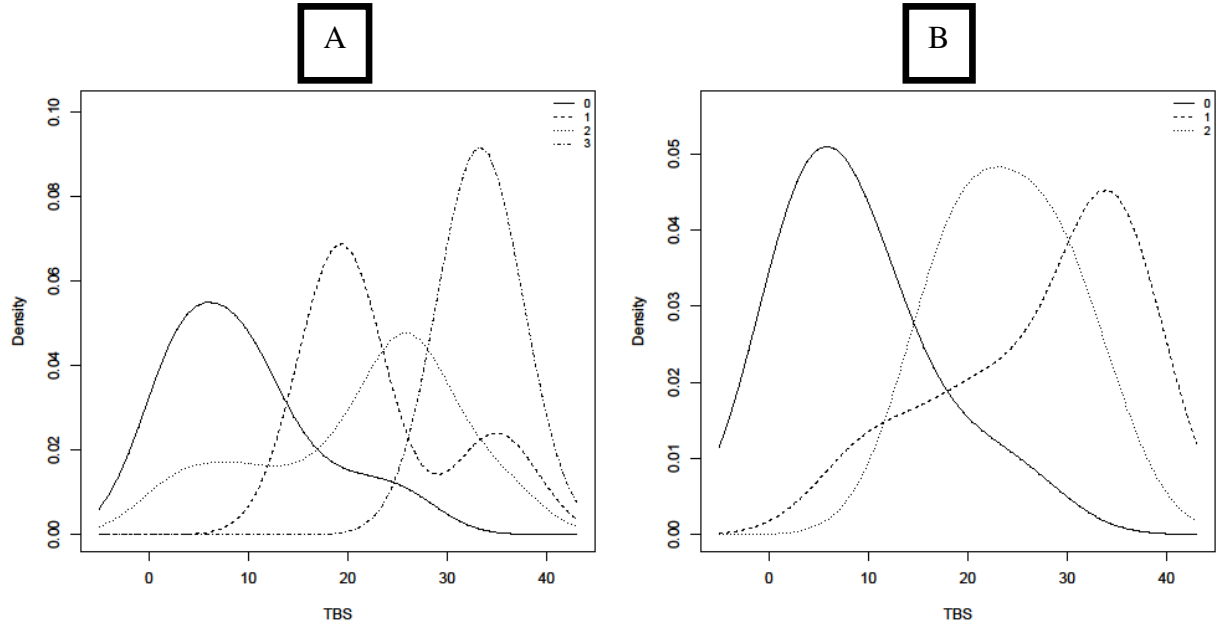

Figure 4.24 Kernel density estimates for the amount of charred bone based on the ranked scores (0,1,2,3) in the metacarpals (A) and metatarsals (B) [TBS = total body score]

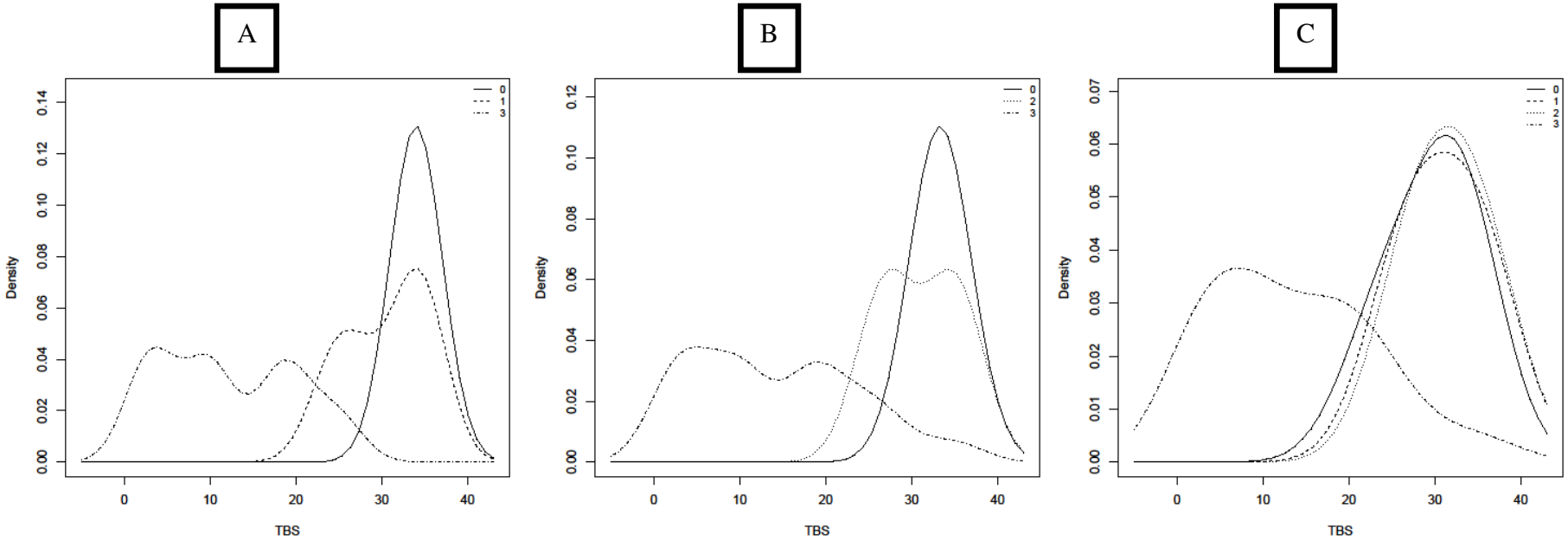

Figure 4.25 Kernel density estimates for the amount of unaltered bone based on the ranked scores (0,1,2,3) in the humerus (A), ulna (B) and radius (C) [TBS = total body score]

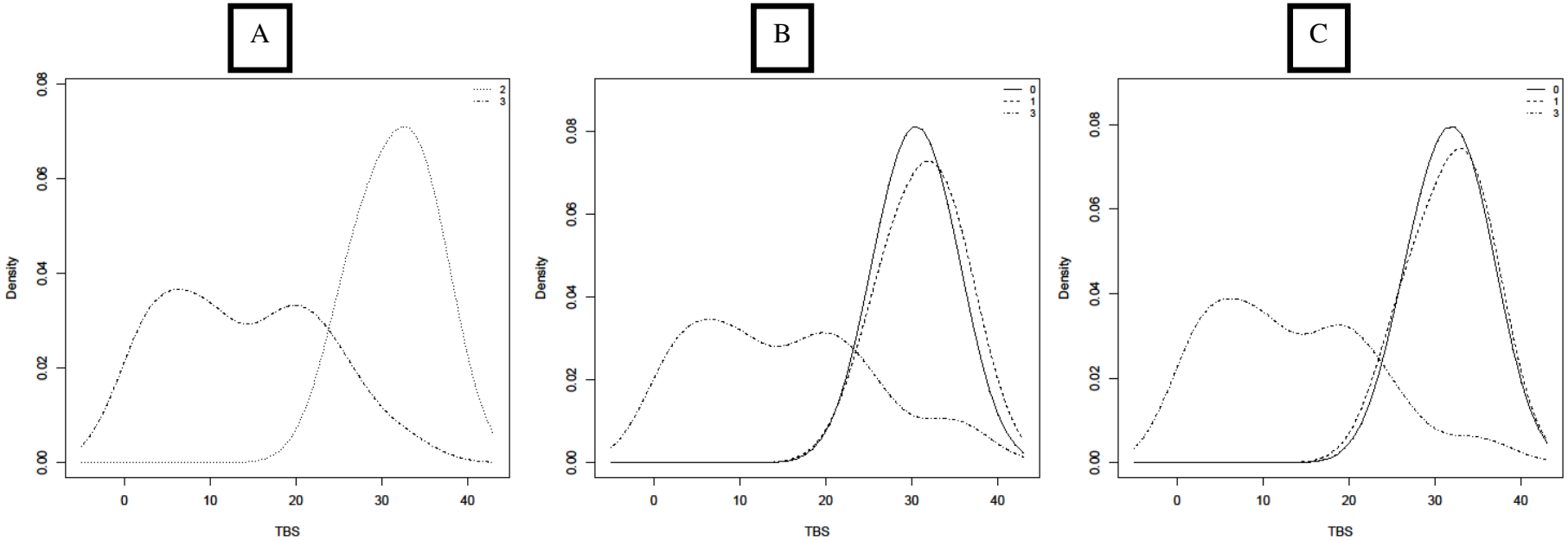

Figure 4.26 Kernel density estimates for the amount of unaltered bone based on the ranked scores (0,1,2,3) in the femur (A), tibia (B) and fibula (C) [TBS = total body score]

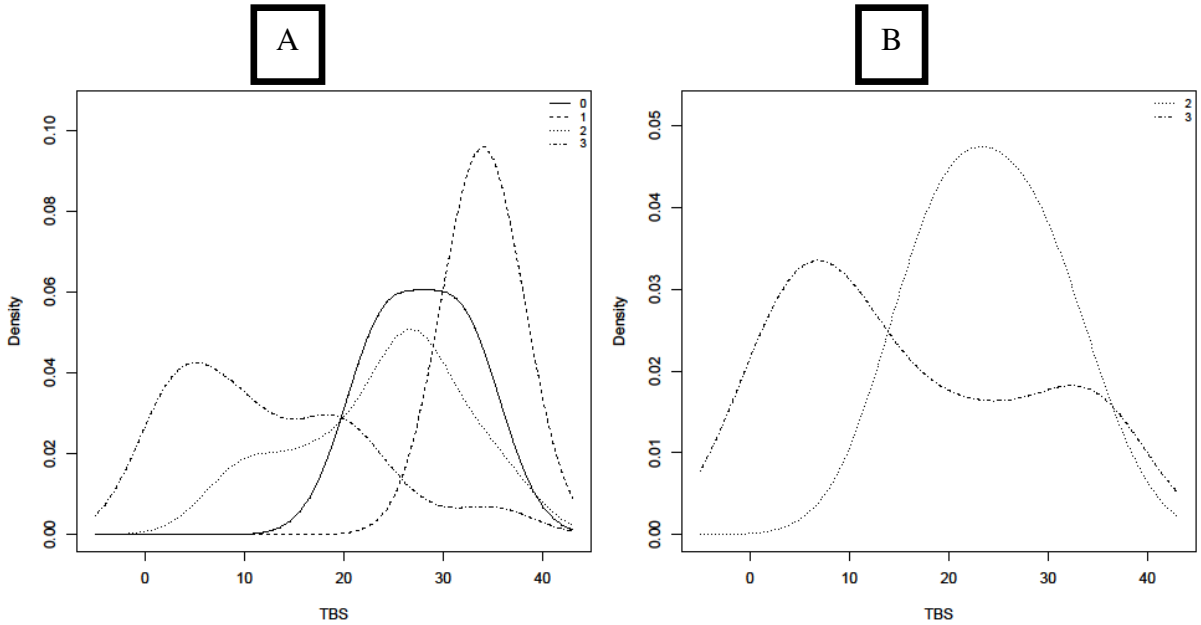

Figure 4.27 Kernel density estimates for the amount of unaltered bone based on the ranked scores (0,1,2,3) in the metacarpals (A) and metatarsals (B) [TBS = total body score]

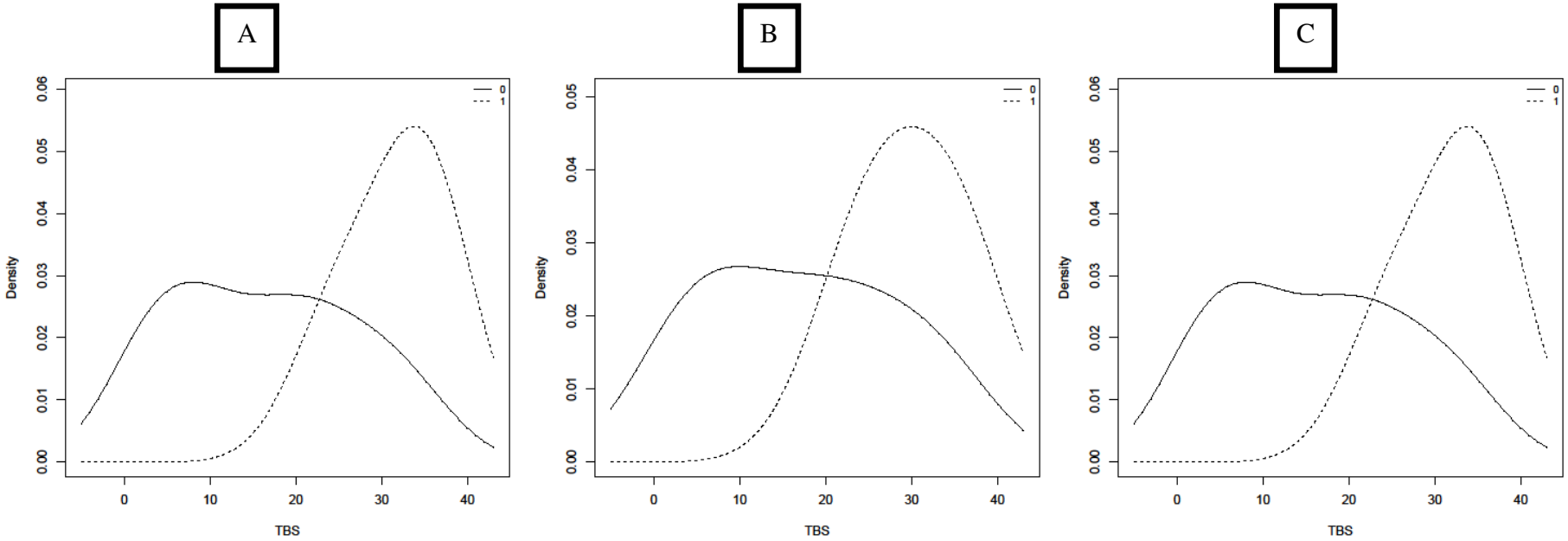

Figure 4.28 Kernel density estimates for brown burn based on the binary scores (0,1) in the radius (A), ulna (B) and tibia (C) [TBS = total body score]

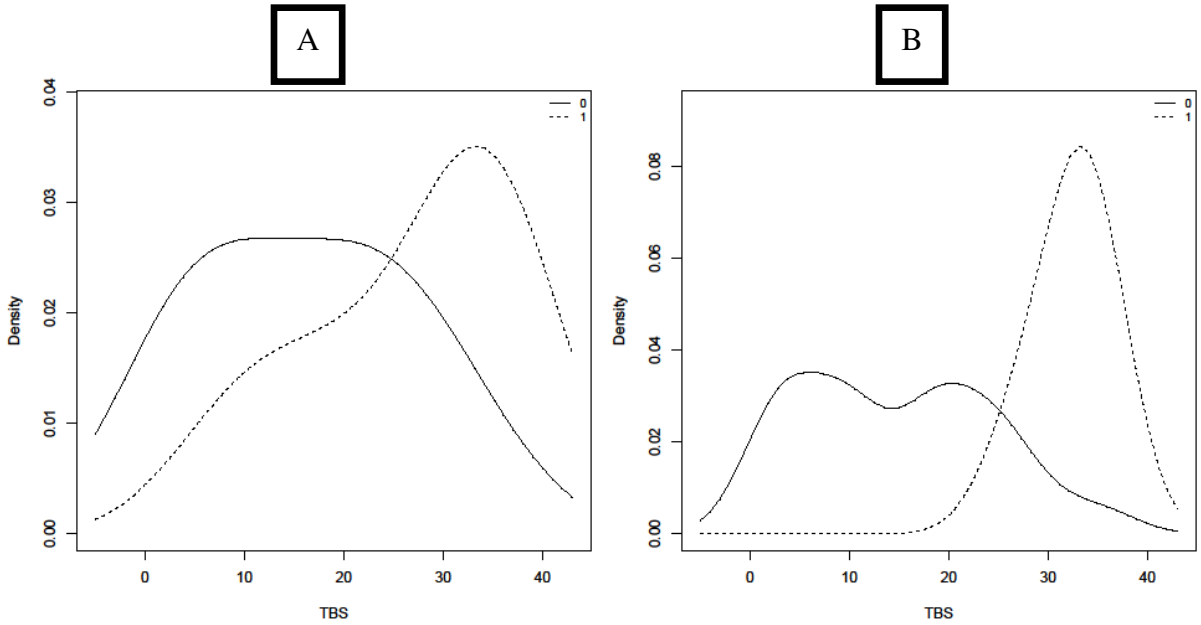

Figure 4.29 Kernel density estimates for brown burn based on the binary scores (0,1) in the metacarpals (A) and metatarsals (B) [TBS = total body score]

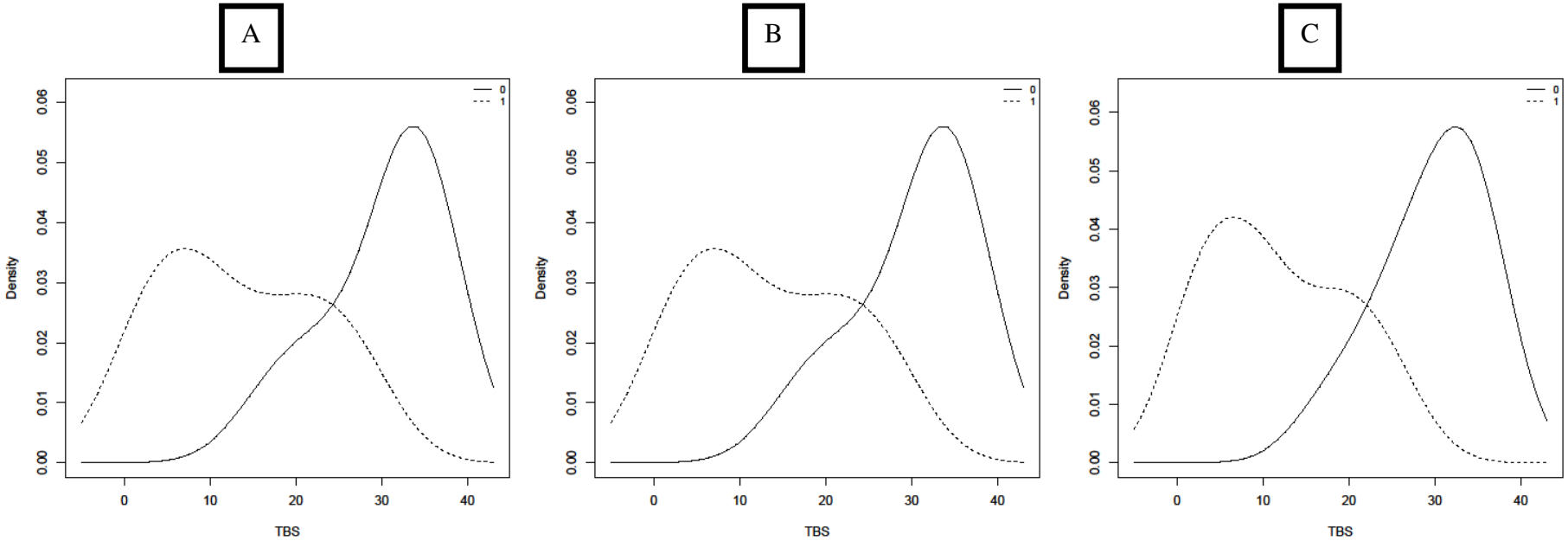

Figure 4.30 Kernel density estimates for greasy bone based on the binary scores (0,1) in the humerus (A), ulna (B) and radius (C) [TBS = total body score]

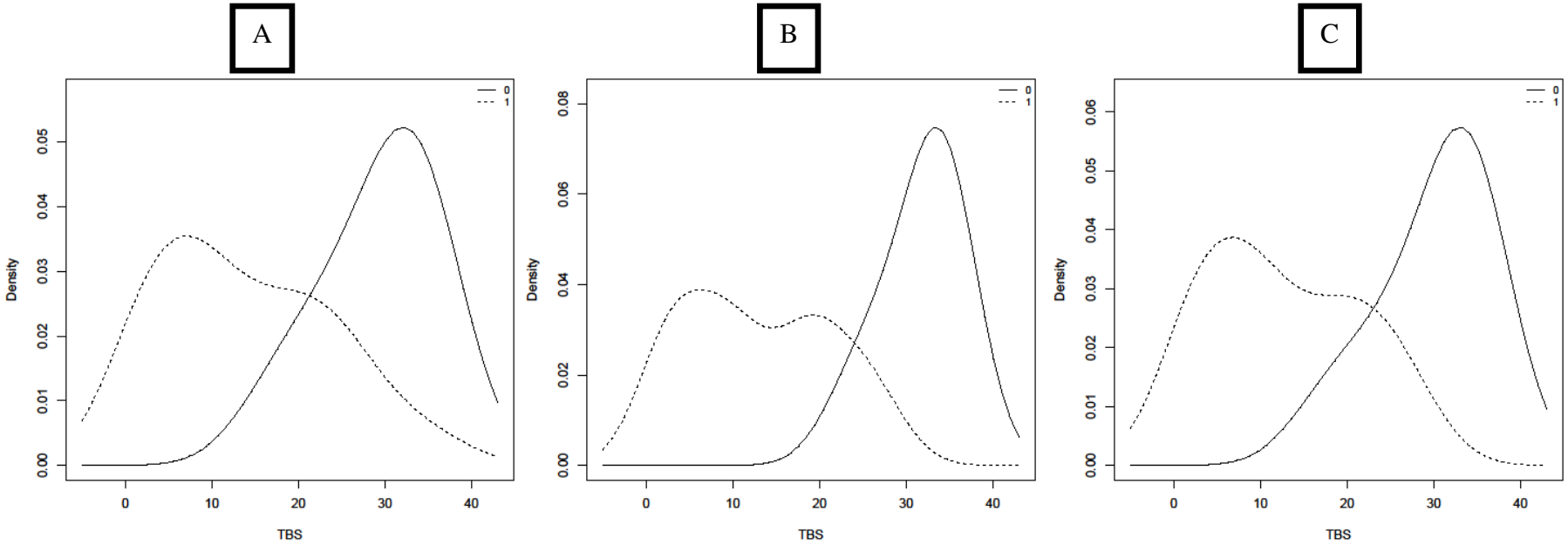

Figure 4.31 Kernel density estimates for greasy bone based on the binary scores (0,1) in the femur (A), tibia (B) and fibula (C) [TBS = total body score]

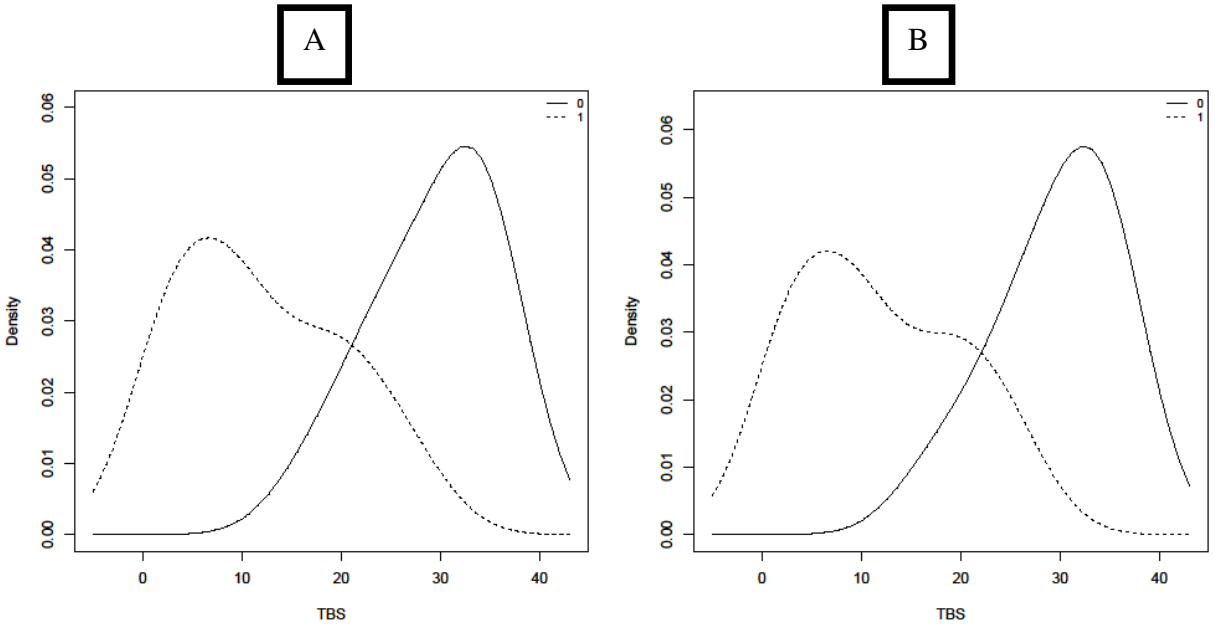

Figure 4.32 Kernel density estimates for greasy bone based on the binary scores (0,1) in the metacarpals (A) and metatarsals (B) [TBS = total body score]

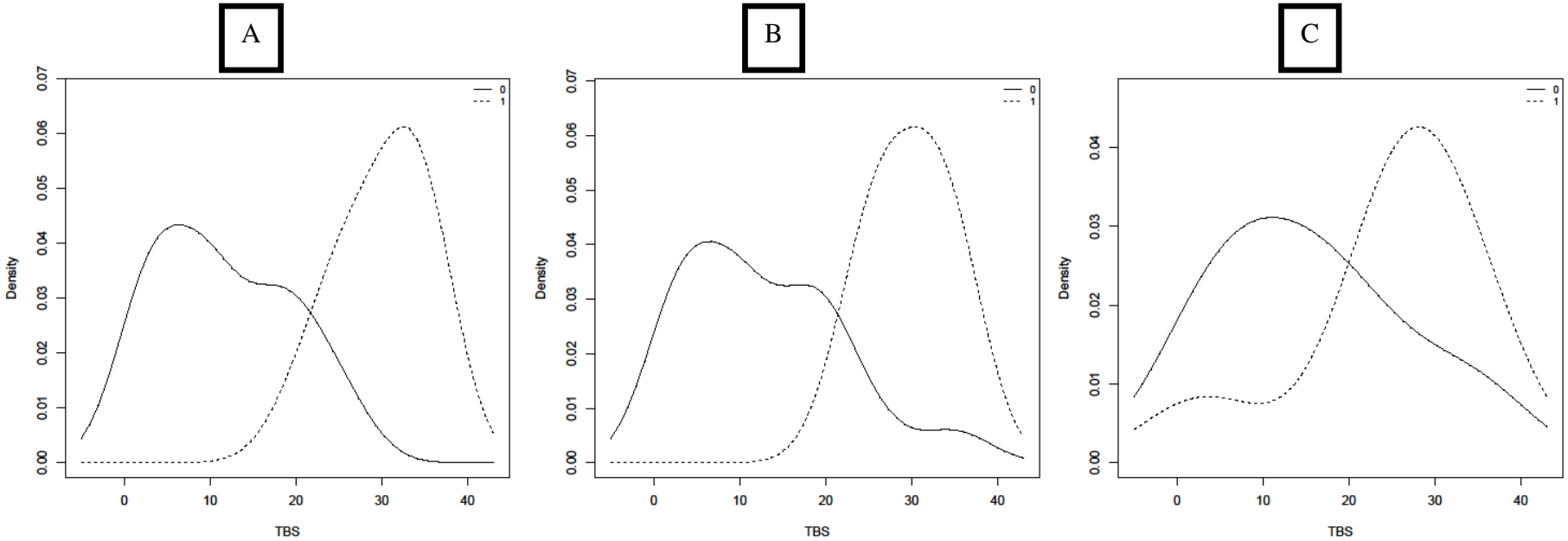

Figure 4.33 Kernel density estimates for delamination based on the binary scores (0,1) in the humerus (A), ulna (B) and radius (C) [TBS = total body score]

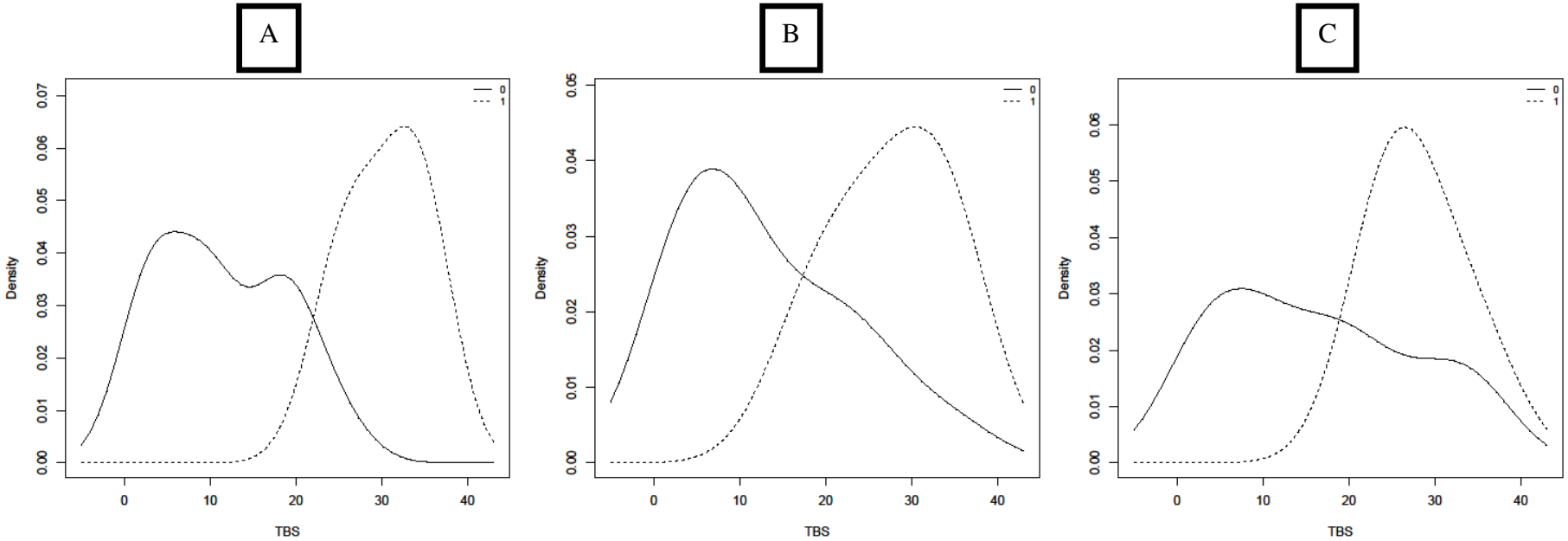

Figure 4.34 Kernel density estimates for delamination based on the binary scores (0,1) in the femur (A), tibia (B) and fibula (C) [TBS = total body score]

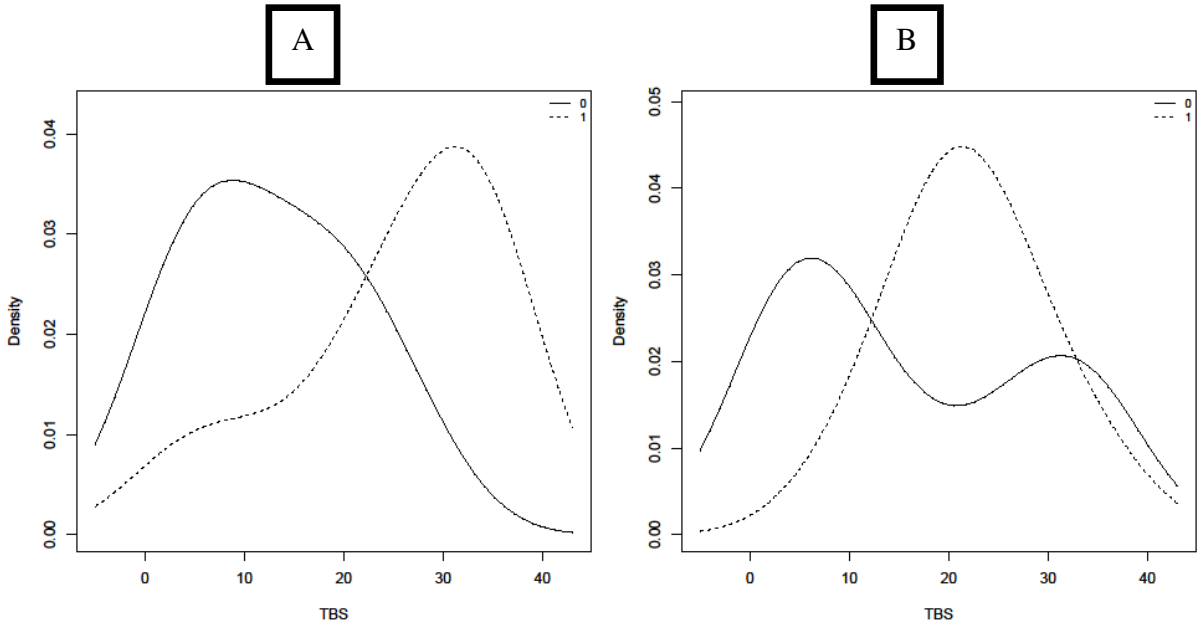

Figure 4.35 Kernel density estimates for delamination based on the binary scores (0,1) in the metacarpals (A) and metatarsals (B) [TBS = total body score]

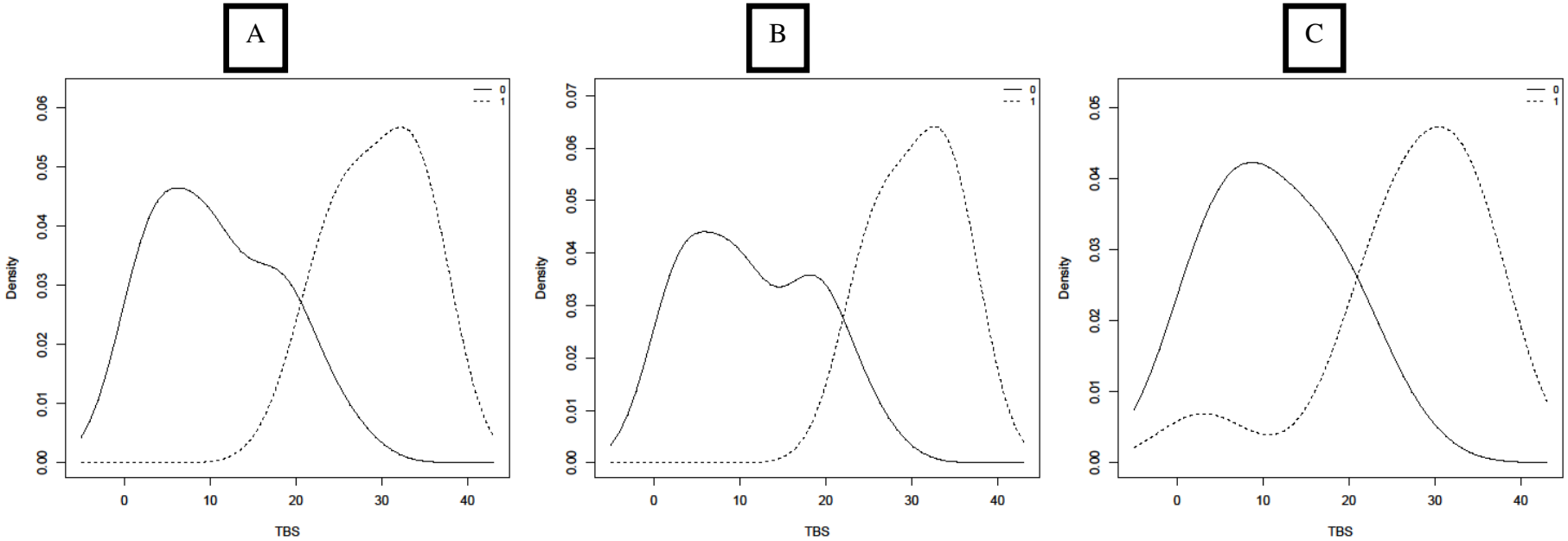

Figure 4.36 Kernel density estimates for heat-induced fractures based on the binary scores (0,1) in the humerus (A), ulna (B) and radius (C) [TBS = total body score]

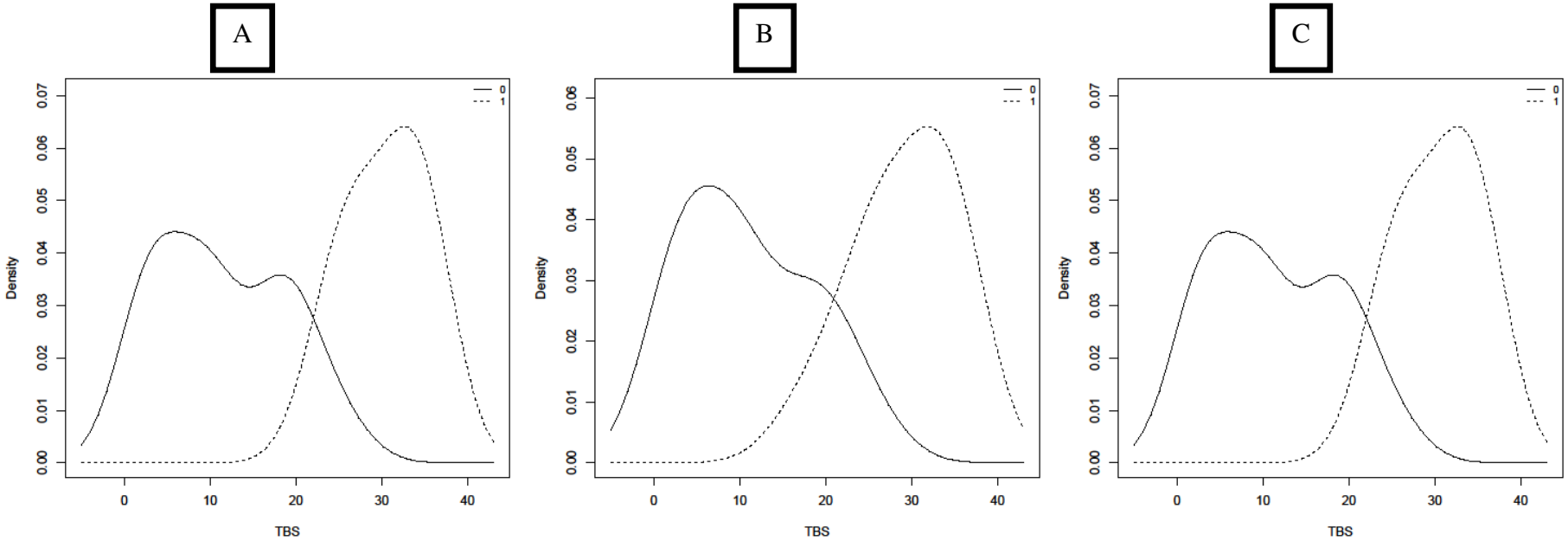

Figure 4.37 Kernel density estimates for heat-induced fractures based on the binary scores (0,1) in the femur (A), tibia (B) and fibula (C) [TBS = total body score]

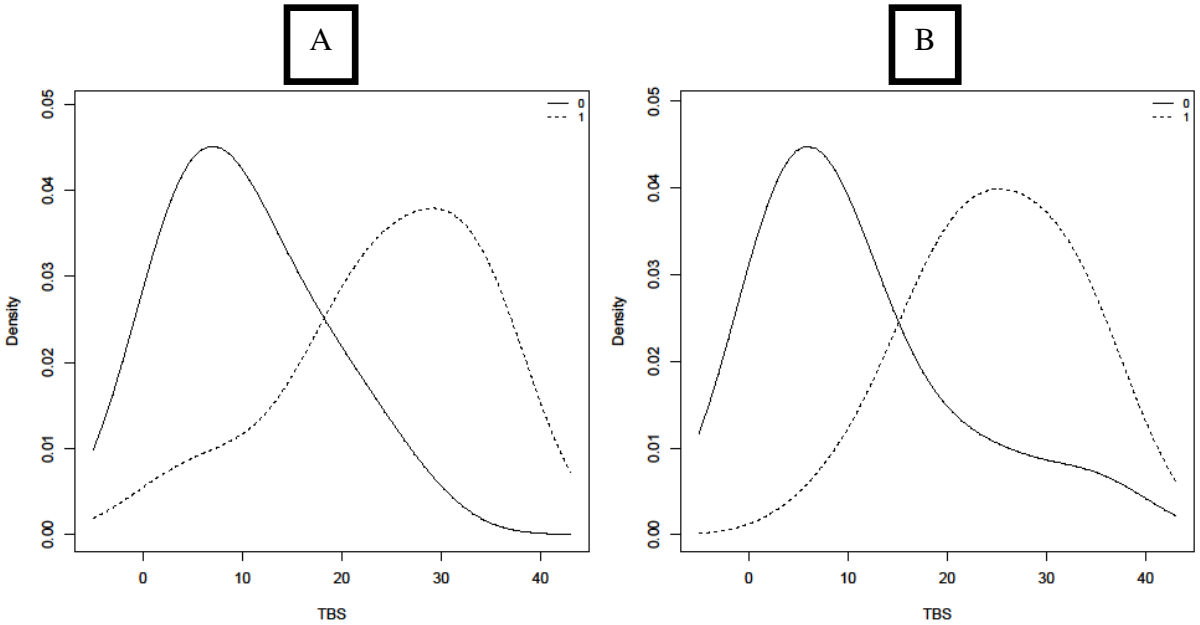

Figure 4.38 Kernel density estimates for heat-induced fractures based on the binary scores (0,1) in the metacarpals (A) and metatarsals (B) [TBS = total body score]

Table 4.1 Frequency distribution for calcined bone scored in the head and neck (HN_Cal) (PSU = primary sampling unit)

Number of strata	= 1	Number of obs	= 75
Number of PSUs	= 25	Population size	= 75
		Design df	= 24

	Stage of decomposition				
HN_Cal	**A**	**B**	**C**	**D**	**E**
0	100	100	60	0	0
1	0	0	27	40	26.7
2	0	0	13	60	40
3	0	0	0	0	33.3
Total	100	100	100	100	100

Key: column proportions

Pearson:				
Uncorrected chi2(12)	=	77.9509		
Design-based F(7.51, 180.15)	=	3.8773	p =	0.0004

Table 4.2 Frequency distribution for charred bone scored in the head and neck (HN_Cha) (PSU = primary sampling unit)

Number of strata	= 1	Number of obs	= 75
Number of PSUs	= 25	Population size	= 75
		Design df	= 24

	Stage of decomposition				
HN_Cha	**A**	**B**	**C**	**D**	**E**
0	100	100	20	0	0
1	0	0	60	13.3	47
2	0	0	20	74.3	40
3	0	0	0	13.3	13
Total	100	100	100	100	100

Key: column proportions

Pearson:				
Uncorrected chi2(12)	=	83.2677		
Design-based F(6.54, 156.90)	=	5.1493	p =	0.0000

Table 4.3 Frequency distribution for unaltered bone scored in the head and neck (HN_Una) (PSU = primary sampling unit)

Number of strata	= 1	Number of obs	= 75
Number of PSUs	= 25	Population size	= 75
		Design df	= 24

	Stage of decomposition				
HN_Una	**A**	**B**	**C**	**D**	**E**
0	0	0	6.7	27	53.3
1	0	0	0	27	33.3
2	0	0	13.3	33	0
3	100	100	80	13	13.3
Total	100	100	100	100	100

Key: column proportions

Pearson:				
Uncorrected chi2(12)	=	65.0807		
Design-based F(7.98, 191.48)	=	3.3799	p =	0.0012

Table 4.4 Frequency distribution for greasy bone scored in the head and neck (HN_Gr) (PSU = primary sampling unit)

Number of strata	= 1	Number of obs	= 75
Number of PSUs	= 25	Population size	= 75
		Design df	= 24

	Stage of decomposition				
HN_Gr	**A**	**B**	**C**	**D**	**E**
0	0	0	33.3	53.3	100
1	100	100	66.7	46.7	0
Total	100	100	100	100	100

Key: column proportions

Pearson:				
Uncorrected chi2(12)	=	44.7948		
Design-based F(3.75, 90.04)	=	4.617	p =	0.0024

Table 4.5 Frequency distribution for delamination scored in the head and neck (HN_D2) (PSU = primary sampling unit)

Number of strata	= 1	Number of obs	= 75
Number of PSUs	= 25	Population size	= 75
		Design df	= 24

	Stage of decomposition				
HN_D2	**A**	**B**	**C**	**D**	**E**
0	100	100	33.3	33.3	33.3
1	0	0	66.7	66.7	66.7
Total	100	100	100	100	100

Key: column proportions

Pearson:				
Uncorrected chi2(12)	=	33.3333		
Design-based F(2.47, 59.28)	=	6.2745	p =	0.0018

Table 4.6 Frequency distribution for heat-induced fractures scored in the head and neck (HN_HIF) (PSU = primary sampling unit)

Number of strata	= 1	Number of obs	= 75
Number of PSUs	= 25	Population size	= 75
		Design df	= 24

	Stage of decomposition				
HN_HIF	**A**	**B**	**C**	**D**	**E**
0	100	100	53.3	0	0
1	0	0	46.7	100	100
Total	100	100	100	100	100

Key: column proportions

Pearson:				
Uncorrected chi2(12)	=	60.064		
Design-based F(3.31, 79.35)	=	6.7116	p =	0.0003

Table 4.7 Frequency distribution for calcined bone scored in the trunk (T_Cal) (PSU = primary sampling unit)

Number of strata	= 1	Number of obs	= 125
Number of PSUs	= 25	Population size	= 125
		Design df	= 24

	Stage of decomposition				
T_Cal	**A**	**B**	**C**	**D**	**E**
0	100	100	100	44	0
1	0	0	0	24	56
2	0	0	0	28	36
3	0	0	0	4	8
Total	100	100	100	100	100

Key: column proportions

Pearson:				
Uncorrected chi2(12)	=	98.0048		
Design-based F(4.70, 112.69)	=	5.1342	p =	0.0004

Table 4.8 Frequency distribution for charred bone scored in the trunk (T_Cha) (PSU = primary sampling unit)

Number of strata	= 1	Number of obs	= 125
Number of PSUs	= 25	Population size	= 125
		Design df	= 24

	Stage of decomposition				
T_Cha	**A**	**B**	**C**	**D**	**E**
0	100	100	84	16	0
1	0	0	16	24	0
2	0	0	0	48	32
3	0	0	0	12	68
Total	100	100	100	100	100

Key: column proportions

Pearson:				
Uncorrected chi2(12)	=	141.3		
Design-based F(5.68, 136.32)	=	5.7857	p =	0.0000

Table 4.9 Frequency distribution for unaltered bone scored in the trunk (T_Una) (PSU = primary sampling unit)

Number of strata	= 1	Number of obs	= 125
Number of PSUs	= 25	Population size	= 125
		Design df	= 24

	Stage of decomposition				
T_Una	**A**	**B**	**C**	**D**	**E**
0	0	0	0	4	12
1	0	0	0	8	64
2	0	0	0	24	16
3	100	100	100	64	8
Total	100	100	100	100	100

Key: column proportions

Pearson:				
Uncorrected chi2(12)	=	100.5072		
Design-based F(4.05, 97.17)	=	3.3602	p =	0.0001

Table 4.10 Frequency distribution for greasy bone scored in the trunk (T_Gr) (PSU = primary sampling unit)

Number of strata	= 1	Number of obs	= 125
Number of PSUs	= 25	Population size	= 125
		Design df	= 24

	Stage of decomposition				
T_Gr	**A**	**B**	**C**	**D**	**E**
0	0	0	20	24	92
1	100	100	80	76	8
Total	100	100	100	100	100

Key: column proportions

Pearson:				
Uncorrected chi2(12)	=	72.479		
Design-based F(3.61, 86.60)	=	4.4366	p =	0.0036

Table 4.11 Frequency distribution for delamination scored in the trunk (T_D2) (PSU = primary sampling unit)

Number of strata	= 1	Number of obs	= 125
Number of PSUs	= 25	Population size	= 125
		Design df	= 24

	Stage of decomposition				
T_D2	**A**	**B**	**C**	**D**	**E**
0	100	100	76	20	0
1	0	0	24	80	100
Total	100	100	100	100	100

Key: column proportions

Pearson:				
Uncorrected chi2(12)	=	89.5061		
Design-based F(3.40, 81.59)	=	7.1188	p =	0.0001

Table 4.12 Frequency distribution for heat-induced fractures scored in the trunk (T_HIF) (PSU = primary sampling unit)

Number of strata	= 1	Number of obs	= 125
Number of PSUs	= 25	Population size	= 125
		Design df	= 24

	Stage of decomposition				
T_HIF	**A**	**B**	**C**	**D**	**E**
0	100	100	88	24	0
1	0	0	12	76	100
Total	100	100	100	100	100

Key: column proportions

Pearson:				
Uncorrected chi2(12)	=	94.3126		
Design-based F(3.28, 78.62)	=	7.8277	p =	0.0001

Table 4.13 Frequency distribution for calcined bone scored in the limbs (L_Cal) (PSU = primary sampling unit)

Number of strata	= 1	Number of obs	= 200
Number of PSUs	= 25	Population size	= 200
		Design df	= 24

	Stage of decomposition				
L_Cal	**A**	**B**	**C**	**D**	**E**
0	100	100	95	40	22.5
1	0	0	5	37.5	52.5
2	0	0	0	17.5	22.5
3	0	0	0	5	2.5
Total	100	100	100	100	100

Key: column proportions

Pearson:				
Uncorrected chi2(12)	=	111.2771		
Design-based F(4.40, 105.56)	=	3.979	p =	0.0036

Table 4.14 Frequency distribution for charred bone scored in the limbs (L_Cha) (PSU = primary sampling unit)

Number of strata	= 1	Number of obs	= 200
Number of PSUs	= 25	Population size	= 200
		Design df	= 24

	Stage of decomposition				
L_Cha	**A**	**B**	**C**	**D**	**E**
0	95	95	65	17.5	0
1	2.5	2.5	25	17.5	17.5
2	2.5	2.5	10	30	22.5
3	0	0	0	35	60
Total	100	100	100	100	100

Key: column proportions

Pearson:				
Uncorrected chi2(12)	=	150.7744		
Design-based F(6.06, 145.53)	=	4.2299	p =	0.0006

Table 4.15 Frequency distribution for unaltered bone scored in the limbs (L_Una) (PSU = primary sampling unit)

Number of strata	= 1	Number of obs	= 200
Number of PSUs	= 25	Population size	= 200
		Design df	= 24

	Stage of decomposition				
L_Una	**A**	**B**	**C**	**D**	**E**
0	0	0	0	10	27.5
1	0	0	0	17.5	27.5
2	0	2.5	10	27.5	17.5
3	100	97.5	90	45	27.5
Total	100	100	100	100	100

Key: column proportions

Pearson:				
Uncorrected chi2(12)	=	102.3605		
Design-based F(4.84, 116.16)	=	3.4803	p =	0.0063

Table 4.16 Frequency distribution for brown burn/borders scored in the limbs (L_BB) (PSU = primary sampling unit)

Number of strata	= 1	Number of obs	= 200
Number of PSUs	= 25	Population size	= 200
		Design df	= 24

	Stage of decomposition				
L_BB	**A**	**B**	**C**	**D**	**E**
0	100	97.5	97.5	90	67.5
1	0	2.5	2.5	10	32.5
Total	100	100	100	100	100

Key: column proportions

Pearson:				
Uncorrected chi2(12)	=	33.3818		
Design-based F(3.10, 74.41)	=	4.7785	p =	0.0039

Table 4.17 Frequency distribution for greasy bone scored in the limbs (L_Gr) (PSU = primary sampling unit)

Number of strata	= 1	Number of obs	= 200
Number of PSUs	= 25	Population size	= 200
		Design df	= 24

	Stage of decomposition				
L_Gr	**A**	**B**	**C**	**D**	**E**
0	0	0	17.5	42.5	97.5
1	100	100	82.5	57.5	2.5
Total	100	100	100	100	100

Key: column proportions

Pearson:				
Uncorrected chi2(12)	=	123.4156		
Design-based F(3.13, 75.05)	=	5.8205	p =	0.0011

Table 4.18 Frequency distribution for delamination scored in the limbs (L_D2) (PSU = primary sampling unit)

Number of strata	= 1	Number of obs	= 200
Number of PSUs	= 25	Population size	= 200
		Design df	= 24

	Stage of decomposition				
L_D2	**A**	**B**	**C**	**D**	**E**
0	95	95	80	32.5	32.5
1	5	5	20	67.5	67.5
Total	100	100	100	100	100

Key: column proportions

Pearson:				
Uncorrected chi2(12)	=	74.4912		
Design-based F(2.67, 63.96)	=	9.7093	p =	0.0000

Table 4.19 Frequency distribution for heat-induced fractures scored in the limbs (L_HIF) (PSU = primary sampling unit)

Number of strata	= 1	Number of obs	= 200
Number of PSUs	= 25	Population size	= 200
		Design df	= 24

	Stage of decomposition				
L_HIF	**A**	**B**	**C**	**D**	**E**
0	95	95	75	20	2.5
1	5	5	25	80	97.5
Total	100	100	100	100	100

Key: column proportions

Pearson:				
Uncorrected chi2(12)	=	123.5806		
Design-based F(2.44, 58.61)	=	12.4352	p =	0.0000

Table 4.20 Results of the multiple regression analysis for categorical variables for the cranium

Source	SS	df	MS
Model	2752.473	5	550.5
Residual	324.5667	19	17.08
Total	3077.04	24	128.2

Number of Obs	= 25
F(5, 19)	= 32.23
Prob > F	= 0.0000
R-squared	= 0.8945
Adj r-squared	= 0.8668
Root MSE	= 4.1331

TBS	Coef	Std. Err.	t	P>|t|	[95% Conf. Interval]		
Cr_Cal							
1	8.333333	3.77298	2.21	0.040	0.4363949	-	16.23027
2	16.5	5.84508	2.82	0.011	4.266116	-	28.73388
3	16.33333	3.77298	4.33	0.000	8.436395	-	24.23027
Cr_Cha							
1	11.6	3.20148	3.62	0.002	4.899226	-	18.30077
2	3.266667	5.74683	0.57	0.576	-8.761592	-	15.29492
_cons	6.4	1.307	4.9	0.000	3.66442	-	9.13558

Table 4.21 Results of the multiple regression analysis for categorical variables for the mandible

Source	SS	df	MS
Model	2766.176	4	691.5
Residual	310.8643	20	15.54
Total	3077.04	24	128.2

Number of Obs	= 25
F(4, 20)	= 44.49
Prob > F	= 0.0000
R-squared	= 0.8990
Adj r-squared	= 0.8788
Root MSE	= 3.9425

TBS	Coef	Std. Err.	t	P>|t|	[95% Conf. Interval]		
Mn_Cal							
1	11.75	3.4143	3.44	0.003	4.627905	-	18.87209
2	21.02857	1.94288	10.82	0.000	16.9758	-	25.08135
3	15.75	3.4143	4.61	0.001	8.627005	-	22.87209
Mn_Cha							
1	11.85	2.33241	5.08	0.000	6.984683	-	16.71532
2	(omitted)						
_cons	6.4	1.24672	5.13	0.000	3.799379	-	9.000621

Table 4.22 Results for the multiple regression analysis for categorical variables for the cervical vertebrae

Source	SS	df	MS
Model	2496.098	4	624
Residual	580.9423	20	29.05
Total	3077.04	24	128.2

Number of Obs	= 25
F(4, 20)	= 21.48
Prob > F	= 0.0000
R-squared	= 0.8112
Adj r-squared	= 0.7734
Root MSE	= 5.3895

TBS	Coef	Std. Err.	t	P>|t|	[95% Conf. Interval]		
CV_Cal							
1	22.09615	3.08159	7.17	0.000	15.66808	-	28.52423
2	28.09615	5.59299	5.02	0.000	16.42939	-	39.76292
CV_Cha							
1	-11.75	4.66748	-2.52	0.02	-21.48619	-	-2.01382
2	-6.25	4.66748	-1.34	0.196	-15.98619	-	3.486185
3	(omitted)						
_cons	9.153846	1.49479	6.12	0.000	6.035771	-	12.27192

Table 4.23 Results for the multiple regression analysis for categorical variables for the ribs

Source	SS	df	MS
Model	2577.524	5	515.5
Residual	499.5157	19	26.29
Total	3077.04	24	128.2

Number of Obs	= 25
F(5, 19)	= 19.61
Prob > F	= 0.0000
R-squared	= 0.8377
Adj r-squared	= 0.7949
Root MSE	= 5.1274

TBS	Coef	Std. Err.	t	P>|t|	[95% Conf. Interval]		
Rb_Cal							
1	5	6.27977	0.8	0.436	-8.143699	-	18.1437
2	10.62963	7.28474	1.46	0.161	-4.617509	-	25.87677
Rb_Cha							
1	10.92308	3.89455	2.8	0.011	2.771701	-	19.07445
2	11.33048	7.22279	1.57	0.133	-3.786998	-	26.44795
3	17.10826	7.61649	2.25	0.037	1.166764	-	33.04976
_cons	9.076923	1.42209	6.38	0.000	6.100461	-	12.05338

Table 4.24 Results for the multiple regression analysis for categorical variables for the scapula

Source	SS	df	MS
Model	2299.39	5	459.9
Residual	777.65	19	40.93
Total	3077.04	24	128.2

Number of Obs	= 25
F(5, 19)	= 11.24
Prob > F	= 0.0000
R-squared	= 0.7473
Adj r-squared	= 0.6808
Root MSE	= 6.3976

TBS	Coef	Std. Err.	t	P>|t|	[95% Conf. Interval]		
Sca_Cha							
1	12.2	4.81592	2.53	0.02	2.120167	-	22.27983
2	20.7	4.81592	4.3	0.000	10.62017	-	30.77983
3	13.2	6.60739	2	0.06	-0.629417	-	27.02942
Sca_Una							
1	9.75	7.15271	1.36	0.189	-5.220783	-	24.72078
2	3	9.04754	0.33	0.744	-15.93671	-	21.93671
3	(omitted)						
_cons	10.8	1.65185	6.54	0.000	7.32646	-	14.25735

Table 4.25 Results for the multiple regression analysis for categorical variables for the os coxa

Source	SS	df	MS
Model	2193.936	4	548.5
Residual	883.1042	20	44.16
Total	3077.04	24	128.2

Number of Obs	= 25
F(4, 20)	= 12.42
Prob > F	= 0.0000
R-squared	= 0.7130
Adj r-squared	= 0.6556
Root MSE	= 6.6449

TBS	Coef	Std. Err.	t	P>|t|	[95% Conf. Interval]		
OsC_Cha							
1	14.5625	4.9837	2.92	0.008	4.166676	-	24.95832
2	16.89583	4.18068	4.04	0.001	8.175083	-	25.61658
3	23.5625	4.9837	4.73	0.000	13.16668	-	33.95832
OsC_Una							
2	5.166667	6.06597	0.85	0.404	-7.486728	-	17.82006
3	(omitted)						
_cons	11.4375	1.66124	6.88	0.000	7.972225	-	14.90277

Table 4.26 Results for the multiple regression analysis for categorical variables for the thoracic vertebrae

Source	SS	df	MS
Model	2289.34	4	572.3
Residual	787.7	20	39.39
Total	3077.04	24	128.2

Number of Obs	= 25
F()	= 14.53
Prob > F	= 0.0000
R-squared	= 0.7440
Adj r-squared	= 0.6928
Root MSE	= 6.2757

TBS	Coef	Std. Err.	t	P>|t|	[95% Conf. Interval]		
TV_Cha							
1	12.2	4.72421	2.58	0.018	2.345469	-	22.05453
2	21.2	6.48156	3.27	0.004	7.679695	-	34.7203
3	22.4	3.24078	6.91	0.000	15.63985	-	29.16015
TV_Una							
1	(omitted)						
2	-6.5		-0.85	0.408	-22.53311	-	9.533109
3	(omitted)						
_cons	10.8		6.67	0.000	7.419924	-	14.18008

Table 4.27 Results for the multiple regression analysis for categorical variables for the lumbar vertebrae

Source	SS	df	MS
Model	2233.603	5	446.7
Residual	843.4375	19	44.39
Total	3077.04	24	128.2

Number of Obs	= 25
F(5, 19)	= 10.06
Prob > F	= 0.0001
R-squared	= 0.7259
Adj r-squared	= 0.6538
Root MSE	= 6.6627

TBS	Coef	Std. Err.	t	P>|t|	[95% Conf. Interval]		
LV_Cha							
1	12.5625	6.86774	1.83	0.083	-1.811854	-	26.93685
2	13.0625	10.1319	1.29	0.213	-8.143792	-	34.26879
3	10.5625	6.86774	2.99	0.007	6.188146	-	34.93685
LV_Una							
1	2.5	7.44912	0.34	0.741	-13.09118	-	18.09118
2	2	11.0488	0.18	0.858	-21.12545	-	25.12545
3	(omitted)						
_cons	11.4375		6.87	0.000	7.951207	-	14.92379

Table 4.28 Results for the multiple regression analysis for categorical variables for the humerus

Source	SS	df	MS
Model	2231	4	557.9
Residual	845.6	20	42.28
Total	3077.04	24	128.2

Number of Obs	= 25
F(4, 20)	= 13.19
Prob > F	= 0.0000
R-squared	= 0.7252
Adj r-squared	= 0.6702
Root MSE	= 6.5023

TBS	Coef	Std. Err.	t	P>|t|	[95% Conf. Interval]		
Hum_Cha							
1	12.2	4.89476	2.49	0.022	1.989711	-	22.41029
3	23.2	4.89476	4.74	0.000	12.98971	-	33.41029
Hum_Una							
1	-3.4	5.44022	-0.62	0.539	-14.7481	-	7.948101
2	-6	7.96367	-0.75	0.46	-22.61192	-	10.61192
3	(omitted)						
_cons	10.8	1.67889	6.43	0.000	7.2979	-	14.3021

Table 4.29 Results for the multiple regression analysis for categorical variables for the ulna

Source	SS	df	MS
Model	2161.04	5	432.2
Residual	916	19	48.21
Total	3077.04	24	128.2

Number of Obs	= 25
F(5, 19)	= 8.97
Prob > F	= 0.0002
R-squared	= 0.7023
Adj r-squared	= 0.6240
Root MSE	= 6.9434

TBS	Coef	Std. Err.	t	P>|t|	[95% Conf. Interval]		
Uln_Cal							
1	5	11.4091	0.44	0.666	-18.8796	-	28.8796
2	6	8.50387	0.71	0.489	-11.7988	-	23.7988
Uln_Cha							
1	7	7.17109	0.98	0.341	-8.009268	-	22.00927
2	14	7.17109	1.95	0.066	-1.009268	-	29.00927
3	15	11.1239	1.35	0.193	-8.282515	-	38.28251
_cons	11	1.79277	6.14	0.000	7.247683	-	14.75232

Table 4.30 Results for the multiple regression analysis for categorical variables for the radius

Source	SS	df	MS
Model	2034.847	4	508.7
Residual	1042.193	20	52.11
Total	3077.04	24	128.2

Number of Obs	= 25
F(4, 20)	= 9.76
Prob > F	= 0.0002
R-squared	= 0.6613
Adj r-squared	= 0.5936
Root MSE	= 7.2187

TBS	Coef	Std. Err.	t	P>|t|	[95% Conf. Interval]		
Rad_Cal							
1	19.58036	3.67324	5.33	0.000	11.91812	-	27.2426
2	15.95536	6.28868	2.54	0.02	2.837397	-	29.07332
Rad_Cha							
1	4.97619	4.5926	1.08	0.291	-4.603813	-	14.55619
2	4.375	6.25158	0.7	0.492	-8.665568	-	17.41557
3	(omitted)						
_cons	11.35714	1.92928	5.89	0.000	7.332736	-	15.38155

Table 4.31 Results for the multiple regression analysis for categorical variables for the metacarpals

Source	SS	df	MS
Model	2211.184	8	276.4
Residual	865.8559	16	54.12
Total	3077.04	24	128.2

Number of Obs	= 25
F(8, 16)	= 5.11
Prob > F	= 0.0027
R-squared	= 0.7186
Adj r-squared	= 0.5779
Root MSE	= 7.3564

TBS	Coef	Std. Err.	t	P>|t|	[95% Conf. Interval]		
MC_Cal							
1	10.23529	5.64207	1.81	0.088	-1.725357	-	22.19595
2	9.941176	8.74066	1.14	0.272	-8.588184	-	28.47054
MC_Cha							
1	13.85	4.35208	3.18	0.006	4.624003	-	23.076
2	-6.4	7.71541	-0.83	0.419	-22.75594	-	9.955944
3	1.305882	15.4205	0.08	0.934	-31.38413	-	33.9959
MC_Una							
1	7.117647	9.44099	0.75	0.462	-12.89635	-	27.13164
2	3	10.4035	0.29	0.777	-19.05435	-	25.05435
3	-11.0588	13.5879	-0.81	0.428	-39.86389	-	17.74624
_cons	20.45882	13.7856	1.48	0.157	-8.765333	-	49.68298

Table 4.32 Results for the multiple regression analysis for categorical variables for the femur

Source	SS	df	MS
Model	2177.703	5	435.5
Residual	899.3375	19	47.33
Total	3077.04	24	128.2

Number of Obs	= 25
F(5, 19)	= 9.20
Prob > F	= 0.0001
R-squared	= 0.7077
Adj r-squared	= 0.6308
Root MSE	= 6.8799

TBS	Coef	Std. Err.	t	P>|t|	[95% Conf. Interval]		
Fem_Cal							
1	23.2625	4.67886	4.97	0.000	13.46953	-	33.05547
2	22.1625	5.59986	3.96	0.001	10.44185	-	33.88315
3	20.9625	8.87085	2.36	0.029	2.395591	-	39.52941
Fem_Cha							
1	12.5625	7.09168	1.77	0.093	-2.280553	-	27.40555
2	-4.4	5.32918	-0.83	0.419	-15.5541	-	6.754096
3	(omitted)						
_cons	11.4375	1.71999	6.65	0.000	7.837531	-	15.03747

Table 4.33 Results for the multiple regression analysis for categorical variables for the tibia

Source	SS	df	MS
Model	2554.417	6	425.7
Residual	522.6225	18	29.03
Total	3077.04	24	128.2

Number of Obs	= 25
F(6, 18)	= 14.66
Prob > F	= 0.0000
R-squared	= 0.8302
Adj r-squared	= 0.7735
Root MSE	= 5.3884

TBS	Coef	Std. Err.	t	P>|t|	[95% Conf. Interval]		
Tib_Cal							
1	8.558824	4.38339	1.95	0.067	-0.650327	-	17.76797
2	12.26471	7.30564	1.68	0.11	-3.083878	-	27.61329
3	9.382353	5.1035	1.84	0.083	-1.339707	-	20.10441
Tib_Cha							
1	12.08333	3.11098	3.88	0.001	5.547407	-	18.61926
2	18.02451	7.11816	2.53	0.021	3.069811	-	32.97921
3	12.31863	5.17275	2.38	0.028	1.451079	-	23.18618
_cons	8.416667	1.55549	5.41	0.000	5.148704	-	11.68463

Table 4.34 Results for the multiple regression analysis for categorical variables for the fibula

Source	SS	df	MS
Model	2108.353	4	527.1
Residual	968.6875	20	48.43
Total	3077.04	24	128.2

Number of Obs	= 25
F(4, 20)	= 10.88
Prob > F	= 0.0001
R-squared	= 0.6852
Adj r-squared	= 0.6222
Root MSE	= 6.9595

TBS	Coef	Std. Err.	t	P>|t|	[95% Conf. Interval]		
Fib_Cal							
1	1.75	6.02709	0.29	0.775	-10.82228	-	14.3228
2	18.5625	5.21961	3.56	0.002	7.674583	-	29.45042
Fib_Cha							
1	23.5625	7.17367	3.28	0.004	8.598489	-	38.52651
2	(omitted)						
3	17.8125	3.89047	4.58	0.000	9.697126	-	25.92787
_cons	11.4375	1.73987	6.57	0.000	7.808194	-	15.06681

Table 4.35 Results for the multiple regression analysis for categorical variables for the metatarsals

Source	SS	df	MS
Model	1872.111	4	468
Residual	1204.929	20	60.25
Total	3077.04	24	128.2

Number of Obs	= 25
F(4, 20)	= 7.77
Prob > F	= 0.0006
R-squared	= 0.6084
Adj r-squared	= 0.5301
Root MSE	= 7.7619

TBS	Coef	Std. Err.	t	P>|t|	[95% Conf. Interval]		
MT_Cal							
1	5.12069	4.67048	1.1	0.286	-4.62176	-	14.86314
MT_Cha							
1	17.14734	3.983	4.31	0.000	8.838947	-	25.45572
2	11.76803	5.02124	2.34	0.03	1.293899	-	22.24215
3	15.18182	8.107	1.87	0.076	-1.729084	-	32.09272
_cons	8.818182	2.34029	3.77	0.001	3.936425	-	13.69994

Table 4.36 The results of the probability mass functions from transition analysis for heat-related changes to the cranium

Cranium		Stage of decomposition				
	Heat-related trait	**A**	**B**	**C**	**D**	**E**
Score = 0	Unaltered bone					67%
	Charred bone	50%	50%			
	Calcined bone	42%	42%			
		A	**B**	**C**	**D**	**E**
Score = 1	Unaltered bone				50%	50%
	Charred bone					50%
	Calcined bone			50%		
		A	**B**	**C**	**D**	**E**
Score = 2	Unaltered bone			67%		
	Charred bone				57%	
	Calcined bone				67%	
		A	**B**	**C**	**D**	**E**
Score = 3	Unaltered bone	33%	33%			
	Charred bone				57%	
	Calcined bone					99%
		Stage of decomposition				
	Heat-related trait	**A**	**B**	**C**	**D**	**E**
Present	Greasy bone	28%	28%			
	Heat border			67%		
	Heat line			99%		
	Delineation			99%		
	Joint shielding			99%		
	Predictable cracking			99%		
	Minimal cracking			99%		
	Delamination			44%		
	Brown burn/border				50%	
	Heat-induced fractures				39%	39%
		Fleshed bone		**Wet bone**		**Dry bone**

Table 4.37 The results of the probability mass functions from transition analysis for heat-related changes to the mandible

Mandible		Stage of decomposition				
	Heat-related trait	**A**	**B**	**C**	**D**	**E**
Score = 0	Unaltered bone				28%	
	Charred bone	50%	50%			
	Calcined bone	36%	36%			
		A	**B**	**C**	**D**	**E**
Score = 1	Unaltered bone				99%	
	Charred bone			50%		
	Calcined bone				50%	50%
		A	**B**	**C**	**D**	**E**
Score = 2	Unaltered bone	31%	31%			
	Charred bone				58%	
	Calcined bone				58%	
		A	**B**	**C**	**D**	**E**
Score = 3	Unaltered bone	31%	31%			
	Charred bone				58%	
	Calcined bone					99%
		Stage of decomposition				
	Heat-related trait	**A**	**B**	**C**	**D**	**E**
Present	Greasy bone	33%	33%			
	Heat border			99%		
	Delamination			45%		
	Brown burn/border			67%		
	Heat-induced fractures				39%	39%
		Fleshed bone		**Wet bone**		**Dry bone**

Table 4.38 The results of the probability mass functions from transition analysis for heat-related changes to the cervical vertebrae

Cervical vertebrae		Stage of decomposition				
	Heat-related trait	**A**	**B**	**C**	**D**	**E**
Score = 0	Unaltered bone					67%
	Charred bone	39%	39%			
	Calcined bone	39%	39%			
		A	**B**	**C**	**D**	**E**
Score = 1	Unaltered bone					60%
	Charred bone			99%		
	Calcined bone				50%	
		A	**B**	**C**	**D**	**E**
Score = 2	Unaltered bone				99%	
	Charred bone				50%	50%
	Calcined bone					75%
		A	**B**	**C**	**D**	**E**
Score = 3	Unaltered bone	33%	33%	33%		
	Charred bone				50%	50%
	Calcined bone					75%
		Stage of decomposition				
	Heat-related trait	**A**	**B**	**C**	**D**	**E**
Present	Greasy bone	31%	31%			
	Heat border			99%		
	Minimal cracking			99%		
	Heat-induced fractures				46%	46%
	Delamination					50%
	Brown burn/border					99%
		Fleshed bone		**Wet bone**		**Dry bone**

Table:4.39 The results of the probability mass functions from transition analysis for heat-related changes to the ribs

Ribs		Stage of decomposition				
	Heat-related trait	**A**	**B**	**C**	**D**	**E**
Score = 0	Unaltered bone					99%
	Charred bone	39%	39%			
	Calcined bone	33%	33%	33%		
		A	**B**	**C**	**D**	**E**
Score = 1	Unaltered bone					99%
	Charred bone			67%		
	Calcined bone				75%	
		A	**B**	**C**	**D**	**E**
Score = 2	Unaltered bone					67%
	Charred bone				57%	
	Calcined bone					67%
		A	**B**	**C**	**D**	**E**
Score = 3	Unaltered bone	26%	26%	26%		
	Charred bone					99%
	Calcined bone					67%
		Stage of decomposition				
	Heat-related trait	**A**	**B**	**C**	**D**	**E**
Present	Greasy bone	28%	28%			
	Predictable cracking			99%		
	Brown burn/border				99%	
	Delamination				39%	39%
	Heat-induced fractures				42%	42%
		Fleshed bone		**Wet bone**		**Dry bone**

Table: 4.40 The results of the probability mass functions from transition analysis for heat-related changes to the scapula

Scapula		Stage of decomposition				
	Heat-related trait	**A**	**B**	**C**	**D**	**E**
Score = 0	Unaltered bone				99%	
	Charred bone	33%	33%			
	Calcined bone	27%	27%	27%		
		A	**B**	**C**	**D**	**E**
Score = 1	Unaltered bone					99%
	Charred bone				50%	
	Calcined bone					67%
		A	**B**	**C**	**D**	**E**
Score = 2	Unaltered bone				99%	
	Charred bone				50%	50%
	Calcined bone					67%
		A	**B**	**C**	**D**	**E**
Score = 3	Unaltered bone	26%	26%	26%		
	Charred bone					67%
	Calcined bone					99%
		Stage of decomposition				
	Heat-related trait	**A**	**B**	**C**	**D**	**E**
Present	Greasy bone	26%	26%			
	Heat border			50%	50%	
	Predictable cracking			99%		
	Brown burn/border			33%	33%	33%
	Minimal cracking				99%	
	Delamination					50%
	Heat-induced fractures					56%
		Fleshed bone		**Wet bone**		**Dry bone**

Table 4.41 The results of the probability mass functions from transition analysis for heat-related changes to the os coxa

Os Coxa		Stage of decomposition				
	Heat-related trait	**A**	**B**	**C**	**D**	**E**
Score = 0	*Unaltered bone**					
	Charred bone	31%	31%	31%		
	Calcined bone	29%	29%	29%		
		A	**B**	**C**	**D**	**E**
Score = 1	Unaltered bone					99%
	Charred bone				99%	
	Calcined bone					67%
		A	**B**	**C**	**D**	**E**
Score = 2	Unaltered bone					99%
	Charred bone					60%
	Calcined bone					67%
		A	**B**	**C**	**D**	**E**
Score = 3	Unaltered bone	24%	24%	24%	24%	
	Charred bone					99%
	Calcined bone				50%	50%
		Stage of decomposition				
	Heat-related trait	**A**	**B**	**C**	**D**	**E**
Present	Greasy bone	28%	28%			
	Brown burn/border				99%	
	Delamination					50%
	Heat-induced fractures					55%
		Fleshed bone		**Wet bone**		**Dry bone**

Table 4.42 The results of the probability mass functions from transition analysis for heat-related changes to the thoracic vertebrae

Thoracic vertebrae		Stage of decomposition				
	Heat-related trait	**A**	**B**	**C**	**D**	**E**
Score = 0	Unaltered bone					99%
	Charred bone	33%	33%			
	Calcined bone	28%	28%	28%		
		A	**B**	**C**	**D**	**E**
Score = 1	Unaltered bone					80%
	Charred bone			50%	50%	
	Calcined bone					80%
		A	**B**	**C**	**D**	**E**
Score = 2	Unaltered bone				99%	
	Charred bone				67%	
	Calcined bone				50%	50%
		A	**B**	**C**	**D**	**E**
Score = 3	Unaltered bone	29%	29%	29%		
	Charred bone					80%
	Calcined bone				50%	50%
		Stage of decomposition				
	Heat-related trait	**A**	**B**	**C**	**D**	**E**
Present	Greasy bone	28%	28%			
	Delamination					55%
	Heat-induced fractures					63%
		Fleshed bone		**Wet bone**		**Dry bone**

Table 4.43 The results of the probability mass functions from transition analysis for heat-related changes to the lumbar vertebrae

Lumbar vertebrae		Stage of decomposition				
	Heat-related trait	**A**	**B**	**C**	**D**	**E**
Score = 0	Unaltered bone					99%
	Charred bone	31%	31%	31%		
	Calcined bone	28%	28%	28%		
		A	**B**	**C**	**D**	**E**
Score = 1	Unaltered bone					80%
	Charred bone				99%	
	Calcined bone					99%
		A	**B**	**C**	**D**	**E**
Score = 2	Unaltered bone				99%	
	Charred bone				99%	
	Calcined bone				99%	
		A	**B**	**C**	**D**	**E**
Score = 3	Unaltered bone	29%	29%	29%		
	Charred bone					99%
	Calcined bone				99%	
		Stage of decomposition				
	Heat-related trait	**A**	**B**	**C**	**D**	**E**
Present	Greasy bone	28%	28%			
	Delamination					56%
	Brown burn/border					99%
	Heat-induced fractures					56%
		Fleshed bone		**Wet bone**		**Dry bone**

Table 4.44 The results of the probability mass functions from transition analysis for heat-related changes to the humerus

Humerus		Stage of decomposition				
	Heat-related trait	**A**	**B**	**C**	**D**	**E**
Score = 0	Unaltered bone					99%
	Charred bone	33%	33%			
	Calcined bone	28%	28%			
		A	**B**	**C**	**D**	**E**
Score = 1	Unaltered bone					60%
	Charred bone					50%
	Calcined bone					50%
		A	**B**	**C**	**D**	**E**
Score = 2	Unaltered bone				99%	
	Charred bone				50%	
	Calcined bone					67%
		A	**B**	**C**	**D**	**E**
Score = 3	Unaltered bone	29%	29%	29%		
	Charred bone					63%
	Calcined bone					67%
		Stage of decomposition				
	Heat-related trait	**A**	**B**	**C**	**D**	**E**
Present	Greasy bone	28%	28%			
	Heat border			99%		
	Predictable cracking			99%		
	Delamination					56%
	Brown burn/border					99%
	Heat-induced fractures					50%
		Fleshed bone		**Wet bone**		**Dry bone**

Table 4.45 The results of the probability mass functions from transition analysis for heat-related changes to the ulna

Ulna		Stage of decomposition				
	Heat-related trait	**A**	**B**	**C**	**D**	**E**
Score = 0	Unaltered bone					99%
	Charred bone	33%	33%			
	Calcined bone	29%	29%	29%		
		A	**B**	**C**	**D**	**E**
Score = 1	Unaltered bone				99%	
	Charred bone			99%		
	Calcined bone					60%
		A	**B**	**C**	**D**	**E**
Score = 2	Unaltered bone				50%	50%
	Charred bone				67%	
	Calcined bone					67%
		A	**B**	**C**	**D**	**E**
Score = 3	Unaltered bone	26%	26%	26%		
	Charred bone					67%
	Calcined bone					67%
		Stage of decomposition				
	Heat-related trait	**A**	**B**	**C**	**D**	**E**
Present	Greasy bone	28%	28%			
	Heat border			99%		
	Heat line			99%		
	Delineation			99%		
	Delamination				50%	50%
	Brown burn/border				50%	50%
	Heat-induced fractures					56%
		Fleshed bone		**Wet bone**		**Dry bone**

Table 4.46 The results of the probability mass functions from transition analysis for heat-related changes to the radius

Radius		Stage of decomposition				
	Heat-related trait	**A**	**B**	**C**	**D**	**E**
Score = 0	Unaltered bone					67%
	Charred bone		36%			
	Calcined bone	29%	29%	29%		
		A	**B**	**C**	**D**	**E**
Score = 1	Unaltered bone				50%	50%
	Charred bone			33%	33%	
	Calcined bone					67%
		A	**B**	**C**	**D**	**E**
Score = 2	Unaltered bone				50%	50%
	Charred bone					99%
	Calcined bone				50%	50%
		A	**B**	**C**	**D**	**E**
Score = 3	Unaltered bone	28%	28%	28%		
	Charred bone				50%	50%
	Calcined bone				50%	50%
		Stage of decomposition				
	Heat-related trait	**A**	**B**	**C**	**D**	**E**
Present	Greasy bone	31%	31%			
	Heat border	50%		50%		
	Predictable cracking	50%		50%		
	Delamination				57%	
	Brown burn/border					67%
	Heat-induced fractures					46%
		Fleshed bone		**Wet bone**		**Dry bone**

Table 4.47 The results of the probability mass functions from transition analysis for heat-related changes to the metacarpals

Metacarpals		Stage of decomposition				
	Heat-related trait	**A**	**B**	**C**	**D**	**E**
Score = 0	Unaltered bone				50%	50%
	Charred bone	40%	40%			
	Calcined bone	28%	28%	28%		
		A	**B**	**C**	**D**	**E**
Score = 1	Unaltered bone					99%
	Charred bone			75%		
	Calcined bone					60%
		A	**B**	**C**	**D**	**E**
Score = 2	Unaltered bone				50%	
	Charred bone				50%	
	Calcined bone				99%	
		A	**B**	**C**	**D**	**E**
Score = 3	Unaltered bone	33%				
	Charred bone					99%
	Calcined bone				99%	
		Stage of decomposition				
	Heat-related trait	**A**	**B**	**C**	**D**	**E**
Present	Greasy bone	31%	31%			
	Heat border			60%		
	Heat line		50%	50%		
	Delineation		50%	50%		
	Predictable cracking			50%		
	Delamination					46%
	Brown burn/border					60%
	Heat-induced fractures					36%
		Fleshed bone		**Wet bone**		**Dry bone**

Table 4.48 The results of the probability mass functions from transition analysis for heat-related changes to the femur

Femur		Stage of decomposition				
	Heat-related trait	**A**	**B**	**C**	**D**	**E**
Score = 0	*Unaltered bone**					
	Charred bone	31%	31%	31%		
	Calcined bone	29%	29%	29%		
		A	**B**	**C**	**D**	**E**
Score = 1	Unaltered bone					99%
	Charred bone				99%	
	Calcined bone					75%
		A	**B**	**C**	**D**	**E**
Score = 2	Unaltered bone					60%
	Charred bone				60%	
	Calcined bone					67%
		A	**B**	**C**	**D**	**E**
Score = 3	Unaltered bone	26%	26%	26%		
	Charred bone					99%
	Calcined bone				99%	
		Stage of decomposition				
	Heat-related trait	**A**	**B**	**C**	**D**	**E**
Present	Greasy bone	28%	28%			
	Delamination					56%
	Heat-induced fractures					56%
		Fleshed bone		**Wet bone**		**Dry bone**

Table 4.49 The results of the probability mass functions from transition analysis for heat-related changes to the tibia

Tibia		Stage of decomposition				
	Heat-related trait	**A**	**B**	**C**	**D**	**E**
Score = 0	Unaltered bone				50%	50%
	Charred bone	42%	42%			
	Calcined bone	31%	31%	31%		
		A	**B**	**C**	**D**	**E**
Score = 1	Unaltered bone	22%	22%	22%		
	Charred bone			42%	42%	
	Calcined bone				50%	50%
		A	**B**	**C**	**D**	**E**
Score = 2	Unaltered bone					67%
	Charred bone					99%
	Calcined bone					99%
		A	**B**	**C**	**D**	**E**
Score = 3	Unaltered bone	25%	25%	25%		
	Charred bone				50%	50%
	Calcined bone				50%	50%
		Stage of decomposition				
	Heat-related trait	**A**	**B**	**C**	**D**	**E**
Present	Greasy bone	28%	28%	28%		
	Heat border			99%		
	Heat line			99%		
	Delineation			99%		
	Predictable cracking			99%		
	Joint shielding				99%	
	Delamination					45%
	Brown burn/border					67%
	Heat-induced fractures					50%
		Fleshed bone		**Wet bone**		**Dry bone**

Table 4.50 The results of the probability mass functions from transition analysis for heat-related changes to the fibula

Fibula		Stage of decomposition				
	Heat-related trait	**A**	**B**	**C**	**D**	**E**
Score = 0	Unaltered bone					67%
	Charred bone	31%	31%	31%		
	Calcined bone	24%	24%	24%		
		A	**B**	**C**	**D**	**E**
Score = 1	Unaltered bone					67%
	Charred bone					99%
	Calcined bone				50%	50%
		A	**B**	**C**	**D**	**E**
Score = 2	Unaltered bone				99%	
	Charred bone				50%	50%
	Calcined bone				50%	50%
		A	**B**	**C**	**D**	**E**
Score = 3	Unaltered bone	28%	28%	28%		
	Charred bone				50%	50%
	Calcined bone				50%	50%
		Stage of decomposition				
	Heat-related trait	**A**	**B**	**C**	**D**	**E**
Present	Greasy bone	29%	29%			
	Delamination				75%	
	Heat-induced fractures					56%
		Fleshed bone		**Wet bone**		**Dry bone**

Table 4.51 The results of the probability mass functions from transition analysis for heat-related changes to the metatarsals

Metatarsals		Stage of decomposition				
	Heat-related trait	**A**	**B**	**C**	**D**	**E**
Score = 0	*Unaltered bone**					
	Charred bone	46%				
	Calcined bone	26%	26%			
		A	**B**	**C**	**D**	**E**
Score = 1	Unaltered bone				99%	
	Charred bone					58%
	Calcined bone				50%	
		A	**B**	**C**	**D**	**E**
Score = 2	Unaltered bone			50%		
	Charred bone			50%		
	Calcined bone				50%	
		A	**B**	**C**	**D**	**E**
Score = 3	Unaltered bone	28%	28%			
	Charred bone				99%	
	Calcined bone				50%	
		Stage of decomposition				
	Heat-related trait	**A**	**B**	**C**	**D**	**E**
Present	Greasy bone	31%	31%			
	Heat border			67%		
	Heat line			67%		
	Delineation			99%		
	Delamination			44%		
	Predictable cracking			67%		
	Heat-induced fractures			31%	31%	31%
	Brown burn/border					80%
		Fleshed bone		**Wet bone**		**Dry bone**

Table 4.52 Analysis of variance for head and neck

Source of Variance	df	ssq	msq	F	p
Between rows	10	360.8182	36.0818	264.6	<0.0001
Within rows	11	2.5	0.2273		
Between columns	1	1.1364	1.1364	8.3333	0.0012
Residual error	10	1.3636	0.1364		
Total overall	21	363.3182			

*Sig of diff between measurements (Cols) / residual F = 8.3333; p = 0.0012
*Sig of diff between measurements (Cols) / cases (rows) F = 0.0315; p = 0.8627

Intraclass Correlations	Single	Meaned
Model 1	0.9875	0.9937
Model 2	0.9875	0.9937
Model 3	0.9925	0.9962

ICC = 0.9875

Table 4.53 Analysis of variance for trunk

Source of Variance	df	ssq	msq	F	p
Between rows	10	271.3636	27.1364	597	<0.0001
Within rows	11	0.5	0.0455		
Between columns	1	0.0455	0.0455	1	0.5
Residual error	10	0.4545	0.0455		
Total overall	21	271.8636			

*Sig of diff between measurements (Cols) / residual F = 3.75; p = 0.0243
*Sig of diff between measurements (Cols) / cases (rows) F = 0.1214; p = 0.7347

Intraclass Correlations	Single	Meaned
Model 1	0.9967	0.9983
Model 2	0.9967	0.9983
Model 3	0.9967	0.9983

ICC = 0.9967

Table 4.54 Analysis of variance for limbs

Source of Variance	df	ssq	msq	F	p
Between rows	10	303.2727	30.3273	30.8889	<0.0001
Within rows	11	13.5	1.2273		
Between columns	1	3.6818	3.6818	3.75	0.0243
Residual error	10	9.8182	0.9818		
Total overall	21	316.7727			

*Sig of diff between measurements (Cols) / residual F = 1; p = 0.5
*Sig of diff between measurements (Cols) / cases (rows) F = 0.0017; p = 0.9682

Intraclass Correlations	Single	Meaned
Model 1	0.9222	0.9595
Model 2	0.9228	0.9599
Model 3	0.9373	0.9676

ICC = 0.9228

Table 4.55 Summary of kappa statistic results from 13 burn-related traits for the head and neck (highlight indicates significant p-values)

Trait	Observer agreement	Symmetry p-value	Agreement %	Kappa	Agreement
Calcined bone	Intra	0.2231	87.5	0.8159	Almost perfect
	Inter	0.2873	79.17	0.7059	Substantial
Charred bone	Intra	0.2615	83.33	0.7538	Substantial
	Inter	0.1353	83.33	0.7377	Substantial
Unaltered bone	Intra	0.3679	91.67	0.8737	Almost perfect
	Inter	0.2231	87.5	0.8204	Almost perfect
Brown burn	Intra	0.1573	91.67	0.7037	Substantial
	Inter	0.3173	95.83	0.8636	Almost perfect
Heat border	Intra	0.3173	95.83	0.7778	Substantial
	Inter	0.1573	91.67	0.7037	Substantial
Heat line	Intra*	-	-	-	-
	Inter	-	-	-	-
Delineation	Intra*	-	-	-	-
	Inter*	-	-	-	-
Greasy	Intra	1.000	100	1.000	Almost perfect
	Inter	1.000	91.67	0.8125	Almost perfect
Joint shielding	Intra*	-	-	-	-
	Inter*	-	-	-	-
Predictable cracking	Intra*	-	-	-	-
	Inter	0.3173	95.83	0.000	Slight
Minimal cracking	Intra*	-	-	-	-
	Inter	0.3173	95.83	0.8333	Almost perfect
Delamination	Intra	1.000	66.67	0.2889	Fair
	Inter	0.6547	79.17	0.5455	Moderate
Heat-induced fractures	Intra	1.000	100	1.000	Almost perfect
	Inter	0.0143	75	0.191	Slight

Table 4.56 Summary of kappa statistic results from 13 burn-related traits for the trunk (highlight indicates significant p-values)

Trait	Observer agreement	Symmetry p-value	Agreement %	Kappa	Agreement
Calcined bone	Intra	0.5134	90	0.8498	Almost perfect
	Inter	0.0074	67.5	0.5307	Moderate
Charred bone	Intra	0.3796	77.5	0.6552	Substantial
	Inter	0.0117	67.5	0.5586	Moderate
Unaltered bone	Intra	0.149	80	0.6998	Substantial
	Inter	0.1116	85	0.7521	Substantial
Brown burn	Intra	0.0503	82.5	0.1566	Slight
	Inter	0.3173	97.5	0.7872	Substantial
Heat border	Intra	1.000	100	1.000	Almost perfect
	Inter	1.000	100	1.000	Almost perfect
Heat line	Intra*	-	-	-	-
	Inter	-	-	-	-
Delineation	Intra*	-	-	-	-
	Inter*	-	-	-	-
Greasy	Intra	1.000	100	1.000	Almost perfect
	Inter	0.0253	87.5	0.7462	Substantial
Joint shielding	Intra*	-	-	-	-
	Inter*	-	-	-	-
Predictable cracking	Intra*	-	-	-	-
	Inter	0.3173	97.5	0.6552	Substantial
Minimal cracking	Intra*	-	-	-	-
	Inter	0.3173	97.5	0.000	Slight
Delamination	Intra	0.0253	87.5	0.6	Moderate
	Inter	0.0143	85	0.6783	Substantial
Heat-induced fractures	Intra	1.000	100	1.000	Almost perfect
	Inter	0.3173	97.5	0.939	Almost perfect

Table 4.57 Summary of kappa statistic results from 13 burn-related traits for the extremities/limbs (highlight indicates significant p-values)

Trait	Observer agreement	Symmetry p-value	Agreement %	Kappa	Agreement
Calcined bone	Intra	0.3208	82.81	0.7433	Substantial
	Inter	0.0302	89.06	0.8315	Almost perfect
Charred bone	Intra	0.2231	75	0.6263	Substantial
	Inter	0.0719	89.06	0.8544	Almost perfect
Unaltered bone	Intra	0.0503	82.81	0.7684	Substantial
	Inter	0.5062	87.5	0.8097	Almost perfect
Brown burn	Intra	0.0047	87.5	0.6859	Substantial
	Inter	0.3173	93.75	0.8072	Almost perfect
Heat border	Intra	0.1573	96.88	0.000	Slight
	Inter	0.6547	92.19	0.5722	Moderate
Heat line	Intra*	-	-	-	-
	Inter	-	-	-	-
Delineation	Intra*	-	-	-	-
	Inter*	-	-	-	-
Greasy	Intra	0.3173	98.44	0.9592	Almost perfect
	Inter	0.1573	96.88	0.9376	Almost perfect
Joint shielding	Intra*	-	-	-	-
	Inter*	-	-	-	-
Predictable cracking	Intra*	-	-	-	-
	Inter	1.000	93.75	0.4667	Moderate
Minimal cracking	Intra*	-	-	-	-
	Inter	1.000	96.88	0.4839	Moderate
Delamination	Intra	0.5271	84.38	0.6541	Substantial
	Inter	0.763	82.81	0.6563	Substantial
Heat-induced fractures	Intra	1.000	100	1.000	Almost perfect
	Inter	0.3173	98.44	0.9631	Almost perfect

Chapter 5: Discussion

The discovery of burned remains often evokes questions as to the condition of the body prior to the burn event. A fundamental question to address is whether macroscopic burn-related signatures (heat-related traits) are useful in providing clues as to condition of bone or the body prior to burning, and if so, can the differences be quantified and used to estimate prior bone condition. This project is interpreted within the context of existing literature on burned skeletal remains, particularly with regard to fleshed, wet and dry burned bone, as a means to address this question. Within the confines of degrading soft tissue (decomposition) and wet/dry bone conditions, heat-related traits such as heat borders, heat lines, delineation, greasy bone, predictable cracking and minimal cracking manifest on fleshed bone as a result of burning. These features are not present when bone burns without the presence of soft tissue; Pope (2007), Symes *et al.* (1999, 2008) and Keough *et al*. (2012) also observed similar burn patterns. Previous research primarily focused on varying fracture patterns in accordance with the condition of the bone (fleshed, wet or dry) (Krogman, 1939; Baby, 1954; Binford, 1963; Thurman & Willmore, 1981; Gonçalves *et al.*, 2011) as well as certain changes in colour (Lisowskii, 1968; Dokladal, 1969; Gejvall, 1969; Hermann, 1970; Shipman *et al*., 1984; Mayne Correira, 1997; Devlin & Herrmann, 2008). This study is the first to quantify the relationship of heat-related traits to the previous bone condition, so that thermal patterns can be elucidated and discussed.

The study was conducted outdoors, within a controlled burning period (30 minutes), and with the use of the surrounding vegetation as fuel, to more closely replicate veldt fire conditions. Veldt fires are generally unpredictable with random heat sources that vary tremendously with changes in local vegetation and climate. Veldt fires devastate grasslands, wildlife and other natural resources as well as cause injuries and death to people and destruction to properties and farmlands (Nkomo & Sassi, 2009; Siwele, 2011). Factors involved in the combustion, sustainability and duration of a veldt fire vary. The source and position of the heat are constantly changing and the body or skeletal remains experience different phases of combustion such as ignition, sustainability and eventual reduction as the fuel source diminishes. No two fires are the same, and by extension, resultant damage to skeletal remains differs in each circumstance with regard to size, magnitude, speed and destruction and also whether they are intentional, accidental or natural (Eckert, 1981). When

conditions of the fire are unknown (which is most likely the case), predicting state of decomposition at time of burning from discovered remains is problematic, if not impossible. While PMI cannot be accurately estimated from burned remains, heat-related characteristics observed on bone exposed to fire are useful to indicate conditions of the skeleton (fleshed, wet or dry).

Most researchers agree that marked thermal characteristics exist among fleshed, wet and dry bone (Krogman, 1939; Baby, 1954; Binford, 1963; Thurman & Willmore, 1981; Gonçalves *et al.*, 2011; Keough *et al.*, 2012) with burn fracture types being similar between wet/green and fleshed bone but not between wet and dry bone (Krogman, 1939; Baby, 1954; Binford, 1963; Thurman & Willmore, 1981; Gonçalves *et al.*, 2011). Of particular interest to this project was changes in colour (Lisowskii, 1968; Dokladal, 1969; Gejvall, 1969; Hermann, 1970; Shipman *et al*., 1984; Mayne Correira, 1997; Devlin & Herrmann, 2008) and other burn-related signatures: for example, heat borders, heat lines, delineation, fractures and joint shielding on fleshed, wet and dry bone (Symes *et al*., 2008; Keough *et al.*, 2012).

With many unknown skeletal remains recovered from the veldt in South Africa, the surrounding environment, duration of exposure and nature of fire are often unknown. Taphonomic conditions are variable and the exact circumstances surrounding and relating to the time of death will always be uncertain and at best remain educated guesses. Differential preservation of certain skeletal elements is linked to the body's position during the burn event and the variable nature of the fire. In a supine position, bones located anterior and lateral are often affected before posterior surfaces, which may be lying against another object (wall, ground, rock) and thus additionally protected. Logic dictates that bones nearest to the posterior surface or the surface in contact with the ground will survive for a longer period than those anterior and directly exposed to fire.

In this study, a directional trend in colour change (unaltered, charred and calcined) is noted across the various stages of decomposition. However, while regression and prediction intervals show promising results for estimating TBS, the formulae should be used with caution if applied to real life cases nor to cases outside of a 30-minute burn period. The same concept applies to the use of transition analysis that shows that certain heat-related traits are more likely associated with certain stages of decomposition than with others. Even though statistical tests assisted in elucidating a clear pattern in burned skeletal remains within the predefined conditions of this study, application to an unknown case is limited, due to the

various other factors that cannot be controlled (duration of exposure, context, climatic conditions, body positioning) (DeHaan, 2012).

Aside from the problems associated with taphonomy, the author strongly suggests that the degree of heat-related/heat-induced changes on bone can be more positively associated with the condition of the bone (fleshed, wet/green, and dry) rather than the possible decomposition stage. The study provides guidelines that can be used to approximate the condition of skeletal remains prior to a burn event. The outcome of the study provides statistical support to previously observed characteristics on wet and dry bone and of the importance of soft tissue in the formation of burn patterns and fracture characteristics.

5.1. Tissue shielding and the effects on fresh, early and advanced decomposed remains

When a fleshed body burns, a predictable sequence of tissue distortion and body repositioning occurs, known as the pugilistic posture, or pose. This pose is merely the reaction of a body to fire and results in flexion of the large, antagonistic muscles of the neck, upper and lower limbs. Because each anatomical area has a distinct arrangement and distribution of soft tissue around bone, tissue and joint shielding present with a unique and predictable burn pattern across the body. Soft tissue offers most protection to bone and is a major influence when assessing patterned thermal destruction on skeletal remains (Smith *et al.*, 2001).

When present, soft tissue affords tissue-shielding properties, and its destruction is the main impetus for patterned thermal destruction of the skeleton. Tissue shielding occurs with either flexion and/or fixed poses, and resultant burn patterns are often the combination of the two observed in the limbs, trunk and neck regions. Flexed shielding is associated with contraction of large, antagonistic muscles or pugilistic alterations in humans, while fixed shielding appears in areas where a mass of overlying tissue is present and the bone/s are in a fixed position (e.g., hip joint: acetabulum and femoral head). While the large, antagonistic muscles present a unique pattern of flexion in the pig extremities, the large areas of soft tissue and muscle also provide differential protection to the underlying skeletal system. The differential thickness of the skin and soft tissue in areas of the neck, trunk and buttocks are greater compared to the lower parts of both fore- and hind legs. The simultaneous destruction

of soft tissue, muscle and bone is explained with colour differentiations as well as other heat-induced changes (heat border, heat lines, joints shielding, etc.).

In the fresh and early stages of decomposition, the skin and muscle tissues maintain structural integrity and protect the underlying bone. This is evident in the results as minimal thermal alteration is scored in these early stages. While marked destruction of skin and muscle tissue, with regard to splitting, stretching and shrinking, is noted on the thinly covered distal limbs, little skeletal involvement is present (Figure 5.1). Similarly, Pope (2007) observes that the skin of fresh/early decomposed remains split and shrink within a few minutes of exposure and opens up gaps for further heat penetration. The rate of destruction of the skin and muscle of a pig in a fire may be different from that to humans, and this variance should be noted. As tissue degrades and decomposition advances a reduction in and sagging of tissues, caving in of flesh of the eyes, throat and abdominal cavity and tissue reduction in the limbs are observed. This leads to eventual exposure of patches of bone on the head, trunk and limbs. In this phase, skin lacks elasticity and is more likely to slough off with minimal resistance to manual force or fire. The fire more quickly consumed denatured soft tissues, and larger charred surface areas are noted when compared to the fresh/early decomposition stages. Although most of the skin is compromised in this stage, the underlying muscle tissue retains structural integrity such that the large, antagonistic flexor muscles are able to contract into a flexed posture.

Skeletal elements of the head and neck (cranium, mandible and cervical vertebrae) show a distinct pattern of thermal damage with regard to colour changes and other heat-induced characteristics. The anatomy of the head and neck (pig and human) is unique from the rest of the body in that specialised distributions of soft tissue are located around the vault, face and neck. The soft tissue distribution influences both decomposition rate and burn pattern. Thin areas of soft tissue (scalp, forehead and nasal region) decompose faster than thicker areas of tissue (lower face, neck and mandible), unevenly exposing the underlying surface to thermal destruction. Cranial morphology also differs from postcranial remains such that fire immediately consumes a broader area unlike the more progressive direction seen with postcranial remains. Although the overall structure of the cranium of a pig differs from that of a human, similarities exist between the protective soft tissues that surround the cranium. Burn patterns observed on the skull mimic differential tissue distribution and are comparable with the level of decomposition that has taken place (Pope, 2007). In fresh tissue a gradual retraction and burning of flesh is noted, but in advanced decomposition, tissues

merely slough off and expose broad areas of underlying bone. Extreme sloughing of the skin (skin slippage) over the cranial and neck elements exposes the area to fire faster than fresh/elastic tissue.

The nasal, incisive, maxillary and zygomatic bones all show the first signs of thermal alteration starting from the most rostral aspect travelling posteriorly towards the base of the skull in the later stages (Figure 5.4). The posterior aspects of the frontal, parietal and occipital bones afforded increased tissue protection from *m. frontoscutularis* and *m. trapezius* and were less inclined to burn within a 30 minute period. The burn patterns on pig crania are similarly observed on fleshed, human remains. Observations conflicting with those of Pope (2007) relate to the pattern of exposure and resultant thermal alteration. Pope (2007) notes that the exposed areas on human skulls in advanced decomposition undergo broad and nondescript patterns of charring and calcination divergent from fresher, fleshed patterns. This more mottled, non-descript pattern can be attributed to differing anatomy and thicker distribution of muscles and skin on pig crania. The mandibula of specimens in the advanced stage show signs of thermal alteration along the anterior aspects (over the mental symphysis) and along the inferior border towards the gonial angle, a directional pattern similar to that observed in burned fleshed human remains.

The cervical vertebrae, due to the thickened tissue mass accumulating over the neck, did not display considerable thermal alteration prior to skeletonisation. In humans, hyperextension of the neck occurs during heat exposure and protects the associated skeletal elements such as the occipital bone and cervical vertebrae (Bohnert *et al*., 1998; Pope, 2007; Symes *et al*., 2008). A similar protective situation is noted with the thick neck muscles of the pig specimens but without neck hyperextension, as exaggerated extension of the neck is not within the normal range of movement in pigs. However, one pig specimen (BP_08) did show minimal calcined and charred surfaces on the occipital bone and cervical vertebrae (Figure 5.5). The burn pattern on BP_08 is explained via varied decomposition (excessive skin slippage) and antemortem positioning of his head prior to exposure.

Areas of soft tissue that take longer than the head and limbs to decompose (trunk, proximal parts of the extremities) are devoid of thermal alteration when the specimens ranged from fully to partially fleshed (fresh – advanced decomposition). The torso, in general, burns slower than other areas of the body on account of high moisture content of the thoracic and abdominal organs and greater tissue mass, which takes longer to decompose when compared to the decomposition rates for the head or limbs. Due to increased tissue shielding and

moisture, elements of the trunk and proximal limbs show no thermal alteration prior to skeletonisation with the exception of one specimen, which displayed some charred areas on the scapula due to the increased skin slippage over the shoulder region (Figure 5.6). The skeletal region of BP_08 that exhibits charring also displays similar features (charring, heat borders, heat lines and predictable cracking) observed in the fully fleshed remains.

Increased amounts of both charred and calcined bone are noted on the extremities in the advanced stages of decomposition when compared to the fresh and early stages. Charred and calcined bone are observed in areas with the least amount of tissue protection such as the medial aspect of the tibia, the dorsal surface of the radius, metacarpals and metatarsals and the olecranon process of the ulna (Figure 5.7). These areas are exposed earlier than other areas due to the thin layers of tissue and flexed nature of the limbs. A completely flexed pose, referred to as a pugilistic posture in humans, is observed on the extremities of all specimens in the fresh, early and advanced stages of decomposition (Figure 5.2). This rearrangement of the limbs is in agreement with numerous studies but for which the duration of burn and condition of the body are different (Adelson, 1955; Bass, 1984; Spitz, 1993; Bohnert *et al*., 1998; DiMaio & DiMaio, 2001; Icove & DeHaan, 2003; Pope 2007; Symes *et al*., 2008). Similar to humans, pig extremities function like a pulley and lever system with adhering muscles creating flexion and extension of the relevant joints. In pigs, the distribution of muscle and adipose tissue in the lower (forearm) extremities is sparse compared to the upper front and hind legs. With flexion, the areas to first burn on a pig are the wrist; the dorsal aspects of the carpals, metacarpals; and the distal radius and ulna. Areas on the pig with accumulating tissue (due to burn progression) or areas with already thickened tissue masses such as the neck (cervical vertebrae), buttock region (pelvis, sacrum), ventral surfaces of the vertebrae, and proximal aspects of the femora, if burning continued for a longer duration, should be the last areas to burn.

A difference in the degree of flexion (slightly flexed to extreme flexion) is noted between the fresh/early stages and advanced stages of decomposition and most likely relates to the denaturing of soft tissues and the duration of exposure. Within a crematorium or similar conditions a similar progression from not flexed to strongly flexed in all specimens is observed, with the main difference being that the more decomposed specimens enter and leave the flexed posture much faster than the fresher specimens. This repositioning of the anatomical joints of the limbs in individuals burned while fleshed is widely noted throughout

the literature (Bass, 1984; Spitz, 1993, 2006; DiMaio & DiMaio, 2001; Smith *et al*., 2001; Icove & DeHaan, 2003; Dolinak *et al*., 2005; DeHaan, 2006).

Few burn studies incorporate or consider decomposition phase as a factor for influencing the formation of the flexed posture (Pope, 2007). The present study shows that the deep lying muscles and tendons present in the early and even advanced stages of decomposition maintain enough structure and stability to produce identifiable hyperflexion of the joints of the upper and lower limbs somewhat comparable to the repositioning of the arms, legs, hands and feet in humans. Due to the flexed position of the distal pig extremities and the rapid consumption of the thin skin covering these parts, the posterior metacarpals and metatarsals burned immediately and created canoe-shaped patterns in the fresh, early and advanced decomposed remains (Figure 5.3). Canoeing is often associated with fleshed remains that display increased flexion of the hands and feet (Symes *et al,* 1999; Pope, 2007). The mechanism of action involves the shrinkage and retraction of muscles and tendons around the metacarpals/tarsals, exposing first the dorsal surface, and often long, linear, and thicker cortical bone covering the trabecular bone burns away and exposes the underlying medullary cavity, creating a canoe-shaped fracture pattern.

In general, bones burned while fleshed (protected by overlying tissue) display multiple surface colours with a non-uniform distribution of thermal damage. These characteristics are attributed to differential combustion of soft tissues, temperature fluctuations and position in relation to heat source (Nicholson, 1993; Buikstra & Ubelaker, 1997; Bennett, 1999; Asmussen, 2009). When protected with soft tissue, bone may display a sequence of unaltered surfaces, heat borders, charred and calcined areas that aid in distinguishing fleshed from dry burned bone (Symes *et al*., 2008, 2012). Often, the external and internal surface of bone differs in colour due to the basic principle of heat conduction through materials. This principle implies that heat flows from areas with a higher temperature (external periosteal surface) to cooler areas located more towards the central cortical and trabecular bone (DeHaan, 2006). In other words, bone burns from the outside to the inside as overlying soft tissues, if present, are consumed. Unprotected bone sequentially destroys from the outside to the inside, and the extent of destruction is dependent on the composition of the bone itself (dry vs wet/green).

The appearance of the pugilistic posture in exposed remains allows for the differential patterns observed on fleshed remains and distinguishes them from patterns observed on remains that lack typical pugilistic arrangement. In order for this contraction to take place

muscle, tendon and ligament integrity needs to be present, and these features are observed in fleshed as well as partially fleshed remains, already in advanced decay. Once the remains progress into skeletonisation, contraction of the joints is impaired, because the integrity of the soft tissues is denatured and unable to react to the fire in the same manner observed in the fresher remains. Although the areas protected by bulkier tissues in advanced decomposed remains show similar heat-related features to fresh or early remains, the combination of mixed signatures (fleshed/wet signatures or dry signatures) observed allows for an assumption as to the relevant stage of decomposition or more so the condition of the bones. If areas are observed that display fleshed/wet signatures (heat border and heat lines) together with areas displaying dry signatures (brown burn and delamination), this may indicate the presence of tissue but not over the entire body. If mixed burn signatures are noted, the remains are most likely in advanced decomposition prior to burning and are neither fresh nor dry but wet.

5.2. No tissue shielding and the effects on skeletonised remains

In the early skeletonisation phase, large areas of wet/greasy bone with some dry or desiccated soft tissue are exposed to heat and flame. No tissue integrity or protection is available on the bones, and no flexed posture recorded so randomised burn patterns form as either patches of burned and unburned bone or patches of charred and calcined bone. During this phase, increased amounts of charred and calcined bone appear when compared to the fresh, early and advanced stages of decomposition and a uniform burn pattern is found across some of the bones, i.e., the entire bone is either calcined, charred or displayed a combination of the two. This is not observed on bones in the earlier stages of decomposition which instead show a more linear progression of colour distribution with areas of unaltered followed by charred bone adjacent to calcined bone.

Some of the calcined bone in early skeletonisation appears shiny and black/grey and results from the reduction environment created in the burning area where the bones remain after being exposed and before collection. This type of environment is smoky and/or without oxygen and allows the porous calcined bone the opportunity to become saturated with superficial carbon and smoke deposits after the fire is extinguished (Pope, 2007). A number

of the calcined remains present with a charred appearance resulting from smoke from the overlying vegetation.

In late skeletonisation, all tissue is absent and the external, visible surface of the bone is dry and in some instances slightly weathered. For these remains, some of the areas remain completely unaltered and are a consequence of the variable nature of the fire and the position of the remains in relation to the heat source. Extreme fragmentation of burned remains is often noted, and recovery of the skeletal elements often incomplete. The preferential preservation of epiphyses and trabecular regions of dry-burned bones reflects the durability and structural integrity of this bone type to dehydration and recrystallization (Gejvall, 1970; Warren & Maples, 1997; Pope, 2007; Symes *et al*., 2008). Bones exposed while dry display more uniform burning with increased areas of calcination when compared to the early skeletonised remains. No distinct areas are found to burn first or last in this stage and areas that previously would not have shown thermal damage now display extensive charring nor calcination (pelvis, ventral aspects of vertebrae, and proximal aspects of the femora). Bones that display incomplete cremation (unaltered surfaces present) but no visible signs nor remnants of soft tissue need to be examined for mixed thermal signatures. If areas normally well protected with tissue (cranial base, articular joint surfaces, vertebral body surfaces, internal surfaces of ribs, or the sacroiliac joint) display thermal alteration, it may be consistent with heat exposure to dry, skeletonised remains or possibly previous trauma, body positioning or location within the fire (Pope, 2007). Areas of the skeleton in contact with the ground often displayed no or minimal thermal alteration, as the ground surface acts as a protective barrier.

In general, burn-related colour alterations were uniform across most of the skeleton. Bone fragments ranged in colour from white calcined to blackened char and combinations of calcined and charred surfaces. Variation in colour for a single element relates to differences between fleshed, defleshed/wet/green, and dry burned bone (Buikstra & Swegle, 1989; Bennett, 1999). Variability in colour provides information to correctly interpreted normal bone structural dynamics and normal burn patterns. Previous authors suggest that the uniform pattern of calcination or charring (single element completely charred/calcined) occurs on defleshed, green bones that are directly exposed to hearth fires in archaeological studies (Stiner *et al*., 1995; Buikstra & Ubelaker, 1997; Cain, 2005; Pope, 2007; Asmussen, 2009). However, the burn uniformity is not necessarily exclusive to defleshed/green bone and also

presents in dry bone. In this instance, the absence of flesh is more important in producing a uniform burn pattern than the wet/dry condition of the bone.

Soft tissue and the organic content of bone play an important role in the presentation of thermal damage to skeletal remains. The manner in which fleshed, wet and dry bones burn and the associated changes in colour differ and provide clues as to the bone condition prior to the burn event. Skeletonised phases (early and late), with little to no soft tissue present with large areas of calcined bone (head and neck: 60% moderate calcination, 33% extensive calcination; trunk: 28% moderate calcination, 8% extensive calcination; limbs: 17.5% moderate calcination, 2.5% extensive calcination). In fleshed remains, not only would it take longer to reach the calcined stage but also the manner in which the bone was exposed to heat would differ (0% calcination observed). With an increase in tissue degradation (decomposition), the colour distribution (charred and calcined) increases with the larger areas of exposed bone, and with a decrease in unaltered bone in all regions of the body. Fresh or fleshed remains burned for a limited duration do not present as completely calcined or even completely charred. The opposite pattern occurs on skeletonised remains lacking tissue in that whole bones could be completely charred or calcined, because tissue shielding is not a factor.

Calcination or extreme charring of the remains indicates a number of conditions independent of the condition of the remains such as increased temperatures, relative position to the source of the fire and increased duration of exposure (Baby, 1954; De Graff, 1961; Binford, 1963; Heglar, 1984; Shipman *et al*., 1984; Bennett, 1998; Pope, 2007; Walker *et al*., 2008). Colour change in burned bone has proven to be quite complex. Recent studies have recognised that various colour alterations can occur on a single skeleton and even on a single bone, especially in cases where the remains were fleshed prior to burning (Shipman *et al*., 1984; Walker & Miller, 2005; Brickley, 2007; Symes *et al*., 2008). Alone, colour alteration cannot aid in distinguishing between fleshed, wet or dry bone, but the relation of colour to other burn signatures (heat line, heat border, joint shielding, and brown burn) may provide more information as to previous bone condition. Increased evidence from this study of brown burn discolouration, delamination, and heat-induced fractures is noted with progressive tissue loss but is most prominent in the skeletal stages, irrespective of whether the bone was wet or dry.

5.3. Heat-related changes on bone

Heat borders, heat lines with distinct delineation and predictable cracking are observed on the remains burned while in the fresh, early and advanced stages of decomposition (Figure 5.9). These specific burn-related traits are more often associated with remains that have been burned while fully fleshed and have not previously been linked to partially fleshed remains (Mayne Correira, 1997; Pope & Smith, 2004; Thompson; 2004; Symes *et al*., 2008; Keough *et al*., 2012). Remains in advanced decomposition continue to display enough structural integrity of the tissue to produce distinctive traits observed on burned fleshed remains that are notably absent in skeletonised remains as discussed above.

A heat border, also known as the initial zone of pyrolysis, is the first transitional colour change that follows the contours of soft tissue specifically as it retracts along the bone surface (Pope, 2007; Symes *et al*., 2008, 2012, 2013). Additionally, a heat line, which lies adjacent to the heat border, is considered the initial transition between unaltered and thermally altered bone (Symes *et al*., 1999, 2008, 2012, 2013). However, a heat border may be observed without the presence of a heat line. The absence of a heat line is often observed in partially fleshed (advanced decomposition) remains. The nature of the tissue in late decomposition or perhaps the denatured periosteum may permit the tissue to burn away with less resistance, thus preventing a distinctive heat line. Therefore, fresh tissue, still adherent to the underlying bone, needs to be present in order for a heat line to be created along the periphery of a heat border.

Predictable cracking patterns also known as heat shrinkage fractures are a consequence of the alteration in bone structure due to direct heat exposure, and often these fractures extend slightly beyond the heat border (Binford, 1963; Stewart, 1979; DeHaan, Symes *et al*., 1999; Herrmann & Bennett, 1999; Symes *et al.,* 2001; Pope & Smith, 2004; Pope, 2007). Delineation is the clear, almost linear, distinction observed between unaltered bone, charred bone and the heat border. As expected, these suites of burn-related traits are absent on skeletonised and dry remains, as soft tissues are necessary to produce them. The traits, however have been observed in advanced decomposition in which a mixture of wet bone and soft tissue is present. Previous literature links these burn-related traits (heat border, heat line and delineation) to fully fleshed bodies (fresh or early decomposition) (Pope, 2007; Symes *et al*., 2008, 2012; Keough *et al*., 2012).

In addition to the heat borders, lines and predictable cracking, a small percentage of the remains in the advanced stage display joint shielding in the head and neck (6.7%) and in the limbs with early skeletonisation (2.5%). This specific trait is associated with articulated remains, so it is expected to observe joint shielding in fleshed or partially fleshed remains exposed to fire. In advanced decomposition or early skeletonisation, joint shielding is noted on the head and neck or limbs. However, the author suggests that joint shielding will be present in earlier stages of decomposition as long as tissue is present and joints are articulated. In both these stages, the condition of the bones appears partially fleshed, articulated and greasy. Joint shielding is not expected in dry, skeletonised and disarticulated remains, as the ligaments holding the joints together have decomposed and the joints are no longer in contact. This is evident in the results of this study that indicate a 0% chance of remains being in late skeletonisation, and no joint shielding is present on any of the dry remains. Joint shielding may not necessarily be linked to the abundance of soft tissue present or specifically ligaments keeping the joints together, but rather if a joint is articulated and remains undisturbed during the burning process, this trait may appear in any decomposition stage.

Previous authors specifically noted a range of observable heat-related traits on burned fleshed remains but not wet, defleshed bone, which appear to display a unique pattern of thermal alteration (Shipman *et al*., 1984; Buikstra & Swegle, 1989; Nelson, 1992; Pope & Smith, 2004; Pope, 2007). The presence of fat/grease in bone is a possible contributing factor to the range of thermal destruction on fresh to early skeletonised remains (wet remains) and not on dry bone which instead presents with non-distinct, uniform charring and calcination with no delineation, heat borders, heat lines or joint shielding. Non-delineated brown borders are observed in wet or early skeletonised and dry bone. The overlying flesh (dried out tissue) of the early skeletonised stage instantaneously burns away, and the greasy/wet bone directly reacts to the heat. When the greasy bones are examined, the borders between altered and unaltered bone are not as well defined as seen in the previous stages (no delineation), and a brown burn/border replaces the previously observed distinctive, off-white heat border and heat line. This has been attributed to the lack of tissue and the presence of, although minimal, moisture and organic content in the bone (Keough *et al.*, 2012). A brown border may be the chemical alteration of bone with remnant organic content and moisture in direct contact with heat or fire. The brown border observed in the late skeletonisation (dry bone) could possibly be attributed to last remnants of organic materials present in the bone. Although not visible to

the eye and even though the surface of the bone appeared dry, the deeper cortex of the bone may have some remaining organic constituents that may account for the presence of the non-delineated borders. Additional burn-related traits observed in this stage include increased delamination and heat-induced fractures.

Heat-induced fractures observed on the remains in this study include longitudinal, transverse, step, patina and delamination. Patina fracturing, also known as superficial checking is only observed with skeletonisation and coincides with large surface areas being directly exposed to the fire (Figure 5.10). Patina/crazing/superficial checking most often occurs in thin cortical bone overlying trabecular bone such as that found in the articular ends of long bones, flat bones of the skull and pelvis, and vertebrae (Herrmann & Bennett, 1999; Pope & Smith, 2004). Delamination is observed on the remains from the fresh stage of decomposition but shows a larger representation in skeletonisation (Figure 5.11). Delamination is most commonly present in the skull due to the presence of diploë (Pope & Smith, 2004) but has also been linked to the separation of cortical and cancellous bone in epiphyseal regions (Herrmann & Bennett, 1999). In the present study, delamination is prevalent on the cranial and trunk elements in the advanced, early and late skeletonisation stages of decomposition (66.7% and 67.5%). Delamination is uncommon in early decomposition. In the limbs, delamination is more prevalent in the early and late stages of skeletonisation (80 – 100%), especially at the epiphyseal regions of the long bones. In the later stages, the cranial elements were too fragmented to observe patterns of delamination. Delamination is not exclusively attributed to heat-related conditions but may result from cooling after fire exposure or from external forces following post-exposure handling and recovery (Herrmann & Bennett, 1999; Pope & Smith, 2004).

The percentage and variability of heat-induced fractures steadily increased with decomposition (0% - 5% fresh & early; 12% - 46.7% advanced; 76% - 100% skeletonisation) and is attributed to a progressive reduction in soft tissue covering and the increasing exposure of bony surfaces. In some cases, areas adjacent to a heat-related fracture may vary in colour from the actual site of the fracture. This organic venting presents such that fracture margins and the area directly surrounding the fracture retain the blackened char, while the remaining bone may be calcined (Figure 5.8) (Bohnert *et al.*, 1998; Pope & Smith, 2004; Symes *et al.*, 2008). With continued exposure, charred areas within fracture lines (or sutures or foramina), eventually lose organic material and become calcined. This is a natural heat-related process

which continues until all organic materials within either the skull or long bone cavities are pyrolyzed (Pope & Smith, 2004; DeHaan, 2006).

The duration of burning, proximity to fire and manner of cooling and other variables may also contribute to the types of observed fractures. No curved transverse fractures are noted in this study, even though previous experimental studies demonstrated these fractures on porcine material (Marciniak, 2009). Not only is the histological nature of porcine material different from human bone, the anatomy of the limbs and how the muscle retracts along the surface of the bone may be different. Perhaps the shape or the underlying structural network of long bones only allows these fractures to occur during prolonged heat exposure, and further research into the formation of curved transverse fractures is needed.

Warping due to thermal exposure affects the dimensional structure of the bones is observed in advanced, early and late skeletonisation and suggests that the feature is not exclusively linked to the specific condition of the bone but possibly more linked to duration of exposure. The deep longitudinal, transverse and diagonal fractures observed in the early stages of decomposition show warping along the edges of the fracture lines as do the remains in late skeletonisation (Figure 5.12). Discrepancies in the literature occur as to whether warping is exclusive to dry, wet/green or fleshed burned remains. Several debates exist that contradict the association of warping with burned bone; some studies state that bone warping is common in remains that are exposed to fire while completely dry (Spenneman & Colley, 1989; Whyte, 2001; Gonçalves *et al*., 2011), whereas others suggest that dry bone does not display signs of warping when exposed to thermal conditions (Baby, 1954; Binford, 1972). Buikstra & Swegle (1989) suggest that warping is observed on both dry burned or wet/green burned bones and concurs with the current study. Bone warping has been linked to collagen content, and it is still unknown at what stage in bone diagenesis the levels of collagen are reduced enough to prevent the bone from warping and distorting from thermal exposure.

To summarise, researchers agree that fleshed bone reacts differently to heat and fire than dry bone with regard to colour, texture and fracture patterning and may be attributed to the contrasting structural properties between bones (Krogman, 1943; Webb and Snow, 1945; Baby, 1954; Trotter & Peterson, 1955; Wells, 1960; Stewart, 1979; Binford, 1963, 1972; Thurman & Willmore, 1980; Bradtmiller & Buikstra, 1984; Shipman *et al*., 1984; Buikstra & Swegel, 1989; Mayne, 1990; Grupe & Hummel, 1991; Nelson, 1992; Stiner *et al*., 1995; Herrmann & Bennett, 1999; Symes *et al*., 2001; Whyte, 2001; de Gruchy & Rogers, 2002; Dunlop, 2004; Symes *et al*., 2008; Gonçalves *et al*.., 2011; Keough *et al*., 2012). However,

wet/green (defleshed) bone displays less distinguishable traits than those observed in fleshed bone and is often classified therein. This close similarity between the two conditions proves the importance of tissue, fat/grease and the organic composition of the bone at time of exposure (Krogman, 1939). With flesh and grease present, the production of heat-induced fractures is greatly influenced, as the process of burning affords moisture loss and subsequent reduction in organic collagen content in bone (Herrmann & Bennett, 1999; Symes *et al*., 1999; Pope, 2007). The loss in organic content results in reduced tensile strength (loss of elasticity in the bone), allowing the bone to pull apart, shrink, distort and form fractures while exposed to heat (Herrmann & Bennett, 1999; Symes *et al*., 1999).

The appearance of heat borders, heat lines, delineation, predictable cracking and greasy bone are most likely associated with the early stages of decomposition (fleshed to partially fleshed). Joint shielding is a trait that is linked to advanced decomposition and early skeletonisation where the bone is wet and articulated. The author suggests that this trait appears where two joints are articulated regardless of the level of decomposition. The fact that joint shielding was only observed in advanced decomposition and early skeletonisation can be attributed to the duration of exposure in this study. Traits including delamination and heat-induced fractures are most likely associated with the later stages of decomposition (wet – dry bone) with chances being between 39 – 99%. Brown borders are specifically linked to the early and late skeletonisation stages of decomposition when bone may still contain trace collagen content with minimal tissue present.

5.4. Limitations of the study

For this study an exposure time interval of 30 minutes was chosen. As previously stated, a human skeleton has been shown to display thermal alteration after just 10 minutes of exposure. This interval was chosen to produce enough thermal alteration on the remains, specifically in the later stages of decomposition, to analyse, interpret and reconstruct the changes associated with burn damage. As mentioned in Chapter 3, an attempt was made to replicate a natural, outdoor veldt fire. Since differential temperatures, ventilation, collapsing debris and reduction of the surrounding environment influence the complexity of natural fires an assesment of energy input and output (heat of combustion, HRR, heat flux etc.) was not recorded. It is acknowledged that the shortfall of not having this data makes comparison

between experimental burn studies difficult.However, this situation reflects the reality of burnt remains as these parameters are not known when a burned body is discovered and assessed.

If remains are discovered after a veldt fire, no information is available to state how long they were exposed to fire prior to discovery and recovery. In addition, not knowing how long the remains stayed undiscovered after being burnt in a veldt fire can also hinder the interpretation especially if the remains underwent extreme weathering from prolonged environmental exposure. The effects of weathering on postmortem burn remains has not been documented or researched in detail. This may affect the recovery of the skeletal elements, but postmortem damage to the remains prior to recovery may influence the interpretation and analysis of those remains. Context of the remains is often unknown, and the skeleton alone is used to make inferences from and construct a demographic profile as well as events related to or surrounding the time of death.

Figure 5.1 Marked destruction of skin and muscle tissue in pigs exposed to fire in the fresh and early stages of decomposition

Figure 5.2 Burn pattern observed on the crania of pigs burned in the advanced stage of decomposition

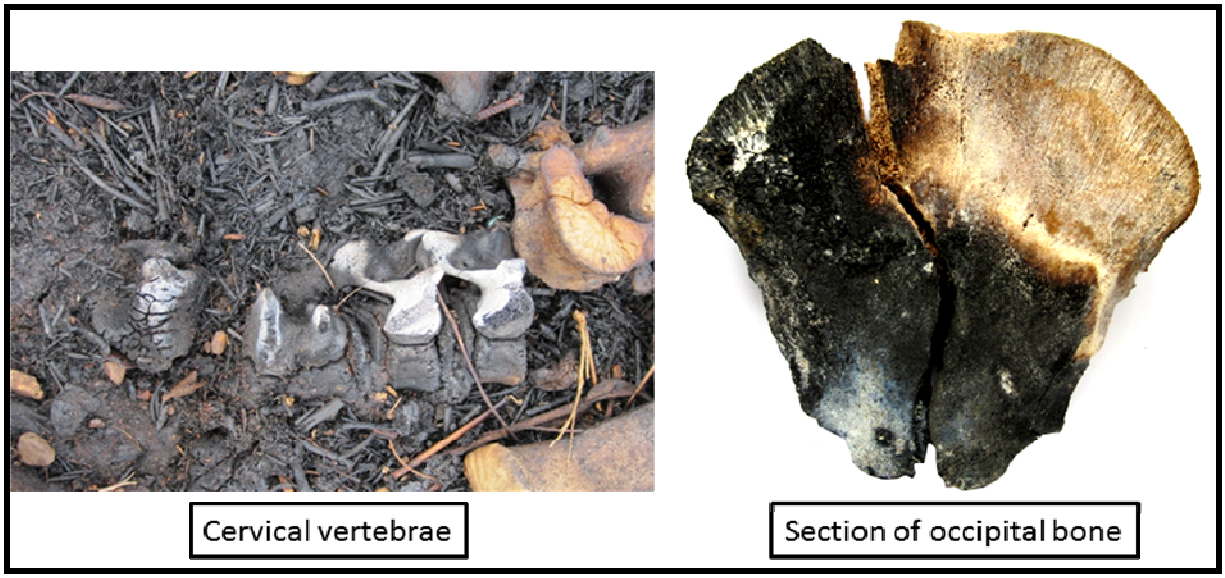

Figure 5.3 Charring and calcination of the occipital bone and cervical vertebrae in pig specimen

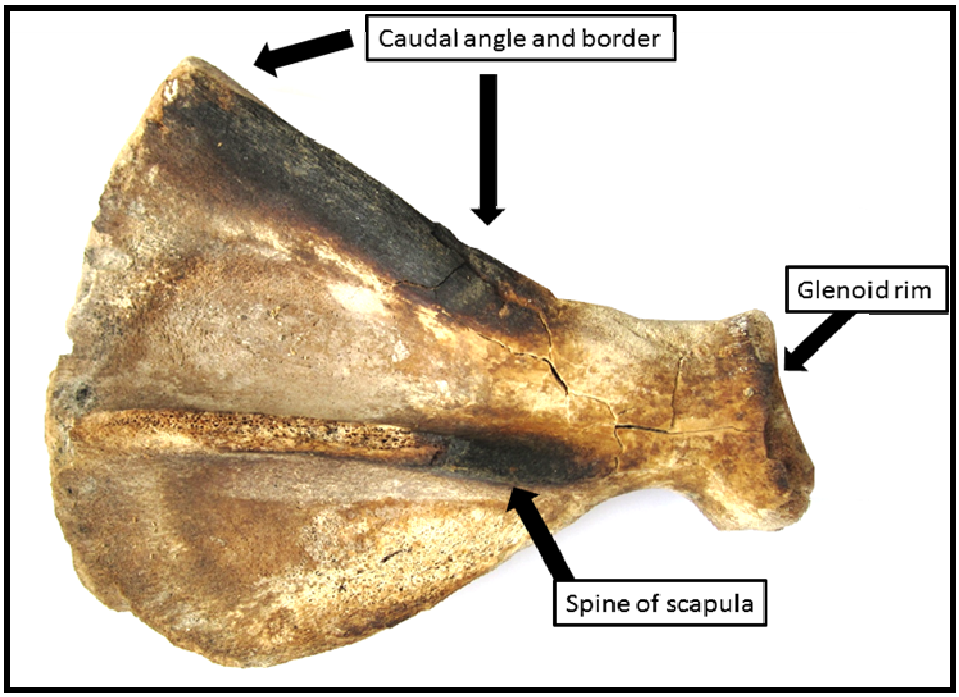

Figure 5.4 Charring of the spine, glenoid rim, caudal angle and border of the scapula

Figure 5.5 Burn damage to the A) metacarpals, B) metatarsals, C) radius, D) olecranon process, and E) medial aspect of the tibia of pig specimens in advanced decomposition

Figure 5.6 Flexion of the extremities due to heat and fire exposure

Figure 5.7 Canoeing burn pattern on the dorsal surface of the metacarpals exposing the medullary cavity

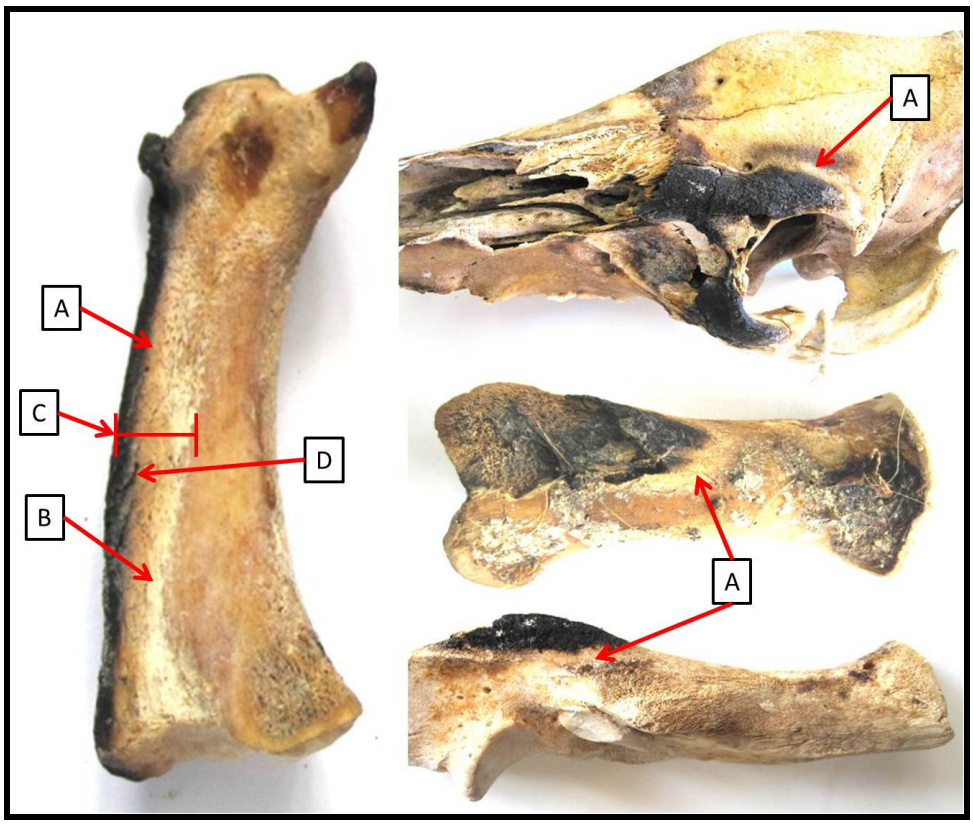

Figure 5.8 Heat border (A), heat line (B), delineation (C) and predictable cracking (D) on remains in early stages of decomposition

Figure 5.9 Patina fracture patterns on the metacarpal and tibial shafts

Figure 5.10 Delamination fracture patterns on the cranium, pelvic and metatarsals

Figure 5.11 Organic venting through a fracture line on the shaft of a tibia

Figure 5.12 Warping along fracture lines in both advanced decomposition and late skeletonisation

Chapter 6: Conclusion

The current study demonstrates a suite of reliable heat-related traits that can be utilised for estimating whether remains were fleshed, wet or dry prior to a burn event when confined to the parameters of this study (30 min burn interval). These conclusions included the following:

1) Soft tissue protects bone, and bone burns progressively when the protective tissue recedes and is destroyed. The more tissue present, the more protection is afforded from tissue shielding, and as decomposition progresses this tissue shielding is reduced and thermal effects on bone are noted.
2) The differential ratio of colour distribution (unaltered, charred or calcined) on the bones is associated with the relative level of decomposition when exposed during a veldt fire.
3) The presence of heat borders, heat lines, delineation and greasy bone are linked to early stages of decomposition when a body is fleshed or partially fleshed.
4) Based on the observations made on remains exposed to a veldt fire while in advanced decomposition, the thermal alterations appear to mimic the burn pattern or burn characteristics previously associated with a body that has been burned while fully fleshed. This is due to the presence of flexion of the extremities and has a major impact on deducing information surrounding the time of death, specifically the state of the remains before exposure, from unknown burned remains.
5) Joint shielding is a trait observed in remains which remain articulated and undisturbed during the burning process. This trait is more common in remains that are fleshed or partially fleshed but is not restricted to a specific bone condition.
6) Delamination and heat-induced fractures are associated with the later stages decomposition, and the more fractures present, the greater the likelihood of the remains being in more advanced decomposition. The number of fractures does not necessarily indicate extreme decomposition, instead, it can be said that the duration of the fire and the percentage of flesh present prior to exposure has a major role in the production of fractures.

Severeal potential research ideas regarding burn-related changes to bone have been found during the course of the present study. Many questions still remain and new questions have been formulated. The study of burned bone is a growing multidisciplinary field and can provide several research ideas and potential discoveries. Several variables encountered during this study can provide future research opportunities and a number of questions can possibly be answered;

1) The duration of fire exposure and its effect on the patterned thermal destruction in the various stages of decomposition;
2) The reproduction of curved transverses fractures and whether they are in actual fact linked to the condition of the bone, percentage of soft tissue or the structure of the bone;
3) The use of accelerants on the body and how this affects the consumption in various stages of decomposition;
4) The replication of this study with other animal specimens with bone structure more similar to human bone (e.g., baboons);
5) The effect of different fire exposure conditions on remains in various stages of decomposition;
6) The effect covering material such as clothing, blankets or plastic on the patterns of thermal destruction in various stages of decomposition;
7) The chemical analysis of burned bones in various stages of decomposition regarding organic content;
8) Histology of burned bone in various stages of decomposition;
9) Applying the results of this study to real life forensic cases to determine applicability;
10) The effects of environmental exposure on burned remains in various stages of decomposition;
11) Measuring the HRR (heat release rate) during the various stages of decomposition to evaluate differences between fleshed, wet and dry bone.

REFERENCE LIST

Adelson, L. 1954/5. Role of the pathologist in arson investigation. *The Journal of Criminal Law, Criminology, and Police Service,* 45(6):760-768

Adlam, R.E., Simmons, T. 2007. The effect of repeated physical disturbance on soft tissue decomposition – are taphonomic studies an accurate reflection of decomposition. *Journal of Forensic Sciences*, 52(5):1007-1014

Agresti, A. 1990. *Categorical data analysis*. New York, NY: John Wiley & Sons

Agricultural Research Council. 1993. Pig production in South Africa. *Irene Animal Production Institute*. Bulletin 427, V & R Printers. Pretoria, South Africa: 19-97

Arora, A.K., Gupta, P., Kapoor, S.S., Mahajan, S. 2010. An analytic review of burnt bones in medicolegal sciences. *Journal of Punjab Academy of Forensic Medicine & Toxicology,* 10:31-36

Asmussen, B. 2009. Intentional or incidental thermal modification? Analysing site occupation via burned bone. *Journal of Archaeological Science*, 36(2):528-536

Aturaliya, S., Lukasewycz, A. 1999. Experimental forensic and bioanthropological aspects of soft tissue taphonomy: 1. Factors influencing postmortem tissue desiccation rates. *Journal of Forensic Sciences*, 44(5):893-896

Baby, R.S. 1954. Hopewell cremation practices. *The Ohio Historical Society Papers in Archaeology*, 1:1-7

Banerjee, M., Capozzoli, M., McSweeny., Sinha, D. 1999. 'Beyond kappa: a review of interrater agreement measure'. *The Canadian Journal of Statistics*, 27:3-23

Bass, W.M. 1984. Is it possible to consume a body completely in a fire? (*In*: Rathbun, T.A. & Buikstra, J.E., (eds). Human identification cases studies in forensic anthropology. Springfield, IL: Charles C. Thomas. pp:159-167

Bass, W.M., Jefferson, J. 2003. Death's acre: Inside the legendary forensic lab the body farm where the dead do tell tales. Putnam's G.P., Sons, New York, NY

Bell, L., Skinner, M.F., Jones, S.J. 1996. The speed of postmortem change to the human skeleton and its taphonomic significance. *Forensic Science International*, 82(2):129-149

Benhin, J.K.A. 2006. Climate change and South African Agriculture: Impacts and adaptation options. CEEPA Discussion paper No. 21 *Center for Environmental Economics and Policy in Africa*, University of Pretoria

Bennett, J. 1999. Thermal alteration of bone. *Journal of Archaeological Science*, 26(1):1-8

Binford, L.R. 1963. An analysis of cremations from three Michigan sites. *Wisconsin Archaeology,* 44(2):98-110

Bohnert, M., Rost, T., Pollak, S. 1998. The degree of destruction of human bodies in relation to the duration of the fire. *Forensic Science International*, 95:11-21

Bohnert, M., Schmidt, U., Perdekamp, G., Pollak, S. 2002. Diagnosis of a captive bolt injury in a skull extremely destroyed by fire. *Forensic Science International*, 127(3):192-197

Bohnert, M., Pollak, S. 2003. Heat-mediated changes to the hands and feet mimicking washerwoman's skin. *International Journal of Legal Medicine*, 2:102-105

Boldsen, J.L., Milner, G.R., Konigsberg, L.W., Wood, J.W. 2002. Transition analysis: a new method for estimating age from skeletons. *In*: Hoppa, R.D. & Vaupel, J.W., (eds). Paleodemography: Age distributions from skeletal samples. United Kingdom: Cambridge. pp:73-106

Bontrager A.B., Nawrocki, S.P. 2008. A taphonomic analysis of human cremains from the Fox Hollow Farm serial homicide site. *In*: Schmidt, C.W., & Symes, S.A., (eds). The analysis of burned human remains. London, Academic Press, pp:211-226

Bornman, E., van Eeden, R., Wentzel, M. 1998. Violence in South Africa: A variety of perspectives. HSRC Publishers. p.19 ISBN 0796918589

Bradtmiller, B., Buikstra, J.E. 1984. Effects of burning on human bone microstructure: a preliminary study. *Journal of Forensic Sciences*, 29(2):535-540

Brickley, M.B. 2007. A case of disposal of a body through burning and recent advances in the study of burned human remains. *In*: Brickely, M.B., Ferllini, R., (eds), Forensic Anthropology, Charles C Thomas, Springfield, pp:69-85

Brooks, T., Suchey, J. 1990. Skeletal age determination based on the os pubis comparison of Ascadi-Nemerski and Suchey-Brooks methods. *Human evolution*, (5):227-238

Buikstra, J.E., Swegle, M. 1989. Bone modification due to burning: experimental evidence. *In*: Bonnichsen, R.B. & Sorg, M.H., (eds). Bone modification. Center for the study of the first Americans, Orono. pp:258-278

Buikstra, J.E., Ubelaker, D.H. 1997. Standards for Data Collection from Human Skeletal Remains. *Arkansas Archaeological Survey,* Fayetteville

Cain, C.R. 2005. Using burned animal bone to look at Middle Stone Age occupation and behaviour. *Journal of Archaeological Science*, 32(6):873-884

Campobasso, C.P., Di Vella, G., Introna, F. 2001. Factors affecting decomposition and Diptera colonization. *Forensic Science International*, 120:18-27

Camps, F.E., Lucas, B.G.B., Robinson, A.E. 1976. Gradwohl's Legal Medicine, 3rd ed, Bristol: John Wright & Sons, pp:120-228

Christensen, A. 2002. Experiments in the combustibility of the human body. *Journal of Forensic Sciences*, 47(3):466-470

Clark, M.A., Worrell, M.B., Pless, J.E. 1997. Postmortem changes in soft tissue. *In*: Haglund, W.D. & Sorg, M.H., (eds). Forensic taphonomy: The postmortem fate of human remains. Boca Raton: CRC Press, pp:151-164

Collins, M.J., Riley, M., Child, A.M., Turner-Walker, G. 1995. A basic mathematical simulation of the chemical degradation of ancient collagen. *Journal of Archaeological Science*, 22:175-183

Collins, M.J., Nielsen-Marsh, C.M., Hiller, J., Smith, C.I., Roberts, J.P., Prigodich, R.V., Wess, T.J., Csapo, J., Millard, A.R., Turner-Walker, G. 2002. The survival of organic matter in bone: a review. Archaeometry, 44(3):383-394

Connelley, H., DesPlaines, L., Kreek, E. 2010. *Ageing and thermal effects on the properties of fleshed and defleshed bones.* Project report (BSc: M.Eng), Worcester Polytechnic Institute

Cook, R., Ide, R. 1985. Principles of fire investigation. *The institution of fire engineers*, Leicester, UK, 134

Cooper, P.N. 2006. Burn injury. *In*: Rutty, G.N., (ed). Essentials of Autopsy Practice: Current methods and modern trends. London, UK: Springer-Verlag. pp:215-232

Cormack, D.H. 1987. Ham's Histology. J.B. Lippincott, Philadelphia

Cotran, R.S., Kumar, V., Robbins, S.L. 1994. Robbins pathologic basis of disease. Saunders, W.B., Philiadelphia

Crosbie, S., Corliss, D. 2012. Are you dense? Using kernel density estimation (KDE) to connect the dots amidst uncertainty. Magnify, a Division of Marketing Associates, LLC, Detroit, Michigan and Wilmington Delaware. Available at:

www.mwsug.org/proceedings/2012/DV/MWSUG-2012-DV06.pdf [Accessed 13 June, 2013]

Cross, P., Simmons, T. 2010. The influence of penetrative trauma on the rate of decomposition. *Journal of Forensic Science*, 55(2):295-301

David, B. 1990. How was this bone burnt? *In*: Solomon, S., Davidson, I., Watson, D., (eds). Problem solving in taphonomy. Vol: 2:65-70

De Gruchy, S., Rogers, T.L. 2002. Identifying chop marks on cremated bone: A preliminary study. *Journal of Forensic Sciences*, 47(5):933-936

De Graff, G. 1961. Gross effects of a primitive hearth. *South African Archaeological Bulletin*, 16:25-26

DeHaan, J.D. 1997. A case of not-so-spontaneous human combustion. *Fire and Arson Investigator*, 47(4):14-16

DeHaan, J.D., Campbell, S.J., Nurbakhsh, S. 1999. Combustion of animal fat and its implications for the consumption of human bodies in fires. *Science & Justice*, 39(1):27-38

DeHaan, J.D., Nurbakhsh, S. 2001. Sustained combustion of an animal carcass and its implications for the consumption of human bodies in fires. *Journal of Forensic Sciences*, 46(5):1076-1081

DeHaan, J.D. 2006. Fire-related deaths and injuries. *In*: DeHaan, J.D. (ed), Kirk's Fire Ivnvestigation, 5th ed, Upper Saddle River: Prentice Hall Inc: pp:362-393

DeHaan, J.D. 2008. Fire and Bodies. In: Schmidt C.W., Symes, S.A., (eds). The analysis of burned human remains, Elsevier, Academic Press, London: pp:1-14

DeHaan, J.D. 2012. Sustained combustion of bodies: some observations. *Journal of Forensic Sciences*, 57(6):1578-1584

Denys, C. 2002. Taphonomy and experimentation. *Archaeometry*, 44(3):469-484

Devlin, J.B., Herrmann, N.P. 2008. Bone colour as an interpretive tool of the depositional history of archaeological cremains. *In*: Schmidt, C.W., Symes, S.A., (eds). The analysis of burned human remains, Elsevier, Academic Press, London: pp:109-128

Dent, B.B., Forbes, S.L., Stuart, B.H. 2004. Review of human decomposition processes in soil. *Environmental Geology*, 45:576-585

DiMaio, D.J., DiMaio, V. 1989. Forensic Pathology. Elsevier, New York

DiMaio, D.J., DiMaio, V. 2001. *Forensic Pathology*, 2nd ed, CRC Press Boca Raton, FL

Dokladal, M. 1969. Uber die heutigen moglichkeiten der personenidentifikation auf grund von verbrannten knochen. *Aktulle Kriminologie*, pp:223-246

Dolinak, D., Mathshes, E., Lew, E. 2005. *Forensic Pathology: Principles and Practice*, Academic Press, Elsevier

Dunlop, J. 2004. Cremation of body parts and foetuses. *Journal of Obstetrics and Gynecology*, 24(4):341-342

Eckert, W. 1981. The medicolegal and forensic aspects of fire. *American Journal of Forensic Medicine and Pathology*, 2(4):347-357

Eckert, W.G., James, S., Karchis, S. 1988. Investigation of cremations and severely burnt bodies. *American Journal of Forensic Medicine and Pathology*, 9(3):188-200

Elston, D.A., Proe, M.F. 1995. Smoothing regression coefficients in an overspecified regression model with interrelated explanatory variables. *Applied Statistics*, 44:395-406

Fairgrieve, S.I. 2008. Forensic cremation: Recovery and analysis. CRC Press/Taylor Francis Group, Boca Raton, Florida

Fanton, L., Jdeed, K., Tilhet-Coartet, S., Malicier, D. 2006. Criminal burning. *Forensic Science International*, 158: 87-93

Fiedler, S., Graw, M. 2003. Decomposition of buried corpses, with special reference to the formation of adipocere. *Naturwissenschaften*, 90:291-300

Fienberg, S.E. 1977. The analysis of cross-classified categorical data. Cambridge, MA: MIT press

Figueiredo, M., Fernando, A., Martins, G., Freita, J., Judas, H., Figueiredo, H. 2010. Effect of the calcination temperature on the composition and microstructure of hydroxyapatite derived from human and animal bone. *Ceramics International*, doi:10.1016/j.ceramint.2010.07.016

Filhani, P. 2011. Is necklacing returning to South Africa? BBC News, Port Elizabeth. www.bbc.co.uk/news/world-africa-14914526

Fisher, B.A.J. 2007. Techniques of crime scene investigation, 7th ed. CRC Press, New York

Forbes, G. 1941. The effects of heat on the histological structure of bone. *Police Journal*, 14(1):50-60

Forbes, S.L.., Stuart, B.H., Dent, B.B. 2005. The effect of the burial environment on adipocere formation. *Forensic Science International*, 154:24-34

Frater, J. 2007. Top 10 gruesome methods of execution. http://listverse.com/2007/09/12/top-10-gruesome-methods-of-execution/

Freemont, A.J. 1998. The tissues we deal with. (I) Bone. *Current Orthopaedics*, 12(3):181-192

Fründ, H., Schoenen, D. 2009. Quantification of adipocere degradation with and without access to oxygen and to the living soil. *Forensic Science International*, 188:18-22

Galloway, A., Birkby, W.B., Jones, A.M., Henry, T.E., Parks, B.O. 1989. Decay rates of human remains in an arid environment. *Journal of Forensic Sciences*, 34:607-616

Galloway, A. 1997. The process of decomposition: A model from the Arizona-Sonoran Desert. *In*: Haglund, W.D. & Sorg, M.H., (eds). Forensic Taphonomy: The postmortem fate of human remains. Boca Raton: CRC Press: pp:93-108

Gejvall, N.G. 1969. Cremations. *In*: Brothwell, D. & Higgs, E., (eds). Science in Archaeology. Praeger, New York: pp:468-479

Gerling, I., Meissner, C., Reiter, A., Oehmichen, M. 2000. Death from thermal effects and burns. *Forensic Science International*, 115:33-41

Gilchrist, R., Mytum, H.C. 1986. Experimental archaeology and burnt animal bones from archaeological sites. *Circaea,* 4(1): 29-38

Gill-King. 1997. Chemical and ultrastructural aspects of decomposition. *In*: Haglund & Sorg, (eds). Forensic Taphonomy and the Postmortem Fate of Human Remains, CRC Press Boca Raton, Florida, 93-108

Glassman, R.M., Crow, D.M. 1996. Standardisation model for describing the extent of burn injury to human remains. *Journal of Forensic Sciences*, 41(1):152-154

Goff, M.L. 2009. Early postmortem changes and stages of decomposition in exposed cadavers. *Exp Appl Acarology*, 49:21-36

Gonçalves, D., Thompson, T.J.U., Cunha, E. 2011. Implications of heat-induced changes in bone on the interpretation of funerary behaviour and practice. *Journal of Archaeological Science*, doi: 10.1016/j.jas2011.01.006

Gordon, I., Shapiro, H.A., Berson, S.D. 1988. Forensic Medicine. A guide to principles. Churchill Livingstone, Edinburgh, pp:1-62

Green, M.A. 2000. Postmortem changes. *In*: Siegal, J., Saukko, P.J., & Knupfer. G.C., (eds). Encyclopaedia of Forensic Science. London: Academic Press: pp:1163-1167

Greenfield, M.L.V.H., Kuhn, J.E., Wojtys, E.M. 1998. A statistic primer: correlation and regression analysis. *American Journal of Sport Medicine*, 26(2):338-343

Grévin, G., Bailet, P., Quatrehomme, G., Ollier, A. 1998. Anatomical reconstruction of fragments of burned human bones: A necessary means for forensic identification. *Forensic Science International*, 96(2-3):129-134

Grupe, G., Hummel, S. 1991. Trace element studies on experimentally cremated bone, I. Alterations of the chemical composition at high temperatures. *Journal of Archaeological Science,* 18:177-186

Gunn, A. 2009. Essential forensic biology: animals, plants and micro-organisms in legal investigations. Wiley, Chichester

Haglund, W.D., Reay, D.T., Swindler, D.R. 1988. Tooth artifacts and survival of bones in animal-scavenged human skeletons. *Journal of Forensic Science*, 33:985-997

Haglund, W.D., Sorg, M.H. 1997. Method and theory of forensic taphonomy research. (*In*: Haglund & Sorg (eds). Forensic Taphonomy: The Postmortem Fate of Human Remains, CRC Press LLC. pp:13-26

Hanson, M., Cain, C.R. 2007. Examining histology to identify burned bone. *Journal of Archaeological Science*, 34(11):1902-1913

Haury, E.W. 1945. The excavation of Los Muertos and neighbouring ruins in the Salt River Valley, Southern Arizona. *Papers of the Peabody Museum of American Archaeology and Ethnology, Harvard University*, 24(1). Cambridge

Hedges, R.E.M., Millard, A.R. 1995. Bones and groundwater: towards the modelling of diagnostic processes. *Journal of Archaeological Science*, 22:155-164

Hedges, R.E.M. 2002. Bone diagenesis: an overview of processes. *Archaeometry*, 44:319-328

Heglar, R. 1984. Burned remains. *In*: Rathbun & Buikstra (eds). Human identification: Case studies in Forensic Anthropology, Charles C Thomas, Springfield, IL, 148-158

Hermann, B. 1970. Anthropologische bearbeitung der leichenbranden von Berlin-Rudow. *Ausgrabungen in Berlin*, 1:61-71

Herrmann, B. 1976. On histological investigations of cremated human remains. *Journal of Human Evolution*, 6:101-103

Herrmann, N.P., Bennett, J.L. 1999. The differentiation of traumatic and heat-related fractures in burned bone. *Journal of Forensic Sciences*, 44(3):461-469

Henssge, C. 2002. Temperature based methods II. *In*: Henssge, Knight, Krompecher, Madea, Nokes (eds). The estimation of the time since death in the early postmortem period, Arnold, London, 46-105

Hewadikaram, K.A., Goff, M.L. 1991. Effect of carcass size on rate of decomposition and arthropod succession patterns. *American Journal of Forensic Medicine and Pathology*, 12(3):235-240

Holck, P. 2005. Cremated bone. Oslo: Anatomical Institute, University of Oslo. pp:113-119

Holden, J.L., Phakey, P.P., Clement, J.G. 1995. Scanning electron microscope observations of heat-treated human bone. *Forensic Science International*, 74:29-45

Icove, D., DeHaan, J. 2003. Forensic fire scene reconstruction an engineering approach, Prentice Hall, Upper Saddle River, NJ.

Institute for digital research and education. 2013. *Regression diagnostics*. Available at: www.ats.uda.edu/stat/stata/webbooks/reg/chapter2/statareg2.htm [Accessed 13 June, 2013]

Institute for digital research and education. 2013. *Regression with categorical variables*. Available at: www.ats.uda.edu/stat/stata/webbooks/reg/chapter3/statareg3.htm [Accessed 13 June, 2013]

Jawetz, E., Melnick, J.L., Adelberg, E.A. 1982. Review of Medical Microbiology, 15th ed. Lang Medical Publications, Los Altos, California

Kahn, H.A. 1983. An Introduction to Epidemiologic Methods. Oxford University Press, Inc

Karmani, S. 2006. The thermal properties of bone and the effects of surgical intervention. *Current Orthopaedics*, 20:52-58

Kelly, J.A., van der Linde, T.C., Anderson, G.S. 2009. The influence of clothing and wrapping on carcass decomposition and arthropod succession during warmer seasons in Central South Africa. *Journal of Forensic Science*, 54(5):1105-1112

Keough, N., Colman, K., L'Abbé, E.N., Symes, S.A., Cabo, L. 2012. Distinguishing features of thermal destruction on fleshed, wet and dry remains. *Proceedings of the American Academy of Forensic Sciences* 18:386

Kolver, J.H., Van der Linde, T.C., Mansell, M.W. 2001. A comparison of the decomposition and insect succession of a hanging carcass versus a carcass lying on the ground, with reference to the theory of island biography. *Proceedings of the Thirteenth Entomology Congress*, Pietermaritzburg (Oral presentation)

Kolver, J.H., Van der Linde T.C., Mansell, M.W. 2003. The influence of internal carcass temperatures on the development of *Chrysomya chloropyga*. *Proceedings of the Fourteenth Entomology Congress*, Pretoria

Kolver, J.H., Van der Linde, T.C. 2005. The effect of burning on decomposition and arthropod assemblages on burnt bodies. *Proceedings of the Fifteenth Entomology Congress*, Grahamstown,(Oral presentation)

Krogman, W.M. 1939. A guide to the identification of human skeletal material. *FBI Law Enforcement Journal*, 8(8):1-29

Krogman, W.M. 1943a. Role of the physical anthropologist in the identification of human skeletal remains, Part 1. *FBI Law Enforcement Journal*, 12(4):17-40

Krogman, W.M. 1943b. Role of the physical anthropologist in the identification of human skeletal remains, Part 2. *FBI Law Enforcement Journal*, 12(5):12-28

Krogman, W.M., Iscan, Y. 1986. The human skeleton in forensic medicine. Charles C. Thomas, Springfield, IL

Lanting, J.N., Aerts-Bijma, A.T., van der Plicht, J. 2001. Dating of cremated bones. *Radiocarbon*, 43:249-254

Lindsey, J.K. 1995a. Modelling frequency and count data. New York: Oxford University press

Lindsey, J.K. 1995b. Introductory statistics: a modelling approach. New York: Oxford University press

Lisowski, F.P. 1968. The investigation of human cremated remains. *Anthropologie und Humangenetik*, 4:76-83

Long, J.S. 1997. Regression models for categorical and limited dependent variables. Thousand Oaks, CA: Sage

Lopes de Carvahlo, L.M., Linhares, A.X. 2001. Seasonality of insect succession and pig carcass decomposition in a natural forest area in Southeastern Brazil. *Journal of Forensic Science*, 46(3):604-608

Lovejoy, O., Meindl, R.S., Pryzbeck, T.R., Mensforth, R.P. 1985. Chronological metamorphosis of the auricular surface of the ilium: a new method for the determination of age at death. *American Journal of Physical Anthropology*, 68:15-28

Mann, R.W., Bass, W.M., Meadows, L. 1990. Time since death and decomposition of the human body: variables and observations in case and experimental field studies. *Journal of Forensic Sciences*, 35(1):103-111

Marciniak, S. 2009. A preliminary assessment of the identification of saw marks on burned bone. *Journal of Forensic Sciences*, 54(4):779-785

Marella, G.L., Perfetti, E., Manciocchi, S., Arcudi, G. 2013. A case of "precocious" mummification. *Journal of Forensic and Legal Medicine*, 20:122-124

Marieb, E. 1992. Human anatomy and physiology, 2nd ed. Benjamin Cummings, San Francisco

Mayne, P.M. 1990. The identification of traumatic fractures in cremated remains: final results. *Paper presented at the annual meeting of the AAFS*, Cincinnati

Mayne Correia, P.M. 1997. Fire modification of bone: a review of the literature. In: Forensic Taphonomy: The Postmortem Fate of Human Remains, Haglund, WD, Sorg, MH, Eds. CRC Press: Boca Raton, pp:275-293

Mayne Correia, P.M., Beatie, O. 2002. A critical look at methods for recovering, evaluating and interpreting cremating human remains. (*In*: Haglund, W.D., Sorg, M.H., (eds). Advances in Forensic Taphonomy: Method, theory and archaeological perspectives. CRC Press, Boca Raton, FL. pp:275-293

Mays, S. 1998. The archaeology of human bones. Routledge, New York

McCullagh, P. 1980. Regression models for ordinal data. *Journal of the Royal Statistical Society*. Series B 42:109-142

McCullagh, P., Nelder, J.A. 1989. Generalised linear models, 2nd ed. New York: Chapman and Hall

McGraw, K.O., Wong, S.P. 1996. Forming inferences about some intraclass correlation coefficients. *Psychological Methods*, 1:30-46. (Correction: 1:390).

Mckern, G., Stewart, T. 1957. Skeletal age changes in young American males, analysed from the standpoint of identification. Technical report EP-45. Headquarters, Quartermaster Research and Development Command, Natick, MA.

Megyesi, M.S., Nawrocki, S.P., Haskell, N.H. 2005. Using accumulated degree-days to estimate the postmortem interval from decomposed human remains. *Forensic Science International*, 50(3):618-626

Micozzi, M.S. 1991. Experimental study of postmortem change under field conditions: effects of freezing, thawing, and mechanical injury. *Journal of Forensic Sciences*, 31(3):983-991

Miles, C.A., Sionkowska, A., Hulin, S.L., Sims, T.J., Avery, N., Bailey, A.J. 2000. Identification of an intermediate stage in the helix-coil degradation of collagen by ultraviolet light. *Journal of Biological Chemisty*, 275: 33014-33020

Moraitis, K., Spiliopoulou, C. 2010. Forensic implications of carnivore scavenging on human remains recovered from outdoor locations in Greece. *Journal of Forensic and Legal Medicine*, 17:298-303

Moritz, A.R., Henriques, F.C. 1947. Studies of thermal injury. II. The relative importance of time and surface temperature in causation of cutaneous burns. *American Journal of Pathology*, 23:695-720

Multiple regression with categorical data. 2013. *Department of political science and international relations,* Available at: www.udel.edu/htr/Statistics/Notes816/class14.PDF. [Accessed 13 June, 2013]

Murad, T.A. 1998. The growing popularity of cremation versus inhumation: Some forensic implications. (*In*: Reichs, K., Forensic osteology: Advances in the identification of human remains., (ed), Charles C Thomas, Springfield, IL. pp:86-105

Murray, K.A., Rose, J.C. 1993. The analysis of cremains: A case involving the inappropriate disposal of mortuary remains. *Journal of Forensic Sciences*, 38(1):98-103

National Injury Mortality Surveillance System (NIMSS); 1999, 2011, 2012

Nelson, R. 1992. A microscopic comparison of fresh and burned bone. *Journal of Forensic Sciences*, 37(4): pp:1055-1060

News24, 2013. Tshwane battling wildfires. [online] Available at: http://www.news24.com/SouthAfrica/News/Tshwane-battling-wildfires-20130817 [Accessed 26th August 2013]

Nicholson, R.A. 1993. A morphological investigation of burnt animal bone and an evaluation of its utility in archaeology. *Journal of Archaeological Science*, 20:411-428

Nielson-Marsh, C.M., Hedges, R.E.M. 1999. Bone porosity and the use of mercury intrusion porosimetry in bone diagenesis studies. *Archaeometry*, 41:165-174

Nkomo, G.V., Sassi, M. 2009. Impact of veld fires on land on smallholder farmers in Cashel Valley in Zimbabwe. *NAF International Working Paper Series*, Paper n. 09/02

O'Brien, R.C., Forbes, S.L. 2007. A preliminary investigation into the scavenging activity on pig carcasses in Western Australia. *Forensic Science and Medical Pathology*, 3:194-199

Owsley, D., Ubelaker, D., Houck, M., Sandness, M., Grant, W., Craig, E., Woltanski, T., Peerwani, M. 1995. The role of forensic anthropology in recovery and analysis of Branch Davidian Compound victims: Techniques and analysis. *Journal of Forensic Sciences*, 40(3):341-348

Parks, C.L. 2011. A study of the human decomposition sequence in Central Texas. *Journal of Forensic Science*, 56(1):19-22

Pauw, J. 1991. In the heart of the whore: the true story of apartheid's death squads. 1st ed; Halfway House: Southern Book Publishers

Pauw, J. 1996. Into the heart of darkness: confessions of apartheid's assassins. 1st ed; Published: J Ball

Pijoan, C., Ma, J., Mansilla, J., Leboreiro, I., Lara, V.H., Bosch, P. 2007. Thermal alteration of archaeological bones. *Archaeometry*, 449(4):713-727

Pike, A., Nielsen-Marsh, C.M., Hedges, R.E.M. 2001. Bone dissolution and hydrology. Proceedings of Archaeological Sciences 1997, British Archaeological Reports, Archaeopress, Oxford, 127-132

Pinheiro, J. 2007. Decay process of a cadaver. *In*: Schmitt, A., Cunha, E., & Pinheiro, J., (eds). Forensic anthropology and medicine: Complementary sciences from recovery to cause of death. Totowa, N.J: Humana Press: pp:85-116

Polsen, C.J., Gee, D.J., Knight, B. 1985. The Essentials of Forensic Medicine, 4th ed. Pergamon Press, Oxford

Pope E.J., Smith, O.C. 2004. Identification of traumatic injury in burned cranial bones: an experimental approach. *Journal of Forensic Sciences*, 49(3):431-440

Pope, E.J. 2007. *The effects of fire on human remains: characteristics of taphonomy and trauma*. Dissertation, (PhD). Fayetteville (AR), University of Arkansas

Pounder, D.J. 2000. Postmortem interval. *In*: Siegal, J., Saukko, P.J., & Knupfer, G.C., (eds). Encyclopaedia of Forensic Sciences. London: Academic Press: pp:1167-1172

Powers, R.H. 2007. The decomposition of human remains. (*In*: Rich, J., Dean, D.E., Powers, R.H., (eds). Forensic medicine of the lower extremity. Humana Press: pp:3-15

Ramirez, J.G. 2009. Statistical Intervals: Confidence, Prediction, Enclosure. [online] Available at: https://www.sas.com/resources/whitepaper/wp_4430.pdf

Raphela, T.D. 2011. *The impact of shack fires on the people of J.B. Mafira informal settlement, Bloemfontein, South Africa.* Thesis, (MSc). Bloemfontein, University of the Free State

Reed, H.B. 1958. A study of dog carcass communities in Tennessee, with special reference to the insects. *Am Midl Nat.,* 59:213-245

Rhine, S., Dawson, J. 1997. Estimation of time since death in the Southwest United States. *In*: Reichs, K., (ed). Forensic Osteology: Advances in the Identification of Human Remains, 2ed. Charles C. Thomas, Springfield, IL, 145-159

Rhine, S. 1998. Bone voyage: a journey in forensic anthropology. University of New Mexico Press, New Mexico

Rockhold, L.A. 1996. Bones: bullets, burns, bludgeons, blunders, and why. *In*: Symes, S.A. (ed), Burned Bone, Proceedings of the bone trauma workshop: American Academy of Forensic Sciences; Feb 19-24, Nashville, TN

Rodriquez, W.C., Bass, W.M. 1985. Decomposition of buried bodies and methods that may aid in their location. *Journal of Forensic Sciences*, 30(3):836-852

Rodriquez, W.C. 1997. Decomposition of buried and submerged bodies. *In*: Haglund, W.D. & Sorg, M.H., (eds). Forensic Taphonomy: The postmortem fate of human remains. Boca Raton: CRC Press, pp:459-467

Rossi, M.L., Shahrom, A.W., Chapman, R.C., Vanezis, P. 1994. Postmortem injuries by indoor pets. *American Journal of Forensic Medicine and Pathology*, 15(2):105-109

Sachs, J. 2000. Corpse, nature, forensic, and the struggle to pinpoint the time of death. Perseus publishing

Samuels, M.L., Witmer, J.A. 2003. Statistics for the Life Sciences (3rd ed), Prentice Hall, NJ, Upper Saddle River

SAPA. Truth comminssion looks at first "Necklace" murder. 4th February, 1997. www.justice.gov.za/trc/media/1997/9702/s970204c.htm

Schoenen, D., Schoenen, H. 2013. Adipocere formation – The result of insufficient microbial degradation. *Forensic Science International*, 226:301e1-301e6

Schultz, J.J., Warren, M.W., Krigbaum, J.S. 2008. Analysis of human cremains: Gross and chemical methods. *In*: Schmidt & Symes (eds). The analysis of burned human remains. Elsevier, pp:75-94

Schurr, M.R., Hayes, R.G., Cook, D.C. 2008. Thermally induced changes in the stable carbon and nitrogen isotope ratios of charred bones. *In*: Schmidt & Symes (eds). The analysis of burned human remains. Elsevier, pp:95-108

Schwark, T., Heinrich, A., Preuße-Prange, A., von Wurmb-Schwark, N. 2010. Reliable genetic identification of burnt human remains. *Forensic Science International*, doi:10.1016/j.fsigen.2010.08.008

Scott, R.M., Buckley, H.R., Spriggs, M., Valentin, F., Bedford, S. 2010. Identification of the first reported Lapita cremation in the Pacific Islands using archaeological, forensic and contemporary burning evidence. *Journal of Archaeological Science*, 37:901-909

Shipman, P., Foster, G., Schoeninger, M. 1984. Burnt bone and teeth: an experimental study of colour, morphology, crystal structure and shrinkage. *Journal of Archaeological Science,* 11:307-325

Shrout, P.E., Fleiss, J.L. 1979. Intraclass correlations: uses in assessing rater reliability. *Psychological Bulletin*, 86:420-428

Simmons, T., Adlam, R.E., Moffat, C. 2010. Debugging decomposition data – Comparative taphonomic studies and the influence of insects and carcass size on decomposition rate. *Journal of Forensic Science*, 55(1):8-13

Simpson, K., Knight, B. 1985. Changes after death: The time of death. (*In*: Forensic Medicine (9th ed), Edward Arnold, London, England, pp:6-10

Siwele, N.D. 2011. A review and assessment for Thaba Chweu local municipality veldfire management in Mpumalanga province. Mini-dissertation (M). University of the Free State

Smith, O.C., Symes, S.A., Pope, E.J., Gardner, C.D. 2001. Burning Observations I: Identification of normal human anatomical patterns in a thermal event. *Proceedings of the American Academy of Forensic Sciences*, 7:214.

Sorg, M.H., Haglund, W.D. 2002. Advancing forensic taphonomy: purpose, theory, and process. *In*: Haglund, W.D., Sorg, M.H., (eds). Advances in Forensic Taphonomy: Method, theory, and archaeological perspectives. CRC Press LLC. pp:3-29

Spenneman, D., Colley, S. 1989. Fire in a pit: the effects of burning on faunal remains. *Archaeozoologia*, 3:51-64

Spitz, W. 1993. Thermal Injuries. *In*: Spitz & Fisher (eds). Medicolegal Investigation of Death Charles C. Thomas, Springfield, IL. pp:413-442

Spitz, W. 2006. Thermal Injuries. *In:* Spitz & Fisher (eds). Medicolegal Investigation of Death, Charles C, Thomas, Springfield, IL, 413-444

Steadman, D.W., Worne, H. 2007. Canine scavenging of human remains in an indoor setting. *Forensic Science International*, 173:78-82

Stiner, M., Kuhn, S., Weiner, S., Bar-Yosef, O. 1995. Differential burning, recrystallization, and fragmentation of archaeological bone. *Journal of Archaeological Science*, 22:223-237

Stewart, T.D. Essentials of Forensic Anthropology. 1979. Charles C Thomas, Springfield, IL

Stockbuger, D.W. 2013. Multiple regression with categorical variables. *Multivariate statistics: Concepts, models, and applications,* Available at: www.psychstat.missouristate.edu/multibook/mlt08.htm [Accessed 13 June, 2013]

Symes, SA, Smith, OC, Berryman, H, Pope, EJ. (1999). Patterned thermal destruction of human remains. Paper presented to the 30th anniversary of the T.D. Stewart "Personal Identification in Mass Disasters" Central Identification Laboratory, Hawaii

Symes, S.A., Pope, E.J., Smith, O.C., Gardner, C.D., Zephro, L.A. 2001. Burning observations III: Analysis of fracture patterns in burned human remains. A paper presented at the American Academy of Forensic Sciences 53rd Annual meeting, February 19-24, Seattle, Washington

Symes, S.A., Rainwater, C.W., Chapman, E.N., Gipson, D.R., Piper, A.L.P. 2008. Patterned thermal destruction of human remains in a forensic setting. *In*: Schmidt, C.W., & Symes, S.A. (eds). The Analysis of Burned Human Remains, Academic Press, London, pp:15-24

Symes, S.A., L'Abbé, E.N., Chapman, E.R., Wolf, I., Dirkmaat, D.C. 2012. Interpreting traumatic injury to bone in Medicolegal invesitigations. (*In*: Dirkmaat, D. (eds). A Companion to Forensic Anthropology. Wiley-Blackwell, 340-389

Symes, S.A., L'Abbè, E.N., Pokines, J.T., Yuzwa, T., Messer, D., Stromquist, A., Keough, N. 2013. Thermal alteration to bone. *In*: Pokines, J.T., & Symes, S.A. (eds). Manual of Forensic Taphonomy, CRC Press, 367-402

Teie, W.C. 2005. Fire manager's handbook on veld and forest fires: Strategy, tactics and safety. South African Institute of Forestry

Thompson, T.J.U. 2002. The assessment of sex in cremated individuals: Some cautionary notes. *Journal of the Canadian Society of Forensic Sciences*, 35(2):49-56

Thompson, T.J.U. 2004. Recent advances in the study of burned bone and their implications for forensic anthropology. *Forensic Science International*, 146S:S203-S205

Thompson, T.J.U. 2005. Heat-induced dimensional changes in bone and their consequences for forensic anthropology. *Journal of Forensic Science,* 50(5):1008-1015

Thompson, M. 2006. Representing data distributions with kernel density estimates. *Analytical Methods Committee*, 4 (revised 2006)

Thompson, T.J.U. 2009. Burned human remains. *In*: Blau, S., & Ubelaker, D.H., (eds). Handbook of Forensic Anthropology and Archaeology. Left Coast Press, Inc.: 295-303

Thurman, M.D., Willmore L.J. 1981. A replicative cremation study experiment. *North American Archaeology,* 2(4):275-283

Todd, T.W. 1920. Age changes in the pubic bone I: the male white pubis. *American Journal of Physical Anthropology*, 3:285-334

Tracqui, A. 2000. Time since death. *In*: Siegal, J., Saukko, P.J., & Knupfer, G.C., (eds). Encyclopaedia of Forensic Sciences. London: Academic Press: pp:1357-1363

Trotter, T., Peterson, R. 1955. Ash weight of human skeletons in percent of their dry, fat-free weight. *Anatomical Records*, 123:341-368

Ubelaker, D.H. 1989. Human Skeletal Remains. Taraxacum, Washington

Van der Linde, T.C. 2003. The influence of wrapping on decomposition of a body – a case study. *Proceedings of the Fourteenth Entomology Congress*, Pretoria (Oral presentation)

Van Vark, G.N. 1970. Some statistical procedures for the investigation of prehistoric human skeletal material. Unpublished PhD dissertation, Rijksuniversiteit de Groningen, Groningen, The Netherlands

Vass, A. 2001. Beyond the grave – Understanding human decomposition. Microbiology Today, 28:190-192

Viguet-Carrin, S., Garnero, P., Delmas, P.D. 2006. The role of collagen in bone strength. *Osteoporosis International*, 17:319-336

Viera, A.J., Garrett, J.M. 2005. Understanding interobserver agreement: The kappa statistic. *Family Medicine*, 37(5):360-363

Walker, P.L., Miller, K.W.P., Richman, R. 2005. Time, temperature, and oxygen availability: an experimental study of the effects of environmental conditions on the colour and organic content of cremated bone. *In*: Schmidt, C.W., (ed). Burned bone, Elsevier Press, 216-217

Warren, M.W., Maples, W.R. 1997. The anthropometry of contemporary cremation. *Journal of Forensic Sciences*, 42:417-423

Webb, W., Snow, C.E. (1945). The Adena people. *Reports in Anthropology and Archaeology*, 6: 59-81, 166-199

Wells, C. 1960. A study of cremation. *Antiquity*, 133(34): 29-37

White, E.M., Hannus, L.A. 1983. Chemical weathering of bone in archaeological soils. *American Antiquity*, 48(2):316-322

Whyte, T. 2001. Special studies – Distinguishing human cremations from burned animal bones. *Journal of Field Archaelogy*, 28(3):437-449

Yoshino, M., Kimijima, T., Miyasaka, S., Sato, H., Seta, S. 1991. Microscopic study on estimation of time since death in skeletal remains. *Forensic Science International*, 49:143-158

Zhou, C., Byard, R.W. 2011. Factors and processes causing accelerated decomposition in human cadavers – An overview. *Journal of Forensic and Legal Medicine*, 18:6-9

Zioupos, P., Currey, J.D., Hamer, A.J. 1999. The role of collagen in the declining mechanical properties of ageing human cortical bone. *Journal of Biomedical Materials Research*, 45:108-116

APPENDIX A: SCORE SHEET

PIG#____	Element	Calcined		Charred		Unaltered		Brown burn	Heat border	Heat line	Delin	Greasy	Joint shield	Pred_cracking	Min_cracking	Delam	HI fractures
	Cranium																
	Mandible																
	Cervical vert.																
		Left	Right	Left	Right	Left	Right										
	Ribs																
	Scapula																
	Os coxa																
	Thoracic vert																
	Lumbar vert																
	Sacrum																
		Left	Right	Left	Right	Left	Right										
	Humerus																
	Ulna																
	Radius																
	Metacarpals																
	Carpals																
	Femur																
	Tibia																
	Fibula																
	Metatarsals																
	Tarsals																

APPENDIX B: ORIGINAL RAW DATA

PIG	Sc_HN	Sc_TK	Sc_LS	TBS	Cr_Cal	Cr_Cha	Cr_Una	Cr_BB	Cr_HB	Cr_HL	Cr_D1	Cr_Gr	Cr_JS	Cr_PC	Cr_MC	Cr_D2	Cr_HIF
BP_07	1	1	1	3	0	0	3	0	0	0	0	1	0	0	0	0	0
BP_15	1	1	1	3	0	0	3	0	0	0	0	1	0	0	0	0	0
BP_17	1	1	1	3	0	0	3	0	0	0	0	1	0	0	0	0	0
BP_19	1	1	1	3	0	0	3	0	0	0	0	1	0	0	0	0	0
BP_21	1	1	1	3	0	0	3	0	0	0	0	1	0	0	0	0	0
BP_01	3	3	2	8	0	0	3	0	0	0	0	1	0	0	0	0	0
BP_02	5	3	2	10	0	0	3	0	0	0	0	1	0	0	0	0	0
BP_22	3	4	3	10	0	0	3	0	0	0	0	1	0	0	0	0	0
BP_23	3	4	3	10	0	0	3	0	0	0	0	1	0	0	0	0	0
BP_20	4	4	3	11	0	0	3	0	0	0	0	1	0	0	0	0	0
BP_03	7	6	5	18	0	1	3	0	0	0	0	0	0	0	0	1	0
BP_05	7	6	5	18	1	2	2	0	0	0	0	1	0	0	0	1	1
BP_06	7	6	5	18	0	1	3	1	0	0	0	1	0	0	0	0	0
BP_04	7	6	6	19	1	1	3	0	1	1	1	1	0	1	0	1	1
BP_08	8	7	5	21	2	2	2	0	1	0	0	0	1	0	1	1	1
BP_14	10	8	6	24	2	2	0	0	0	0	0	0	0	0	0	1	1
BP_12	8	9	8	25	2	2	2	0	0	0	0	1	0	0	0	1	1
BP_18	10	9	6	25	1	1	3	0	0	0	0	1	0	0	0	1	1
PIG_029	12	7	8	27	2	2	1	1	0	0	0	1	0	0	0	0	1
PIG_028	11	7	10	28	2	2	1	1	1	0	0	0	0	0	0	0	1
PIG_002	13	10	9	32	2	2	0	0	0	0	0	0	0	0	0	1	1
PIG_003	11	12	10	33	3	1	0	0	0	0	0	0	0	0	0	0	1
PIG_009	13	12	10	35	1	1	3	1	0	0	0	0	0	0	0	0	1
PIG_010	13	12	10	35	3	1	1	0	0	0	0	0	0	0	0	1	1
PIG_011	13	12	10	35	3	1	1	0	0	0	0	0	0	0	0	0	1

PIG	Sc_HN	Sc_TK	Sc_LS	TBS	Mn_Cal	Mn_Cha	Mn_Una	Mn_BB	Mn_HB	Mn_HL	Mn_D1	Mn_Gr	Mn_JS	Mn_PC	Mn_MC	Mn_D2	Mn_HIF
BP_07	1	1	1	3	0	0	3	0	0	0	0	1	0	0	0	0	0
BP_15	1	1	1	3	0	0	3	0	0	0	0	1	0	0	0	0	0
BP_17	1	1	1	3	0	0	3	0	0	0	0	1	0	0	0	0	0
BP_19	1	1	1	3	0	0	3	0	0	0	0	1	0	0	0	0	0
BP_21	1	1	1	3	0	0	3	0	0	0	0	1	0	0	0	0	0
BP_01	3	3	2	8	0	0	3	0	0	0	0	1	0	0	0	0	0
BP_02	5	3	2	10	0	0	3	0	0	0	0	1	0	0	0	0	0
BP_22	3	4	3	10	0	0	3	0	0	0	0	1	0	0	0	0	0
BP_23	3	4	3	10	0	0	3	0	0	0	0	1	0	0	0	0	0
BP_20	4	4	3	11	0	0	3	0	0	0	0	1	0	0	0	0	0
BP_03	7	6	5	18	0	1	3	0	0	0	0	0	0	0	0	1	0
BP_05	7	6	5	18	0	1	3	1	0	0	0	1	0	0	0	1	1
BP_06	7	6	5	18	0	1	3	1	0	0	0	1	0	0	0	1	0
BP_04	7	6	6	19	0	1	3	0	1	0	0	1	0	0	0	1	1
BP_08	8	7	5	21	2	2	0	0	0	0	0	0	0	0	0	1	1
BP_14	10	8	6	24	2	2	0	0	0	0	0	0	0	0	0	1	1
BP_12	8	9	8	25	2	2	2	0	0	0	0	1	0	0	0	0	1
BP_18	10	9	6	25	1	1	3	0	0	0	0	1	0	0	0	1	1
PIG_029	12	7	8	27	2	2	0	0	0	0	0	0	0	0	0	0	1
PIG_028	11	7	10	28	2	2	2	0	0	0	0	0	0	0	0	1	1
PIG_002	13	10	9	32	2	2	0	0	0	0	0	0	0	0	0	1	1
PIG_003	11	12	10	33	3	1	0	0	0	0	0	0	0	0	0	1	1
PIG_009	13	12	10	35	1	1	3	0	0	0	0	0	0	0	0	0	1
PIG_010	13	12	10	35	3	1	0	0	0	0	0	0	0	0	0	0	1
PIG_011	13	12	10	35	2	2	0	0	0	0	0	0	0	0	0	1	1

PIG	Sc_HN	Sc_TK	Sc_LS	TBS	CV_Cal	CV_Cha	CV_Una	CV_BB	CV_HB	CV_HL	CV_D1	CV_Gr	CV_JS	CV_PC	CV_MC	CV_D2	CV_HIF
BP_07	1	1	1	3	0	0	3	0	0	0	0	1	0	0	0	0	0
BP_15	1	1	1	3	0	0	3	0	0	0	0	1	0	0	0	0	0
BP_17	1	1	1	3	0	0	3	0	0	0	0	1	0	0	0	0	0
BP_19	1	1	1	3	0	0	3	0	0	0	0	1	0	0	0	0	0
BP_21	1	1	1	3	0	0	3	0	0	0	0	1	0	0	0	0	0
BP_01	3	3	2	8	0	0	3	0	0	0	0	1	0	0	0	0	0
BP_02	5	3	2	10	0	0	3	0	0	0	0	1	0	0	0	0	0
BP_22	3	4	3	10	0	0	3	0	0	0	0	1	0	0	0	0	0
BP_23	3	4	3	10	0	0	3	0	0	0	0	1	0	0	0	0	0
BP_20	4	4	3	11	0	0	3	0	0	0	0	1	0	0	0	0	0
BP_03	7	6	5	18	1	1	3	0	0	0	0	0	0	0	0	1	0
BP_05	7	6	5	18	0	0	3	0	0	0	0	1	0	0	0	0	0
BP_06	7	6	5	18	0	0	3	0	0	0	0	1	0	0	0	0	0
BP_04	7	6	6	19	0	0	3	0	0	0	0	1	0	0	0	0	0
BP_08	8	7	5	21	1	1	3	0	1	0	0	1	0	0	1	0	1
BP_14	10	8	6	24	2	2	0	0	0	0	0	0	0	0	0	0	1
BP_12	8	9	8	25	1	2	2	0	0	0	0	1	0	0	0	1	1
BP_18	10	9	6	25	1	2	2	0	0	0	0	1	0	0	0	1	1
PIG_029	12	7	8	27	1	3	1	0	0	0	0	0	0	0	0	1	1
PIG_028	11	7	10	28	1	3	1	0	0	0	0	0	0	0	0	1	1
PIG_002	13	10	9	32	2	2	1	0	0	0	0	0	0	0	0	1	1
PIG_003	11	12	10	33	2	2	0	0	0	0	0	0	0	0	0	1	1
PIG_009	13	12	10	35	1	3	1	1	0	0	0	0	0	0	0	1	1
PIG_010	13	12	10	35	1	3	0	0	0	0	0	0	0	0	0	1	1
PIG_011	13	12	10	35	2	2	1	0	0	0	0	0	0	0	0	1	1

PIG	Sc_HN	Sc_TK	Sc_LS	TBS	Rb_Cal	Rb_Cha	Rb_Una	Rb_BB	Rb_HB	Rb_HL	Rb_D1	Rb_Gr	Rb_JS	Rb_PC	Rb_MC	Rb_D2	Rb_HIF
BP_07	1	1	1	3	0	0	3	0	0	0	0	1	0	0	0	0	0
BP_15	1	1	1	3	0	0	3	0	0	0	0	1	0	0	0	0	0
BP_17	1	1	1	3	0	0	3	0	0	0	0	1	0	0	0	0	0
BP_19	1	1	1	3	0	0	3	0	0	0	0	1	0	0	0	0	0
BP_21	1	1	1	3	0	0	3	0	0	0	0	1	0	0	0	0	0
BP_01	3	3	2	8	0	0	3	0	0	0	0	1	0	0	0	0	0
BP_02	5	3	2	10	0	0	3	0	0	0	0	1	0	0	0	0	0
BP_22	3	4	3	10	0	0	3	0	0	0	0	1	0	0	0	0	0
BP_23	3	4	3	10	0	0	3	0	0	0	0	1	0	0	0	0	0
BP_20	4	4	3	11	0	0	3	0	0	0	0	1	0	0	0	0	0
BP_03	7	6	5	18	0	0	3	0	0	0	0	0	0	0	0	1	0
BP_05	7	6	5	18	0	0	3	0	0	0	0	1	0	0	0	0	0
BP_06	7	6	5	18	0	0	3	0	0	0	0	1	0	0	0	0	0
BP_04	7	6	6	19	0	1	3	0	0	0	0	1	0	0	0	1	1
BP_08	8	7	5	21	0	1	3	0	0	0	0	1	0	1	0	1	1
BP_14	10	8	6	24	1	2	2	0	0	0	0	0	0	0	0	1	1
BP_12	8	9	8	25	1	2	3	1	0	0	0	1	0	0	0	1	1
BP_18	10	9	6	25	1	1	3	0	0	0	0	1	0	0	0	1	1
PIG_029	12	7	8	27	2	2	3	0	0	0	0	1	0	0	0	1	1
PIG_028	11	7	10	28	2	2	3	0	0	0	0	0	0	0	0	1	1
PIG_002	13	10	9	32	2	2	2	0	0	0	0	0	0	0	0	1	1
PIG_003	11	12	10	33	1	3	1	0	0	0	0	0	0	0	0	1	1
PIG_009	13	12	10	35	2	2	0	0	0	0	0	0	0	0	0	1	1
PIG_010	13	12	10	35	2	3	1	0	0	0	0	0	0	0	0	1	1
PIG_011	13	12	10	35	2	2	2	0	0	0	0	1	0	0	0	1	1

PIG	Sc_HN	Sc_TK	Sc_LS	TBS	Sca_Cal	Sca_Cha	Sca_Una	Sca_BB	Sca_HB	Sca_HL	Sca_D1	Sca_Gr	Sca_JS	Sca_PC	Sca_MC	Sca_D2	Sca_HIF
BP_07	1	1	1	3	0	0	3	0	0	0	0	1	0	0	0	0	0
BP_15	1	1	1	3	0	0	3	0	0	0	0	1	0	0	0	0	0
BP_17	1	1	1	3	0	0	3	0	0	0	0	1	0	0	0	0	0
BP_19	1	1	1	3	0	0	3	0	0	0	0	1	0	0	0	0	0
BP_21	1	1	1	3	0	0	3	0	0	0	0	1	0	0	0	0	0
BP_01	3	3	2	8	0	0	3	0	0	0	0	1	0	0	0	0	0
BP_02	5	3	2	10	0	0	3	0	0	0	0	1	0	0	0	0	0
BP_22	3	4	3	10	0	0	3	0	0	0	0	1	0	0	0	0	0
BP_23	3	4	3	10	0	0	3	0	0	0	0	1	0	0	0	0	0
BP_20	4	4	3	11	0	0	3	0	0	0	0	1	0	0	0	0	0
BP_03	7	6	5	18	0	0	3	0	0	0	0	0	0	0	0	1	0
BP_05	7	6	5	18	0	0	3	0	0	0	0	1	0	0	0	0	0
BP_06	7	6	5	18	0	0	3	0	0	0	0	1	0	0	0	0	0
BP_04	7	6	6	19	0	0	3	0	0	0	0	1	0	0	0	0	0
BP_08	8	7	5	21	0	1	3	0	1	0	0	1	0	1	0	1	1
BP_14	10	8	6	24	0	3	0	0	0	0	0	0	0	0	0	1	1
BP_12	8	9	8	25	0	1	3	0	0	0	0	1	0	0	0	0	0
BP_18	10	9	6	25	0	0	3	0	0	0	0	1	0	0	0	0	0
PIG_029	12	7	8	27	1	3	2	1	0	0	0	1	0	0	0	1	1
PIG_028	11	7	10	28	2	2	3	0	1	0	0	1	0	0	1	1	1
PIG_002	13	10	9	32	1	3	1	0	0	0	0	0	0	0	0	1	1
PIG_003	11	12	10	33	1	3	1	0	0	0	0	0	0	0	0	1	1
PIG_009	13	12	10	35	2	3	1	0	0	0	0	0	0	0	0	1	1
PIG_010	13	12	10	35	3	3	1	0	0	0	0	0	0	0	0	1	1
PIG_011	13	12	10	35	2	2	3	0	0	0	0	1	0	0	0	1	1

PIG	Sc_HN	Sc_TK	Sc_LS	TBS	OsC_Cal	OsC_Cha	OsC_Una	OsC_BB	OsC_HB	OsC_HL	OsC_D1	OsC_Gr	OsC_JS	OsC_PC	OsC_MC	OsC_D2	OsC_HIF
BP_07	1	1	1	3	0	0	3	0	0	0	0	1	0	0	0	0	0
BP_15	1	1	1	3	0	0	3	0	0	0	0	1	0	0	0	0	0
BP_17	1	1	1	3	0	0	3	0	0	0	0	1	0	0	0	0	0
BP_19	1	1	1	3	0	0	3	0	0	0	0	1	0	0	0	0	0
BP_21	1	1	1	3	0	0	3	0	0	0	0	1	0	0	0	0	0
BP_01	3	3	2	8	0	0	3	0	0	0	0	1	0	0	0	0	0
BP_02	5	3	2	10	0	0	3	0	0	0	0	1	0	0	0	0	0
BP_22	3	4	3	10	0	0	3	0	0	0	0	1	0	0	0	0	0
BP_23	3	4	3	10	0	0	3	0	0	0	0	1	0	0	0	0	0
BP_20	4	4	3	11	0	0	3	0	0	0	0	1	0	0	0	0	0
BP_03	7	6	5	18	0	0	3	0	0	0	0	0	0	0	0	1	0
BP_05	7	6	5	18	0	0	3	0	0	0	0	1	0	0	0	0	0
BP_06	7	6	5	18	0	0	3	0	0	0	0	1	0	0	0	0	0
BP_04	7	6	6	19	0	0	3	0	0	0	0	1	0	0	0	0	0
BP_08	8	7	5	21	0	0	3	0	0	0	0	1	0	0	0	0	0
BP_14	10	8	6	24	0	1	3	1	0	0	0	0	0	0	0	1	1
BP_12	8	9	8	25	1	2	3	0	0	0	0	1	0	0	0	1	1
BP_18	10	9	6	25	0	0	3	0	0	0	0	1	0	0	0	0	0
PIG_029	12	7	8	27	2	2	3	0	0	0	0	1	0	0	0	1	1
PIG_028	11	7	10	28	3	1	3	0	0	0	0	1	0	0	0	1	1
PIG_002	13	10	9	32	3	2	2	0	0	0	0	0	0	0	0	1	1
PIG_003	11	12	10	33	1	2	3	0	0	0	0	0	0	0	0	1	1
PIG_009	13	12	10	35	2	3	1	0	0	0	0	0	0	0	0	1	1
PIG_010	13	12	10	35	2	2	2	0	0	0	0	0	0	0	0	1	1
PIG_011	13	12	10	35	1	3	1	0	0	0	0	0	0	0	0	1	1

PIG	Sc_HN	Sc_TK	Sc_LS	TBS	TV_Cal	TV_Cha	TV_Una	TV_BB	TV_HB	TV_HL	TV_D1	TV_Gr	TV_JS	TV_PC	TV_MC	TV_D2	TV_HIF
BP_07	1	1	1	3	0	0	3	0	0	0	0	1	0	0	0	0	0
BP_15	1	1	1	3	0	0	3	0	0	0	0	1	0	0	0	0	0
BP_17	1	1	1	3	0	0	3	0	0	0	0	1	0	0	0	0	0
BP_19	1	1	1	3	0	0	3	0	0	0	0	1	0	0	0	0	0
BP_21	1	1	1	3	0	0	3	0	0	0	0	1	0	0	0	0	0
BP_01	3	3	2	8	0	0	3	0	0	0	0	1	0	0	0	0	0
BP_02	5	3	2	10	0	0	3	0	0	0	0	1	0	0	0	0	0
BP_22	3	4	3	10	0	0	3	0	0	0	0	1	0	0	0	0	0
BP_23	3	4	3	10	0	0	3	0	0	0	0	1	0	0	0	0	0
BP_20	4	4	3	11	0	0	3	0	0	0	0	1	0	0	0	0	0
BP_03	7	6	5	18	0	0	3	0	0	0	0	0	0	0	0	0	0
BP_05	7	6	5	18	0	0	3	0	0	0	0	1	0	0	0	0	0
BP_06	7	6	5	18	0	0	3	0	0	0	0	1	0	0	0	0	0
BP_04	7	6	6	19	0	0	3	0	0	0	0	1	0	0	0	0	0
BP_08	8	7	5	21	0	1	3	0	0	0	0	1	0	0	0	0	0
BP_14	10	8	6	24	0	2	2	0	0	0	0	0	0	0	0	1	1
BP_12	8	9	8	25	0	1	3	0	0	0	0	1	0	0	0	1	0
BP_18	10	9	6	25	0	0	3	0	0	0	0	1	0	0	0	0	0
PIG_029	12	7	8	27	2	2	2	0	0	0	0	1	0	0	0	1	1
PIG_028	11	7	10	28	1	3	1	0	0	0	0	1	0	0	0	1	1
PIG_002	13	10	9	32	2	2	0	0	0	0	0	0	0	0	0	1	1
PIG_003	11	12	10	33	1	3	1	0	0	0	0	0	0	0	0	1	1
PIG_009	13	12	10	35	1	3	1	0	0	0	0	0	0	0	0	1	1
PIG_010	13	12	10	35	1	3	1	0	0	0	0	0	0	0	0	1	1
PIG_011	13	12	10	35	1	3	1	0	0	0	0	0	0	0	0	1	1

PIG	Sc_HN	Sc_TK	Sc_LS	TBS	LV_Cal	LV_Cha	LV_Una	LV_BB	LV_HB	LV_HL	LV_D1	LV_Gr	LV_JS	LV_PC	LV_MC	LV_D2	LV_HIF
BP_07	1	1	1	3	0	0	3	0	0	0	0	1	0	0	0	0	0
BP_15	1	1	1	3	0	0	3	0	0	0	0	1	0	0	0	0	0
BP_17	1	1	1	3	0	0	3	0	0	0	0	1	0	0	0	0	0
BP_19	1	1	1	3	0	0	3	0	0	0	0	1	0	0	0	0	0
BP_21	1	1	1	3	0	0	3	0	0	0	0	1	0	0	0	0	0
BP_01	3	3	2	8	0	0	3	0	0	0	0	1	0	0	0	0	0
BP_02	5	3	2	10	0	0	3	0	0	0	0	1	0	0	0	0	0
BP_22	3	4	3	10	0	0	3	0	0	0	0	1	0	0	0	0	0
BP_23	3	4	3	10	0	0	3	0	0	0	0	1	0	0	0	0	0
BP_20	4	4	3	11	0	0	3	0	0	0	0	1	0	0	0	0	0
BP_03	7	6	5	18	0	0	3	0	0	0	0	0	0	0	0	0	0
BP_05	7	6	5	18	0	0	3	0	0	0	0	1	0	0	0	0	0
BP_06	7	6	5	18	0	0	3	0	0	0	0	1	0	0	0	0	0
BP_04	7	6	6	19	0	0	3	0	0	0	0	1	0	0	0	0	0
BP_08	8	7	5	21	0	0	3	0	0	0	0	1	0	0	0	0	0
BP_14	10	8	6	24	0	1	3	0	0	0	0	0	0	0	0	1	1
BP_12	8	9	8	25	0	2	2	0	0	0	0	1	0	0	0	1	1
BP_18	10	9	6	25	0	0	3	0	0	0	0	1	0	0	0	0	0
PIG_029	12	7	8	27	2	2	1	0	0	0	0	1	0	0	0	1	1
PIG_028	11	7	10	28	2	2	2	0	0	0	0	1	0	0	0	1	1
PIG_002	13	10	9	32	1	3	0	0	0	0	0	0	0	0	0	1	1
PIG_003	11	12	10	33	1	3	1	0	0	0	0	0	0	0	0	1	1
PIG_009	13	12	10	35	1	3	1	1	0	0	0	0	0	0	0	1	1
PIG_010	13	12	10	35	1	3	1	0	0	0	0	0	0	0	0	1	1
PIG_011	13	12	10	35	1	3	1	0	0	0	0	0	0	0	0	1	1

PIG	Sc_HN	Sc_TK	Sc_LS	TBS	Hum_Cal	Hum_Cha	Hum_Una	Hum_BB	Hum_HB	Hum_HL	Hum_D1	Hum_Gr	Hum_JS	Hum_PC	Hum_MC	Hum_D2	Hum_HIF
BP_07	1	1	1	3	0	0	3	0	0	0	0	1	0	0	0	0	0
BP_15	1	1	1	3	0	0	3	0	0	0	0	1	0	0	0	0	0
BP_17	1	1	1	3	0	0	3	0	0	0	0	1	0	0	0	0	0
BP_19	1	1	1	3	0	0	3	0	0	0	0	1	0	0	0	0	0
BP_21	1	1	1	3	0	0	3	0	0	0	0	1	0	0	0	0	0
BP_01	3	3	2	8	0	0	3	0	0	0	0	1	0	0	0	0	0
BP_02	5	3	2	10	0	0	3	0	0	0	0	1	0	0	0	0	0
BP_22	3	4	3	10	0	0	3	0	0	0	0	1	0	0	0	0	0
BP_23	3	4	3	10	0	0	3	0	0	0	0	1	0	0	0	0	0
BP_20	4	4	3	11	0	0	3	0	0	0	0	1	0	0	0	0	0
BP_03	7	6	5	18	0	0	3	0	0	0	0	0	0	0	0	0	0
BP_05	7	6	5	18	0	0	3	0	0	0	0	1	0	0	0	0	0
BP_06	7	6	5	18	0	0	3	0	0	0	0	1	0	0	0	0	0
BP_04	7	6	6	19	0	0	3	0	0	0	0	1	0	0	0	0	0
BP_08	8	7	5	21	1	1	3	0	1	0	0	1	0	1	0	1	1
BP_14	10	8	6	24	0	3	1	0	0	0	0	0	0	0	0	0	1
BP_12	8	9	8	25	0	1	3	0	0	0	0	1	0	0	0	1	1
BP_18	10	9	6	25	0	0	3	0	0	0	0	1	0	0	0	0	0
P_029	12	7	8	27	2	3	1	0	0	0	0	1	0	0	0	1	1
P_028	11	7	10	28	1	3	2	0	0	0	0	1	0	0	0	1	1
P_002	13	10	9	32	2	3	1	0	0	0	0	0	0	0	0	1	1
P_003	11	12	10	33	0	3	0	0	0	0	0	0	0	0	0	1	1
P_009	13	12	10	35	1	3	0	0	0	0	0	0	0	0	0	1	1
P_010	13	12	10	35	1	3	1	1	0	0	0	0	0	0	0	1	1
P_011	13	12	10	35	2	3	1	0	0	0	0	0	0	0	0	1	1

PIG	Sc_HN	Sc_TK	Sc_LS	TBS	Uln_Cal	Uln_Cha	Uln_Una	Uln_BB	Uln_HB	Uln_HL	Uln_D1	Uln_Gr	Uln_JS	Uln_PC	Uln_MC	Uln_D2	Uln_HIF
BP_07	1	1	1	3	0	0	3	0	0	0	0	1	0	0	0	0	0
BP_15	1	1	1	3	0	0	3	0	0	0	0	1	0	0	0	0	0
BP_17	1	1	1	3	0	0	3	0	0	0	0	1	0	0	0	0	0
BP_19	1	1	1	3	0	0	3	0	0	0	0	1	0	0	0	0	0
BP_21	1	1	1	3	0	0	3	0	0	0	0	1	0	0	0	0	0
BP_01	3	3	2	8	0	0	3	0	0	0	0	1	0	0	0	0	0
BP_02	5	3	2	10	0	0	3	0	0	0	0	1	0	0	0	0	0
BP_22	3	4	3	10	0	0	3	0	0	0	0	1	0	0	0	0	0
BP_23	3	4	3	10	0	0	3	0	0	0	0	1	0	0	0	0	0
BP_20	4	4	3	11	0	0	3	0	0	0	0	1	0	0	0	0	0
BP_03	7	6	5	18	0	0	3	0	0	0	0	0	0	0	0	0	0
BP_05	7	6	5	18	0	0	3	0	0	0	0	1	0	0	0	0	0
BP_06	7	6	5	18	0	1	3	0	1	1	1	1	0	0	0	0	0
BP_04	7	6	6	19	0	0	3	0	0	0	0	1	0	0	0	0	0
BP_08	8	7	5	21	0	0	3	0	0	0	0	1	0	0	0	0	0
BP_14	10	8	6	24	1	3	1	0	0	0	0	0	0	0	0	1	1
BP_12	8	9	8	25	0	2	3	0	0	0	0	1	0	0	0	1	1
BP_18	10	9	6	25	0	0	3	0	0	0	0	1	0	0	0	0	0
PIG_029	12	7	8	27	2	2	2	0	0	0	0	1	0	0	0	1	1
PIG_028	11	7	10	28	1	3	3	0	0	0	0	1	0	0	0	1	1
PIG_002	13	10	9	32	2	3	0	0	0	0	0	0	0	0	0	1	1
PIG_003	11	12	10	33	1	3	0	0	0	0	0	0	0	0	0	1	1
PIG_009	13	12	10	35	1	3	0	0	0	0	0	0	0	0	0	1	1
PIG_010	13	12	10	35	2	2	3	1	0	0	0	0	0	0	0	1	1
PIG_011	13	12	10	35	1	3	2	0	0	0	0	0	0	0	0	0	1

PIG	Sc_HN	Sc_TK	Sc_LS	TBS	Rad_Cal	Rad_Cha	Rad_Una	Rad_BB	Rad_HB	Rad_HL	Rad_D1	Rad_Gr	Rad_JS	Rad_PC	Rad_MC	Rad_D2	Rad_HIF
BP_07	1	1	1	3	0	1	3	0	1	0	0	1	0	1	0	1	1
BP_15	1	1	1	3	0	0	3	0	0	0	0	1	0	0	0	0	0
BP_17	1	1	1	3	0	0	3	0	0	0	0	1	0	0	0	0	0
BP_19	1	1	1	3	0	0	3	0	0	0	0	1	0	0	0	0	0
BP_21	1	1	1	3	0	0	3	0	0	0	0	1	0	0	0	0	0
BP_01	3	3	2	8	0	0	3	0	0	0	0	1	0	0	0	0	0
BP_02	5	3	2	10	0	0	3	0	0	0	0	1	0	0	0	0	0
BP_22	3	4	3	10	0	0	3	0	0	0	0	1	0	0	0	0	0
BP_23	3	4	3	10	0	0	3	0	0	0	0	1	0	0	0	0	0
BP_20	4	4	3	11	0	0	3	0	0	0	0	1	0	0	0	0	0
BP_03	7	6	5	18	0	0	3	0	0	0	0	0	0	0	0	0	0
BP_05	7	6	5	18	0	0	3	0	0	0	0	1	0	0	0	0	0
BP_06	7	6	5	18	0	0	3	0	0	0	0	1	0	0	0	0	0
BP_04	7	6	6	19	0	0	3	0	0	0	0	1	0	0	0	0	0
BP_08	8	7	5	21	0	1	3	0	1	0	0	1	0	1	0	0	1
BP_14	10	8	6	24	1	3	0	0	0	0	0	0	0	0	0	1	1
BP_12	8	9	8	25	0	1	3	0	0	0	0	1	0	0	0	1	1
BP_18	10	9	6	25	0	0	3	0	0	0	0	1	0	0	0	0	0
P_029	12	7	8	27	2	3	1	0	0	0	0	0	0	0	0	1	1
P_028	11	7	10	28	1	3	2	0	0	0	0	0	0	0	0	1	1
P_002	13	10	9	32	2	2	0	0	0	0	0	0	0	0	0	1	1
P_003	11	12	10	33	1	3	0	0	0	0	0	0	0	0	0	0	1
P_009	13	12	10	35	1	2	2	1	0	0	0	0	0	0	0	1	1
P_010	13	12	10	35	1	3	3	1	0	0	0	0	0	0	0	0	1
PG_011	13	12	10	35	1	3	1	0	0	0	0	0	0	0	0	0	1

PIG	Sc_HN	Sc_TK	Sc_LS	TBS	MC_Cal	MC_Cha	MC_Una	MC_BB	MC_HB	MC_HL	MC_D1	MC_Gr	MC_JS	MC_PC	MC_MC	MC_D2	MC_HIF
BP_07	1	1	1	3	0	2	3	0	1	0	0	1	0	1	0	1	1
BP_15	1	1	1	3	0	0	3	0	0	0	0	1	0	0	0	0	0
BP_17	1	1	1	3	0	0	3	0	0	0	0	1	0	0	0	0	0
BP_19	1	1	1	3	0	0	3	0	0	0	0	1	0	0	0	0	0
BP_21	1	1	1	3	0	0	3	0	0	0	0	1	0	0	0	0	0
BP_01	3	3	2	8	0	0	3	0	0	0	0	1	0	0	0	0	0
BP_02	5	3	2	10	0	2	2	0	1	1	1	1	0	1	0	1	1
BP_22	3	4	3	10	0	0	3	0	0	0	0	1	0	0	0	0	0
BP_23	3	4	3	10	0	0	3	0	0	0	0	1	0	0	0	0	0
BP_20	4	4	3	11	0	0	3	0	0	0	0	1	0	0	0	0	0
BP_03	7	6	5	18	0	2	2	0	0	0	0	0	0	0	0	0	0
BP_05	7	6	5	18	0	0	3	0	0	0	0	1	0	0	0	0	0
BP_06	7	6	5	18	0	1	3	0	1	0	0	1	0	0	0	0	1
BP_04	7	6	6	19	0	1	3	0	1	1	1	1	0	1	0	1	1
BP_08	8	7	5	21	0	1	3	0	1	0	0	1	0	1	0	0	1
BP_14	10	8	6	24	2	2	0	0	0	0	0	0	0	0	0	1	1
BP_12	8	9	8	25	1	2	2	0	0	0	0	0	0	0	0	1	1
BP_18	10	9	6	25	0	0	3	0	0	0	0	1	0	0	0	0	0
PIG_029	12	7	8	27	2	2	2	0	0	0	0	1	0	0	0	0	1
PIG_028	11	7	10	28	1	2	2	0	0	0	0	0	0	0	0	1	1
PIG_002	13	10	9	32	1	3	0	0	0	0	0	0	0	0	0	1	1
PIG_003	11	12	10	33	1	3	1	1	0	0	0	0	0	0	0	1	1
PIG_009	13	12	10	35	0	1	3	0	0	0	0	0	0	0	0	1	1
PIG_010	13	12	10	35	1	2	2	1	0	0	0	0	0	0	0	1	1
PIG_011	13	12	10	35	0	3	1	0	0	0	0	0	0	0	0	1	1

PIG	Sc_HN	Sc_TK	Sc_LS	TBS	Fem_Cal	Fem_Cha	Fem_Una	Fem_BB	Fem_HB	Fem_HL	Fem_D1	Fem_Gr	Fem_JS	Fem_PC	Fem_MC	Fem_D2	Fem_HIF
BP_07	1	1	1	3	0	0	3	0	0	0	0	1	0	0	0	0	0
BP_15	1	1	1	3	0	0	3	0	0	0	0	1	0	0	0	0	0
BP_17	1	1	1	3	0	0	3	0	0	0	0	1	0	0	0	0	0
BP_19	1	1	1	3	0	0	3	0	0	0	0	1	0	0	0	0	0
BP_21	1	1	1	3	0	0	3	0	0	0	0	1	0	0	0	0	0
BP_01	3	3	2	8	0	0	3	0	0	0	0	1	0	0	0	0	0
BP_02	5	3	2	10	0	0	3	0	0	0	0	1	0	0	0	0	0
BP_22	3	4	3	10	0	0	3	0	0	0	0	1	0	0	0	0	0
BP_23	3	4	3	10	0	0	3	0	0	0	0	1	0	0	0	0	0
BP_20	4	4	3	11	0	0	3	0	0	0	0	1	0	0	0	0	0
BP_03	7	6	5	18	0	0	3	0	0	0	0	0	0	0	0	0	0
BP_05	7	6	5	18	0	0	3	0	0	0	0	1	0	0	0	0	0
BP_06	7	6	5	18	0	0	3	0	0	0	0	1	0	0	0	0	0
BP_04	7	6	6	19	0	0	3	0	0	0	0	1	0	0	0	0	0
BP_08	8	7	5	21	0	0	3	0	0	0	0	1	0	0	0	0	0
BP_14	10	8	6	24	0	1	3	0	0	0	0	0	0	0	0	1	1
BP_12	8	9	8	25	2	2	3	0	0	0	0	1	0	0	0	1	1
BP_18	10	9	6	25	0	0	3	0	0	0	0	1	0	0	0	0	0
P_029	12	7	8	27	1	2	2	0	0	0	0	1	0	0	0	1	1
P_028	11	7	10	28	3	2	2	0	0	0	0	0	0	0	0	1	1
P_002	13	10	9	32	2	2	3	0	0	0	0	0	0	0	0	1	1
P_003	11	12	10	33	1	3	2	0	0	0	0	0	0	0	0	1	1
P_009	13	12	10	35	1	2	2	0	0	0	0	1	0	0	0	1	1
P_010	13	12	10	35	2	3	1	0	0	0	0	0	0	0	0	1	1
PG_011	13	12	10	35	1	3	2	0	0	0	0	0	0	0	0	1	1

PIG	Sc_HN	Sc_TK	Sc_LS	TBS	Tib_Cal	Tib_Cha	Tib_Una	Tib_BB	Tib_HB	Tib_HL	Tib_D1	Tib_Gr	Tib_JS	Tib_PC	Tib_MC	Tib_D2	Tib_HIF
BP_07	1	1	1	3	0	0	3	0	0	0	0	1	0	0	0	0	0
BP_15	1	1	1	3	0	0	3	0	0	0	0	1	0	0	0	0	0
BP_17	1	1	1	3	0	0	3	0	0	0	0	1	0	0	0	0	0
BP_19	1	1	1	3	0	0	3	0	0	0	0	1	0	0	0	0	0
BP_21	1	1	1	3	0	0	3	0	0	0	0	1	0	0	0	0	0
BP_01	3	3	2	8	0	0	3	0	0	0	0	1	0	0	0	0	0
BP_02	5	3	2	10	0	0	3	0	0	0	0	1	0	0	0	0	0
BP_22	3	4	3	10	0	0	3	0	0	0	0	1	0	0	0	0	0
BP_23	3	4	3	10	0	0	3	0	0	0	0	1	0	0	0	0	0
BP_20	4	4	3	11	0	0	3	0	0	0	0	1	0	0	0	0	0
BP_03	7	6	5	18	0	1	3	0	1	1	1	1	0	0	0	1	1
BP_05	7	6	5	18	0	0	3	0	0	0	0	1	0	0	0	0	0
BP_06	7	6	5	18	0	1	3	0	1	1	1	1	0	1	0	1	0
BP_04	7	6	6	19	0	0	3	0	0	0	0	1	0	0	0	0	0
BP_08	8	7	5	21	0	1	3	0	0	0	0	1	0	0	0	0	0
BP_14	10	8	6	24	1	3	3	0	0	0	0	0	0	0	0	1	1
BP_12	8	9	8	25	1	1	3	0	0	0	0	1	0	0	0	1	1
BP_18	10	9	6	25	0	1	3	0	0	0	0	1	0	0	0	0	0
PIG_029	12	7	8	27	1	3	1	0	0	0	0	1	1	0	0	0	1
PIG_028	11	7	10	28	3	1	0	0	0	0	0	0	0	0	0	1	1
PIG_002	13	10	9	32	3	3	1	0	0	0	0	0	0	0	0	1	1
PIG_003	11	12	10	33	2	3	0	0	0	0	0	0	0	0	0	1	1
PIG_009	13	12	10	35	1	1	3	0	0	0	0	0	0	0	0	1	1
PIG_010	13	12	10	35	1	2	3	1	0	0	0	0	0	0	0	0	1
PIG_011	13	12	10	35	1	3	1	1	0	0	0	0	0	0	0	1	1

PIG	Sc_HN	Sc_TK	Sc_LS	TBS	Fib_Cal	Fib_Cha	Fib_Una	Fib_BB	Fib_HB	Fib_HL	Fib_D1	Fib_Gr	Fib_JS	Fib_PC	Fib_MC	Fib_D2	Fib_HIF
BP_07	1	1	1	3	0	0	3	0	0	0	0	1	0	0	0	0	0
BP_15	1	1	1	3	0	0	3	0	0	0	0	1	0	0	0	0	0
BP_17	1	1	1	3	0	0	3	0	0	0	0	1	0	0	0	0	0
BP_19	1	1	1	3	0	0	3	0	0	0	0	1	0	0	0	0	0
BP_21	1	1	1	3	0	0	3	0	0	0	0	1	0	0	0	0	0
BP_01	3	3	2	8	0	0	3	0	0	0	0	1	0	0	0	0	0
BP_02	5	3	2	10	0	0	3	0	0	0	0	1	0	0	0	0	0
BP_22	3	4	3	10	0	0	3	0	0	0	0	1	0	0	0	0	0
BP_23	3	4	3	10	0	0	3	0	0	0	0	1	0	0	0	0	0
BP_20	4	4	3	11	0	0	3	0	0	0	0	1	0	0	0	0	0
BP_03	7	6	5	18	0	0	3	0	0	0	0	0	0	0	0	0	0
BP_05	7	6	5	18	0	0	3	0	0	0	0	1	0	0	0	0	0
BP_06	7	6	5	18	0	0	3	0	0	0	0	1	0	0	0	0	0
BP_04	7	6	6	19	0	0	3	0	0	0	0	1	0	0	0	0	0
BP_08	8	7	5	21	0	0	3	0	0	0	0	1	0	0	0	0	0
BP_14	10	8	6	24	0	3	2	0	0	0	0	0	0	0	0	1	1
BP_12	8	9	8	25	0	3	3	0	0	0	0	1	0	0	0	1	1
BP_18	10	9	6	25	0	0	3	0	0	0	0	1	0	0	0	0	0
PIG_029	12	7	8	27	1	3	1	0	0	0	0	1	0	0	0	0	1
PIG_028	11	7	10	28	2	2	0	0	0	0	0	0	0	0	0	1	1
PIG_002	13	10	9	32	2	2	0	0	0	0	0	0	0	0	0	0	1
PIG_003	11	12	10	33	0	3	1	0	0	0	0	0	0	0	0	0	1
PIG_009	13	12	10	35	0	1	3	0	0	0	0	0	0	0	0	1	1
PIG_010	13	12	10	35	1	3	1	0	0	0	0	0	0	0	0	0	1
PIG_011	13	12	10	35	0	3	0	0	0	0	0	0	0	0	0	0	1

PIG	Sc_HN	Sc_TK	Sc_LS	TBS	MT_Cal	MT_Cha	MT_Una	MT_BB	MT_HB	MT_HL	MT_D1	MT_Gr	MT_JS	MT_PC	MT_MC	MT_D2	MT_HIF
BP_07	1	1	1	3	0	0	3	0	0	0	0	1	0	0	0	0	0
BP_15	1	1	1	3	0	0	3	0	0	0	0	1	0	0	0	0	0
BP_17	1	1	1	3	0	0	3	0	0	0	0	1	0	0	0	0	0
BP_19	1	1	1	3	0	0	3	0	0	0	0	1	0	0	0	0	0
BP_21	1	1	1	3	0	0	3	0	0	0	0	1	0	0	0	0	0
BP_01	3	3	2	8	0	0	3	0	0	0	0	1	0	0	0	0	0
BP_02	5	3	2	10	0	1	3	0	1	0	0	1	0	1	0	1	1
BP_22	3	4	3	10	0	0	3	0	0	0	0	1	0	0	0	0	0
BP_23	3	4	3	10	0	0	3	0	0	0	0	1	0	0	0	0	0
BP_20	4	4	3	11	0	0	3	0	0	0	0	1	0	0	0	0	0
BP_03	7	6	5	18	0	0	3	0	0	0	0	0	0	0	0	0	0
BP_05	7	6	5	18	0	2	2	0	0	0	0	1	0	0	0	1	1
BP_06	7	6	5	18	1	2	2	0	0	0	0	1	0	0	0	1	1
BP_04	7	6	6	19	0	1	3	0	1	1	1	1	0	1	0	1	1
BP_08	8	7	5	21	0	2	2	0	1	1	1	1	0	1	0	1	1
BP_14	10	8	6	24	0	3	1	0	0	0	0	0	0	0	0	1	1
BP_12	8	9	8	25	1	1	3	0	0	0	0	1	0	0	0	1	1
BP_18	10	9	6	25	0	0	3	0	0	0	0	1	0	0	0	0	0
PIG_029	12	7	8	27	1	2	2	1	0	0	0	0	0	0	0	0	1
PIG_028	11	7	10	28	1	2	2	0	0	0	0	0	0	0	0	1	1
PIG_002	13	10	9	32	1	2	2	1	0	0	0	0	0	0	0	0	1
PIG_003	11	12	10	33	0	1	3	1	0	0	0	0	0	0	0	0	1
PIG_009	13	12	10	35	0	1	3	0	0	0	0	0	0	0	0	0	1
PIG_010	13	12	10	35	0	1	3	1	0	0	0	0	0	0	0	0	0
PIG_011	13	12	10	35	1	1	3	1	0	0	0	0	0	0	0	1	1

APPENDIX C: Codes in R

For one variable: (glm, transition analysis)

```
pigdata <- read.csv(file.choose(), header = T)

attach(pigdata)

head(pigdata)

ordered(pigdata$Ordinal_Tag)

ordered(pigdata$Cr_Cal)

library(VGAM)

fit.Cr_Cal  <- vglm(Cr_Cal ~ Ordinal_Tag, cratio(parallel=F), pigdata)

summary(fit.Cr_Cal)
```

Repeat the above code substituting each instance of Cr_Cal above with the respective variables that follow.

For the binary variables:

Replace

```
fit.Cr_BB  <- vglm(Cr_Cal ~ Ordinal_Tag, cratio(parallel=F), pigdata)
```

with

```
fit.Cr_BB  <- glm(Cr_BB ~ Ordinal_Tag, binomial, pigdata)
```

Density plots:

```
library(XLConnect)
library(sm)
library(reshape2)
library(sqldf)
setwd("C:/Documents and Settings/User/Desktop/PhD")
Odata <- read.table("C:/Documents and
Settings/User/Desktop/PhD/Pig_Data1.csv",header=TRUE,sep=",")

#template
data <- Odata[, c(6,)]
data
melt <- melt(data, id.vars=c("TBS"), variable.name="color", value.name="score")
melt
#2's are a problem
melt <- sqldf("SELECT * FROM melt WHERE score != ")
pdf(".pdf")
sm.density.compare(melt$TBS, melt$score, xlab="TBS", lty=c(1,2,3,4), col=c("black",
"black", "black", "black"))
legend("topright", legend=c("0", "1", "2", "3"), col=c("black", "black", "black", "black"),
lty=c(1, 2, 3, 4), cex=.75, bty="n")
dev.off()
```

APPENDIX D: FREQUENCY DISTRIBUTIONS

Table D1 Frequency distribution for the amount of brown burn/border scored in the head and neck (HN_BB)

Number of strata	= 1	Number of obs	= 75
Number of PSUs	= 25	Population size	= 75
		Design df	= 24

	Stage of decomposition				
HN_BB	**1**	**2**	**3**	**4**	**5**
0	100	100	80	80	87
1	0	0	60	20	13
Total	100	100	100	100	100

Key: column proportions

Pearson:				
Uncorrected chi2(12)	=	6.4366		
Design-based F(6.54, 156.90)	=	0.8161	p =	0.5062

Table D2 Frequency distribution for the amount of heat borders scored in the head and neck (HN_HB)

Number of strata	= 1	Number of obs	= 75
Number of PSUs	= 25	Population size	= 75
		Design df	= 24

	Stage of decomposition				
HN_HB	**1**	**2**	**3**	**4**	**5**
0	100	100	73	93	100
1	0	0	27	7	0
Total	100	100	100	100	100

Key: column proportions

Pearson:				
Uncorrected chi2(12)	=	12.8571		
Design-based F(6.54, 156.90)	=	1.4566	p =	0.2293

Table D3 Frequency distribution for the amount of heat lines scored in the head and neck (HN_HL)

Number of strata	= 1	Number of obs	= 75
Number of PSUs	= 25	Population size	= 75
		Design df	= 24

	Stage of decomposition				
HN_HL	**1**	**2**	**3**	**4**	**5**
0	100	100	93	100	100
1	0	0	7	0	0
Total	100	100	100	100	100

Key: column proportions

Pearson:				
Uncorrected chi2(12)	=	4.0541		
Design-based F(6.54, 156.90)	=	0.3950	p =	0.7868

Table D4 Frequency distribution for the amount of delineation scored in the head and neck (HN_D1)

Number of strata	= 1	Number of obs	= 75
Number of PSUs	= 25	Population size	= 75
		Design df	= 24

	Stage of decomposition				
HN_D1	**1**	**2**	**3**	**4**	**5**
0	100	100	93	100	100
1	0	0	7	0	0
Total	100	100	100	100	100

Key: column proportions

Pearson:				
Uncorrected chi2(12)	=	4.0541		
Design-based F(6.54, 156.90)	=	0.3950	p =	0.7868

Table D5 Frequency distribution for the amount of joint shielding scored in the head and neck (HN_JS)

Number of strata	= 1	Number of obs	= 75
Number of PSUs	= 25	Population size	= 75
		Design df	= 24

	Stage of decomposition				
HN_JS	**1**	**2**	**3**	**4**	**5**
0	100	100	93	100	100
1	0	0	7	0	0
Total	100	100	100	100	100

Key: column proportions

Pearson:				
Uncorrected chi2(12)	=	4.0541		
Design-based F(6.54, 156.90)	=	0.3950	p =	0.7868

Table D6 Frequency distribution for the amount of predictable cracking scored in the head and neck (HN_PC)

Number of strata	= 1	Number of obs	= 75
Number of PSUs	= 25	Population size	= 75
		Design df	= 24

	Stage of decomposition				
HN_PC	**1**	**2**	**3**	**4**	**5**
0	100	100	93	100	100
1	0	0	7	0	0
Total	100	100	100	100	100

Key: column proportions

Pearson:				
Uncorrected chi2(12)	=	4.0541		
Design-based F(6.54, 156.90)	=	0.3950	p =	0.7868

Table D7 Frequency distribution for the amount of minimal cracking scored in the head and neck (HN_MC)

Number of strata	= 1	Number of obs	= 75
Number of PSUs	= 25	Population size	= 75
		Design df	= 24

	Stage of decomposition				
HN_MC	**1**	**2**	**3**	**4**	**5**
0	100	100	87	100	100
1	0	0	13	0	0
Total	100	100	100	100	100

Key: column proportions

Pearson:				
Uncorrected chi2(12)	=	8.2192		
Design-based F(6.54, 156.90)	=	0.7298	p =	0.5692

Table D8 Frequency distribution for the amount of brown burn/border scored in the trunk (T_BB)

Number of strata	= 1	Number of obs	= 75
Number of PSUs	= 25	Population size	= 75
		Design df	= 24

	Stage of decomposition				
T_BB	**1**	**2**	**3**	**4**	**5**
0	100	96	96	88	96
1	0	4	4	12	4
Total	100	100	100	100	100

Key: column proportions

Pearson:				
Uncorrected chi2(12)	=	4.2017		
Design-based F(6.54, 156.90)	=	1.1330	p =	0.3448

Table D9 Frequency distribution for the amount of heat borders scored in the trunk (T_HB)

Number of strata	= 1	Number of obs	= 75
Number of PSUs	= 25	Population size	= 75
		Design df	= 24

	Stage of decomposition				
T_HB	**1**	**2**	**3**	**4**	**5**
0	100	100	96	96	100
1	0	0	4	4	0
Total	100	100	100	100	100

Key: column proportions

Pearson:				
Uncorrected chi2(12)	=	3.0488		
Design-based F(6.54, 156.90)	=	0.2502	p =	0.8382

Table D10 Frequency distribution for the amount of predictable cracking scored in the trunk (T_PC)

Number of strata	= 1	Number of obs	= 75
Number of PSUs	= 25	Population size	= 75
		Design df	= 24

	Stage of decomposition				
T_PC	**1**	**2**	**3**	**4**	**5**
0	100	100	92	100	100
1	0	0	8	0	0
Total	100	100	100	100	100

Key: column proportions

Pearson:				
Uncorrected chi2(12)	=	8.1301		
Design-based F(6.54, 156.90)	=	0.4666	p =	0.7399

Table D11 Frequency distribution for the amount of minimal cracking scored in the trunk (T_MC)

Number of strata	= 1	Number of obs	= 75
Number of PSUs	= 25	Population size	= 75
		Design df	= 24

	Stage of decomposition				
T_MC	**1**	**2**	**3**	**4**	**5**
0	100	100	100	96	100
1	0	0	0	4	0
Total	100	100	100	100	100

Key: column proportions

Pearson:				
Uncorrected chi2(12)	=	4.0323		
Design-based F(6.54, 156.90)	=	0.2445	p =	0.8824

Table D12 Frequency distribution for the amount of heat borders scored in the limbs (L_HB)

Number of strata	= 1	Number of obs	= 75
Number of PSUs	= 25	Population size	= 75
		Design df	= 24

	Stage of decomposition				
L_HB	**1**	**2**	**3**	**4**	**5**
0	95	95	75	100	100
1	5	5	25	0	0
Total	100	100	100	100	100

Key: column proportions

Pearson:				
Uncorrected chi2(12)	=	26.4209		
Design-based F(2.36, 56.70)	=	1.9338	p =	0.1468

Table D13 Frequency distribution for the amount of heat lines scored in the limbs (L_HL)

Number of strata	= 1	Number of obs	= 75
Number of PSUs	= 25	Population size	= 75
		Design df	= 24

	Stage of decomposition				
L_HL	**1**	**2**	**3**	**4**	**5**
0					
1					
Total	100	100	100	100	100

Key: column proportions

Pearson:				
Uncorrected chi2(12)	=	20.1332		
Design-based F(2.37, 56.88)	=	1.1048	p =	0.3458

Table D14 Frequency distribution for the amount of delineation scored in the limbs

Number of strata	= 1	Number of obs	= 75
Number of PSUs	= 25	Population size	= 75
		Design df	= 24

	Stage of decomposition				
L_HB	**1**	**2**	**3**	**4**	**5**
0	100	97.5	85	100	100
1	0	2.5	15	0	0
Total	100	100	100	100	100

Key: column proportions

Pearson:				
Uncorrected chi2(12)	=	20.1332		
Design-based F(2.37, 56.88)	=	1.1048	p =	0.3458

Table D15 Frequency distribution for the amount of joint shielding scored in the limbs (L_JS)

Number of strata	= 1	Number of obs	= 75
Number of PSUs	= 25	Population size	= 75
		Design df	= 24

	Stage of decomposition				
L_JS	**1**	**2**	**3**	**4**	**5**
0	100	100	100	97.5	100
1	0	0	0	2.5	0
Total	100	100	100	100	100

Key: column proportions

Pearson:				
Uncorrected chi2(12)	=	4.0201		
Design-based F(3.20, 76.76)	=	0.1555	p =	0.9346

APPENDIX E: KERNEL DENSITY PLOTS

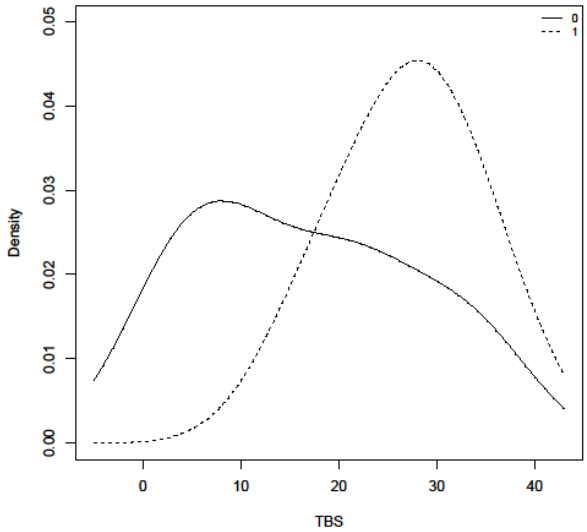

Figure E.1: Kernel density estimates for brown burn/border based on the binary scores (0,1) in the cranium [TBS = total body score]

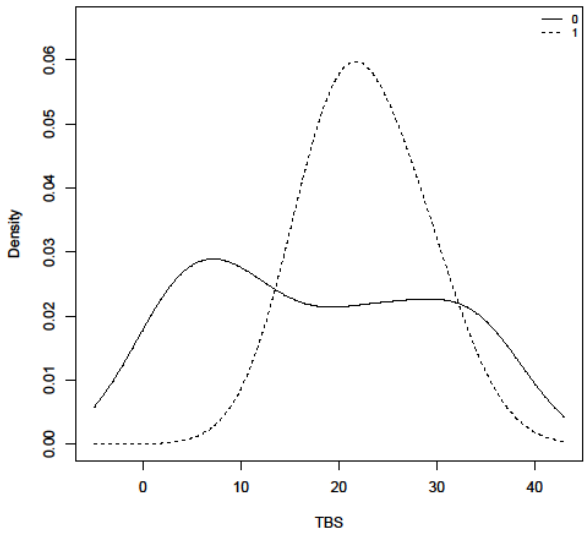

Figure E.2: Kernel density estimates for heat border based on the binary scores (0,1) in the cranium [TBS = total body score]

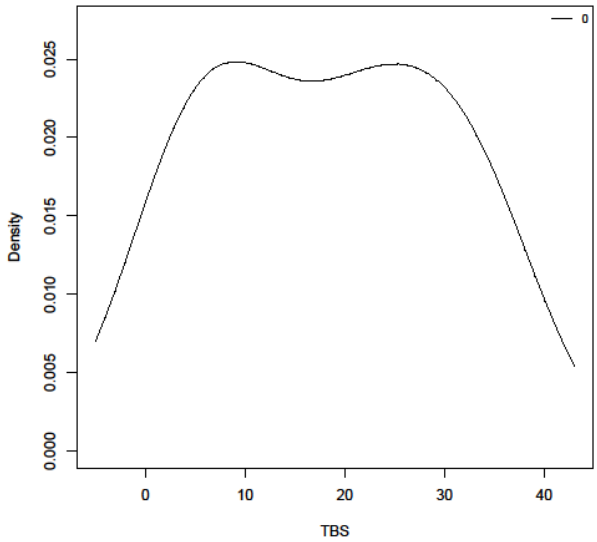

Figure E.3: Kernel density estimates for heat line, delineation, joint shielding, minimal and predictable cracking based on the binary scores (0,1) in the cranium [TBS = total body score]

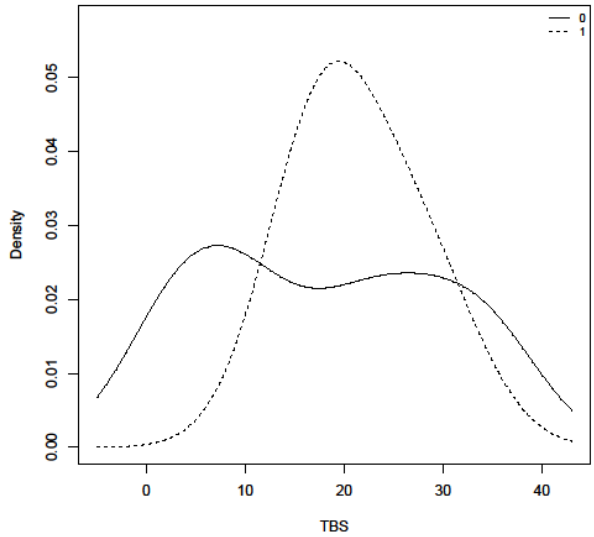

Figure E.4: Kernel density estimates for brown burn/border based on the binary scores (0,1) in the mandible [TBS = total body score]

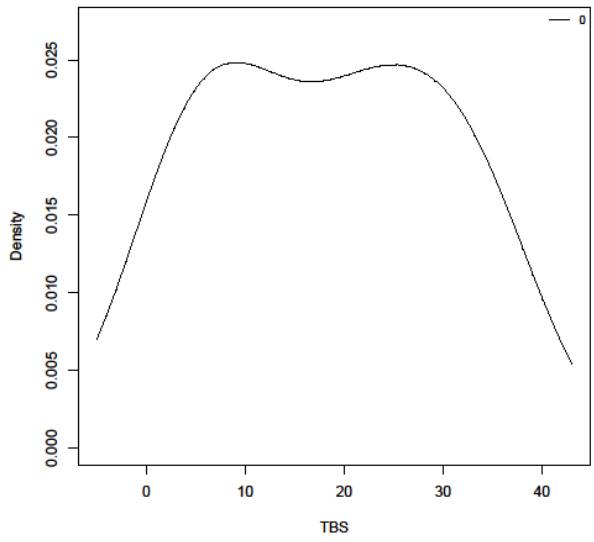

Figure E.5: Kernel density estimates for heat border, heat line, delineation, joint shielding, predictable and minimal cracking based on the binary scores (0,1) in the mandible [TBS = total body score]

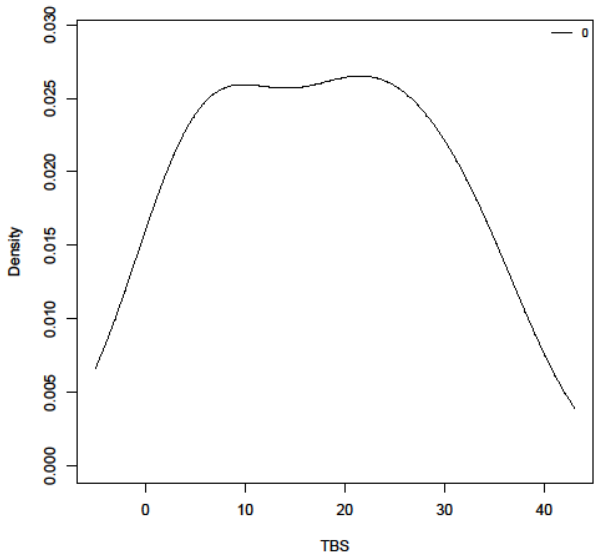

Figure E.6: Kernel density estimates for brown burn/border, heat line, delineation, joint shielding and predictable cracking on the cervical vertebrae based on the binary scores (0,1) in the mandible [TBS = total body score]

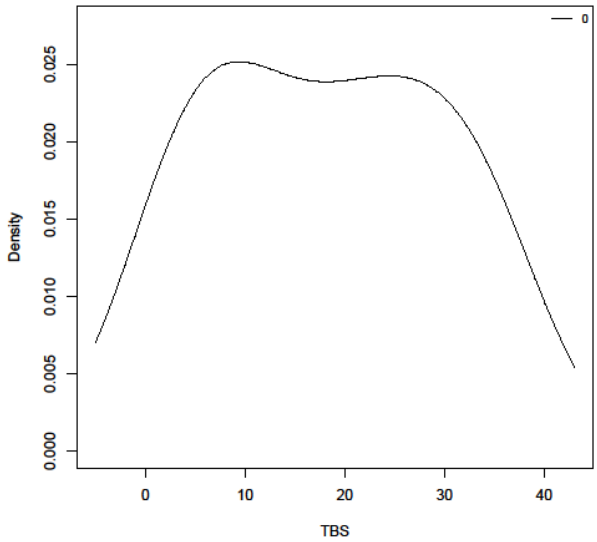

Figure E.7: Kernel density estimates for heat border and minimal cracking on the cervical vertebrae [TBS = Total Body Score; 0 = absent; 1 = present]

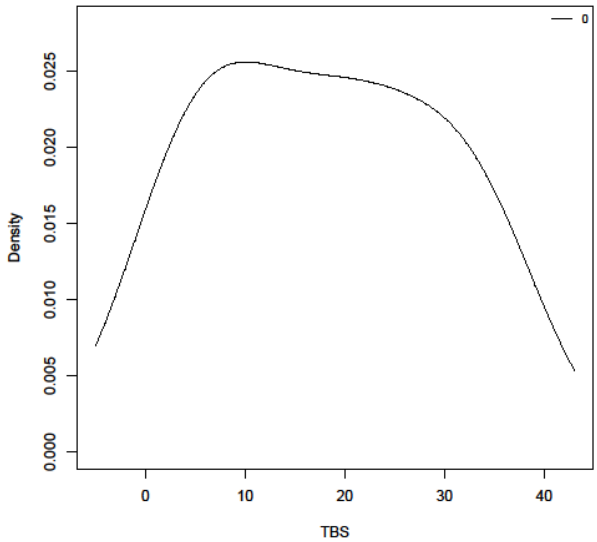

Figure E.8: Kernel density estimates for brown burn/border on the ribs [TBS = Total Body Score; 0 = absent; 1 = present]

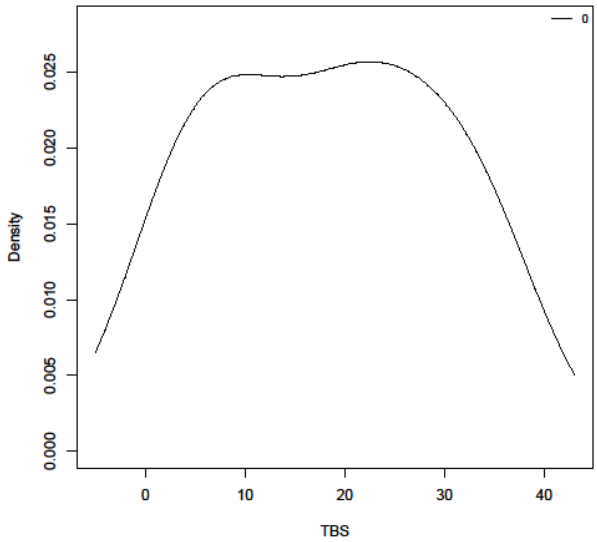

Figure E.9: Kernel density estimates for heat border, heat line, delineation, joint shielding, and minimal cracking on the ribs [TBS = Total Body Score; 0 = absent; 1 = present]

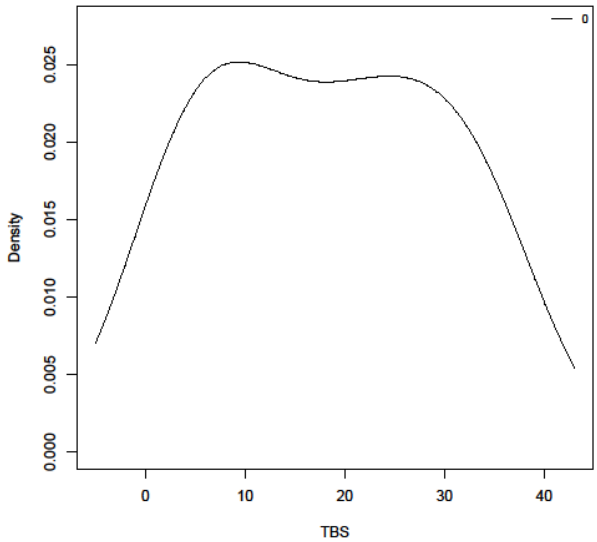

Figure E.10: Kernel density estimates for predictable cracking on the ribs [TBS = Total Body Score; 0 = absent; 1 = present]

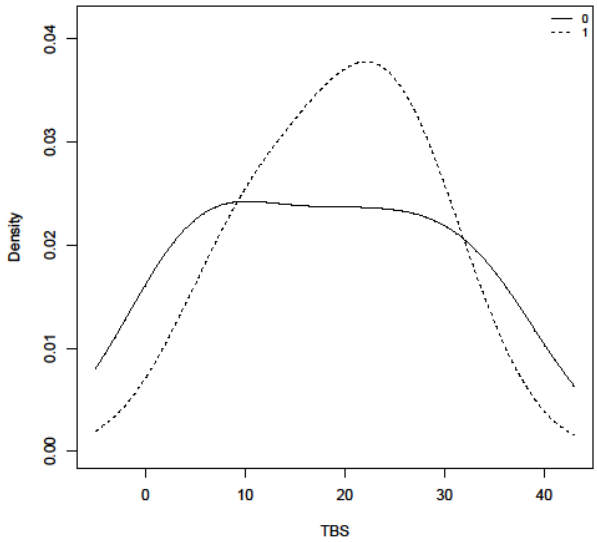

Figure E.11: Kernel density estimates for brown burn/border on the scapula [TBS = Total Body Score; 0 = absent; 1 = present]

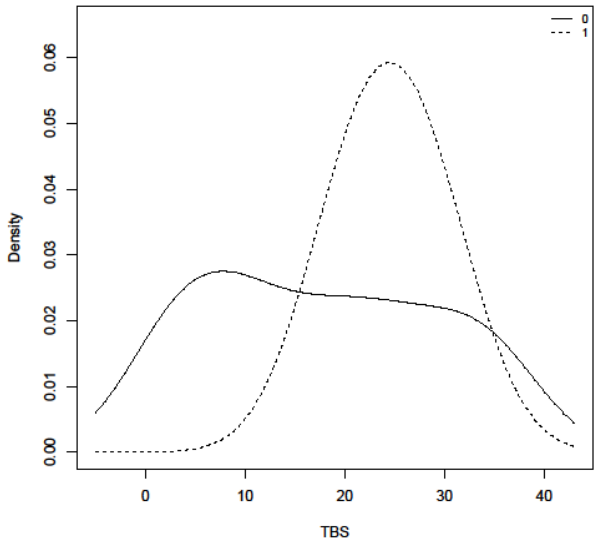

Figure E.12: Kernel density estimates for heat border on the scapula [TBS = Total Body Score; 0 = absent; 1 = present]

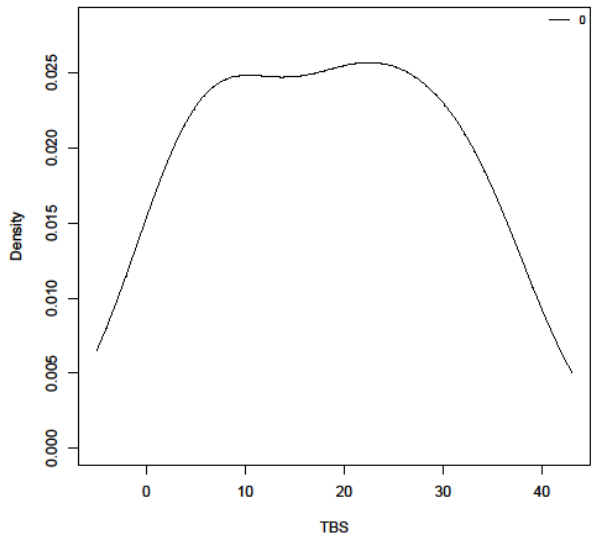

Figure E.13: Kernel density estimates for heat line, delineation and joint shielding on the scapula [TBS = Total Body Score; 0 = absent; 1 = present]

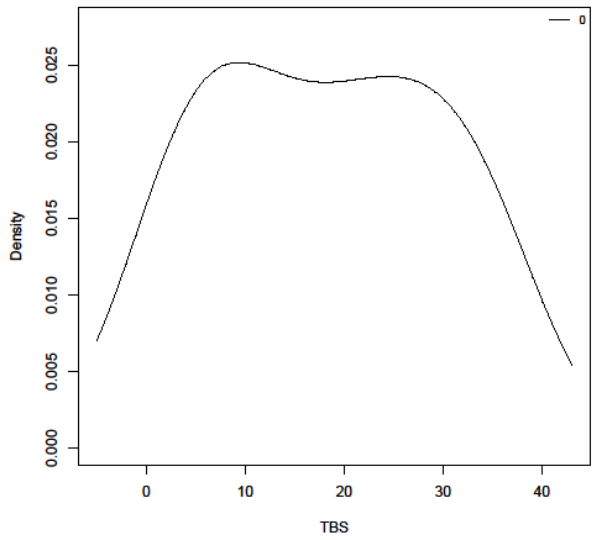

Figure E.14: Kernel density estimates for predictable cracking on the scapula [TBS = Total Body Score; 0 = absent; 1 = present]

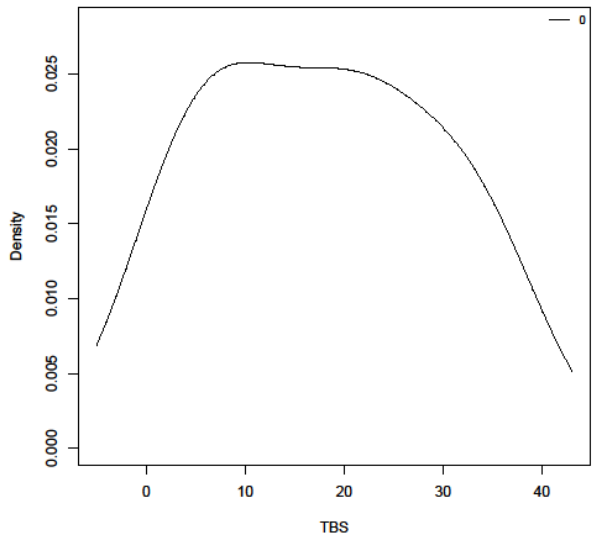

Figure E.15: Kernel density estimates for minimal cracking on the scapula [TBS = Total Body Score; 0 = absent; 1 = present]

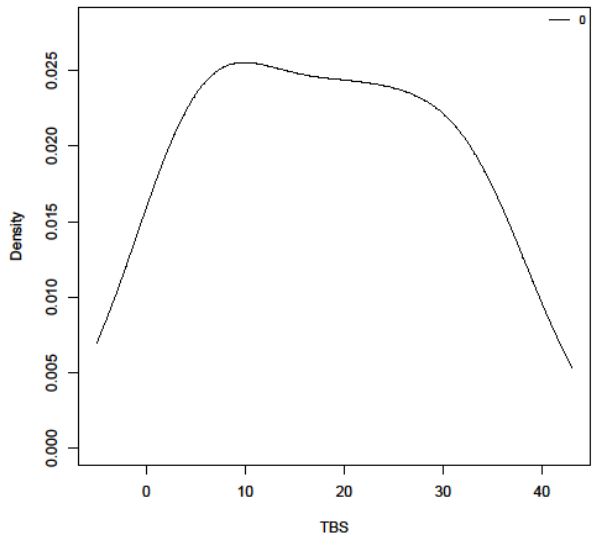

Figure E.16: Kernel density estimates for brown burn/border on the os coxa [TBS = Total Body Score; 0 = absent; 1 = present]

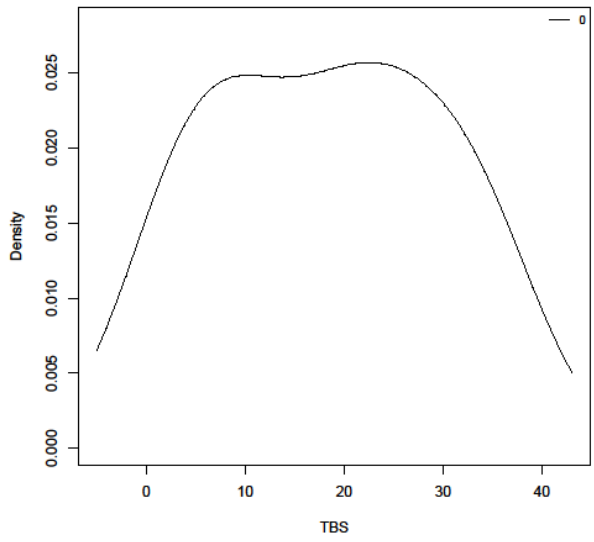

Figure E.17: Kernel density estimates for heat border, heat line, delineation, joint shielding, predictable and minimal cracking on the os coxa [TBS = Total Body Score; 0 = absent; 1 = present]

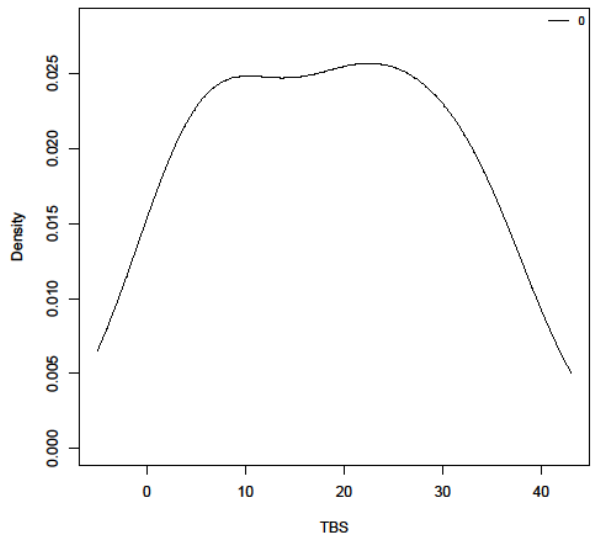

Figure E.18: Kernel density estimates for brown burn/border, heat border, heat line, delineation, joint shielding, predictable and minimal cracking on the thoracic vertebrae [TBS = Total Body Score; 0 = absent; 1 = present]

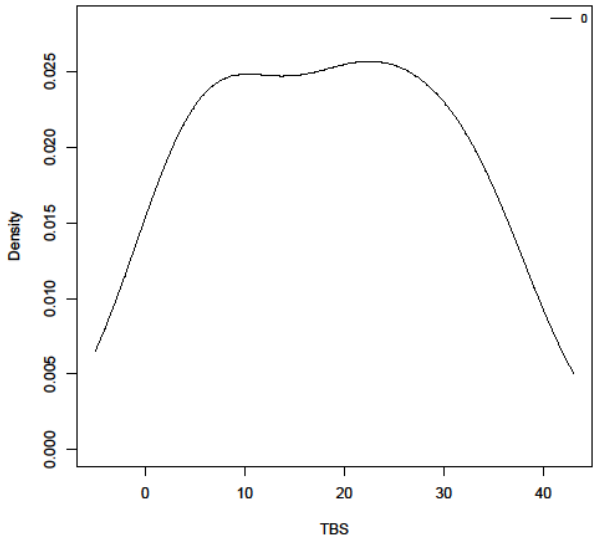

Figure E.19: Kernel density estimates for brown burn/border, heat border, heat line, delineation, joint shielding, predictable and minimal cracking on the lumbar vertebrae [TBS = Total Body Score; 0 = absent; 1 = present]

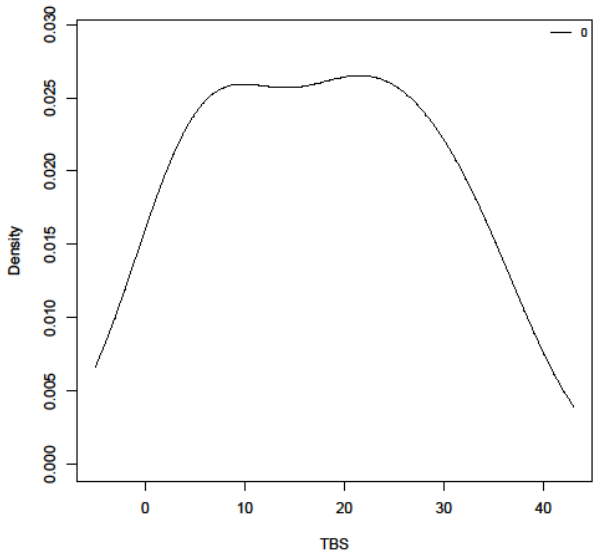

Figure E.20: Kernel density estimates for brown burn/border on the humerus [TBS = Total Body Score; 0 = absent; 1 = present]

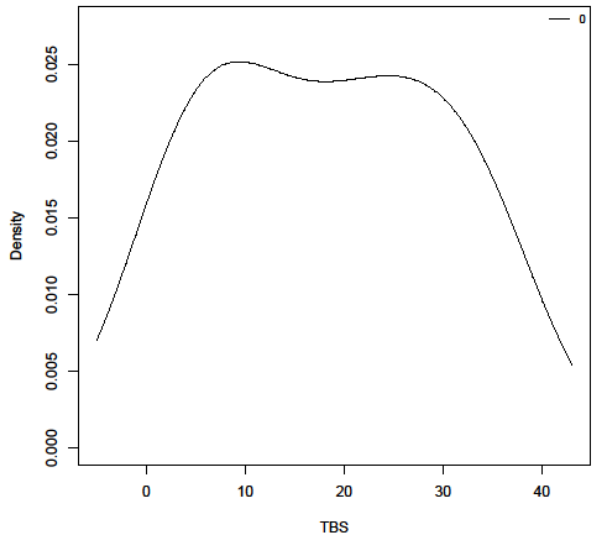

Figure E.21: Kernel density estimates for heat border and predictable cracking on the humerus [TBS = Total Body Score; 0 = absent; 1 = present]

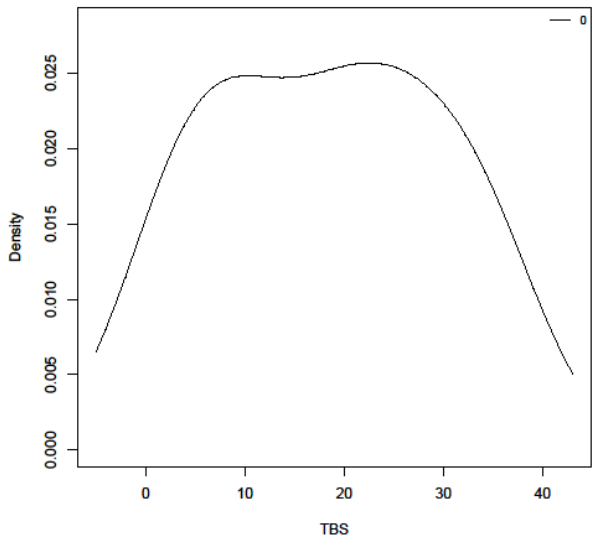

Figure E.22: Kernel density estimates for heat line, delineation, joint shielding and minimal cracking on the humerus [TBS = Total Body Score; 0 = absent; 1 = present]

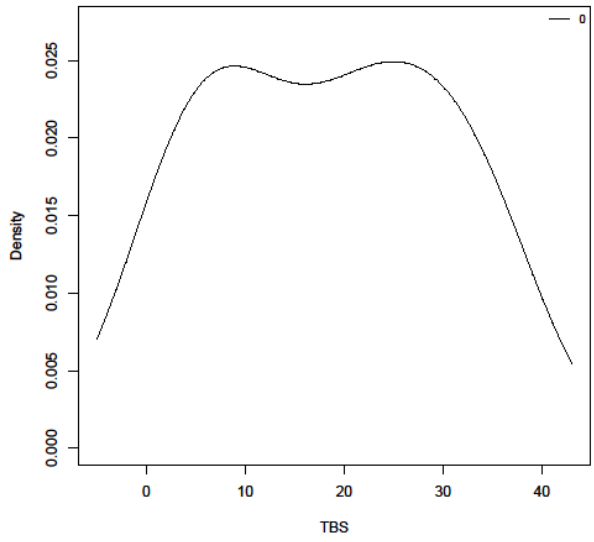

Figure E.23: Kernel density estimates for heat border, heat line, delineation, joint shielding, predictable and minimal cracking on the ulna [TBS = Total Body Score; 0 = absent; 1 = present]

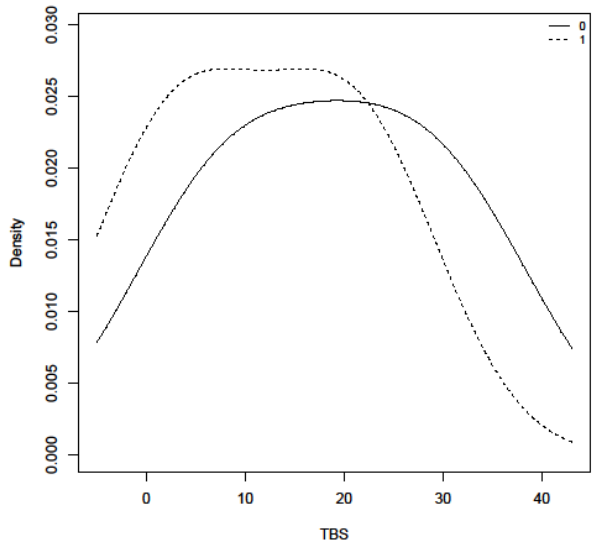

Figure E.24: Kernel density estimates for heat border on the radius [TBS = Total Body Score; 0 = absent; 1 = present]

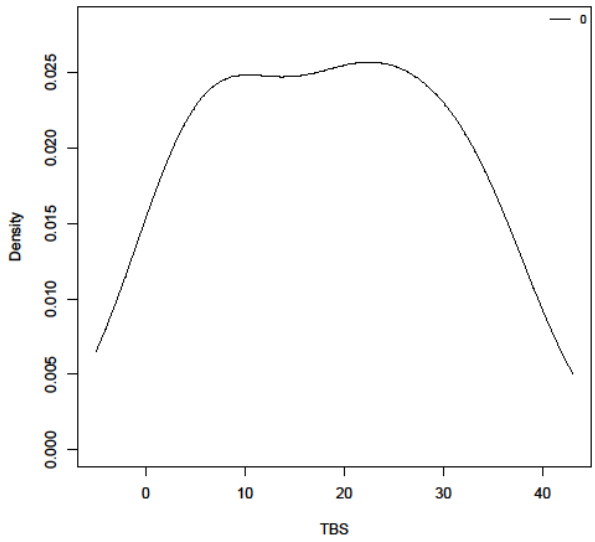

Figure E.25: Kernel density estimates for heat line, delineation, joint shielding, predictable and minimal cracking on the radius [TBS = Total Body Score; 0 = absent; 1 = present]

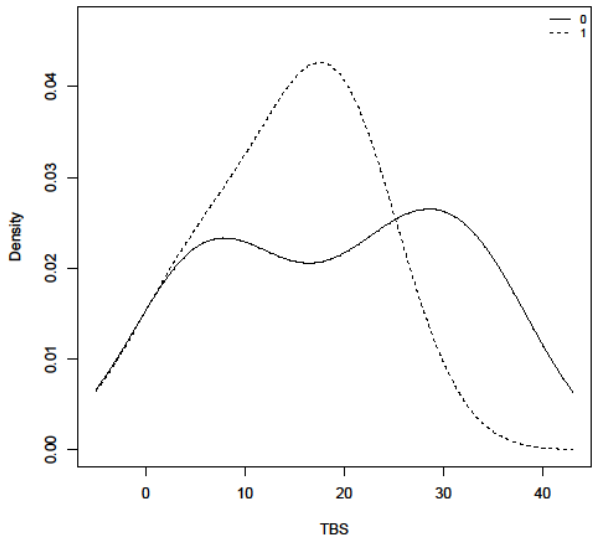

Figure E.26: Kernel density estimates for heat border on the metacarpals [TBS = Total Body Score; 0 = absent; 1 = present]

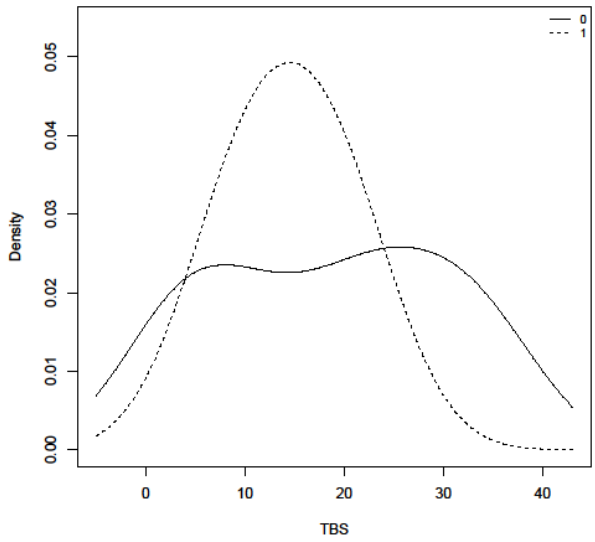

Figure E.27: Kernel density estimates for heat line and delineation on the metacarpals [TBS = Total Body Score; 0 = absent; 1 = present]

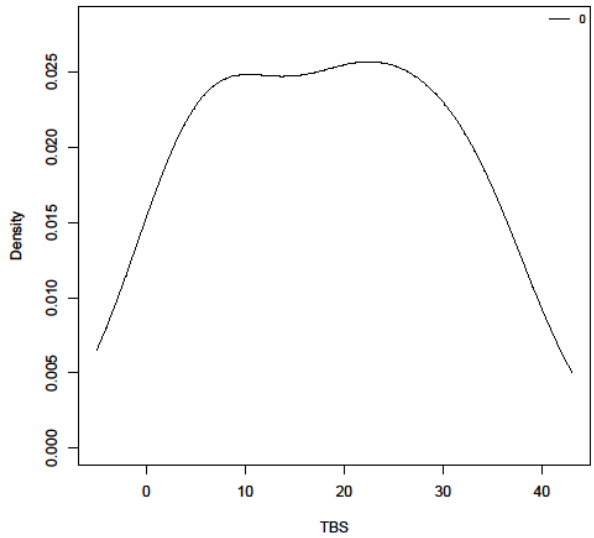

Figure E.28: Kernel density estimates for joint shielding and minimal cracking on the metacarpals [TBS = Total Body Score; 0 = absent; 1 = present]

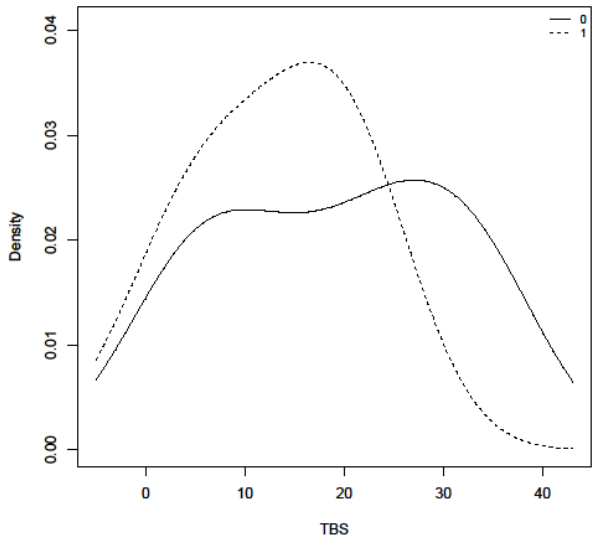

Figure E.29: Kernel density estimates for predictable cracking on the metacarpals [TBS = Total Body Score; 0 = absent; 1 = present]

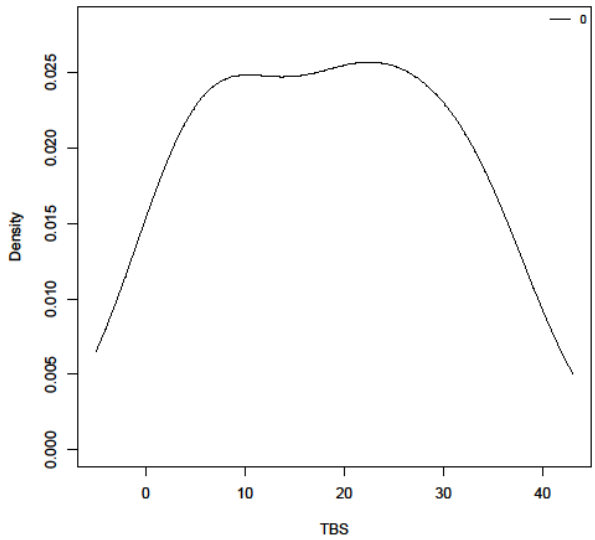

Figure E.30: Kernel density estimates for brown burn/border, heat border, heat line, delineation, joint shielding, predictable and minimal cracking on the femur [TBS = Total Body Score; 0 = absent; 1 = present]

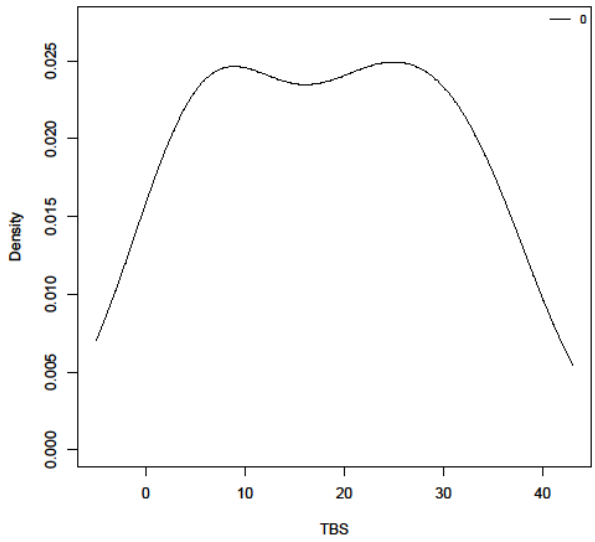

Figure E.31: Kernel density estimates for heat border, heat line, delineation and predictable cracking on the tibia [TBS = Total Body Score; 0 = absent; 1 = present]

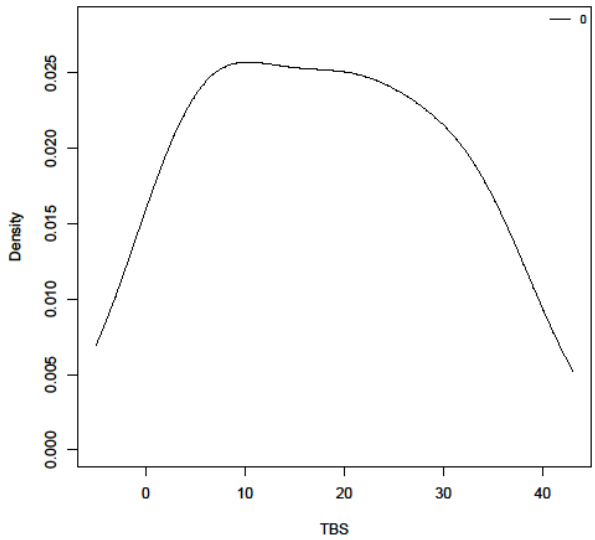

Figure E.32: Kernel density estimates for joint shielding on the tibia [TBS = Total Body Score; 0 = absent; 1 = present]

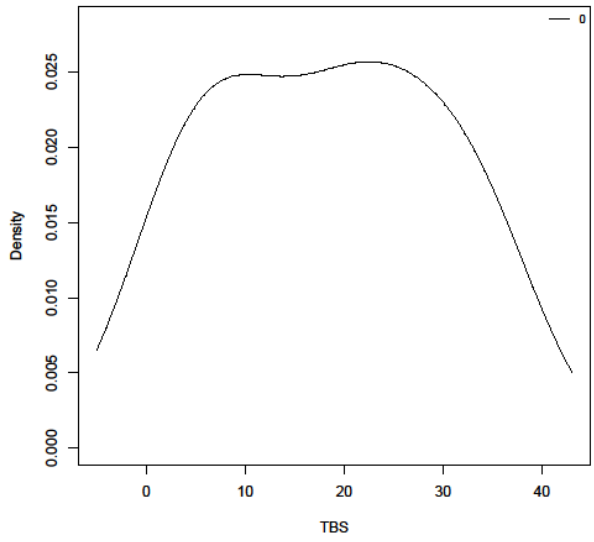

Figure E.33: Kernel density estimates for minimal cracking on the tibia [TBS = Total Body Score; 0 = absent; 1 = present]

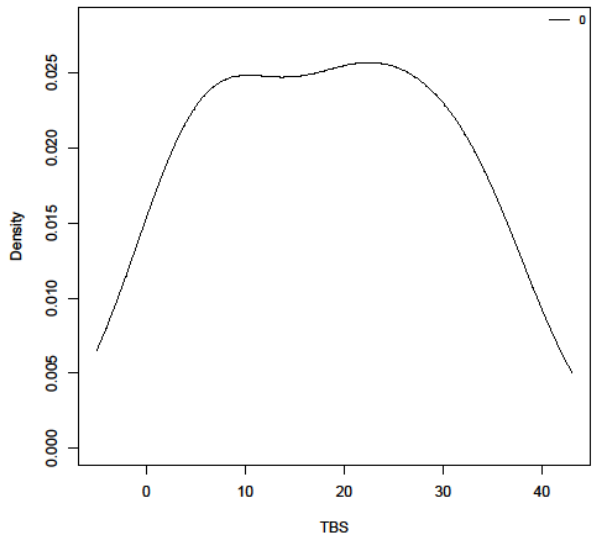

Figure E.34: Kernel density estimates for brown burn/border, heat border, heat line, delineation, joint shielding, predictable and minimal cracking on the fibula [TBS = Total Body Score; 0 = absent; 1 = present]

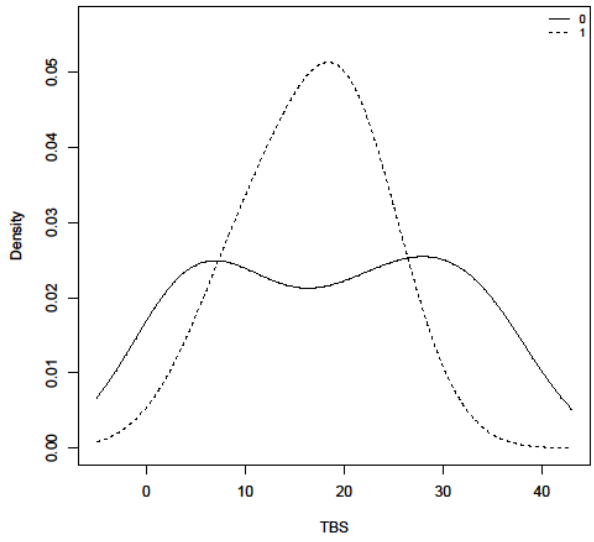

Figure E.35: Kernel density estimates for heat border on the metatarsals [TBS = Total Body Score; 0 = absent; 1 = present]

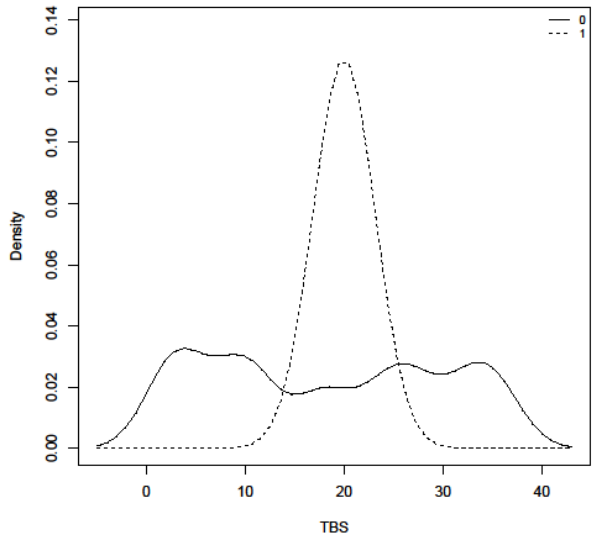

Figure E.36: Kernel density estimates for heat line and delineation on the metatarsals [TBS = Total Body Score; 0 = absent; 1 = present]

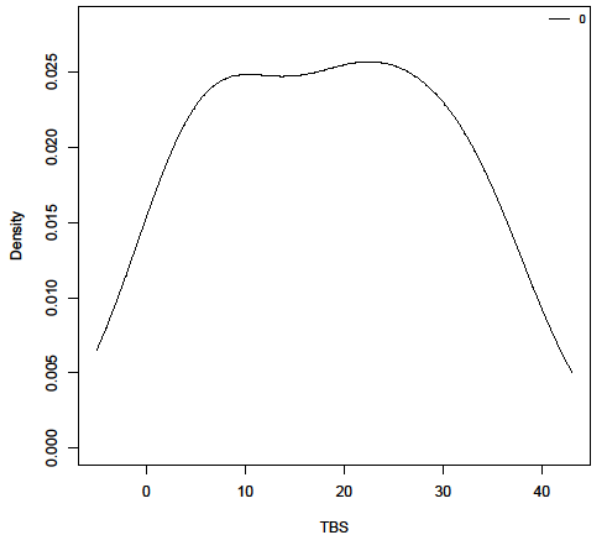

Figure E.37: Kernel density estimates for joint shielding and minimal cracking on the metatarsals [TBS = Total Body Score; 0 = absent; 1 = present]

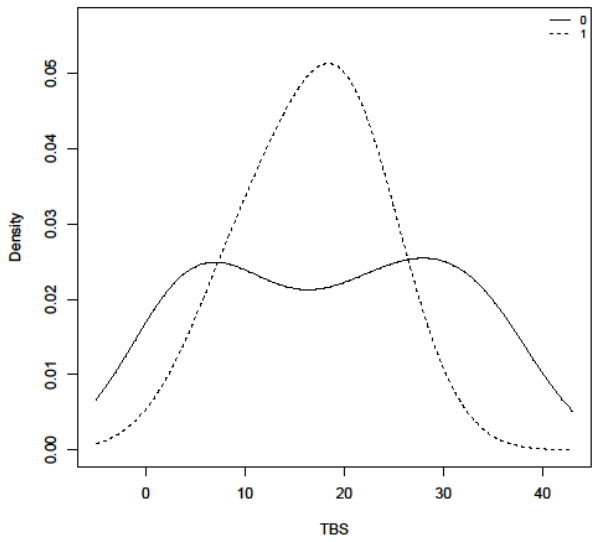

Figure E.38: Kernel density estimates for predictable cracking on the metatarsals [TBS = Total Body Score; 0 = absent; 1 = present]

APPENDIX F: MULTIPLE REGRESSION

Table F1 Results of the multiple regression analysis for categorical variables for the cranium

Source	SS	df	MS		
Model	2782.97333	7	397.567619	Number of obs =	25
Residual	294.066667	17	17.2980392	F(7, 17) =	22.98
Total	3077.04	24	128.21	Prob > F =	0.0000
				R-squared =	0.9044
				Adj R-squared =	0.8651
				Root MSE =	4.1591

tbs	Coef.	Std. Err.	t	P>|t|	[95% Conf.	Interval]
cr_cal						
1	8.333333	3.796713	2.19	0.042	.3229682	16.3437
2	13.33333	6.353117	2.10	0.051	-.0705712	26.73724
3	16	4.362092	3.67	0.002	6.796791	25.20321
cr_cha						
1	11.6	3.221618	3.60	0.002	4.80298	18.39702
2	7.766667	7.000794	1.11	0.283	-7.003717	22.53705
cr_una						
1	.5	3.221618	0.16	0.878	-6.29702	7.29702
2	-4.5	3.94566	-1.14	0.270	-12.82462	3.824616
3	(omitted)					
_cons	6.4	1.31522	4.87	0.000	3.625128	9.174872

Table F2 Results of the multiple regression analysis for categorical variables for the cranium

Source	SS	df	MS		
Model	2558.70667	6	426.451111	Number of obs =	25
Residual	518.333333	18	28.7962963	F(6, 18) =	14.81
Total	3077.04	24	128.21	Prob > F =	0.0000
				R-squared =	0.8315
				Adj R-squared =	0.7754
				Root MSE =	5.3662

tbs	Coef.	Std. Err.	t	P>|t|	[95% Conf.	Interval]
cr_cal						
1	18	3.463879	5.20	0.000	10.72266	25.27734
2	23	7.429193	3.10	0.006	7.391846	38.60815
3	29.5	8.512971	3.47	0.003	11.61491	47.38509
cr_una						
1	.5	4.156655	0.12	0.906	-8.232807	9.232807
2	-4.5	5.090841	-0.88	0.388	-15.19546	6.195461
3	3.833333	8.019459	0.48	0.638	-13.01493	20.68159
_cons	4.5	8.167706	0.55	0.588	-12.65971	21.65971

Table F3 Results of the multiple regression analysis for categorical variables for the cranium

Source	SS	df	MS		
				Number of obs =	25
				F(5, 19) =	25.87
Model	2682.97333	5	536.594667	Prob > F =	0.0000
Residual	394.066667	19	20.7403509	R-squared =	0.8719
				Adj R-squared =	0.8382
Total	3077.04	24	128.21	Root MSE =	4.5542

tbs	Coef.	Std. Err.	t	P>|t|	[95% Conf.	Interval]
cr_cha						
1	16.6	2.494415	6.65	0.000	11.37913	21.82087
2	10.1	4.320453	2.34	0.030	1.057188	19.14281
cr_una						
1	.5	3.527635	0.14	0.889	-6.883425	7.883425
2	-6.166667	3.899948	-1.58	0.130	-14.32935	1.996017
3	-11	4.073362	-2.70	0.014	-19.52565	-2.474355
_cons	17.4	4.320453	4.03	0.001	8.357188	26.44281

Table F4 Results of the multiple regression analysis for categorical variables for the mandible

Source	SS	df	MS		
				Number of obs =	25
				F(5, 19) =	34.11
Model	2768.59	5	553.718	Prob > F =	0.0000
Residual	308.45	19	16.2342105	R-squared =	0.8998
				Adj R-squared =	0.8734
Total	3077.04	24	128.21	Root MSE =	4.0292

tbs	Coef.	Std. Err.	t	P>|t|	[95% Conf.	Interval]
mn_cal						
1	11.75	3.489364	3.37	0.003	4.446678	19.05332
2	21.4	2.206867	9.70	0.000	16.78097	26.01903
3	15.75	3.489364	4.51	0.000	8.446678	23.05332
mn_cha						
1	11.85	2.383689	4.97	0.000	6.860881	16.83912
2	(omitted)					
mn_una						
2	-1.3	3.371045	-0.39	0.704	-8.355679	5.755679
3	(omitted)					
_cons	6.4	1.274135	5.02	0.000	3.733204	9.066796

Table F5 Results of the multiple regression analysis for categorical variables for the mandible

```
      Source |       SS       df       MS              Number of obs =      25
-------------+------------------------------           F(  4,    20) =   16.68
       Model |  2367.38286     4  591.845714           Prob > F      =  0.0000
    Residual |  709.657143    20  35.4828571           R-squared     =  0.7694
-------------+------------------------------           Adj R-squared =  0.7232
       Total |     3077.04    24      128.21           Root MSE      =  5.9567

------------------------------------------------------------------------------
         tbs |      Coef.   Std. Err.      t    P>|t|     [95% Conf. Interval]
-------------+----------------------------------------------------------------
      mn_cal |
          1  |   20.21429   4.502879     4.49   0.000     10.82144    29.60713
          2  |   18.01429   3.103395     5.80   0.000     11.54072    24.48785
          3  |   24.21429   4.502879     5.38   0.000     14.82144    33.60713
             |
      mn_una |
          2  |       -1.3   4.983774    -0.26   0.797    -11.69597     9.09597
          3  |  (omitted)
             |
       _cons |   9.785714   1.592008     6.15   0.000     6.464844    13.10658
------------------------------------------------------------------------------
```

Table F6 Results of the multiple regression analysis for categorical variables for the mandible

```
      Source |       SS       df       MS              Number of obs =      25
-------------+------------------------------           F(  4,    20) =   26.24
       Model |  2584.50667     4  646.126667           Prob > F      =  0.0000
    Residual |  492.533333    20  24.6266667           R-squared     =  0.8399
-------------+------------------------------           Adj R-squared =  0.8079
       Total |     3077.04    24      128.21           Root MSE      =  4.9625

------------------------------------------------------------------------------
         tbs |      Coef.   Std. Err.      t    P>|t|     [95% Conf. Interval]
-------------+----------------------------------------------------------------
      mn_cha |
          1  |   15.76667   2.562638     6.15   0.000      10.4211    21.11223
          2  |   9.566667   4.879116     1.96   0.064     -.610992    19.74433
             |
      mn_una |
          2  |       -1.3   4.151947    -0.31   0.757     -9.96081     7.36081
          3  |  -11.83333   4.051886    -2.92   0.008    -20.28542   -3.381248
             |
       _cons |   18.23333   4.345163     4.20   0.000     9.169481    27.29719
------------------------------------------------------------------------------
```

Table F7 Results of the multiple regression analysis for categorical variables for the cervical vertebrae

```
      Source |       SS       df       MS              Number of obs =      25
-------------+------------------------------           F(  5,    19) =   16.36
       Model |  2496.99055     5   499.39811           Prob > F      =  0.0000
    Residual |  580.049451    19  30.5289184           R-squared     =  0.8115
-------------+------------------------------           Adj R-squared =  0.7619
       Total |     3077.04    24      128.21           Root MSE      =  5.5253

------------------------------------------------------------------------------
         tbs |      Coef.   Std. Err.      t    P>|t|     [95% Conf. Interval]
-------------+----------------------------------------------------------------
      cv_cal |
          1  |   21.56044   4.448986     4.85   0.000     12.24861    30.87227
          2  |    27.2033   7.754693     3.51   0.002     10.97254    43.43406
             |
      cv_cha |
          1  |  -11.21429   5.719227    -1.96   0.065    -23.18477    .7561936
          2  |  -5.714286   5.719227    -1.00   0.330    -17.68477    6.256194
          3  |  (omitted)
             |
      cv_una |
          1  |   .7142857   4.176733     0.17   0.866    -8.027716    9.456288
          2  |  (omitted)
          3  |  (omitted)
             |
       _cons |   9.153846   1.532442     5.97   0.000     5.946408    12.36128
------------------------------------------------------------------------------
```

Table F8 Results of the multiple regression analysis for categorical variables for the cervical vertebrae

```
      Source |       SS       df       MS              Number of obs =      25
-------------+------------------------------           F(  5,    19) =   16.36
       Model |  2496.99055     5   499.39811           Prob > F      =  0.0000
    Residual |  580.049451    19  30.5289184           R-squared     =  0.8115
-------------+------------------------------           Adj R-squared =  0.7619
       Total |     3077.04    24      128.21           Root MSE      =  5.5253

------------------------------------------------------------------------------
         tbs |      Coef.   Std. Err.      t    P>|t|     [95% Conf. Interval]
-------------+----------------------------------------------------------------
      cv_cal |
          1  |   10.34615   4.196765     2.47   0.023     1.562223    19.13008
          2  |   10.27473   5.828174     1.76   0.094    -1.923784    22.47323
             |
      cv_una |
          1  |   .7142857   4.176733     0.17   0.866    -8.027716    9.456288
          2  |  -5.714286   5.719227    -1.00   0.330    -17.68477    6.256194
          3  |  -11.21429   5.719227    -1.96   0.065    -23.18477    .7561936
             |
       _cons |   20.36813   5.920974     3.44   0.003     7.975391    32.76087
------------------------------------------------------------------------------
```

Table F9 Results of the multiple regression analysis for categorical variables for the cervical vertebrae

Source	SS	df	MS		
Model	2496.99055	5	499.39811	Number of obs =	25
Residual	580.049451	19	30.5289184	F(5, 19) =	16.36
Total	3077.04	24	128.21	Prob > F =	0.0000
				R-squared =	0.8115
				Adj R-squared =	0.7619
				Root MSE =	5.5253

tbs	Coef.	Std. Err.	t	P>|t|	[95% Conf.	Interval]
cv_cha						
1	10.34615	4.196765	2.47	0.023	1.562223	19.13008
2	21.48901	3.787068	5.67	0.000	13.56259	29.41543
3	21.56044	4.448986	4.85	0.000	12.24861	30.87227
cv_una						
1	.7142857	4.176733	0.17	0.866	-8.027716	9.456288
2	-5.642857	5.220916	-1.08	0.293	-16.57036	5.284645
3	(omitted)					
_cons	9.153846	1.532442	5.97	0.000	5.946408	12.36128

Table F10 Results of the multiple regression analysis for categorical variables for the ribs

Source	SS	df	MS		
Model	2616.96541	7	373.852201	Number of obs =	25
Residual	460.074592	17	27.0632113	F(7, 17) =	13.81
Total	3077.04	24	128.21	Prob > F =	0.0000
				R-squared =	0.8505
				Adj R-squared =	0.7889
				Root MSE =	5.2022

tbs	Coef.	Std. Err.	t	P>|t|	[95% Conf.	Interval]
rb_cal						
1	5	6.371406	0.78	0.443	-8.442492	18.44249
2	9.909091	7.440199	1.33	0.200	-5.788358	25.60654
rb_cha						
1	10.92308	3.951378	2.76	0.013	2.586397	19.25976
2	9.317016	7.632722	1.22	0.239	-6.78662	25.42065
3	10.77156	9.628216	1.12	0.279	-9.542198	31.08532
rb_una						
1	(omitted)					
2	-3.030303	6.142025	-0.49	0.628	-15.98884	9.928238
3	-6.69697	6.142025	-1.09	0.291	-19.65551	6.261571
_cons	15.77389	6.30922	2.50	0.023	2.462601	29.08518

Table F11 Results of the multiple regression analysis for categorical variables for the ribs

```
      Source |       SS       df       MS              Number of obs =      25
-------------+------------------------------           F(  5,    19) =   13.69
       Model |  2408.51821     5  481.703641           Prob > F      =  0.0000
    Residual |  668.521795    19  35.1853576           R-squared     =  0.7827
-------------+------------------------------           Adj R-squared =  0.7256
       Total |     3077.04    24      128.21           Root MSE      =  5.9317

------------------------------------------------------------------------------
         tbs |      Coef.   Std. Err.      t    P>|t|     [95% Conf. Interval]
-------------+----------------------------------------------------------------
      rb_cal |
          1  |   13.44744   3.898959     3.45   0.003     5.286822    21.60805
          2  |    17.9859   3.898959     4.61   0.000     9.825283    26.14651
             |
      rb_una |
          1  |   1.269231    7.53909     0.17   0.868    -14.51027    17.04873
          2  |  -3.153846   6.979842    -0.45   0.656    -17.76282    11.45513
          3  |  -6.480769   6.931201    -0.94   0.362    -20.98794    8.026401
             |
       _cons |    17.0141   7.098397     2.40   0.027     2.156987    31.87122
------------------------------------------------------------------------------
```

Table F12 Results of the multiple regression analysis for categorical variables for the ribs

```
      Source |       SS       df       MS              Number of obs =      25
-------------+------------------------------           F(  5,    19) =   18.65
       Model |  2556.11692     5  511.223385           Prob > F      =  0.0000
    Residual |  520.923077    19   27.417004           R-squared     =  0.8307
-------------+------------------------------           Adj R-squared =  0.7862
       Total |     3077.04    24      128.21           Root MSE      =  5.2361

------------------------------------------------------------------------------
         tbs |      Coef.   Std. Err.      t    P>|t|     [95% Conf. Interval]
-------------+----------------------------------------------------------------
      rb_cha |
          1  |   12.58974   3.353804     3.75   0.001     5.570151    19.60934
          2  |   17.58974   3.353804     5.24   0.000     10.57015    24.60934
          3  |   16.58974   7.236954     2.29   0.033     1.442624    31.73686
             |
      rb_una |
          1  |  (omitted)
          2  |  -4.666667   6.046156    -0.77   0.450    -17.32142    7.988084
          3  |  -8.333333   6.046156    -1.38   0.184    -20.98808    4.321417
             |
       _cons |   17.41026   6.218119     2.80   0.011     4.395583    30.42493
------------------------------------------------------------------------------
```

Table F13 Results of the multiple regression analysis for categorical variables for the scapula

Source	SS	df	MS		
Model	2305.64	7	329.377143	Number of obs =	25
Residual	771.4	17	45.3764706	F(7, 17) =	7.26
Total	3077.04	24	128.21	Prob > F =	0.0004
				R-squared =	0.7493
				Adj R-squared =	0.6461
				Root MSE =	6.7362

tbs	Coef.	Std. Err.	t	P>|t|	[95% Conf.	Interval]
sca_cal						
1	3	9.526434	0.31	0.757	-17.09902	23.09902
2	5.5	12.60229	0.44	0.668	-21.0885	32.0885
3	5.5	12.60229	0.44	0.668	-21.0885	32.0885
sca_cha						
1	12.2	5.070832	2.41	0.028	1.50148	22.89852
2	15.2	13.58422	1.12	0.279	-13.46019	43.86019
3	13.2	6.957124	1.90	0.075	-1.478248	27.87825
sca_una						
1	5.5	8.250134	0.67	0.514	-11.90626	22.90626
2	(omitted)					
3	(omitted)					
_cons	10.8	1.739281	6.21	0.000	7.130438	14.46956

Table F14 Results of the multiple regression analysis for categorical variables for the scapula

Source	SS	df	MS		
Model	2285.47333	6	380.912222	Number of obs =	25
Residual	791.566667	18	43.9759259	F(6, 18) =	8.66
Total	3077.04	24	128.21	Prob > F =	0.0002
				R-squared =	0.7428
				Adj R-squared =	0.6570
				Root MSE =	6.6314

tbs	Coef.	Std. Err.	t	P>|t|	[95% Conf.	Interval]
sca_cal						
1	6.666667	7.657321	0.87	0.395	-9.420768	22.7541
2	11	9.378265	1.17	0.256	-8.703003	30.703
3	11	9.378265	1.17	0.256	-8.703003	30.703
sca_cha						
1	12.2	4.991963	2.44	0.025	1.712276	22.68772
2	9.7	10.6241	0.91	0.373	-12.62041	32.02041
3	13.2	6.848916	1.93	0.070	-1.189039	27.58904
_cons	10.8	1.712229	6.31	0.000	7.20274	14.39726

Table F15 Results of the multiple regression analysis for categorical variables for the scapula

Source	SS	df	MS
Model	2042.98118	6	340.496863
Residual	1034.05882	18	57.4477124
Total	3077.04	24	128.21

Number of obs =	25
F(6, 18) =	5.93
Prob > F =	0.0015
R-squared =	0.6639
Adj R-squared =	0.5519
Root MSE =	7.5794

tbs	Coef.	Std. Err.	t	P>|t|	[95% Conf.	Interval]
sca_cal						
1	16.76471	10.87542	1.54	0.141	-6.083698	39.61311
2	19.26471	5.665963	3.40	0.003	7.36096	31.16845
3	19.26471	12.1243	1.59	0.129	-6.207495	44.73691
sca_una						
1	-8.264706	12.1243	-0.68	0.504	-33.73691	17.2075
2	-13.76471	15.26991	-0.90	0.379	-45.84559	18.31618
3	-11.76471	7.799166	-1.51	0.149	-28.15015	4.620734
_cons	24	7.579427	3.17	0.005	8.076215	39.92379

Table F16 Results of the multiple regression analysis for categorical variables for the os coxa

Source	SS	df	MS
Model	2207.95964	7	315.422806
Residual	869.080357	17	51.1223739
Total	3077.04	24	128.21

Number of obs =	25
F(7, 17) =	6.17
Prob > F =	0.0010
R-squared =	0.7176
Adj R-squared =	0.6013
Root MSE =	7.15

tbs	Coef.	Std. Err.	t	P>|t|	[95% Conf.	Interval]
osc_cal						
1	8.142857	15.75781	0.52	0.612	-25.10322	41.38894
2	7	14.29998	0.49	0.631	-23.17033	37.17033
3	4	10.11161	0.40	0.697	-17.33364	25.33364
osc_cha						
1	12.5625	7.370042	1.70	0.106	-2.98693	28.11193
2	9.133929	15.62692	0.58	0.567	-23.83599	42.10385
3	15.99107	15.62692	1.02	0.321	-16.97885	48.96099
osc_una						
2	7.428571	9.361536	0.79	0.438	-12.32254	27.17969
3	(omitted)					
_cons	11.4375	1.787498	6.40	0.000	7.666209	15.20879

Table F17 Results of the multiple regression analysis for categorical variables for the os coxa

```
      Source |       SS       df       MS              Number of obs =      25
-------------+------------------------------           F(  6,    18) =    7.24
       Model |  2175.76917     6  362.628194           Prob > F      =  0.0005
    Residual |  901.270833    18  50.0706019           R-squared     =  0.7071
-------------+------------------------------           Adj R-squared =  0.6095
       Total |     3077.04    24      128.21           Root MSE      =  7.0761

------------------------------------------------------------------------------
         tbs |      Coef.   Std. Err.      t    P>|t|     [95% Conf. Interval]
-------------+----------------------------------------------------------------
     osc_cal |
          1  |   1.333333   13.07955     0.10   0.920    -26.14578    28.81244
          2  |   2.666667   13.07955     0.20   0.841    -24.81244    30.14578
          3  |          4   10.00706     0.40   0.694    -17.02405    25.02405
             |
     osc_cha |
          1  |    12.5625   7.293834     1.72   0.102    -2.761277    27.88628
          2  |    16.5625    12.3831     1.34   0.198    -9.453432    42.57843
          3  |    21.5625   13.81645     1.56   0.136    -7.464775    50.58978
             |
       _cons |    11.4375   1.769015     6.47   0.000     7.720938    15.15406
------------------------------------------------------------------------------
```

Table F18 Results of the multiple regression analysis for categorical variables for the os coxa

```
      Source |       SS       df       MS              Number of obs =      25
-------------+------------------------------           F(  5,    19) =    7.65
       Model |  2056.26172     5  411.252344           Prob > F      =  0.0004
    Residual |  1020.77828    19  53.7251727           R-squared     =  0.6683
-------------+------------------------------           Adj R-squared =  0.5810
       Total |     3077.04    24      128.21           Root MSE      =  7.3297

------------------------------------------------------------------------------
         tbs |      Coef.   Std. Err.      t    P>|t|     [95% Conf. Interval]
-------------+----------------------------------------------------------------
     osc_cal |
          1  |   16.66968    5.08824     3.28   0.004     6.019875    27.31949
          2  |    16.0543   5.844279     2.75   0.013     3.822082    28.28652
          3  |   14.90045   6.513141     2.29   0.034     1.268291    28.53261
             |
     osc_una |
          2  |  -.6153846   8.257702    -0.07   0.941    -17.89895    16.66818
          3  |  -6.461538   6.587367    -0.98   0.339    -20.24906     7.32598
             |
       _cons |   18.63801   6.823028     2.73   0.013     4.357247    32.91877
------------------------------------------------------------------------------
```

Table F19 Results of the multiple regression analysis for categorical variables for the thoracic vertebrae

```
      Source |       SS       df       MS              Number of obs =      25
-------------+------------------------------           F(  5,    19) =   11.13
       Model |     2293.84     5     458.768           Prob > F      =  0.0000
    Residual |       783.2    19  41.2210526           R-squared     =  0.7455
-------------+------------------------------           Adj R-squared =  0.6785
       Total |     3077.04    24      128.21           Root MSE      =  6.4204

------------------------------------------------------------------------------
         tbs |      Coef.   Std. Err.      t    P>|t|     [95% Conf. Interval]
-------------+----------------------------------------------------------------
      tv_cal |
          1  |       22.4   3.315461     6.76   0.000     15.46066    29.33934
          2  |          3   9.079764     0.33   0.745    -16.00416    22.00416
             |
      tv_cha |
          1  |       12.2   4.833073     2.52   0.021     2.084262    22.31574
          2  |       18.2   11.24327     1.62   0.122    -5.332445    41.73244
          3  |  (omitted)
             |
      tv_una |
          1  |  (omitted)
          2  |         -5   9.079764    -0.55   0.588    -24.00416    14.00416
          3  |  (omitted)
             |
       _cons |       10.8    1.65773     6.51   0.000      7.33033    14.26967
------------------------------------------------------------------------------
```

Table F20 Results of the multiple regression analysis for categorical variables for the thoracic vertebrae

```
      Source |       SS       df       MS              Number of obs =      25
-------------+------------------------------           F(  4,    20) =   14.34
       Model |     2281.34     4     570.335           Prob > F      =  0.0000
    Residual |       795.7    20      39.785           R-squared     =  0.7414
-------------+------------------------------           Adj R-squared =  0.6897
       Total |     3077.04    24      128.21           Root MSE      =  6.3075

------------------------------------------------------------------------------
         tbs |      Coef.   Std. Err.      t    P>|t|     [95% Conf. Interval]
-------------+----------------------------------------------------------------
      tv_cal |
          1  |       22.4   3.257197     6.88   0.000     15.60561    29.19439
          2  |        5.5   7.725121     0.71   0.485    -10.61432    21.61432
             |
      tv_cha |
          1  |       12.2    4.74814     2.57   0.018     2.295554    22.10445
          2  |       13.2   6.514394     2.03   0.056    -.3887884    26.78879
          3  |  (omitted)
             |
       _cons |       10.8   1.628599     6.63   0.000     7.402803     14.1972
------------------------------------------------------------------------------
```

Table F21Results of the multiple regression analysis for categorical variables for the thoracic vertebrae

```
      Source |       SS       df       MS              Number of obs =      25
-------------+------------------------------           F(  4,    20) =    9.71
       Model |  2031.18118     4  507.795294           Prob > F      =  0.0002
    Residual |  1045.85882    20  52.2929412           R-squared     =  0.6601
-------------+------------------------------           Adj R-squared =  0.5921
       Total |     3077.04    24      128.21           Root MSE      =  7.2314

------------------------------------------------------------------------------
         tbs |      Coef.   Std. Err.      t    P>|t|     [95% Conf. Interval]
-------------+----------------------------------------------------------------
      tv_cal |
          1  |        4.2    12.9359     0.32   0.749    -22.78381    31.18381
          2  |          3   10.22672     0.29   0.772    -18.33257    24.33257
             |
      tv_una |
          1  |  (omitted)
          2  |         -5   10.22672    -0.49   0.630    -26.33257    16.33257
          3  |  -16.76471   12.64733    -1.33   0.200    -43.14657    9.617156
             |
       _cons |         29   12.52513     2.32   0.031     2.873041    55.12696
------------------------------------------------------------------------------
```

Table F22 Results of the multiple regression analysis for categorical variables for the lumbar vertebrae

```
      Source |       SS       df       MS              Number of obs =      25
-------------+------------------------------           F(  6,    18) =    8.00
       Model |   2238.1025     6  373.017083           Prob > F      =  0.0003
    Residual |    838.9375    18  46.6076389           R-squared     =  0.7274
-------------+------------------------------           Adj R-squared =  0.6365
       Total |     3077.04    24      128.21           Root MSE      =   6.827

------------------------------------------------------------------------------
         tbs |      Coef.   Std. Err.      t    P>|t|     [95% Conf. Interval]
-------------+----------------------------------------------------------------
      lv_cal |
          1  |    20.5625   7.037089     2.92   0.009     5.778125    35.34687
          2  |          3   9.654806     0.31   0.760    -17.28399    23.28399
             |
      lv_cha |
          1  |    12.5625   7.037089     1.79   0.091    -2.221875    27.34687
          2  |    10.0625   14.17729     0.71   0.487    -19.72287    39.84787
          3  |  (omitted)
             |
      lv_una |
          1  |        2.5   7.632794     0.33   0.747    -13.53591    18.53591
          2  |        3.5   12.30751     0.28   0.779    -22.35712    29.35712
          3  |  (omitted)
             |
       _cons |    11.4375   1.706745     6.70   0.000     7.851762    15.02324
------------------------------------------------------------------------------
```

Table F23 Results of the multiple regression analysis for categorical variables for the lumbar vertebrae

```
      Source |       SS       df       MS              Number of obs =      25
-------------+------------------------------           F(  4,    20) =   13.22
       Model |   2232.6025     4  558.150625           Prob > F      =  0.0000
    Residual |    844.4375    20   42.221875           R-squared     =  0.7256
-------------+------------------------------           Adj R-squared =  0.6707
       Total |     3077.04    24      128.21           Root MSE      =  6.4978

------------------------------------------------------------------------------
         tbs |      Coef.   Std. Err.      t    P>|t|     [95% Conf. Interval]
-------------+----------------------------------------------------------------
      lv_cal |
          1  |    22.5625    3.32915     6.78   0.000     15.61801    29.50699
          2  |        2.5   7.958192     0.31   0.757     -14.1005     19.1005
             |
      lv_cha |
          1  |    12.5625   6.697816     1.88   0.075      -1.4089     26.5339
          2  |    13.5625   6.697816     2.02   0.056    -.4088998     27.5339
          3  |  (omitted)
             |
       _cons |    11.4375   1.624459     7.04   0.000     8.048938    14.82606
------------------------------------------------------------------------------
```

Table F24 Results of the multiple regression analysis for categorical variables for the lumbar vertebrae

```
      Source |       SS       df       MS              Number of obs =      25
-------------+------------------------------           F(  5,    19) =    8.04
       Model |  2089.56941     5  417.913882           Prob > F      =  0.0003
    Residual |  987.470588    19  51.9721362           R-squared     =  0.6791
-------------+------------------------------           Adj R-squared =  0.5946
       Total |     3077.04    24      128.21           Root MSE      =  7.2092

------------------------------------------------------------------------------
         tbs |      Coef.   Std. Err.      t    P>|t|     [95% Conf. Interval]
-------------+----------------------------------------------------------------
      lv_cal |
          1  |       10.5   12.99652     0.81   0.429    -16.70202    37.70202
          2  |          3   10.19531     0.29   0.772    -18.33902    24.33902
             |
      lv_una |
          1  |        2.5   8.060097     0.31   0.760    -14.36998    19.36998
          2  |        3.5   12.99652     0.27   0.791    -23.70202    30.70202
          3  |  -9.323529   14.96458    -0.62   0.541    -40.64476     21.9977
             |
       _cons |       21.5   14.86209     1.45   0.164    -9.606702     52.6067
------------------------------------------------------------------------------
```

Table F25 Results of the multiple regression analysis for categorical variables for the humerus

```
      Source |       SS       df       MS              Number of obs =      25
-------------+------------------------------           F(  6,    18) =    8.15
       Model |  2248.97333     6  374.828889           Prob > F      =  0.0002
    Residual |  828.066667    18  46.0037037           R-squared     =  0.7309
-------------+------------------------------           Adj R-squared =  0.6412
       Total |     3077.04    24      128.21           Root MSE      =  6.7826

------------------------------------------------------------------------------
         tbs |      Coef.   Std. Err.      t    P>|t|     [95% Conf. Interval]
-------------+----------------------------------------------------------------
     hum_cal |
          1  |          3   5.537972     0.54   0.595    -8.634848    14.63485
          2  |   3.333333   6.782603     0.49   0.629    -10.91639    17.58305
             |
     hum_cha |
          1  |       10.7   5.808274     1.84   0.082    -1.502731    22.90273
          3  |       21.7   5.808274     3.74   0.002     9.497269    33.90273
             |
     hum_una |
          1  |       -4.5   6.782603    -0.66   0.515    -18.74972     9.74972
          2  |       -7.5   8.756303    -0.86   0.403    -25.89631    10.89631
          3  |  (omitted)
             |
       _cons |       10.8   1.751261     6.17   0.000     7.120738    14.47926
------------------------------------------------------------------------------
```

Table F26 Results of the multiple regression analysis for categorical variables for the humerus

```
      Source |       SS       df       MS              Number of obs =      25
-------------+------------------------------           F(  4,    20) =   12.73
       Model |  2209.26745     4  552.316863           Prob > F      =  0.0000
    Residual |  867.772549    20  43.3886275           R-squared     =  0.7180
-------------+------------------------------           Adj R-squared =  0.6616
       Total |     3077.04    24      128.21           Root MSE      =   6.587

------------------------------------------------------------------------------
         tbs |      Coef.   Std. Err.      t    P>|t|     [95% Conf. Interval]
-------------+----------------------------------------------------------------
     hum_cal |
          1  |   1.764706   5.052002     0.35   0.731    -8.773585      12.303
          2  |   1.392157    5.68584     0.24   0.809     -10.4683    13.25261
             |
     hum_cha |
          1  |   11.31765   5.564851     2.03   0.055    -.2904292    22.92572
          3  |   19.14118   4.556148     4.20   0.000     9.637219    28.64513
             |
       _cons |       10.8   1.700757     6.35   0.000     7.252283    14.34772
------------------------------------------------------------------------------
```

Table F27 Results of the multiple regression analysis for categorical variables for the humerus

Source	SS	df	MS		
Model	2092.85061	5	418.570121	Number of obs =	25
Residual	984.189394	19	51.7994418	F(5, 19) =	8.08
Total	3077.04	24	128.21	Prob > F =	0.0003
				R-squared =	0.6802
				Adj R-squared =	0.5960
				Root MSE =	7.1972

tbs	Coef.	Std. Err.	t	P>|t|	[95% Conf.	Interval]
hum_cal						
1	7.863636	5.16571	1.52	0.144	-2.948319	18.67559
2	5.765152	7.059557	0.82	0.424	-9.010671	20.54097
hum_una						
1	-4.5	7.197183	-0.63	0.539	-19.56388	10.56388
2	-9.931818	9.185331	-1.08	0.293	-29.15694	9.2933
3	-18.29545	5.842991	-3.13	0.005	-30.52497	-6.065934
_cons	30.06818	5.707089	5.27	0.000	18.12311	42.01326

Table F28 Results of the multiple regression analysis for categorical variables for the ulna

Source	SS	df	MS		
Model	2228.79	8	278.59875	Number of obs =	25
Residual	848.25	16	53.015625	F(8, 16) =	5.26
Total	3077.04	24	128.21	Prob > F =	0.0024
				R-squared =	0.7243
				Adj R-squared =	0.5865
				Root MSE =	7.2812

tbs	Coef.	Std. Err.	t	P>|t|	[95% Conf.	Interval]
uln_cal						
1	8.25	13.12634	0.63	0.539	-19.5766	36.0766
2	6.25	9.6321	0.65	0.526	-14.16914	26.66914
uln_cha						
1	7	7.519973	0.93	0.366	-8.941631	22.94163
2	14	7.519973	1.86	0.081	-1.941631	29.94163
3	12.5	13.75097	0.91	0.377	-16.65075	41.65075
uln_una						
1	-10	8.917591	-1.12	0.279	-28.90445	8.904449
2	-2.75	8.14061	-0.34	0.740	-20.00732	14.50732
3	-2.25	8.14061	-0.28	0.786	-19.50732	15.00732
_cons	13.25	8.354873	1.59	0.132	-4.46154	30.96154

Table F29 Results of the multiple regression analysis for categorical variables for the ulna

```
      Source |       SS       df       MS              Number of obs =      25
-------------+------------------------------           F(  5,    19) =    7.15
       Model |  2008.83118     5  401.766235           Prob > F      =  0.0006
    Residual |  1068.20882    19   56.221517           R-squared     =  0.6528
-------------+------------------------------           Adj R-squared =  0.5615
       Total |     3077.04    24      128.21           Root MSE      =  7.4981

------------------------------------------------------------------------------
         tbs |      Coef.   Std. Err.      t    P>|t|     [95% Conf. Interval]
-------------+----------------------------------------------------------------
     uln_cal |
          1  |   19.81471   6.312775     3.14   0.005     6.601915     33.0275
          2  |   18.71471   6.312775     2.96   0.008     5.501915     31.9275
             |
     uln_una |
          1  |       -9.7   8.871873    -1.09   0.288    -28.26904    8.869043
          2  |      -2.15   6.912907    -0.31   0.759    -16.61888    12.31888
          3  |      -1.65   6.912907    -0.24   0.814    -16.11888    12.81888
             |
       _cons |   13.88529   7.148107     1.94   0.067    -1.075866    28.84645
------------------------------------------------------------------------------
```

Table F30 Results of the multiple regression analysis for categorical variables for the ulna

```
      Source |       SS       df       MS              Number of obs =      25
-------------+------------------------------           F(  6,    18) =    7.57
       Model |   2203.8019     6  367.300317           Prob > F      =  0.0004
    Residual |  873.238095    18  48.5132275           R-squared     =  0.7162
-------------+------------------------------           Adj R-squared =  0.6216
       Total |     3077.04    24      128.21           Root MSE      =  6.9651

------------------------------------------------------------------------------
         tbs |      Coef.   Std. Err.      t    P>|t|     [95% Conf. Interval]
-------------+----------------------------------------------------------------
     uln_cha |
          1  |          7    7.19357     0.97   0.343    -8.113129    22.11313
          2  |   17.57143   4.901591     3.58   0.002     7.273567    27.86929
          3  |   19.85714   6.155203     3.23   0.005     6.925542    32.78874
             |
     uln_una |
          1  |  -9.333333   8.042655    -1.16   0.261    -26.23032    7.563658
          2  |  -1.190476   7.129052    -0.17   0.869    -16.16806    13.78711
          3  |   -2.47619   7.129052    -0.35   0.732    -17.45377    12.50139
             |
       _cons |   13.47619   7.352387     1.83   0.083    -1.970602    28.92298
------------------------------------------------------------------------------
```

Table F31 Results of the multiple regression analysis for categorical variables for the radius

```
      Source |       SS       df       MS              Number of obs =      25
-------------+------------------------------           F(  7,    17) =    5.10
       Model |  2084.97723     7  297.85389            Prob > F      =  0.0029
    Residual |  992.062771    17  58.3566336           R-squared     =  0.6776
-------------+------------------------------           Adj R-squared =  0.5448
       Total |     3077.04    24      128.21           Root MSE      =  7.6392

------------------------------------------------------------------------------
         tbs |      Coef.   Std. Err.      t    P>|t|     [95% Conf. Interval]
-------------+----------------------------------------------------------------
     rad_cal |
          1  |   23.64286   7.907273     2.99   0.008      6.95997    40.32574
          2  |   17.27922   11.69603     1.48   0.158    -7.397239    41.95568
             |
     rad_cha |
          1  |    4.97619   4.860097     1.02   0.320    -5.277718     15.2301
          2  |   8.636364   8.618125     1.00   0.330    -9.546291    26.81902
          3  |  (omitted)
             |
     rad_una |
          1  |   5.272727   7.978833     0.66   0.518    -11.56114    22.10659
          2  |  -1.727273   7.978833    -0.22   0.831    -18.56114    15.10659
          3  |   6.090909   9.213163     0.66   0.517    -13.34717    25.52898
             |
       _cons |   5.266234   9.436668     0.56   0.584     -14.6434    25.17586
------------------------------------------------------------------------------
```

Table F32 Results of the multiple regression analysis for categorical variables for the radius

```
      Source |       SS       df       MS              Number of obs =      25
-------------+------------------------------           F(  5,    19) =    6.72
       Model |  1965.19546     5  393.039092           Prob > F      =  0.0009
    Residual |  1111.84454    19  58.5181336           R-squared     =  0.6387
-------------+------------------------------           Adj R-squared =  0.5436
       Total |     3077.04    24      128.21           Root MSE      =  7.6497

------------------------------------------------------------------------------
         tbs |      Coef.   Std. Err.      t    P>|t|     [95% Conf. Interval]
-------------+----------------------------------------------------------------
     rad_cal |
          1  |   22.76471   7.871491     2.89   0.009     6.289485    39.23993
          2  |   21.33613   10.58862     2.02   0.058    -.8260924    43.49836
             |
     rad_una |
          1  |   1.571429    7.08226     0.22   0.827    -13.25191    16.39477
          2  |   1.357143   7.371449     0.18   0.856    -14.07148    16.78576
          3  |   4.857143   9.143158     0.53   0.601    -14.27971    23.99399
             |
       _cons |   7.378151     9.3295     0.79   0.439    -12.14872    26.90502
------------------------------------------------------------------------------
```

Table F33 Results of the multiple regression analysis for categorical variables for the radius

```
      Source |       SS       df       MS              Number of obs =      25
-------------+------------------------------           F(  6,    18) =    6.02
       Model |  2053.15905     6  342.193175           Prob > F      =  0.0014
    Residual |  1023.88095    18  56.8822751           R-squared     =  0.6673
-------------+------------------------------           Adj R-squared =  0.5563
       Total |     3077.04    24      128.21           Root MSE      =   7.542

------------------------------------------------------------------------------
         tbs |      Coef.   Std. Err.      t    P>|t|     [95% Conf. Interval]
-------------+----------------------------------------------------------------
     rad_cha |
          1  |    4.97619    4.79831     1.04   0.313    -5.104685    15.05707
          2  |   28.64286   10.47385     2.73   0.014     6.638115     50.6476
          3  |   23.64286   7.806747     3.03   0.007     7.241491    40.04422
             |
     rad_una |
          1  |          3   7.267686     0.41   0.685    -12.26884    18.26884
          2  |          1   6.982567     0.14   0.888    -13.66983    15.66983
          3  |          7   9.014455     0.78   0.448    -11.93867    25.93867
             |
       _cons |   4.357143   9.237067     0.47   0.643    -15.04922     23.7635
------------------------------------------------------------------------------
```

Table F34 Results of the multiple regression analysis for categorical variables for the metacarpals

```
      Source |       SS       df       MS              Number of obs =      25
-------------+------------------------------           F(  5,    19) =    7.24
       Model |  2018.21051     5  403.642103           Prob > F      =  0.0006
    Residual |  1058.82949    19  55.7278677           R-squared     =  0.6559
-------------+------------------------------           Adj R-squared =  0.5653
       Total |     3077.04    24      128.21           Root MSE      =  7.4651

------------------------------------------------------------------------------
         tbs |      Coef.   Std. Err.      t    P>|t|     [95% Conf. Interval]
-------------+----------------------------------------------------------------
      mc_cal |
          1  |   12.38462   5.071544     2.44   0.025     1.769753    22.99948
          2  |   11.85897    6.60167     1.80   0.088     -1.95848    25.67643
             |
      mc_cha |
          1  |      13.85   4.416419     3.14   0.005      4.60633    23.09367
          2  |   4.241026   4.614207     0.92   0.370     -5.41662    13.89867
          3  |   15.67692   5.964906     2.63   0.017     3.192232    28.16161
             |
       _cons |        9.4   2.360675     3.98   0.001      4.45905    14.34095
------------------------------------------------------------------------------
```

Table F35 Results of the multiple regression analysis for categorical variables for the metacarpals

Source	SS	df	MS		
Model	1544.97452	5	308.994905	Number of obs =	25
Residual	1532.06548	19	80.6350251	F(5, 19) =	3.83
Total	3077.04	24	128.21	Prob > F =	0.0144
				R-squared =	0.5021
				Adj R-squared =	0.3711
				Root MSE =	8.9797

tbs	Coef.	Std. Err.	t	P>|t|	[95% Conf.	Interval]
mc_cal						
1	10.78571	6.788016	1.59	0.129	-3.421766	24.99319
2	7.464286	9.294873	0.80	0.432	-11.99011	26.91868
mc_una						
1	9.732143	10.11107	0.96	0.348	-11.43057	30.89485
2	-1.678571	7.959654	-0.21	0.835	-18.33832	14.98118
3	-6.208333	9.802554	-0.63	0.534	-26.72532	14.30865
_cons	18.875	9.524411	1.98	0.062	-1.059821	38.80982

Table F36 Results of the multiple regression analysis for categorical variables for the metacarpals

Source	SS	df	MS		
Model	2021.05667	6	336.842778	Number of obs =	25
Residual	1055.98333	18	58.6657407	F(6, 18) =	5.74
Total	3077.04	24	128.21	Prob > F =	0.0017
				R-squared =	0.6568
				Adj R-squared =	0.5424
				Root MSE =	7.6594

tbs	Coef.	Std. Err.	t	P>|t|	[95% Conf.	Interval]
mc_cha						
1	13.85	4.531336	3.06	0.007	4.330016	23.36998
2	-6.4	8.033201	-0.80	0.436	-23.27713	10.47713
3	1.6	13.48569	0.12	0.907	-26.73238	29.93238
mc_una						
1	2	9.380757	0.21	0.834	-17.70824	21.70824
2	-.1666667	8.27305	-0.02	0.984	-17.5477	17.21437
3	-21	10.83197	-1.94	0.068	-43.75712	1.757116
_cons	30.4	11.09946	2.74	0.013	7.080896	53.7191

Table F37 Results of the multiple regression analysis for categorical variables for the femur

```
      Source |       SS       df       MS              Number of obs =      25
-------------+------------------------------           F(  6,    18) =    7.32
       Model |   2182.6025     6  363.767083           Prob > F      =  0.0004
    Residual |    894.4375    18  49.6909722           R-squared     =  0.7093
-------------+------------------------------           Adj R-squared =  0.6124
       Total |     3077.04    24      128.21           Root MSE      =  7.0492

------------------------------------------------------------------------------
         tbs |      Coef.   Std. Err.      t    P>|t|     [95% Conf. Interval]
-------------+----------------------------------------------------------------
     fem_cal |
          1  |    19.0625   14.20808     1.34   0.196    -10.78757    48.91257
          2  |    20.0625   8.811478     2.28   0.035     1.550272    38.57473
          3  |    16.0625   18.05816     0.89   0.385    -21.87628    54.00128
             |
     fem_cha |
          1  |    12.5625   7.266131     1.73   0.101    -2.703075    27.82807
          2  |         -3   7.049182    -0.43   0.675    -17.80978    11.80978
          3  |  (omitted)
             |
     fem_una |
          2  |  (omitted)
          3  |       -3.5   11.14574    -0.31   0.757    -26.91632    19.91632
             |
       _cons |    14.9375    11.2842     1.32   0.202     -8.76972    38.64472
------------------------------------------------------------------------------
```

Table F38 Results of the multiple regression analysis for categorical variables for the femur

```
      Source |       SS       df       MS              Number of obs =      25
-------------+------------------------------           F(  4,    20) =    9.63
       Model |  2025.06941     4  506.267353           Prob > F      =  0.0002
    Residual |  1051.97059    20  52.5985294           R-squared     =  0.6581
-------------+------------------------------           Adj R-squared =  0.5897
       Total |     3077.04    24      128.21           Root MSE      =  7.2525

------------------------------------------------------------------------------
         tbs |      Coef.   Std. Err.      t    P>|t|     [95% Conf. Interval]
-------------+----------------------------------------------------------------
     fem_cal |
          1  |   13.82353   9.754048     1.42   0.172    -6.523059    34.17012
          2  |   16.32353   5.421558     3.01   0.007     5.014357     27.6327
          3  |   9.323529   11.60131     0.80   0.431    -14.87638    33.52343
             |
     fem_una |
          2  |  (omitted)
          3  |       -6.5   8.882443    -0.73   0.473    -25.02845    12.02845
             |
       _cons |   18.67647   9.054934     2.06   0.052    -.2117902    37.56473
------------------------------------------------------------------------------
```

Table F39 Results of the multiple regression analysis for categorical variables for the femur

```
      Source |       SS       df       MS              Number of obs =      25
-------------+------------------------------           F(  5,    19) =    9.19
       Model |   2176.6025     5    435.3205           Prob > F      =  0.0001
    Residual |    900.4375    19  47.3914474           R-squared     =  0.7074
-------------+------------------------------           Adj R-squared =  0.6304
       Total |     3077.04    24      128.21           Root MSE      =  6.8841

------------------------------------------------------------------------------
         tbs |      Coef.   Std. Err.      t    P>|t|     [95% Conf. Interval]
-------------+----------------------------------------------------------------
     fem_cha |
          1  |    12.5625   7.096014     1.77   0.093    -2.289628    27.41463
          2  |    17.0625   5.163108     3.30   0.004      6.25599    27.86901
          3  |    21.0625     8.1333     2.59   0.018     4.039308    38.08569
             |
     fem_una |
          2  |         -1   8.431321    -0.12   0.907    -18.64696    16.64696
          3  |       -2.5    10.5157    -0.24   0.815    -24.50962    19.50962
             |
       _cons |    13.9375   10.65561     1.31   0.206    -8.364947    36.23995
------------------------------------------------------------------------------
```

Table F40 Results of the multiple regression analysis for categorical variables for the tibia

```
      Source |       SS       df       MS              Number of obs =      25
-------------+------------------------------           F(  8,    16) =   10.82
       Model |  2597.12333     8  324.640417           Prob > F      =  0.0000
    Residual |  479.916667    16  29.9947917           R-squared     =  0.8440
-------------+------------------------------           Adj R-squared =  0.7660
       Total |     3077.04    24      128.21           Root MSE      =  5.4768

------------------------------------------------------------------------------
         tbs |      Coef.   Std. Err.      t    P>|t|     [95% Conf. Interval]
-------------+----------------------------------------------------------------
     tib_cal |
          1  |        9.5   4.743005     2.00   0.062    -.5547208    19.55472
          2  |       21.5   14.22901     1.51   0.150    -8.664163    51.66416
          3  |       10.5   8.215125     1.28   0.219    -6.915287    27.91529
             |
     tib_cha |
          1  |   12.08333   3.162003     3.82   0.002     5.380186    18.78648
          2  |   17.08333   7.415555     2.30   0.035      1.36306    32.80361
          3  |   6.083333   7.415555     0.82   0.424     -9.63694    21.80361
             |
     tib_una |
          1  |         10   10.24606     0.98   0.344    -11.72068    31.72068
          3  |          3   9.486009     0.32   0.756    -17.10944    23.10944
             |
       _cons |   5.416667   9.616857     0.56   0.581    -14.97016    25.80349
------------------------------------------------------------------------------
```

Table F41: Results of the multiple regression analysis for categorical variables for the tibia

```
      Source |       SS       df       MS              Number of obs =      25
-------------+------------------------------           F(  5,    19) =    8.15
       Model |   2098.3525     5    419.6705           Prob > F      =  0.0003
    Residual |    978.6875    19  51.5098684           R-squared     =  0.6819
-------------+------------------------------           Adj R-squared =  0.5982
       Total |     3077.04    24      128.21           Root MSE      =   7.177

------------------------------------------------------------------------------
         tbs |      Coef.   Std. Err.      t    P>|t|     [95% Conf. Interval]
-------------+----------------------------------------------------------------
     tib_cal |
          1  |    18.3125   4.012086     4.56   0.000     9.915108    26.70989
          2  |    24.3125   14.01361     1.73   0.099    -5.018331    53.64333
          3  |    19.3125   9.662383     2.00   0.060    -.9110991     39.5361
             |
     tib_una |
          1  |          4   10.14986     0.39   0.698    -17.24391    25.24391
          3  |       2.75   11.90177     0.23   0.820    -22.16069    27.66069
             |
       _cons |     8.6875   12.03626     0.72   0.479    -16.50468    33.87968
------------------------------------------------------------------------------
```

Table F42: Results of the multiple regression analysis for categorical variables for the tibia

```
      Source |       SS       df       MS              Number of obs =      25
-------------+------------------------------           F(  5,    19) =   15.44
       Model |  2469.24614     5  493.849228           Prob > F      =  0.0000
    Residual |   607.79386    19  31.9891505           R-squared     =  0.8025
-------------+------------------------------           Adj R-squared =  0.7505
       Total |     3077.04    24      128.21           Root MSE      =  5.6559

------------------------------------------------------------------------------
         tbs |      Coef.   Std. Err.      t    P>|t|     [95% Conf. Interval]
-------------+----------------------------------------------------------------
     tib_cha |
          1  |   15.00439   2.777891     5.40   0.000     9.190192    20.81858
          2  |   26.58333   5.886842     4.52   0.000     14.26203    38.90464
          3  |   17.05702   4.955106     3.44   0.003     6.685861    27.42817
             |
     tib_una |
          1  |  -.1929825   5.705293    -0.03   0.973     -12.1343    11.74833
          3  |  -6.052632   4.854993    -1.25   0.228    -16.21425    4.108985
             |
       _cons |    14.4693   5.122179     2.82   0.011     3.748455    25.19014
------------------------------------------------------------------------------
```

Table F43 Results of the multiple regression analysis for categorical variables for the fibula

```
      Source |       SS       df       MS              Number of obs =      25
-------------+------------------------------           F(  7,    17) =    6.10
       Model |   2201.1025     7  314.443214           Prob > F      =  0.0011
    Residual |    875.9375    17  51.5257353           R-squared     =  0.7153
-------------+------------------------------           Adj R-squared =  0.5981
       Total |     3077.04    24      128.21           Root MSE      =  7.1781

------------------------------------------------------------------------------
         tbs |      Coef.   Std. Err.      t    P>|t|     [95% Conf. Interval]
-------------+----------------------------------------------------------------
     fib_cal |
          1  |         -2   8.791394    -0.23   0.823    -20.54822    16.54822
          2  |     8.5625   11.49064     0.75   0.466    -15.68062    32.80562
             |
     fib_cha |
          1  |    23.5625    7.39906     3.18   0.005     7.951847    39.17315
          2  |  (omitted)
          3  |    13.5625    7.39906     1.83   0.084    -2.048153    29.17315
             |
     fib_una |
          1  |         -2   10.15143    -0.20   0.846    -23.41764    19.41764
          2  |        -11   10.15143    -1.08   0.294    -32.41764    10.41764
          3  |        -10   10.15143    -0.99   0.338    -31.41764    11.41764
             |
       _cons |    21.4375   10.30882     2.08   0.053    -.3122151    43.18722
------------------------------------------------------------------------------
```

Table F44 Results of the multiple regression analysis for categorical variables for the fibula

```
      Source |       SS       df       MS              Number of obs =      25
-------------+------------------------------           F(  5,    19) =    3.80
       Model |     1538.54     5     307.708           Prob > F      =  0.0149
    Residual |      1538.5    19  80.9736842           R-squared     =  0.5000
-------------+------------------------------           Adj R-squared =  0.3684
       Total |     3077.04    24      128.21           Root MSE      =  8.9985

------------------------------------------------------------------------------
         tbs |      Coef.   Std. Err.      t    P>|t|     [95% Conf. Interval]
-------------+----------------------------------------------------------------
     fib_cal |
          1  |         -2   11.02091    -0.18   0.858    -25.06704    21.06704
          2  |         -5   11.02091    -0.45   0.655    -28.06704    18.06704
             |
     fib_una |
          1  |         -2   12.72585    -0.16   0.877    -28.63552    24.63552
          2  |        -11   12.72585    -0.86   0.398    -37.63552    15.63552
          3  |      -21.5   9.245119    -2.33   0.031    -40.85026   -2.149744
             |
       _cons |         35   8.998538     3.89   0.001     16.16584    53.83416
------------------------------------------------------------------------------
```

Table F45 Results of the multiple regression analysis for categorical variables for the fibula

```
      Source |       SS       df       MS              Number of obs =      25
-------------+------------------------------           F(  6,    18) =    7.51
       Model |  2198.43583     6  366.405972           Prob > F      =  0.0004
    Residual |  878.604167    18  48.8113426           R-squared     =  0.7145
-------------+------------------------------           Adj R-squared =  0.6193
       Total |     3077.04    24      128.21           Root MSE      =  6.9865

------------------------------------------------------------------------------
         tbs |      Coef.   Std. Err.      t    P>|t|     [95% Conf. Interval]
-------------+----------------------------------------------------------------
     fib_cha |
          1  |    23.5625   7.201531     3.27   0.004     8.432644    38.69236
          2  |     8.5625   11.18388     0.77   0.454    -14.93395    32.05895
          3  |    13.5625   7.201531     1.88   0.076    -1.567356    28.69236
             |
     fib_una |
          1  |  -3.333333   8.067329    -0.41   0.684    -20.28216     13.6155
          2  |        -11   9.880419    -1.11   0.280    -31.75799    9.757991
          3  |        -10   9.880419    -1.01   0.325    -30.75799    10.75799
             |
       _cons |    21.4375   10.03361     2.14   0.047     .3576609    42.51734
------------------------------------------------------------------------------
```

Table F46 Results of the multiple regression analysis for categorical variables for the metatarsals

```
      Source |       SS       df       MS              Number of obs =      25
-------------+------------------------------           F(  4,    20) =    7.77
       Model |  1872.11053     4  468.027633           Prob > F      =  0.0006
    Residual |  1204.92947    20  60.2464734           R-squared     =  0.6084
-------------+------------------------------           Adj R-squared =  0.5301
       Total |     3077.04    24      128.21           Root MSE      =  7.7619

------------------------------------------------------------------------------
         tbs |      Coef.   Std. Err.      t    P>|t|     [95% Conf. Interval]
-------------+----------------------------------------------------------------
    1.mt_cal |     5.12069   4.670479     1.10   0.286     -4.62176    14.86314
             |
      mt_cha |
          1  |   17.14734   3.982998     4.31   0.000     8.838947    25.45572
          2  |   11.76803   5.021241     2.34   0.030     1.293899    22.24215
          3  |   15.18182   8.106999     1.87   0.076    -1.729084    32.09272
             |
      mt_una |
          2  |  (omitted)
          3  |  (omitted)
             |
       _cons |   8.818182   2.340289     3.77   0.001     3.936425    13.69994
------------------------------------------------------------------------------
```

Table F47 Results of the multiple regression analysis for categorical variables for the metatarsals

```
      Source |       SS       df       MS              Number of obs =      25
-------------+------------------------------           F(  3,    21) =    2.28
       Model |  755.492381     3  251.830794           Prob > F      =  0.1091
    Residual |  2321.54762    21  110.549887           R-squared     =  0.2455
-------------+------------------------------           Adj R-squared =  0.1377
       Total |     3077.04    24      128.21           Root MSE      =  10.514

------------------------------------------------------------------------------
         tbs |      Coef.   Std. Err.      t    P>|t|     [95% Conf. Interval]
-------------+----------------------------------------------------------------
    1.mt_cal |   11.85714   5.961031     1.99   0.060       -.5395    24.25379
             |
      mt_una |
          2  |  -7.904762   12.03195    -0.66   0.518    -32.92656    17.11704
          3  |  -9.261905   10.82267    -0.86   0.402    -31.76888    13.24507
             |
       _cons |         24   10.51427     2.28   0.033     2.134377    45.86562
------------------------------------------------------------------------------
```

Table F48 Results of the multiple regression analysis for categorical variables for the metatarsals

```
      Source |       SS       df       MS              Number of obs =      25
-------------+------------------------------           F(  3,    21) =    9.86
       Model |  1799.68935     3   599.89645           Prob > F      =  0.0003
    Residual |  1277.35065    21  60.8262214           R-squared     =  0.5849
-------------+------------------------------           Adj R-squared =  0.5256
       Total |     3077.04    24      128.21           Root MSE      =  7.7991

------------------------------------------------------------------------------
         tbs |      Coef.   Std. Err.      t    P>|t|     [95% Conf. Interval]
-------------+----------------------------------------------------------------
      mt_cha |
          1  |   18.61039   3.770824     4.94   0.000     10.76853    26.45225
          2  |   15.18182   3.958202     3.84   0.001     6.950287    23.41335
          3  |   15.18182   8.145912     1.86   0.076    -1.758533    32.12217
             |
      mt_una |
          2  |  (omitted)
          3  |  (omitted)
             |
       _cons |   8.818182   2.351522     3.75   0.001     3.927924    13.70844
------------------------------------------------------------------------------
```

The Research Ethics Committee, Faculty Health Sciences, University of Pretoria complies with ICH-GCP guidelines and has US Federalwide Assurance. FWA 00002567, Approved dd 22 May 2002 and Expires 24 Jan 2009.
IRB 0000 2235 IORG0001762 Approved dd Jan 2006 and Expires 21 Nov 2008.

100 1923 - 2008
UNIVERSITEIT VAN PRETORIA
UNIVERSITY OF PRETORIA
YUNIBESITHI YA PRETORIA
Faculty of Health Sciences Research Ethics Committee
Fakulteit van Gesondheidswetenskappe Navorsingsetiekkomitee

PROTOCOL NO.	**134/2008**
PROTOCOL TITLE	Skeletal changes after post-mortem exposure to fire as an indicator of decomposition stage
INVESTIGATOR	**Principle Investigator:** Ms N Keough
SUBINVESTIGATOR	None
SUPERVISOR	Dr E N L'abbè ericka.labbe@up.ac.za
DEPARTMENT	**Dept:** Dept Anatomy **Phone:** 012-3192244 **Fax:** **E-Mail:** Natalie.keough@up.ac.za **Cell:** 0823938519
STUDY DEGREE	PhD: Anatomy
SPONSOR	None
MEETING DATE OF THIS STUDY	30/07/2008

This **Protocol** has been considered by the Faculty of Health Sciences Research Ethics Committee, University of Pretoria on 30/07/2008 and found to be acceptable.

*Dr A Nienaber	(female) BA (Hons) (Wits); LLB; LLM (UP); Dipl.Datametrics (UNISA)
*Prof V.O.L. Karusseit	MBChB; MFGP (SA); MMed (Chir); FCS (SA): Surgeon
*Prof M Kruger	(female) MB.ChB. (Pta); MMed. Pead. (Pret); PhD. (Leuven)
Dr N K Likibi	MB.BCh; Med.Adviser (Gauteng Dept.of Health)
*Dr T S Marcus	(female) BSc (LSE), PhD (University of Lodz, Poland)
*Mrs M C Nzeku	(female) BSc (NUL); MSc Biochem (UCL, UK)
*Snr Sr J. Phatoli	(female) BCur (Eet.A) BTec (Oncology Nursing Sience)Snr Nursing-Sister
*Dr L Schoeman	(female) BP harm, BA Hons (PSy), PhD
*Dr R Sommers	(female) MBChB; MMed (Int); MPhar.Med;
Mr Y Sikweyiya	MPH; Master Level Fellowship in Research Ethics; BSC (Health Promotion) Postgraduate Dip in Health Promotion
*Prof TJP Swart	BChD, MSc (Odont), MChD (Oral Path), PGCHE
Dr A P van Der Walt	BChD, DGA (Pret) Director: Clinical Services of the Pretoria Academic Hospital
*Prof C W van Staden	MBChB; MMed (Psych); MD; FCPsych; FTCL; UPLM; Dept of Psychiatry

Dr R Sommers; MBChB; MMed (Int); MPhar.Med.
SECRETARIAT of the Faculty of Health Sciences Research Ethics Committee, University of Pretoria, Pretoria Academic Hospital
♦ H W Snyman Building (South) Level 2-34 ♦ P.O.BOX 667 Pretoria, South Africa, 0001 ♦ Tel:(012)3541330 ♦
♦ Fax: (012)3541367 / 0866515924 ♦ E-Mail: manda@med.up.ac.za ♦ Web: //www.healthethics-up.co.za ♦